ELECTRONIC VALVES
BOOK IX

JUNCTION TRANSISTORS IN PULSE CIRCUITS

by

P. A. Neeteson

The transistor with all its advantages will play a dominant part in the development of such applications, for which numerous electronic switches are required; especially where bulky equipment is concerned.

This book studies the behaviour of networks in which junction transistors are used as switches, with a view to efficient use and new applications.
The introductory chapters on the different types switches and fundamental pulse circuits are followed by a thorough study of the junction transistor in various circuits.

The treatment will be acceptable to a very large circle of readers, since in describing the potentialities of the new semiconductor device, mathematics and circuit analysis have been kept at a minimum.

This book will be of great use for students in technical colleges, radio schools, engineers, and technical men and others interested in the further development of electronics.

PHILIPS TECHNICAL LIBRARY

ELECTRONIC VALVES BOOK XIV

TELEVISION DEFLECTION SYSTEMS

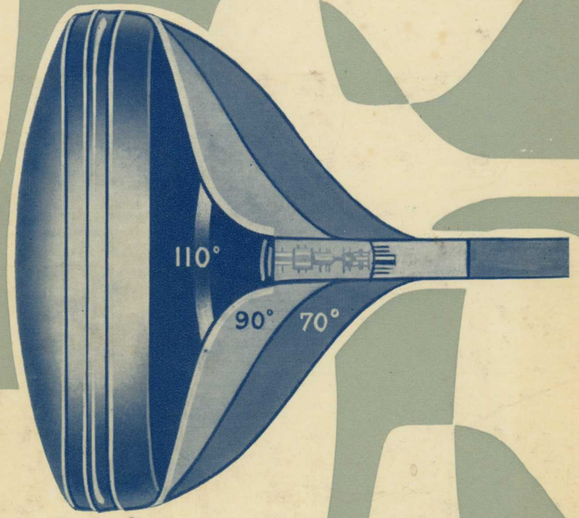

A. BOEKHORST AND
J. STOLK

PHILIPS TECHNICAL LIBRARY

The deflection system which is the subject of this book consists of two parts, each of which is responsible for one of the components, horizontal or vertical, of the deflection field. The coil unit which unites these two components to form one deflection field requires separate consideration. The design and characteristics of a coil unit depend so much on the picture tube with which it is to be used, that the latter can be regarded as the starting point for the design of the deflection system.
Following an introductory first chapter, some attention is paid to the picture tube itself and to its auxiliary components, including focusing and iron trap magnets.

More detailed attention is given to the picture faults which may occur. Mathematical analysis of these faults would lead us to far from our subject, and has therefore been omitted, only a physical interpretation having been given.

After a short analysis of a deflection unit for 110° deflection, which has been developed in the Mullard Research Laboratory at Salfords, the greater part of this work is devoted to the theory and design of the line-deflection circuits.

TELEVISION DEFLECTION SYSTEMS

TELEVISION DEFLECTION SYSTEMS

BY

A. BOEKHORST

AND

J. STOLK

1962

PHILIPS TECHNICAL LIBRARY

Translated by P. J. Arthern, A.I.L., London

Publisher's note:

This book will be published in the German, French, Spanish and English languages
It contains 232 pages, 142 illustrations and
4 pages photographs on art paper

U.D.C. 621.397.33

First edition 1962

FOREWORD

A great variety of general literature has been published in the field of television. Yet there is much demand for a series of books in which the subjects are dealt with in more detail, such as the books on "I. F. Stages" and "Flywheel Synchronisation", by A. G. W. Uitjens and Dr. P. A. Neeteson respectively.

The present book is another volume pertaining to this series. It deals with the problems relating to the deflection of the electron beam in the television picture tube.

In the course of many years of work in the field of deflection circuit techniques in the Applications Laboratories of N.V. Philips' Gloeilampenfabrieken, the authors have made a thorough study of the problems concerned. Both have prepared many publications on this subject, and thus made a considerable contribution to the present-day circuitry.

In my opinion it is an excellent idea to extend and combine these publications in a logical sequence.

In the first part of the book all details around the picture tube and the deflection coils are investigated. The second part deals wit modern deflection circuits; these circuits have found their way in television receivers, not only in Europe but also in other continents. The requirements imposed by the deflection circuits on the valves are extensively discussed, and so are the problems relating to the design of line and field output transformers.

Although the calculations have been based on the use of modern Philips picture tubes, components and receiving valves, the set-up of the book is such that it doesn't present the reader much trouble to adapt the chosen examples to his particular case.

I am convinced that this book will be a most welcome aid to everyone who is involved in the investigation or design of this important part of the T.V. receiver around the picture tube.

March 1962 Dr. B. G. Dammers

ACKNOWLEDGMENT

This book could not have been accomplished without the cooperation of many members of the application and development groups for electron valves and picture tubes of N.V. Philips' Gloeilampenfabrieken. The deflection unit described in this book was developed in Mullard Research Laboratories at Salfords, England. The authors wish to express their great debt to all these cooperators and to Mr. P. Arthern, who translated this book with meticulous care.

The authors

CONTENTS

CHAPTER 1

INTRODUCTION

1.1. The function of the deflection system in a television receiver

Before we enter on a detailed treatment, it may be useful to sketch, in broad outline, the object of the deflection system, and the standards which are generally accepted for it. Our attention will be directed primarily to black-and-white television, but much of the subject matter may also be applicable to colour television.

To transmit a picture, it is not sufficient to transmit a given quantity of light; the gradations in intensity, as well as the relative position of each small part of the picture, must all be faithfully reproduced.

It is obvious that the smaller the component parts of the picture (picture elements), the greater can be the definition and the richness of detail.

If it was desired to transmit a complete picture by electrical means at one and the same instant, it would be necessary to transmit a separate electrical signal for each picture element, in order to convey information concerning its intensity. As several hundred thousand of these picture elements are required for reasonable reproduction of a picture, however, this would lead to an impossibly complicated system of cables, transmitters, camera tube and picture tube.

Thanks to the persistence of vision, there is no need for this; it is sufficient to transmit the information concerning all the picture elements *in succession.* If this is done quickly enough, the eye still receives the illusion of a complete picture. In this system, the picture must be scanned according to an agreed method at both the transmitting end and the receiving end, and a single channel is sufficient for the successive transmission of information concerning the intensity of all the picture elements as they are scanned.

In a television receiver, several different principal functions can be distinguished. These are shown in the block diagram of Fig. 1.1.

First of all, there is the picture tube. This contains the electron gun which consists basically of a hot emissive cathode and a control electrode, while the beam of electrons is attracted to the screen by a high positive potential. The screen is coated with a phosphor which lights up when it is struck by the electron beam. The gun may also contain additional electrodes which produce a sharply focused spot of light on the screen. The number of electrons reaching the screen at any instant determines the intensity of the

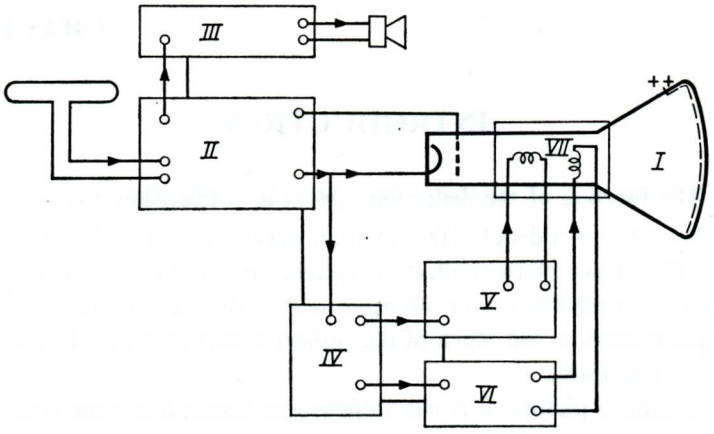

Fig. 1.1. Block diagram of a television receiver. I. Picture tube, II. video receiver, III. audio receiver, IV. synchronising pulse separator, V. line timebase, VI. field timebase, VII. deflection unit.

spot of light. The flow of electrons is regulated by the control electrode, otherwise known as the first grid, which is connected to the output of the video receiver. This receiver detects, amplifies and demodulates the modulated carrier wave which is received from the transmitter.

The associated sound is transmitted by means of a separate carrier wave, and reaches the loudspeaker via an audio receiver. Parts of the video and audio receivers are in common.

Finally there is the deflection system, the function of which is to ensure that the electron beam in the picture tube always strikes the screen at the position corresponding to the video signal which is being received. This is achieved by means of a magnetic field which is set up in the path of the electron beam between the cathode and the screen of the picture tube. The magnetic field can deflect the beam both horizontally and vertically, so that the position where the beam strikes the screen can be precisely controlled by varying the horizontal and vertical components of the field.

The deflection system which is the subject of this book thus consists of two parts, each of which is responsible for one of the components of the deflection field. The coil unit which unites these two components to form one deflection field requires separate consideration. The design and characteristics of a coil unit depend so much on the picture tube with which it is to be used, that the latter can be regarded as the starting point for the design of the deflection system.

In other words, once the picture tube has been chosen, the deflection coil unit must be designed around it, and the design of the rest of the

deflection circuits must be adapted to the characteristics of the combination of coils and picture tube.

We will deal with the various parts of the system in this order.

1.2. The scanning process

We may now enquire which method of scanning has been chosen for the reproduction of television pictures. Although no international agreement has been reached concerning the number of picture elements which is required to give good reproduction, the method by which the picture is scanned is the same everywhere.

The procedure which is followed in all the T.V. standards now in use can best be explained with the aid of Fig. 1.2.

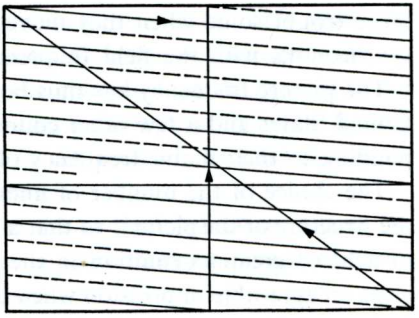

Fig. 1.2. Schematic representation of scanning of the picture screen. Solid lines: first field; dotted lines: second field.

At the beginning of each field, the light spot is moved to the top left-hand corner of the picture tube by means of the magnetic field of the deflection coil. The electron beam is then moved rapidly to and fro across the screen by means of sawtooth currents flowing through the 'horizontal' or line deflection coils, the scan being much slower than the flyback. Simultaneously, another sawtooth current, with a much lower frequency, is passed through the 'vertical' or field deflection coils, so that the light spot also moves slowly downwards, and then flies rapidly upwards again when it reaches the bottom of the screen. The scanning takes place in such a way that this vertical deflection occurs twice in the reproduction of one complete picture. By this means, the flicker frequency is doubled, so that the picture appears steadier. In order to obtain the required number of lines per picture, however, care must be taken to see that the lines of the second field do not coincide with the lines of the first field, but come exactly half-way between them.

In Fig. 1.2 this is indicated by using dotted lines for the second field. To obtain this interlaced scanning, it is necessary to choose an uneven number

of lines, because each field must consist of a certain number of lines plus half a line.

Just as in film projection, the limit at which flickering becomes troublesome plays a great part in the choice of the number of pictures to be scanned in each second. For the observation of moving pictures, only about 16 pictures per second are necessary, but a much larger number are required if flickering is to be prevented to a sufficient extent. For films, therefore, the number which has been chosen is 24 pictures per second, and flickering is suppressed by illuminating each picture twice. The number employed in television is 25 pictures per second, i.e. 50 fields per second. In the choice of this number, attention has also been paid to the difficulties which may arise if the picture repetition frequency differs from the mains frequency. Slight mains hum in the television receiver can cause variations of brightness which are far more troublesome when they move across the screen, than when they are synchronous with the field frequency.

The picture frequency has thus been fixed at 25 per second, except in the United States and a few other countries, where it is 30 per second, corresponding to their mains frequency of 60 c/s.

The choice of the number of lines per picture determines the fineness of the structure of the picture, so that a large number of lines makes it possible to achieve greater definition in the vertical direction. As the picture only gives an agreeable impression when the definition in the horizontal direction is comparable to the vertical definition, many more picture elements are required for the 819-line system, for example, than for 625 or 405 lines. However, if real benefit is to be obtained from this large number of lines, the information concerning brightness must cover a much larger number of picture elements per second; the bandwidth of the whole transmission system must increase quadratically with the number of lines. The size of the light spot in the picture tube must also be adapted to the number of lines.

It is obvious that any choice is a compromise, and that the numbers of lines which have been selected can only vary as a result of differing ideas about the difficulties and possibilities of television transmission in the early stages of its development. The numbers which were originally chosen in different countries have since become firmly established, because of the large numbers of viewers who possess television sets built to the selected standard.

We must thus continue to take different numbers of lines into account. These are, 405 lines for the United Kingdom, 819 lines for France and some Belgian transmitters, 525 lines in the United States of America and a few other countries and 625 lines for the rest of the world.

1.3. **The flyback period**

As already mentioned, the electron beam returns to the left-hand side of the screen, or to the top, very much more quickly than it moves during the scan. During the flyback, no picture information is transmitted, but the time is used to send a synchronising signal. This signal, which normally consists of a single pulse for the lines and a series of pulses for the fields, is the time signal which indicates to the receiver that a line or field has been completed, and that a new line or field is about to commence.

If it was desired to make the fullest possible use of the time which is available for transmitting picture information, the flyback period would have to be made extremely short. For practical reasons connected with deflection techniques, however, a longer time – up to about 18% of a cycle – is left, in which no picture information is given. This gives the receiver the opportunity of allowing a small deviation in the precise instant at which the flyback must commence; the coherence of the picture is not disturbed as long as the deviation is the same for every line. A longer flyback period offers further great advantages in the receiver, because the losses will be smaller, as will be explained later on.

To a lesser extent, this also applies to the vertical deflection, but as the times involved here are so much longer, a total blanking period of about 6% of a cycle is considered to be sufficient.

There is, of course, no necessity to make the flyback period as long as the blanking period. On the contrary, it is recommended that a slightly shorter time should be taken, since this leaves time to allow for some delay in the synchronisation. It is true that this will produce black edges round the picture, but these can be made to fall outside the picture screen, so that no disturbance is experienced.

On the other hand, if the flyback period is too long, the picture information for a new line is being received before the flyback has been completed. Unless special precautions are taken, this gives a disturbing effect, because the high velocity of the flyback means that this picture information may extend over a fairly large area of the screen; the viewer sees part of the picture "folded over" at the left-hand side of the screen, and stretched out through the normal picture.

To prevent this, the flyback period of the line timebase may either be limited to 14 to 16% of a cycle or a longer blanking pulse has to be applied to the picture tube. For the field time base, where a small flyback ratio does not give rise to any particular difficulties, 2 to 4% of a cycle is usual.

As an illustration of the deflection process, Figs. 1.3.1. and 1.3.2. show

a picture signal as a function of time, for one line period and one field period respectively. The figures also indicate how the horizontal and vertical deflection on the screen of the picture tube must vary.

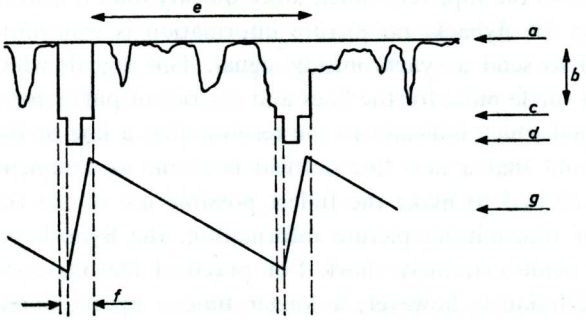

Fig. 1.3.1 Synthesis of a typical television picture. Top: picture signal during one line period. Bottom: synchronous horizontal scanning of the picture screen.
a. signal level for the white areas, *b.* grey shades, *c.* black level, *d.* synchronising pulses, *e.* line period, *f.* blanking period, *g.* horizontal deflection.

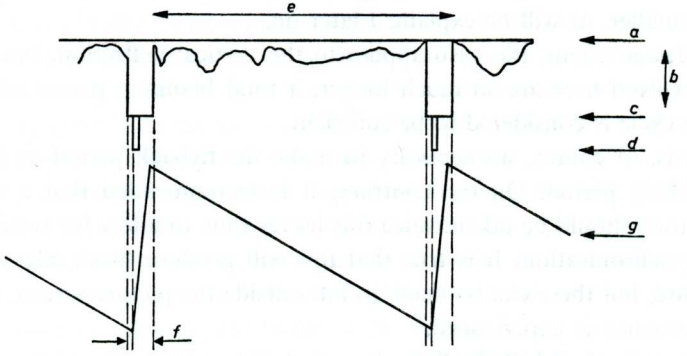

Fig. 1.3.2 Top: picture signal during one field period. Bottom: vertical scanning of the picture screen. For the sake of clarity the line pulses are omitted from this figure.
a. to *d* and *f* see Fig. 1.3.1, *e.* field period, *g.* vertical deflection.

We may note here that, as the flyback periods are normally kept shorter than the blanking periods, and the traced area must occupy the whole of the picture screen, the total deflections must be a few percent greater than exactly to the edges of the screen. It is often necessary to increase the horizontal deflection still further in order to obtain the correct ratio of height to width (3 : 4). The dimensions of the screens of the picture tubes have ratios, slightly deviating from the transmitted 3 : 4 picture aspect ratio.

CHAPTER 2

THE PICTURE TUBE

The picture tube is the last link in the chain of television reception, and must give an accurate reproduction of the scene being televised. The picture can either be watched on the picture tube itself, in which case the tube is referred to as a direct-viewing tube, or it is projected onto a screen from a projection tube, by means of an optical system.

We may distinguish three principal components of the tube:

1. A bulb with a cylindrical neck.
2. A fluorescent screen applied to the inside of the face of the tube.
3. An electron gun, situated in the neck of the tube.

2.1. The bulb

At the present time, almost all the bulbs for monochrome television tubes are made of glass. As the tube is completely evacuated, the glass must be able to withstand the pressure of the atmosphere, and thus the wall is fairly thick. In the centre of the screen, for example, the glass is about 8 mm thick for a 21-inch tube. In addition, the screen is not flat, but is slightly curved, and can be regarded as part of a sphere. A disadvantage of the curvature is that if the picture is being watched from an angle, it is not free from geometrical distortion.

Projection tubes do not have this disadvantage, and they also have the advantages of less danger of implosion and of permitting a larger picture to be obtained. Against this, a relatively expensive and bulky apparatus is required, and the resulting picture is much less brilliant.

At present, the projection tube has yielded the field almost entirely to the direct-viewing tube with a more or less rectangular screen.

The sides of the rectangle are in the ratio of 4 : 5, while the picture which is broadcast by the transmitters has a ratio 3 : 4. As a result, about 6% of the picture information in the horizontal direction is lost if the full height of the screen is utilised. For a given diagonal, a 4 : 5 aspect ratio gives a slightly greater picture area, and the time in which the superfluous picture information is transmitted can be used to increase the horizontal flyback period, with a consequent appreciable decrease in the peak currents and voltages in the deflection circuit.

The size of a picture tube is expressed by the length of the diagonal across the screen. In general the bigger the screen, the longer is the tube and thus

the greater is the depth of the television set, because the depth is determined by the length of the tube.

To limit the depth of the cabinet, the picture tube has been shortened in successive stages, while keeping the same screen dimensions. One way of doing this has been to increase the maximum angle of deflection of the electron beam which is produced by the gun, and which describes a raster on the screen as indicated in Chapter 1. This means that the depth of the bulb is decreased. In addition, it has been possible to decrease the length of the neck, thanks to modifications to the gun.

The maximum angle of deflection is the angle measured across the diagonal of the screen. It has increased in a relatively short time from 55° through 70° and 90° to 110°. Fig. 2.1. clearly illustrates the resulting saving in the length of the tube. All the screens have a diagonal of 21 inches, but the maximum angles of deflection are respectively 70°, 90° and 110°.

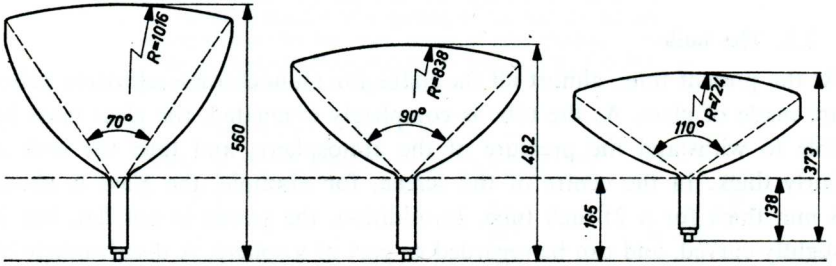

Fig. 2.1. Picture tubes with the same diagonal screen diameter, 21 inches, but different angles of deflection, 70°, 90° and 110° respectively, measured across the diagonal. (All dimensions in mm)

The development towards larger angles of deflection is not only accompanied by technical difficulties in the manufacture of the tubes, but also leads to difficulties in the design of deflection coils and circuits, as will be evident in subsequent chapters.

2.2. **The fluorescent screen**

The screen is composed of certain fluorescent materials, also called phosphors, and glows when it is struck by electrons moving at a sufficient velocity. In the first place, the brightness of the point of impact is proportional to the accelerating velocity to which the electrons have been subjected, and also to the beam current, i.e. the number of electrons striking the point of impact in unit time. The electron beam which, in a normally operating receiver, scans the screen in a raster pattern as already mentioned, is modulated in intensity. The modulation is proportional to the strength

of the incoming television signal, and so the screen will glow more brightly or less brightly in different places, producing a black and white picture with grey intermediate zones.

As the picture screen is scanned 50 times per second, the phosphor must not continue to glow for more than 20 msec., because if it does, a troublesome blur is produced in pictures of moving objects.

It may be asked whether the screen does not become negatively charged due to the continuous electron bombardment, with a consequent retarding effect on the approaching electrons. The answer is that in modern tubes there is also an extremely thin conductive coating of aluminium deposited on the back of the phosphor coating, covering the whole of the inside surface of the bulb. The E.H.T. contact is on one side of the bulb and is connected to the aluminium coating. At the end of the bulb cone, the aluminium coating gives place to a graphite coating (aquadag). The accelerating anode of the electron gun is connected to this graphite coating by spring contacts, with the result that all the space in the tube beyond this anode is free from electric fields. As a result, the charge on the screen is conveyed to the E.H.T. contact via the aluminium coating.

The most important argument in favour of the aluminium backing, however, is the increased output of light. The glowing phosphor does not only emit light from the front of the screen, but also at the back, and this latter component, which is otherwise lost, is now reflected forwards by the aluminium backing. At the usual accelerating voltages of 15 to 18 kV, only very little of this gain is wasted in loss of energy of the electrons in their passage through the aluminium coating. The lower the potential of the accelerating anode, however, the more important is this loss of energy, until it finally becomes predominant. The value of the E.H.T. voltage beneath which the light output becomes less than that of a non-aluminised tube is termed the crossover potential. It is obvious that the crossover potential will increase as the thickness of the aluminium coating increases.

A third advantage of the aluminised tube is the improved contrast. Due to the fact that the screen is slightly spherical, the white areas in the picture illuminate the black areas, resulting in a reduction in contrast. This effect is prevented by the aluminium coating. Unfortunately, the ambient light incident on the screen is reflected to a greater extent, and this reduces the contrast again. In its turn, the use of neutral filter glass improves the contrast (see 3.4).

For the sake of completeness, it should be mentioned here that it is possible to dispense with the ion trap and its associated magnet if the metallic coating is thick enough, (see 2.3.4), and this enables the gun and thus the picture tube to be made shorter.

2.3. The electron gun

The function of the electron gun is to produce a thin beam of electrons which strike the fluorescent screen, causing a luminous spot at the point of impact. In the ideal case, the spot will be circular, whatever its position on the screen, and its diameter will equal the height of the picture divided by the number of lines in a complete raster. Before describing the operation of the gun, we will examine some of the principles on which this is based.

2.3.1. A FEW ELECTRON OPTICAL PRINCIPLES.

There is a far-reaching analogy between the laws governing the path of an electron in an electric field, and the optical laws associated with refraction of rays of light in lenses. For example, a beam of electrons is refracted according to Snell's law at the boundary between two spaces having different potentials, the refractive indices being replaced by the roots of the potentials which exist in the two spaces.

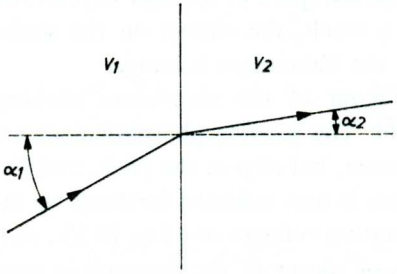

Fig. 2.3.1.1. Refraction of an electron path at the boundary of two spaces at different potentials.

Fig. 2.3.1.1. shows the path of such an electron beam; in this case

$$\sqrt{V_1}\sin\alpha_1 = \sqrt{V_2}\sin\alpha_2$$

so that, if the potential in the right-hand space is higher than the potential in the left-hand space ($V_2 > V_1$), the electron beam is refracted towards the normal. In practice, the transition from one potential to the other will not be abrupt, but gradual, so that the electron beam will be deflected along a flowing curve, instead of being sharply bent.

Fig. 2.3.1.2 shows the path of an electron in a radially symmetrical field. The field is caused by the potential difference between two co-axial cylindrical electrodes. Once again it is assumed that $V_2 > V_1$, so that the first part of the field has a converging action and the second part of the field has a diverging action on the path of the electron.

The two parts of the field thus correspond respectively to a positive lens and a negative lens. The total effect of the system is convergent because the electron passes through the converging part of the field more slowly than

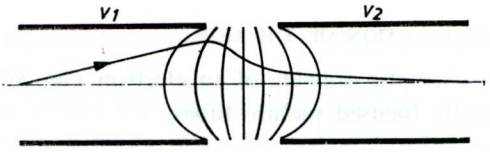

Fig. 2.3.1.2. Path of an electron in a gradually increasing radially symmetrical electric field. This is termed an accelerating lens, because the final velocity of the electrons is greater than their initial velocity. ($V_2 > V_1$)

it does through the diverging part. This is because the velocity of an electron at any point is proportional to the root of the potential at that point, and the lower its velocity, the longer the electron is subjected to electrostatic forces. As the electrons increase in velocity in passing through this electron "lens", it is sometimes termed an accelerating lens.

If the electron enters the field from the opposite direction, it follows the same path in the reverse sense.

As follows from the law of refraction, the degree of convergence, and thus the focal lenght of the electron lens, depends on the ratio of the potentials, and is independent of the charge on and the mass of the charge carriers. Consequently, ions will follow the same paths as electrons, although with a lower velocity.

The so-called unipotential lens is also frequently used. This consists of three cylindrical electrodes, of which the central one is at a much lower potential than the end ones. This means that $V_1 \ll V_2$ in Fig. 2.3.1.3. [1]) The

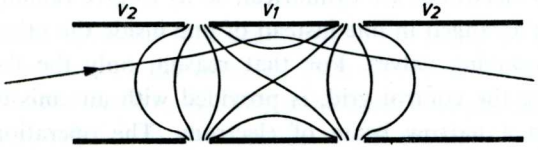

Fig. 2.3.1.3. Path of electrons in a unipotential lens. The electrons enter and leave the lens with the same velocity.

unipotential lens can be regarded as two accelerating lenses placed one after the other, with the first one arranged back to front, so that the field causes the beam of electrons entering the lens to diverge, converge and diverge in succession. The electrons pass through the converging section considerably more slowly than through the other two parts so, that the total effect is still convergent. Here too, the focal lenght depends not only on the geometry of the system, but on the ratio V_2/V_1.

[1]) In fact the name *unipotential lens* applies to this lens only in case the potential of the central electrode equals zero.

2.3.2. The construction of the gun

Fig. 2.3.2.1 is a schematic drawing of an electron gun as used in Philips 110° electrostatically focused picture tubes.

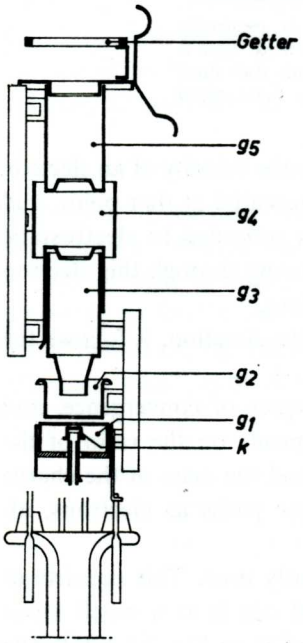

Fig. 2.3.2.1. Longitudinal section of a gun, as used in picture tubes with a diagonal angle of deflection of 110°.

The various electrodes are cylindrical, so as to give radially symmetrical fields, and are arranged in line instead of one inside the other as is usually the case in receiving valves. For that reason, only the flat face of the cathode, facing the control grid, is provided with an emissive coating, so as to produce a narrow beam of electrons. The operation of cathode, control grid and anode is very similar to that of the triode radio valve. The simplest form of the gun is thus the triode, with the accelerating voltage of 12 to 18 kV on g_2, the accelerating anode. In practice, however, there are serious objections to this gun:

a. The E.H.T. cannot be chosen at will, because this voltage determines the grid base.

b. The E.H.T. voltage has an extra effect on the light intensity, because in a triode gun the E.H.T. voltage is one of the factors determining the emission current, while the light intensity is proportional both to the E.H.T. voltage and to the screen current.

For this reason, the tetrode gun has come into general use. In this gun, g_2 serves as a screen grid and is often termed the first anode. The cut-off

voltage can be adjusted by means of the voltage on this anode (in many cases in the region of 300 V).

The grid g_1 is termed the control grid, although in practice the video signal is fed to the cathode with reversed polarity. Amongst other advantages, this gives a greater slope for the picture tube, as illustrated in Fig. 2.3.2.2.

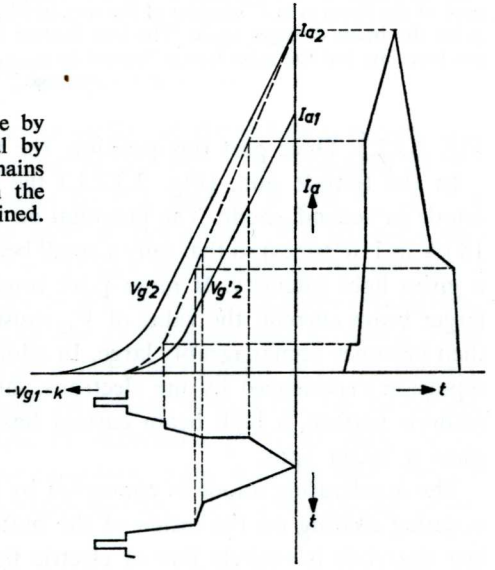

Fig. 2.3.2.2. Driving the picture tube by modulation of the cathode potential by means of the video signal. V_{g1} remains constant. As V_{g2-k} also varies with the video signal, a gain in slope is obtained.

The video signal drives the tube exactly to its full extent with a first anode voltage of V_{g2}' relative to the cathode. With the control voltage on g_1 the beam current varies from 0 to I_{a1}. When the drive is applied to the cathode, the voltage on g_2 relative to the cathode is not constant, but depends on the video signal and varies between V_{g2}' and V_{g2}'' where $V_{g2}'' - V_{g2}'$ is the peak-to-peak value of the video signal. Consequently, the tube is not driven according to the characteristic associated with V_{g2}', but according to the characteristic indicated by the broken line, which lies between those for V_{g2}' and V_{g2}''.

The grids g_1 and g_2 have only a small circular aperture on their axis, and with the difference in their potentials they constitute a strongly convergent lens which, of course, is also affected by the cathode potential. Because of this, the electrons emitted from the cathode, which may have radial as well as axial initial velocities, are converged towards the axis, with the result that the electron beam has its smallest cross-sectional area somewhere between g_1 and g_2. This is the so-called crossover area, indicated by C in

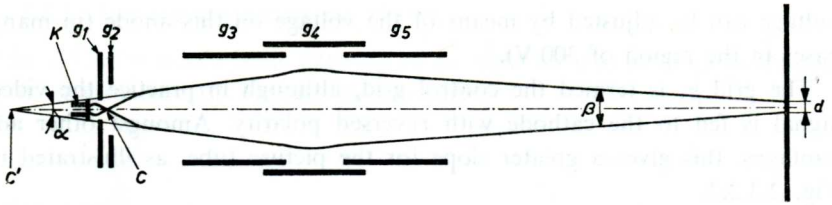

Fig. 2.3.2.3. The completely undeflected electron beam. The smallest cross-sectional area of the beam is at C because of the way in which k, g_1 and g_2 act as a lens. After this point the beam diverges again. The lens formed by g_2 and g_3 gives a certain degree of pre-focusing, but the main lens is formed by g_3, g_4 and g_5. Both g_3 and g_5 are at E.H.T. voltage.

Fig. 2.3.2.3. Once past this position, the beam diverges again.

In the tetrode gun, (Fig. 2.3.2.1.) the electrode g_3 is the accelerating anode or second anode. The potential on this electrode is very high (up to 18 kV in 110° tubes) so that only a small beam current is required to produce a given light intensity. If more peak brightness is to be obtained with a larger beam current, the value of V_{g2} must be increased, but the grid base then becomes unmanageably large. In addition due to the mutual forces of repulsion experienced by the electrons, and because of the larger emissive cathode surface, a high beam current has a larger cross-section and thus gives a larger spot.

The accelerating anode is connected by means of spring contacts to the aquadag coating on the inside of the bulb, so that all the space after the last electrode is entirely free of electric fields.

Electrode g_2, which is at a low potential, and g_3 which is at the high accelerating voltage, constitute another lens, whose effect is to make the beam less divergent, i.e. to pre-focus it to a certain extent. The degree of pre-focusing is determined by the ratio V_{g3}/V_{g2} and can thus be adjusted by means of V_{g2}. The lens $g_2 - g_3$ in fact produces a virtual image of the crossover, as indicated by C' in Fig. 2.3.2.3. In practice, this virtual image lies a few centimetres behind the first grid.

2.3.3. The focusing system

Before a sharp luminous spot appears on the screen, a second focusing operation is required, i.e. the actual focusing brought about by the main lens.

The main lens produces an image of the virtual crossover on the screen, and may be either magnetic or electrostatic. Magnetic focusing will be examined in Chapter 3.2 so that we shall limit ourselves here to electrostatic focusing.

In the latter case, the main lens is obtained by extending the tetrode gun with two more electrodes, i.e. g_4 and g_5. Together with g_3, these electrodes form a unipotential lens. Electrodes g_3 and g_5 are connected together, and are held at the accelerating potential, while V_{g4} is in the region of 0 volt. The formation of an image of the virtual crossover on the screen is governed by Abbe's sine law, which will be familiar from optics, the refractive indices again being replaced by the roots of the respective potentials:

$$c' \sin \alpha \sqrt{V_c} = d \sin \beta \sqrt{V_a}.$$

In this expression, c' is the cross section of the virtual crossover, α is the angle of origin of the electron beam, V_c is the potential at the virtual crossover (in this case equal to V_a), and d, β and V_a are the corresponding quantities for the spot on the screen. The left-hand side of the expression is constant for a constant beam current. We see that d decreases as V_a increases, so we try to get the highest possible accelerating voltage. The spot also decreases in size as the main lens is moved closer to the screen, as this gives a larger β and thus a smaller d. In this respect, a tube with a large maximum angle of deflection thus has the advantage over tubes with a smaller angle of deflection, provided there is no decrease in the distance from the crossover to the focusing lens. Finally, β also becomes larger, and the spot smaller, with a decreasing degree of pre-focusing.

It is not desirable for β to be too large, however, because this means that the cross-sectional area of the beam is too great, both in the main lens and in the magnetic deflection field. The first causes spherical aberration and the second gives rise to more deflection defocusing. Both phenomena will be examined in more detail later on. They can be limited by keeping the beam narrow, and in this case the size of the spot at the edges of the screen is reduced at the expense of a somewhat larger area at the centre, so that more uniformity is obtained.

The curve representing the area of the spot as a function of the focusing voltage is fairly flat over a wide voltage range, (see Fig. 2.3.3.), so that the focusing voltage is not very critical.

To make the gun and thus the picture tube still shorter, the unipotential lens (Fig. 2.3.1.3.) is replaced by the accelerating lens (Fig. 2.3.1.2.) in some types of tube. In addition to its shortness, the advantage of the latter is less spherical aberration. Its disadvantages, on the other hand, are that the correct focusing voltage is more critical, and that it has less depth of focus.

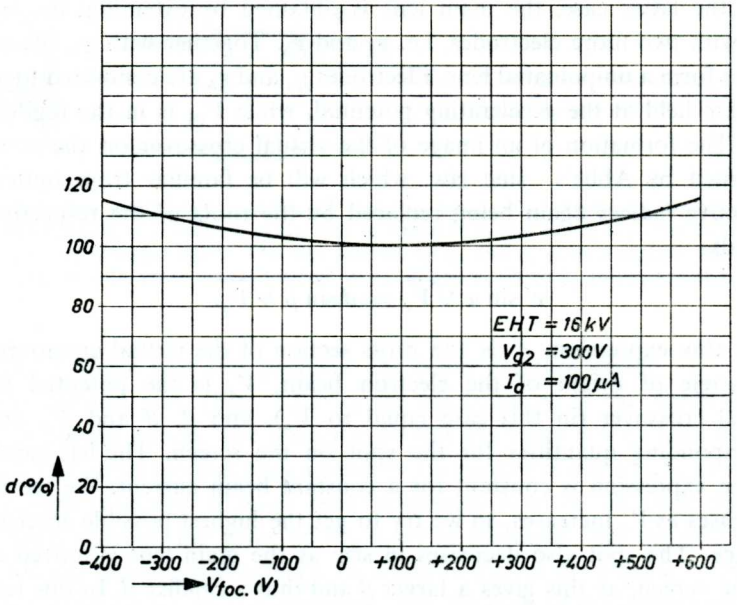

Fig. 2.3.3. The diameter of the spot in an average 110° picture tube with unipotential lens, as a function of the focusing voltage V_{g4}.

2.3.4. The ion trap

There are not only electrons present in the picture tube, but also ions, both positive and negative. The positive ions generally move towards the cathode, from which they are then removed. The negative ions which are produced in the cathode or in its immediate neighbourhood are accelerated like the electrons and finally reach the screen. They are not distributed over the whole of the screen to form a raster, as a result of magnetic deflection, like the electrons are, but always arrive at the centre of the screen. As we shall see in Chapter 4, this is because the deflection of charge-carriers in a magnetic field depends on the ratio of their charge to their mass, in contrast to their deflection in an electric field.

Since this ratio is very much smaller for ions then it is for electrons, the path of the ions remains almost unaffected by the magnetic deflection field, which is dimensioned for deflecting electrons. Consequently the ions always strike the centre of the screen and are responsible for the occurrence of ion burn. The effect is worse in electrostatically focused tubes than in tubes with magnetic focusing because in the former the ion beam is also focused.

There are two possible ways of preventing ion burn. The first is to fit the gun with an ion trap, which can take various forms. In the type illustrated

in Fig. 2.3.4., the anode is bent, so that the electrons are emitted at an angle of approximately 11° to the axis of the tube. The path of the electrons is bent towards the axis of the tube by a magnetic field which is applied in a direction perpendicular to the plane of the drawing. As already mentioned, the magnetic field leaves the path of the ions almost unaffected, so that these are absorbed by the bent anode. In the figure, the continuous line represents the path followed by the electrons, and the broken line indicates the path followed by the ions.

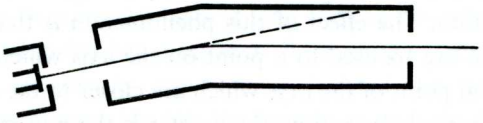

Fig. 2.3.4. Electrode g_3 is bent, so that the electrons are emitted at an angle of about 11° to the axis of the tube. A magnetic field deflects the electrons along the axis (solid line). Any negative ions in the beam carry straight on and are intercepted by g_3 (broken line).

Instead of using an ion trap, ion burn can be prevented by increasing the thickness of the aluminium coating applied to the back of the phosphor screen so that the ions no longer penetrate it. This also means some loss of energy for the electrons, and thus a slightly lower light intensity and a movement of the crossover voltage to higher values (see Chapter 2.2).

The difference in light intensity, however, is scarcely measurable, and is far outweighed by the advantage of omitting the ion trap and associated magnet, with the resulting possibility of a further decrease in the length of the tube. In tubes with 110° deflection, therefore, the ion trap is generally omitted.

The omission of the ion trap does make greater demands on the concentricity of the gun, but against this it is often possible to obtain better spot quality, because we are no longer confronted with distortions caused by the magnetic field of the ion trap.

2.3.5. Distortion of the spot

The spot can be distorted in two ways:

a. it does not remain circular;

b. its diameter increases.

In so far as these distortions are due to the gun, a lack of roundness of the spot is caused by asymmetry of the electrodes, which may be produced to a greater or lesser extent in the manufacture of a gun. Because of this asymmetry, the beam is not uniformly focused, and a slightly oval spot is

produced instead of a round one. Distortion of the focusing electrodes, incorrect distribution of the field of the ion trap magnet, and a deflection field which just penetrates the focusing lens, all have similar effects on the spot.

Variation of the diameter of the spot is caused by modulation defocusing. The beam current varies with the signal voltage applied to the control grid or the cathode. If the grid voltage rises, for example, the beam current increases and with it the cross-section of the crossover and of its image on the screen. A beam of larger cross-section also gives more trouble with spherical aberration. The effect of this phenomenon is that the rays at the edge of the beam are focused to a point on the axis which is nearer to the lens than the focal point of the rays which are closer to the axis. The greater the degree of spherical aberration, the greater is the minimum cross-section of the beam, and thus of the spot. (Fig. 2.3.5.) An increase in V_{g1} also

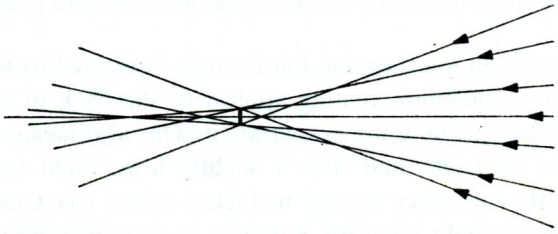

Fig. 2.3.5. Spherical aberration, i.e. the rays at the edge of the beam are focused to a point on the axis which is nearer to the lens than the focal point of the rays which are closer to the axis.

results in a weaker pre-focusing lens, so that the crossover moves in the direction of the focusing lens. The object distance is changed, and so the image on the screen is no longer sharp. To keep this effect as small as possible, the focusing lens must be adjusted for optimum sharpness with the average beam current.

2.4. Screen burn

A dark spot at the centre of the screen is not necessarily an ion burn. It may also be due to burning by electrons inmediately after the television set is switched off.

The filter capacitors which are charged up to the supply voltage have a very short discharge time, so that the voltage on all the electrodes except the final anode will disappear within a few seconds after the set is switched off. The same applies to the line and field deflection.

The tube capacitance, i.e. the capacitance between the conductive alu-

minium and/or aquadag coating inside the tube, and the aquadag coating on the outside of the tube, plus the final anode voltage capacitance, can only be discharged through the tube.

The tube capacitance alone is of the order of 2,000 pF, while the tube presents a resistance of about $10^8\ \Omega$ to the discharge. The time constant is thus very large, so that electrons continue to be attracted to the screen for some time, as the cathode continues to emit electrons for a few minutes after the set is switched off. If the beam current drops to a low value immediately after switching off, because V_{g2} falls to zero almost directly, for example, the tube capacitance takes a long time to discharge, and it is just this which maintains the beam current. Because the deflection fields also collapse almost immediately, the beam is directed onto the centre of the screen, and burns it, even though the current is very small. On the other hand, if the beam current after switching off is large, the tube capacitance becomes discharged and the accelerating voltage drops to zero before the deflection fields have disappeared completely.

One of the most frequently used methods of achieving this is to have a large time constant for the voltage on the first anode, so that this voltage does not disappear immediately.

The first anode voltage is often obtained, via a voltage divider, from the booster voltage in the line timebase circuit (600 to 800 V). If a capacitor is connected to g_2 so that the time constant for the discharge is at least 1 second, V_{g2} remains at a high value long enough to guarantee rapid discharge of the tube capacitance.

If the beam current is zero when the set is switched off, either because the brightness control has been turned off beforehand or because, in the case of negative modulation (black level), the carrier wave is no longer conveying any information, or, in the case of positive modulation, because the transmitter is no longer on the air, the luminous spot still appears at the centre of the screen. In all these cases, the first grid is at a fairly high negative potential relative to the cathode, and some time is necessary for the voltages to collapse far enough for the difference between the grid and cathode potentials to become sufficiently small for the beam current to appear once more. In the meantime, the deflection has also disappeared.

To avoid screen burn in these cases a circuit may be applied which feeds a positive pulse to the first grid at the instant of switching off.

CHAPTER 3

EXTERNAL ACCESSORIES

It is required of a good picture tube that it should produce a sufficiently small circular spot of light exactly at the centre of the screen when no deflection is being applied, but this does not usually happen of its own accord. As already explained, in some types of tube the electron beam does not leave the cathode axially, or else it is electrostatically deflected so as to prevent negative ions from reaching the screen. To bend the electron beam back to the axis an ion-trap magnet is required. After this, the beam is focused, and if this is not done electrostatically, a focusing magnet will be required.

To keep the spot at the centre of the screen when the deflection coils are not operating, or to displace it a certain distance from this point, the tube must be fitted with a centring magnet.

There are a number of diaphragms in the electron gun, and the beam must pass exactly through the centre of all of them. A good ion-trap magnet can take care of this, but, if the gun has no ion trap, an auxiliary centring magnet can be used in the very few cases when the beam requires some correction.

Finally, glass filters are sometimes used to increase the contrast of the picture on the screen.

3.1. **The ion-trap magnet**

With the introduction of tubes with 110° deflection, the ion-trap magnet is doomed to disappear, and so we shall merely look at it in passing.

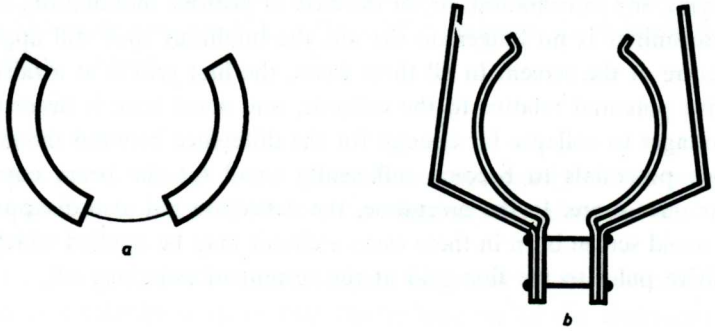

Fig. 3.1. Ion trap magnets. Type *a* consists of two permanent magnets which are pressed against the neck of the tube by means of a metal spring. Type *b* consists of a single magnet provided with pole shoes. In both cases the magnetic field is perpendicular to the axis of the tube.

Figures 3.1*a* and 1*b* show two frequently used types. Type *a* consists of two segments placed diametrically opposite each other round the neck of the tube, while type *b* is a Ticonal magnet fitted with two pole shoes. The latter type is attached to the neck of the tube by a spring of non-magnetic material. Another method which is often employed is to clamp the magnet system directly onto the neck by means of the pole shoes.

Both types of magnet give a permanent field which is not adjustable, and which is perpendicular to the axis of the tube. Part of the field, however, comes behind the cathode and is thus inoperative. The deflection of the electron beam can now be adjusted by moving the magnet system along the neck of the tube.

3.2. **The focusing magnet**

Magnetic focusing has now gone completely out of favour for direct viewing tubes as used in television sets. It is only used where exceptionally high quality is required (e.g. in projection tubes).

Magnetic focusing is performed by means of a radially symmetrical field. The axis of symmetry coincides with the axis of the tube, which is thus also the electron-optical axis of the magnetic lens. The field is produced by a current through a coil, or by permanent magnets.

The focusing power of a magnetic lens is proportional to the square of the field strength, and inversely proportional to the potential difference traversed by the electrons.

For permanent magnetic lenses, a choice is usually made between two possible constructions. The oldest consists of an axially magnetised piece of magnet steel fitted with pole shoes (Fig. 3.2.1) and a movable iron ring which serves to adjust the required field strength. The biggest objection to this construction is the extent of the field along the axis of the tube, because the focusing magnet is placed between the ion-trap magnet and the deflection magnet, so that there is a danger of an axial field extending into the ion trap and also into the deflection system.

If the field strength or the position of the focusing magnet is changed, this also changes the deflection of the electron beam in the ion trap, so that the beam no longer passes through the centre of the last diaphragm. The result may be that the beam is intercepted, or that the picture is displaced on the screen. If the focusing field penetrates into the deflection field, this produces distortion and rotation of the picture.

The other magnet construction consists of two rings magnetised axially in opposite directions, giving a short field. The field strength is adjusted by means of the distance between the rings.

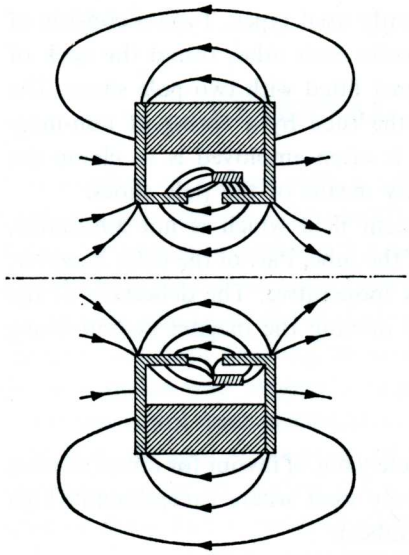

Fig. 3.2.1. Focusing magnet, consisting of an axially magnetized piece of magnet steel fitted with pole shoes, and a movable soft iron ring, by means of which the flux density on the axis can be adjusted.

For television sets, permanent magnets were preferred to focusing coils. They are cheaper, and do not require any power supplies. When a very high field quality is required, as in picture tubes for flying spot scanning, and in projection tubes, focusing coils are used.

Fig. 3.2.2. shows the situation for a field produced by a coil with a soft iron shroud. This construction gives a short magnetic field. The focusing effect of this field can be visualised as follows. Let us consider an electron which enters the field with a velocity having both radial and axial components. (Fig. 3.2.3) At this point, the magnetic field also has radial and axial components. In the case under discussion, both the combination of the axial velocity of the electron v_a and the radial component of the field H_r, and the combination of the radial velocity of the electron v_r and the axial component of the field H_a, exercise a force on the electron which is directed

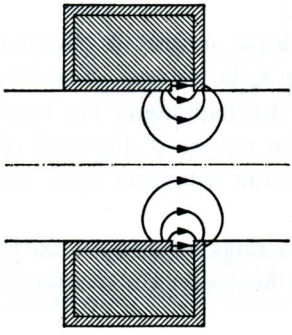

Fig. 3.2.2. Focusing unit consisting of a coil having a soft iron shroud with a gap. The flux density on the axis is adjusted by means of the current through the coil.

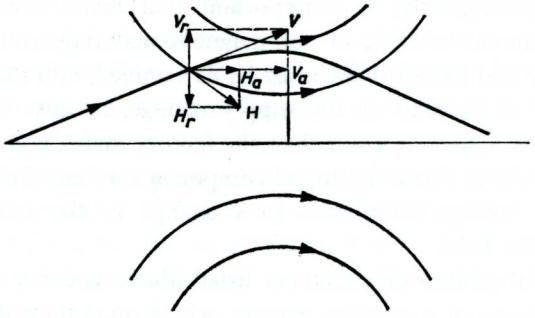

Fig. 3.2.3. Focusing with magnetic lens.

towards the reader. This force imparts a new velocity component (tangential) to the electron which, together with the axial component of the field H_a, results in a force acting towards the axis.

When the electron reaches the second half of the field, the radial component of the field H_r changes in sign. This reduces the tangential velocity component, and thus also the force acting towards the axis. When the electron leaves the field, it still has a small radial velocity component, and it reaches the axis at the screen, provided that the strength of the lens was adjusted to the correct value. As we see, the focusing action is based partly on the tangential component, so that the electrons follow spiral paths.

The magnetic lens has the advantage of a fairly large cross-sectional area, and this reduces the spherical aberration. Nevertheless, it is now quite possible to obtain good spot quality in electrostatically focused picture tubes. Easy adjustment is possible now.

3.3. **The centring magnet**

The centre of the picture should coincide with the centre of the screen. This is not by any means always the case. There are many reasons for this:

a. Tolerances in the construction of the tube.
b. The earth's magnetic field.
c. The line and field flybacks do not occur exactly in the middle of the respective blanking periods.
d. Non-linearity of the picture.
e. The presence of stray fields.
f. Voltage variations.

Stray fields may originate from metal components, from the loudspeaker or perhaps from a transformer. Even very slight fields in the neighbourhood of the electron beam can result in a noticeable displacement of the spot on

the screen. Consequently, it is important that metal components in a television set should be made of non-magnetic material, while the position of loudspeaker and transformers must be determined with the utmost care.

An increase or decrease in the supply voltage, because the customer's mains voltage is higher or lower than the factory mains voltage, or a drop in the supply voltage due to ageing of components, often results in a change in the E.H.T. voltage. This leads to a change in the influence of the earth's magnetic field.

The causes of picture displacement listed above under *a* to *d* are compensated by means of a centring magnet, which must therefore be capable of displacing the picture horizontally as well as vertically, without affecting the quality of the spot.

3.3.1. Tolerances in the construction of the tube

These tolerances refer to:

a. The neck of the tube being sealed on at a slight angle.

b. The gun being mounted at an angle.

c. The gun being displaced parallel to the axis of the tube.

d. The electron beam not leaving the gun along the axis owing to electrodes not being completely radially symmetrical or placed slightly off centre with respect to each other.

Because of the tolerances, an electron beam which passes through all the diaphragms completely centrally can still be at an angle to, or be displaced parallel to, the imaginary axis constructed at the centre of the screen and perpendicular to the screen. Tube manufacturers subject themselves to the necessary limitations, and often publish a maximum distance for each type of tube, through which the focused and undeflected spot can move from the centre of the screen. This displacement may of course be in any direction and is about 10 mm for the 53 cm (21″) tube with 110° deflection and 8 mm for the 43 cm (17″) tube.

3.3.2. The earth's magnetic field

The size of the picture displacement due to the earth's magnetic field depends on:

a. The geographical location of the set.

b. Possible local magnetic screening, such as reinforced concrete.

c. The position of the picture tube in relation to the horizontal component of the local terrestrial magnetic field.

The amount and direction of the picture displacement due to the vertical

component of the earth's field are constant for a given location. The right-hand rule shows at once that the spot will be deflected to the left in the northern hemisphere and to the right in the southern hemisphere. These displacements are a maximum at the poles and practically non-existent at the equator.

The effect of the horizontal component depends on the direction in which the set is pointing. If the axis of the tube coincides with the direction of the horizontal component, i.e. generally in a $N - S$ direction, this component has no effect at all. The effect is a maximum when the set is placed with the tube lying $E - W$.

In this case let us regard the earth's field as having one component along the axis of the tube, and one at right angles to it. The latter is operative during the whole path of the electron from the cathode right up to the screen, and makes the electron move along a circular arc. The error in the calculation of the path is negligible if the electrostatic potential is the same as the accelerating anode potential from the cathode onwards. Let the distance from the cathode to the screen be l, the final angle of deflection φ, the displacement of the spot on the screen y, and the component of the field perpendicular to the path H. In Fig. 3.3.2, H is considered to be

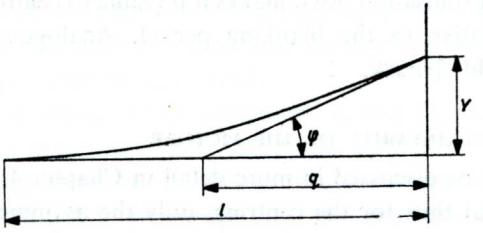

Fig. 3.3.2. The deflection of the electron beam under the influence of the earth's magnetic field, which is considered to be perpendicular to the plane of the drawing.

perpendicular to the plane of the drawing. In Chapter 4.2.1 it is shown that

$$\sin\varphi = \frac{0.3\ H\ l}{\sqrt{V}}.$$

For small angles φ, $q = \frac{1}{2}\ l$ and thus $y = \frac{1}{2}\ l \sin\varphi = \dfrac{0.15\ Hl^2}{\sqrt{V}}$.

For example, for $H = 0.5$ oersted, $V = 16$ kV and $l = 31.7$ cm (approximately the dimension for a 21″ tube with 110° deflection) we have $y = 0.6$ cm.

3.3.3. The line and field flybacks

The line and field flybacks do not usually coincide with the centre of the corresponding blanking periods. The difference in the length of the sections of the blanking periods before and after the flyback depends on the time-base circuits which are employed. If the line period is T sec., then the line blanking period in the C.C.I.R. 625-line system, for example, is $0.18\,T$ sec. and $0.82\,T$ sec are available for the picture information. Most tubes have an aspect ratio of 5 : 4 for the horizontal and vertical dimensions of the screen, while the transmitted picture has a ratio of 4 : 3. If the picture exactly fills the screen in the vertical direction, there is about 6% of over-deflection in the horizontal direction, i.e. the screen is scanned horizontally in $^3/_4 \times {}^5/_4 \times 0.82 = 0.77\,T$ sec. If the vertical over-scan is also 6%, the horizontal or line scan takes place in $0.72\,T$ sec. If the line flyback starts $0.01\,T$ sec after the blanking, for example, and is completed $0.02\,T$ sec. before the end of the blanking period, the centre of the picture will lie to the right of the centre of the screen, at a distance corresponding to $0.005\,T$ sec. This is $\frac{0.005}{0.72}\,W$ mm, where W is the width of the screen in mm. For $W = 490$ mm the displacement is 3.4 mm.

Flywheel synchronisation often makes it possible to centre the line flyback satisfactorily relative to the blanking period. Analogous considerations apply to the field flyback.

3.3.4. The non-linearity of the picture

This subject will be discussed in more detail in Chapter 4. For the picture displacement, and thus for the centring, only the asymmetrical distortion is important. We need only mention here that the vertical non-linear distortion is rather arbitrary, and is difficult to forecast.

The horizontal non-linear distortion which, like the vertical distortion, originates in the timebase circuit and deflection coils, shows itself as an extention of the picture at the left side of the screen and a contraction at the right side. To the extent that this distortion is not eliminated, it means that the picture must be shifted to the right, and if it is over-compensated the picture must be shifted in the opposite direction.

The vertical non-linear distortion is more difficult to control, and often necessitates shifting the picture several millimetres.

3.3.5. Centring

All the above causes of picture displacement combine to give a resultant

displacement. This can be eliminated by means of a centring disc as used with magnetically focused tubes or a centring magnet as used with electrostatically focused tubes.

There are various arrangements of the centring magnet, of which the two most important are:

a. Two discs magnetised diametrically, and capable of being rotated relative to each other. If the like poles coincide, the field at the axis of the tube is a maximum; if the unlike poles coincide, it is a minimum, and should in theory be zero. The direction of displacement of the picture is adjusted by rotating the complete magnetic unit.

b. A rotatable magnet clamped round the neck of the tube by two pole shoes. The magnet is magnetised radially. If the north and south poles are each opposite a pole shoe, the field is a maximum. Here too, the whole unit can be turned round the neck of the tube.

In both cases the centring magnets are placed close to the deflection coils.

3.3.6. The auxiliary centring magnet

This is very occasionally recommended for tubes without an ion trap. When it is present, the ion-trap magnet directs the electron beam exactly through the centres of the diaphragms, so that small shortcomings in the gun are eliminated. If there is no ion-trap, there is no ion-trap magnet, and thus no final adjustment of the beam through the diaphragms, so that the gun tolerances must be very small.

However, the problem is not completely solved by smaller tolerances. In the attempt to make very short tubes with very short necks, the gun is continually coming closer to the deflection field and the centring field. As soon as the centring field penetrates into the gun, there is once more a chance of the beam being intercepted, with the consequent reduction in luminous intensity of the spot. At the same time the focusing deteriorates, because the axis of the beam no longer coincides with that of the focusing lens, resulting in undesirable distortion of the spot. An auxiliary centring magnet (auxiliary beam alignment magnet) is sometimes employed to provide the necessary correction. This little magnet, usually consisting of a single ring magnetised in two diametrically opposite places, with a field strength of about 7 oersteds at the axis, is placed where the ion-trap magnet would otherwise be. The field is adjusted in the same way, i.e. by moving the magnet.

3.4. Filters

There are limits to the maximum contrast, i.e. the relationship between the

whitest and the blackest parts of the picture, which is obtainable with a picture tube. The limit of maximum intensity occurs when the phosphor becomes saturated, i.e. it does not radiate any more light when the beam current or the accelerating voltage are increased further. Before this limit is reached, however, as far as the beam current is concerned, the modulation defocusing becomes so great that the resulting loss in detail contrast is unacceptable. Moreover, the potential of the final anode cannot be increased without limit, because of the resulting danger of flashover in the tube.

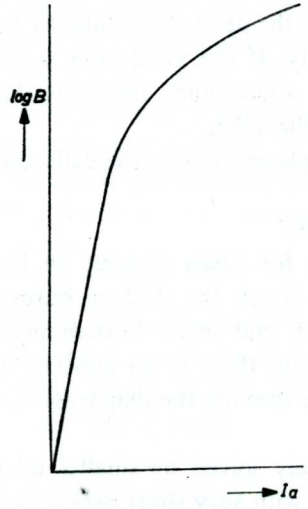

Fig. 3.4.1. The logarithm of the brightness of the screen as a function of the beam current.

Fig. 3.4.1 shows the brightness of the screen as a function of the beam current, for a given accelerating voltage. The brightness scale is logarithmic because the eye reacts logarithmically to visual impressions.

On the other hand, the dark areas cannot be made dark enough, certainly not black, as we should like.

The reasons for this are:

a. Internal reflections in the glass.

b. The ambient light incident on the screen.

As far as internal reflections in the glass are concerned, we must make a distinction between the two cases when the phosphor grains are and are not in optical contact with the glass. Fig. 3.4.2. represents the situation in the first case. The phosphor particles which are struck by the electron beam radiate light in all directions.

The rays of light which penetrate the glass may make any angle with the external face of the glass. In passing through this face they are refracted

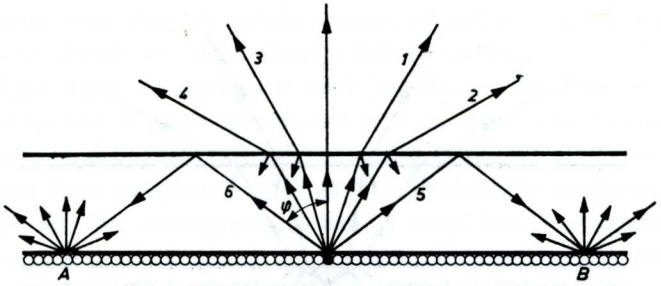

Fig. 3.4.2. Section through the screen of the picture tube. The phosphor grains make optical contact with the glass. An excited phosphor grain radiates light in all directions. The rays of light which penetrate the glass at a smaller angle to the normal than the critical angle (φ), are only reflected to a very slight extent, and produce a bright circular area of diameter *A–B* round the spot. Rays which make a greater angle than (φ) to the normal, are totally reflected and produce halo rings.

away from the normal towards the glass (rays 1 to 4), in accordance with Snell's law (the refractive index for glass is about 1.5) while a small proportion (about 4%) are reflected. These reflected rays illuminate the surrounding phosphor grains, producing a more or less bright circular area round the spot.

The amount of light which is reflected only increases slightly with increasing angle of incidence until the critical angle is reached or exceeded, when all the light is reflected. (rays 5 and 6). The totally reflected rays may strike the phosphor grains which are in optical contact with the glass, and illuminate them so that a bright ring is formed round the spot, enclosing the above-mentioned circular area. On the other hand, these rays may be reflected again at the internal glass face, producing a second ring and perhaps further rings; the latter decrease rapidly in intensity. These rings constitute the so-called halo effect.

Fig. 3.4.3 illustrates the situation when the phosphor grains are not in optical contact with the glass. The crystals which are struck by the electron beam again radiate light in all directions but, in accordance with Snell's law, the rays which penetrate the glass are those whose angle to the glass face is less than the critical angle. As a result, this also applies at the external glass face, so that the internal reflections at the external glass face may produce an illuminated circular area round the spot, as described above, but not halo rings.

In practice, both cases occur in picture tubes.

The effects of internal reflections in the glass are limited quite considerably by the use of a neutral filter glass for the screen, instead of clear

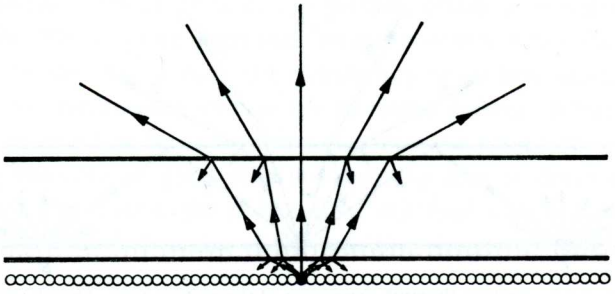

Fig. 3.4.3. The phosphor grains do not make optical contact with the glass. The rays of light which penetrate the glass from excited phosphor grains are always at a smaller angle to the normal than the critical angle. This means that a bright circular area can be produced, but no halo rings round the spot.

glass. The rays of light which cause these effects have to pass through the glass three times, and that at an oblique angle, before they reach the viewer's eye, so that they are attenuated several times more than the desired direct rays. In practice, the absorption of the glass is about 25%.

The second case is that of incident ambient light, much of which is reflected from the tube. The contrast is closely associated with the number of contrast steps which the eye can just distinguish. If it has just to distinguish two grey shades in the picture, the difference in brightness must be a certain minimum. This minimum depends on the absolute brightness of the areas being observed. It is possible to define a more or less constant threshold value for the eye: $T = \frac{B + \triangle B}{B}$. This means that in the darker areas, where B is low, $\triangle B$ also has a low value, or in other words, that the threshold values lie much closer together than in the high lights. It should be noted, however, that the value of T is not absolutely constant, but is determined by the degree of adaptation of the eye, amongst other things. In turn, the degree of adaptation depends on the average brightness of the screen and of the ambient light.

The ambient light blurs the contrast steps in the dark areas of the picture, so that the gradation is incorrect. To correct this, the basic brightness, i.e. the brightness of the darkest areas occuring in the picture, must be increased to that of the reflected ambient light. This, however, considerably reduces the maximum number of contrast stages and thus the contrast as well. The greatest contrast is obtained by viewing the picture in complete darkness, but this is very inadvisable, because it has a painful effect on

the eyes after some time. A certain amount of ambient light is necessary, but the lamp should not shine directly into the screen.

In daylight, when the contrast is often insufficient, the situation is more difficult to control. A glass filter placed in front of the screen compels the ambient light to pass twice through the screen as against only once for the desired light from the picture. This method reduces the brightness of the top whites, but this corresponds to only a small loss in contrast stages, while the gain in the dark areas is much greater, because the basic brightness can be lowered.

Disadvantages of these grey filters are:

a. The picture appears less sunny. There is a tendency to increase the maximum brightness, with a consequent increase in the average and peak beam currents, which may result in defocusing of the spot. For this reason, the transmission factor of the filter must not be too small.

b. The filter is usually fixed permanently in position, although each type of ambient lighting really needs its own transmission factor for optimum results. In artificial light, the filter may be dispensed with completely; nevertheless, a less sunny picture has to be accepted.

In place of the neutral grey filters, selective filters are sometimes used, i.e. the filter effect is a function of the wavelength of the incident light. The transmission characteristic of the selective filter is adapted to the emission characteristic of the picture tube, which shows maximum in the blue and in the yellow. As the eye is also selective, however, the effect of a selective filter is hardly any better than that of a neutral filter.

CHAPTER 4

DEFLECTION OF THE ELECTRON BEAM

4.1. Deflection of the Electron Beam

Although electrostatic deflection of the electron beam is used in oscilloscope tubes, magnetic deflection has been found to be more suitable for the television picture tube. Before discussing the coils which have to provide the correct magnetic fields, we will examine the reasons for this choice.

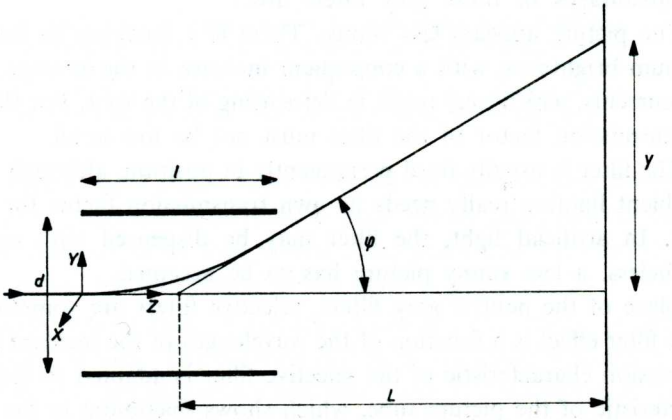

Fig. 4.1.1. The deflection of an electron beam in a uniform electric field. The path of the electron is a parabola.

4.1.1. Electrostatic deflection

In Fig. 4.1.1, which represents the deflection of an electron beam by one set of deflection plates,

d = distance between the plates,

l = length of the plates,

L = distance from the centre of the plates to the screen,

y = displacement of the spot on the screen,

φ = the angle of deflection of the electron beam.

In addition, V_d is the deflecting voltage between the plates and V_a is the accelerating voltage acting on the electrons.

To simplify the calculation, the field is assumed to be uniform between the plates and zero outside them. The axes of co-ordinates originate from that point on the axis of the tube where the field begins. The z axis coincides with the axis of the tube and the y axis with the direction of the field. The

velocity v, with which the electron enters the field along the axis of the tube is $v = \dfrac{dz}{dt}$.

In the field the electron experiences a force

$$F = \frac{e\,V_d}{d} = m\frac{d^2y}{dt^2}\,.$$

where e and m are respectively the charge and the mass of an electron. The equation for the path of the electrons between the plates

$$y = \tfrac{1}{2}\,\frac{e}{m}\,\frac{V_d}{d}\,\frac{z^2}{v}\,.$$

follows from these two equations and from the initial conditions that $\dfrac{dy}{dt} = 0$ and $y = 0$ for $t = 0$.

If we neglect the threshold potential of the electrons relative to the accelerating voltage, the kinetic energy of the electrons is $\frac{1}{2}mv^2 = eV_a$.

From $\tan\varphi = \left(\dfrac{dy}{dz}\right)_{z=l} = \tfrac{1}{2}\,\dfrac{V_d}{V_a}\,\dfrac{l}{d}$ and $y_{z=l} = \tfrac{1}{4}\,\dfrac{V_d}{V_a}\,\dfrac{l^2}{d} = \tfrac{1}{2}\,l\tan\varphi$

it follows that the deflection of the spot on the screen is

$$y = \tfrac{1}{2}\,\frac{V_d}{V_a}\,\frac{l\;L}{d}$$

and that the deflection sensitivity is:

$$\frac{y}{V_d} = \frac{l\;L}{2\,V_a\;d}\,.$$

The deflection sensitivity is thus independent of the specific charge and mass of the charge-carriers and inversely proportional to the E.H.T. voltage.

There is a limit to the deflection sensitivity, because the quantities which determine it cannot be chosen at will. If l is too large or d is too small, the electron beam is intercepted by the deflection plates at a particular value of φ. A large value of L makes the tube unmanageably large, and finally a small value of V_a reduces the brightness of the screen.

4.1.2. Magnetic deflection

To calculate the electron path in a magnetic field, this field is also assumed to be uniform, to start and end abruptly, and to be of length l. In Fig. 4.1.2

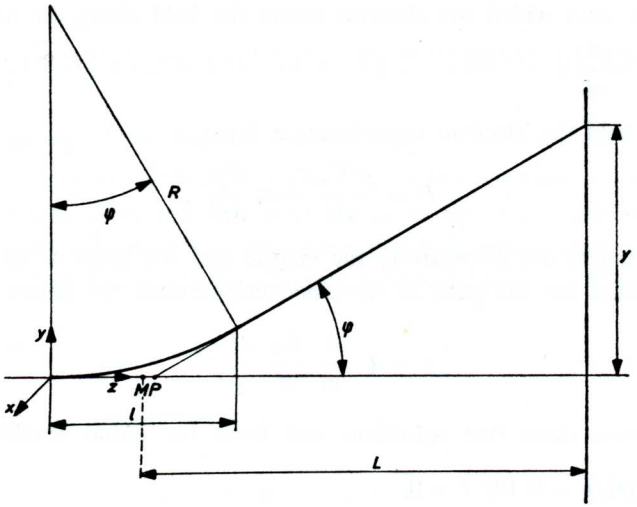

Fig. 4.1.2. The deflection of the electron beam in a uniform magnetic field. The path of the electron is a circle of radius R.

the field is perpendicular to the plane of the drawing, and is directed towards the reader. Axes of co-ordinates again originate at the beginning of the field.

The magnetic field is acting parallel to the x-axis, and the electrons which enter it along the z-axis with a velocity v experience a force

$$m \frac{\mathrm{d}^2 y}{\mathrm{d}t^2} = e \frac{\mathrm{d}z}{\mathrm{d}t} B \qquad (4.1.2.1.)$$

in the y direction. B represents the magnetic induction. The force acting on the electrons gives them a velocity component in the y direction which, with the field, results in a force operating in the z direction:

$$m \frac{\mathrm{d}^2 z}{\mathrm{d}t^2} = -e \frac{\mathrm{d}y}{\mathrm{d}t} B \qquad (4.1.2.2.)$$

Substituting (4.1.2.2) in the equation obtained by differentiation of (4.1.2.1) we have

$$\frac{\mathrm{d}^3 y}{\mathrm{d}t^3} + a^2 \frac{\mathrm{d}y}{\mathrm{d}t} = 0 \ .$$

where $a = eB/m$.

The general solution for this differential equation is

$$y = C_1 + C_2 \mathrm{e}^{\mathrm{j}at} + C_3 \mathrm{e}^{-\mathrm{j}at}.$$

Introduction of the initial conditions $y = z = 0$, $\frac{dy}{dt} = 0$ and $\frac{dz}{dt} = v$ for $t = 0$ finally gives

$$y = \frac{mv}{eB}\left[1 - \cos\frac{e}{m} Bt\right].$$

Since $z = 0$ for $t = 0$, it follows from this equation and (4.1.2.1) that

$$z = \frac{mv}{eB} \sin\frac{e}{m} Bt.$$

Elimination of t gives the equation for the path of the electron in the magnetic field.

$$\left[y - \frac{mv}{eB}\right]^2 + z^2 = \left[\frac{mv}{eB}\right]^2 \qquad (4.1.2.3.)$$

This is the equation of a circle with radius $R = mv/eB$ with its centre on the y axis.

The electrons leave the field along a tangent to the circle. This tangent forms an angle φ – the angle of deflection – with the axis of the tube, which is given by

$$\tan\varphi = \frac{l}{\sqrt{R^2 - l^2}}$$

as can be seen from Fig. 4.1.2.

The point where the tangent cuts the axis is termed the deflection point. For various considerations associated with deflection it is often assumed for the sake of simplicity that the electrons follow the axis of the tube until they reach the deflection point (P in the figure) and that they suddenly turn there to continue on their way at an angle φ to the axis.

It is a simple matter to deduce from Fig. 4.1.2 that the distance from the deflection point to the centre of the field is given by

$$PM = l\frac{1 - \cos\varphi}{2(1 + \cos\varphi).}$$

For $\varphi = 0$, i.e. when there is no deflection, P coincides with M, and with increasing deflection the deflection point moves towards the screen. For example, when $\varphi = 45°$ (the maximum deflection in a 90° picture tube) the displacement of P is equal to 0.086 l. As $l \ll L$, no serious error is made if it is assumed that the deflection point P coincides with the centre of the magnetic field. In this case the expression

$$y = L\tan\varphi = \frac{l\ L}{\sqrt{R^2 - l^2}}.$$

can be taken as a good approximation for the displacement of the spot on the screen.

The quantity R depends, amongst other things, on the velocity v of the electrons. This can be eliminated by means of the kinetic energy equation

$$\tfrac{1}{2} mv^2 = eV_a.$$

For small angles of deflection we also have $l^2 \ll R^2$ so that in this case

$$y \approx \sqrt{\frac{e}{2\,m\,V_a}}\, L\, l\, B\ .$$

The deflection in a magnetic field thus depends on the charge/mass ratio of the charge carriers, a fact which has been turned to advantage in the ion trap. In addition, the displacement on the screen is inversely proportional to the root of the accelerating voltage and directly proportional to the magnetic field strength. These conclusions are only approximately correct for small angles of deviation.

That the deflection sensitivity is again confined within certain limits can be seen in the same way as for the electrostatic deflection.

4.1.3. Comparison of magnetic deflection with electrostatic deflection

In deducing the energies for deflection it is assumed that the fields in question are uniform and occupy only the space inside the coil or between the plates for magnetic and electrostatic deflection respectively. Suppose that the magnetic field is produced by a current i amperes flowing through a coil with a self inductance L henrys. The amount of magnetic energy stored in the field is thus $W_m = \tfrac{1}{2} Li^2$.

If the coil has a cross-sectional area S (m^2) a length l (m) and if the number of turns is n, we have $L = \dfrac{\mu n^2 S}{l}$ where μ is the permeability.

As the field strength $H = \dfrac{ni}{l}$, the expression for the magnetic field energy becomes

$$W_m = \tfrac{1}{2}\,\mu\, H^2\, S\, l \text{ or } W_m = \tfrac{1}{2}\,\frac{B^2}{\mu}\ V\ .$$

where $V = Sl$, the volume occupied by the field.

The magnetic energy per unit volume is thus

$$W_m = \tfrac{1}{2}\frac{B^2}{\mu} \qquad (4.1.3.1.)$$

We assume that the electric field is caused by a potential difference V between the plates of a capacitor. If the plates are parallel, each of surface area S (m^2), and the distance between them is d (m), the capacitance of the capacitor is $C = \dfrac{\varepsilon S}{d}$ where ε is the relative permittivity of the medium in which the field is situated.

The energy stored in the field of the capacitor is now

$$\tfrac{1}{2} C V^2 = \tfrac{1}{2} \frac{\varepsilon S}{d} \; E^2 \; d^2 = \varepsilon \frac{E^2}{2} \times \text{volume.}$$

In this expression E is the field strength between the plates so that $V = Ed$ while the volume of the field is $S\,d$.

The electric energy per unit volume is thus

$$W_e = \tfrac{1}{2}\varepsilon E^2.$$

For equal energies per unit volume, the ratio of the magnetic flux density to the electric field strength is

$$\frac{B}{E} = \sqrt{\mu\varepsilon} = \frac{1}{c} \; .$$

where c is the velocity of light. The force experienced by an electron in this case will not be the same for the magnetic field as for the electric field. The ratio of the two forces is

$$\frac{F_m}{F_e} = \frac{e \; v \; B}{e \; E} = \frac{v}{c} \; .$$

If the accelerating voltage acting on the electron is 18 kV for example

$$\frac{v}{c} = \sqrt{\frac{2eV}{mc^2}} = 0.27.$$

In this case, then, the electrostatic force is nearly four times as large as the magnetic force. In addition, for a given diameter of the neck of the picture tube, the volume of the magnetic field is much greater than that of the electric field.

This is because the coils for magnetic deflection are placed outside the neck of the tube while the plates for electrostatic deflection are situated inside the neck. As a result, the amount of energy required to produce a given deflection magnetically is many times the amount of energy required to produce it electrostatically.

However, there are various considerations which make magnetic deflection

an attractive choice for television tubes, so that electrostatic deflection is not used for this purpose:

1. For electrostatic deflection, the necessary maximum deflection voltage is of the same order of magnitude as the final anode voltage (about 18 kV). The production of such high sawtooth voltages and possibly the recovery of the energy at the end of the scan make very heavy demands on circuit techniques.

With the usual coils, magnetic deflection requires sawtooth currents with peak values of the order of one ampere. It is easier to produce these currents, and a considerable portion of the energy which is stored in the field at the end of the scan can be recovered. This is only worthwhile, however, for the horizontal deflection, which occurs 10,000 to 20,000 times per second, depending on the particular television system; vertical deflection occurs only 50 or 60 times per second.

2. With electrostatic deflection of the beam, the spot suffers seriously from distortion, losing its focus and its circularity. Astigmatism occurs. This distortion is proportional to the square of the tangent of the angle of deflection, and results principally from the fact that, in electrostatic deflection, the electrons do not all pass through the same difference of potential. This can easily be seen with the aid of Fig. 4.1.3. in which the

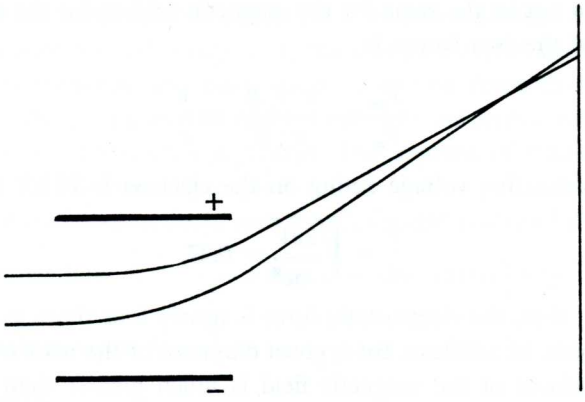

Fig. 4.1.3. Astigmatism due to the deflection of an electron beam in an electric field.

upper plate is positively charged relative to the lower plate. When they reach the field, the electrons at the top of the beam have already traversed a slightly greater potential difference, and have thus attained a greater velocity, than the electrons lower down in the beam. As a result, the former

are less sensitive to deflection, so that the cross-section of the beam, and therefore the spot, loses its circular shape. Consequently the picture becomes blurred at the edges of the screen. Very large maximum angles of deflection are now used in picture tubes so as to avoid having to have an unmanageably long tube to obtain a large screen, and if electrostatic deflection is employed, a heavy loss of focus at the edges of the screen has to be accepted, unless diaphragms are employed to produce a narrow beam. The latter solution, however, is associated with a loss in intensity which is unacceptable for television.

Magnetic deflection also causes distortion of the spot proportional to the square of the tangent of the angle of deflection, but in this case the proportionality factor is many times smaller. In addition, astigmatism can be kept within acceptable limits by suitable formation of the field, even for very large angles of deflection.

3. The magnetic picture tube is cheaper. If the tube in a receiver has to be replaced it is not necessary to replace the deflection system as well, while any displacement of the picture can be corrected by rotating the deflection coil unit. Electrostatic deflection is preferred for oscilloscope tubes because the deflecting plates draw almost no current from the circuit on which measurements are being made, and the displacement of the spot on the screen depends almost solely on the instantaneous voltage applied between the deflecting plates, and is independent of the frequency of the input signal, provided the frequency is not too high. Against this, magnetic deflection is very dependent on current and frequency. There is no objection to this in television applications, because the currents which are applied are constant in form and in frequency of repetition, so that they can be taken into account in the design of the circuits.

4.2. Geometrical distortion of the picture

The picture on the television screen must be a faithful reproduction of the scene which is being transmitted. The raster must be rectangular when viewed from a point some distance away, in line with the axis of the tube. The long sides of the rectangle must be accurately horizontal, and the picture must possess the same linear relationships as the original. Various types of distortion do occur, however, and in general these are due to one or more of the following causes.

1. The flatness of the screen. This may lead to non-linear distortion, and to pincushion or barrel distortion of the picture.

2. For some reason the electron beam does not enter the deflection field along the axis of symmetry. This may lead to sagging of the original straight

lines, non-linearity, keystone distortion of the raster, or a combination of these.

3. Penetration of an axial magnetic field into the radial deflection field. In practice, this can only occur with one of the decreasing number of tubes with magnetic focusing which are still in use, and causes tilting of the picture.

4. Electrical imperfections in the timebase circuits, which have to provide the correct currents through the deflection coils. Departures from the correct current form are visible on the screen as asymmetric non-linear distortions, and have nothing to do with the picture tube and the magnetic deflection system as such.

4.2.1. Symmetrical non-linear distortion

This picture fault is also called ladder distortion and can occur when the electron beam is being deflected by only one of the deflection fields. As already mentioned, it is caused by the flatness of the screen. In section 4.1.2. it is shown that in a uniform magnetic field which begins and ends abruptly, the electron beam is deflected along a circular path of radius $R = \frac{mv}{eH}$. Fig. 4.1.2 also shows that $\sin\varphi = \frac{l}{R}$ so that $\sin\varphi$ must equal $\frac{leH}{mv}$. Using the expression $\frac{1}{2}mv^2 = eV_a$ it is possible to eliminate v so that, after substitution of $e = 1.6 \times 10^{-19}$ coulomb and $m = 9.11 \times 10^{-31}$ kg, we have: $\sin\varphi = \frac{0.3\,lH}{\sqrt{V_a}}$.

In this expression l must be in cm, H in oersteds and V_a in volts.

If the screen is part of a sphere with the deflection point P as centre and L (= distance from P to the screen) as radius, (see Fig. 4.2.1.1) the displacement y of the spot on the screen equals $L \sin\varphi$ and is thus proportional to the field strength H. If the latter varies uniformly with time, the spot moves over the screen at constant velocity, and there is no question of non-linearity. For a flat screen, the displacement of the spot on the screen is $y_2 = L \tan\varphi$ and thus increases more than proportionally with H. If we again assume a linear relationship between the field strength and the time, a pattern of originally equidistant lines appears as in Fig. 4.2.1.2. The picture is compressed at the centre and extended at the edges.

In practice, the screen of a picture tube is not flat, but has a radius equal to several times L, so that the ladder distortion would be less than for a flat screen, but still quite serious. This distortion can be prevented, either

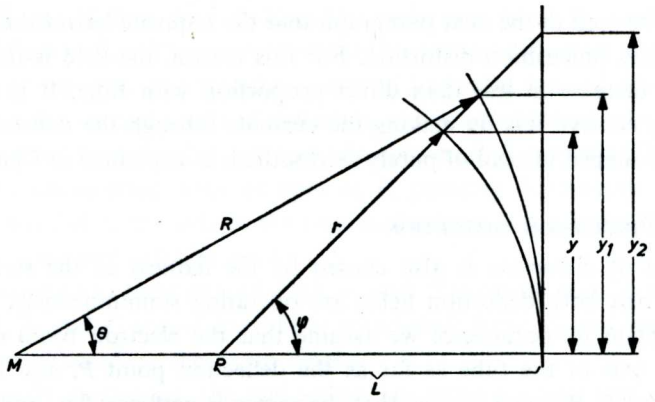

Fig. 4.2.1.1. The displacement of the spot on the screen with an angle of deflection φ for a convex screen of radius $r = L$, a flatter screen with $R > L$ and an absolutely flat screen.

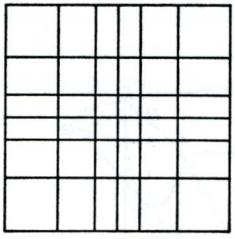

Fig. 4.2.1.2. Symmetrical non-linear distortion of originally equidistant lines.

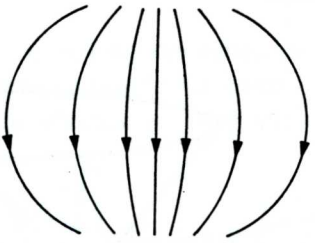

Fig. 4.2.1.3. Cross-section perpendicular to the axis of a barrel-shaped field for horizontal deflection of the electron beam. The field decreases in strength towards the edges.

by making the deflection field non-uniform, or by arranging for the field strength to increase less than proportionally with time.

If the first solution is chosen, the field must be a maximum on the axis, and must decrease in strength towards the edge in the direction of deflection. This can be obtained by means of a barrel-shaped field. Fig. 4.2.1.3 shows a cross-section perpendicular to the axis of such a field for horizontal deflection only. The electrons pass through the field with a velocity such that the field may be regarded as stationary for each electron individually. The electrons which enter the field at the instant when it has just reached its maximum value are sharply deflected, and quickly arrive at the edge of the field. Because the field is not so strong at the edges as at the axis, the angle of deflection for these electrons increases less quickly than it would in a uniform field. In this way, the spot can be given a constant velocity across the screen.

It will be seen in the next paragraph that the requisite barrel-shaped field causes extra pincushion distortion. For this reason, the field is in practice made to increase in less than direct proportion with time. It is a simple matter to achieve this by making the currents through the deflection coils slightly *S*-shaped instead of purely sawtoothed, as explained in Chapter 7.5.

4.2.2. Pincushion distortion

This type of distortion is also caused by the flatness of the screen, and occurs when both deflection fields are operating simultaneously.

To explain its occurrence we assume that the electron beam coincides with the axis of the tube as far as the deflection point *P*, and that it is deflected at *P*. We also assume that the screen is perfectly flat, and that the vertical angle of deflection φ is constant. For a uniform deflection field this means that the current through the field deflection coils must be kept constant.

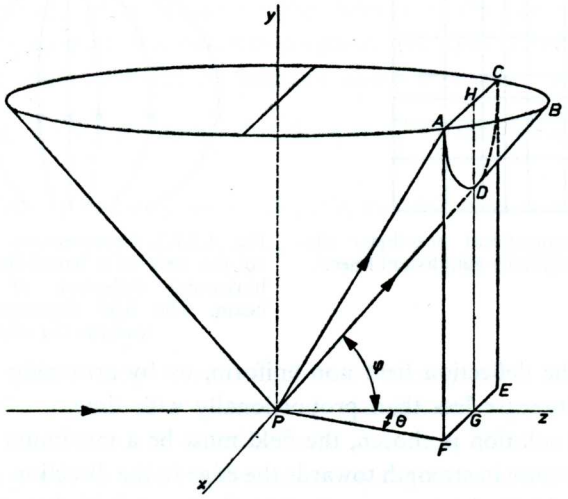

Fig. 4.2.2.1. Deflection of the electron beam with the field being varied for horizontal deflection, and with a constant vertical angle of deflection (φ). The beam describes a section of the surface of a cone and strikes a flat screen *A C E F* along an arc of a hyperbola *A D C*.

Fig. 4.2.2.1 shows only the top part of the screen (*ACEF*). If there is no horizontal deflection the electron beam strikes the screen at *D*, directly above the centre of the screen *G*. If the beam is also deflected in the horizontal direction, for example through an angle Θ towards us, it strikes the screen at *A*. This point is higher than *D*, or in other words $AF > DG$,

because it lies further than D from the deflection point P, owing to the flatness of the screen. The same applies to horizontal deflection to the other side (C), so that the spot describes a curved line ADC instead of a straight line. Since the vertical angle of deflection φ is kept constant, the electron beam describes a sector of the surface of a cone from P onwards. Fig. 4.2.2.1 shows the whole cone, with its apex at P, pointing downwards. The flat screen is parallel to the axis of the cone and intersects it along a hyperbola of which the curve ADC is part.

If the screen had been part of a sphere with P as centre and PG as radius, points A, D and C would have been equidistant from P, and would thus have been situated at the same height.

As already mentioned, the real screen lies between these two extremes. Instead of a straight line we have a line which is curved, although not an arc of a hyperbola; a rectangle becomes distorted to a figure with the shape of a pincushion and a pattern of originally equidistant lines takes on the form shown in Fig. 4.2.2.2.

Pincushion distortion can be countered by making the deflection field itself cushion-shaped. The field then increases towards the edges in the direction of deflection. Fig. 4.2.2.3 shows the situation occuring when both

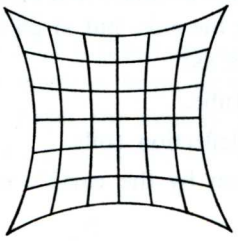

Fig. 4.2.2.2. Pincushion distortion of the raster on a relatively flat screen, due to uniform deflection fields.

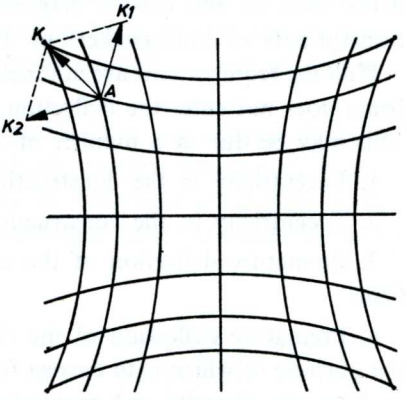

Fig. 4.2.2.3. Cushion shaped deflection fields in horizontal and vertical direction, which exercise forces K_1 and K_2 respectively on an electron. K is the resultant force.

the line and field deflection fields are a maximum, i.e. the electrons experience a resultant force in the diagonal direction, towards the top left-hand corner of the drawing, if their axial velocity is directed towards the plane of the drawing. An electron which has reached point A there ex-

periences a force K_1 due to the field deflection field, and a force K_2 due to the line deflection field. Because the fields are cushion-shaped, the two forces make an obtuse angle with each other so that the resultant force K is smaller than it would be if they were perpendicular to each other. In other words, the electrons are deflected less strongly in the diagonal direction than they would be in uniform magnetic fields. The opposite is true for purely horizontal or vertical deflections because the fields then increase toward the edges in the direction of deflection. The two effects together restore the pincushion raster to its rectangular shape, but the latter increases the non-linear distortion which in its turn can be countered by making the currents through the deflecting coils vary in time according to an *S*-shaped curve, as we saw in the previous section.

4.2.3. Faults due to decentring of the electron beam

In the ideal case, the electron beam is deflected in such a way that a completely rectangular raster, free from non-linearity, is produced on the screen.

It is obvious that this is only possible if not only the tube but also the deflection coils meet the highest requirements, and if external interfering fields such as the earth's magnetic field or the fields originating from transformers or loudspeakers in the television set are excluded.

If all the requirements are not met, there is quite a chance that the electron beam does not enter the deflection field along the axis, but at an angle. This may be due to a number of causes, such as:

1. Eccentricity in the construction of the tube.
2. Eccentricity in the construction of the deflection coils.
3. Premature deflection of the electron beam by the earth's magnetic field.
4. Premature deflection of the electron beam by the centring magnet, the purpose of which is to correct for imperfections in the timebase circuit, such as non-linearity and eccentricity of the field and line flybacks in the respective blanking periods.

The types of distortion which may result from the decentring of the electron beam, i.e. non-linearity, bending of originally straight lines, and keystone distortion, are shown in Fig. 4.2.3.

These types of distortion cannot be caused by decentring of the electron beam alone, but also require the deflection field to be non-uniform. Non-linearity is caused by a change in field strength in the direction of deflection, together with decentring of the beam, while the other picture faults are

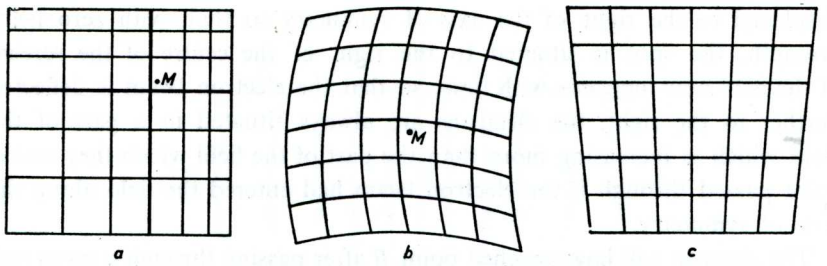

Fig. 4.2.3. Picture distortions due to the electron beam entering the deflection field at an angle.
a. Asymmetrical non-linearity, *b*. Asymmetrical pincushion distortion, *c*. Keystone distortion.

also influenced by the variation of the field along the axis as a function of the z co-ordinate.

Exact mathematical analysis of these picture faults is particularly cumbersome, and would take us too far from our subject. For this reason, we will content ourselves with indicating the origin of the faults.

4.2.3.1. *Asymmetrical non-linearity*

If the field is not uniform in planes perpendicular to the axis of symmetry asymmetrical non-linearity occurs either in the horizontal or vertical direction in case the beam is off centre in the horizontal or vertical direction respectively.

Fig. 4.2.3.1.1. illustrates a cushion-shaped field in the vertical direction, with the electron beam directed towards the reader. Because of its pincushion shape, the field in the direction of deflection is stronger at the edges than it is at the centre. The undeflected beam is taken as being

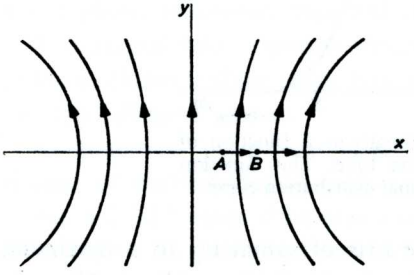

Fig. 4.2.3.1.1. Cross section perpendicular to the axis of a cushion-shaped field for horizontal deflection of the electron beam. The field increases in strength towards the edges.

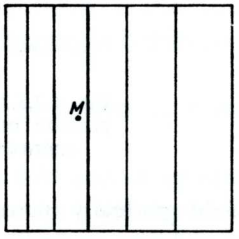

Fig. 4.2.3.1.2. Horizontal asymmetrical non-linearity.

displaced to the right of the axis of symmetry so that, with zero field-strength, the spot is situated to the right of the centre of the screen. If the field now increases with time, so that the electron beam is deflected further to the right, the electrons are always situated in a part of the field which is increasing more than the part of the field which they would have passed through if the electron beam had entered the field along the axis of symmetry.

The electron will have reached point *B* after passing through a given section of the field, instead of point *A*. At point *B* the force acting towards the right is greater, so that the displacement of the spot on the screen is also greater. If the beam is deflected to the left the opposite effect occurs, so that a system of originally equidistant vertical lines is reproduced on the screen as in Fig. 4.2.3.1.2. The point *M* is the centre of the screen. Finally, Fig. 4.2.3. *a* shows the situation when the displacement of the spot is directed to the bottom left-hand corner, both deflection fields being cushion-shaped.

4.2.3.2. *Asymmetrical pincushion distortion*

This is the second effect which may occur if the electron beam does not enter the field along the axis of symmetry. The bending of originally straight lines is in the first place due to the fact that the magnetic deflection field can neither commence nor finish abruptly. The deflection coils used in practice cause a distribution of field along the axis of symmetry, which shows great similarity with the normal statistical distribution curve. (Fig. 4.2.3.2.1). As

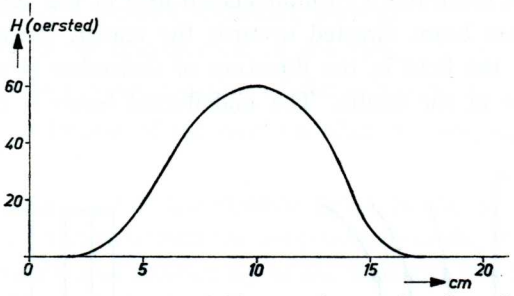

Fig. 4.2.3.2.1. The field strength as a function of position on the axis of the tube. This function approximates to the normal distribution curve.

the field gradually increases along the axis of symmetry to a maximum value, and then gradually decreases again, the distribution of lines of force in the field which is responsible for horizontal deflection of the electron beam towards the reader is approximately as shown in Fig. 4.2.3.2.2. The further the lines of force are from the deflection point *P*, the more curved they are,

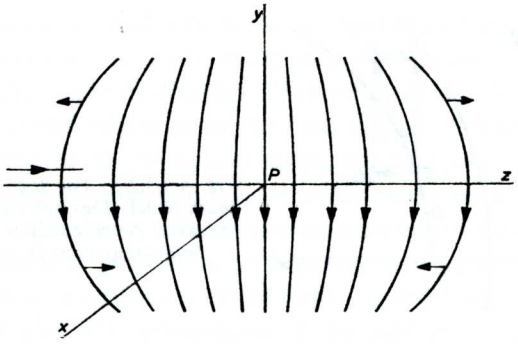

Fig. 4.2.3.2.2. Cross section through the axis of the field for horizontal deflection of the electron beam.

i.e. at all points outside the $x - z$ plane, the field has an axial component. The field possesses mirror symmetry with respect to the $x - y$ plane and mirror symmetry with change of direction with respect to the $x - z$ plane. The result is that electrons which enter the field from the left-hand side, and which already have a vertical upward displacement, not only experience the normal force directed towards us, but are also subject to a vertical force due to the axial component of the field and to the velocity which they have acquired in the x direction. This force is directed upwards in the first half of the field and downwards in the second half. Since the x velocity component in the first half of the field is still slight in comparison with that in the second half, the resultant movement is downwards, and increases in proportion to the final deflection in the x direction. Horizontal lines on the screen are thus distorted to curved lines, with the curve upwards.

If the undeflected beam passes through the deflection coils below the $x - z$ plane, horizontal lines will curve downwards.

As a general rule, originally straight lines become curved in the direction of the eccentricity of the beam. In Fig. 4.2.3.*b* the eccentricity is thus towards the top left-hand corner.

Asymmetrical pincushion distortion may also be caused by a barrel-shaped or cushion-shaped field.

Fig. 4.2.3.2.3 again illustrates a cushion-shaped field and an upward eccentricity of the electron beam. After passing through a given section of the field, the beam will now have reached point *C* instead of point *D*. At point *C*, however, the curvature of the lines of force involves that the x-component of the field is greater than at *D*. The combination of this field component and the axial velocity component of the electrons results

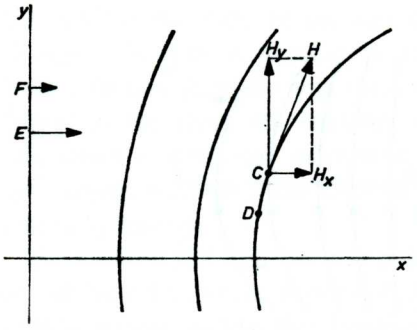

Fig. 4.2.3.2.3. The forces on an electron beam which does not enter the field along the axis. As a result a larger horizontal field component H_x affects the beam.

in a force acting downwards and which is consequently greater at point *C* than at point *D*.

The lines again become curved in the same way as described above. Consequently, it is also possible to eliminate asymmetrical pincushion distortion by giving the field the correct barrel shape.

4.2.3.3. *Keystone distortion*

Non-linearity and asymmetrical pincushion distortion can occur when there is deflection in only one direction, either horizontal or vertical. Keystone distortion can only occur, however, if both deflection fields are present, and like asymmetrical pincushion distortion, it is in the first instance due to the gradual increase and then decrease of the field along the axis of symmetry.

We will again consider the situation represented in Fig. 4.2.3.2.2, but with this difference, that the field-deflection field is also present, so that the electron beam is also bent upwards. Because of the original upward eccentricity of the electron beam, the lines of force of the vertical field are cut at points which are higher than would normally be the case. Their density, and thus the strength of the field, is greater, with a resultant increase in the horizontal deflection, independent of whether this is towards us or away from us. If the field-deflection field changes in sign, the beam is deflected downwards, and analagous reasoning shows that the deflection in the horizontal direction is smaller. The result is keystone distortion, as illustrated in Fig. 4.2.3.*c*.

A second possible cause of keystone distortion is a cushion-shaped or barrel-shaped field.

If we illustrate this by again considering pincushion fields in both directions of deflection, and an electron beam which is displaced upwards from the axis of symmetry, the vertical deflection of the beam due to the hori-

zontally-directed (field) field will be more rapid than would normally be the case, so producing the above-mentioned non-linearity. As a result of this, however, the vertically-directed (line) field will also be cut at higher positions than would otherwise be the case, e.g. at *F* instead of *E*. (Fig. 4.2.3.2.3.) Because of its pincushion shape, the field here will be weaker, so that the horizontal deflection will be smaller than normal.

This acts in opposition to the keystone distortion which we have just described, so that it is possible to arrange for compensation by means of suitable pincushion distribution of the field. In this case, when we move away from the axis, the compression of the field in the axial direction (Fig. 4.2.3.2.2) is compensated by stretching it out in a direction perpendicular to this (Fig. 4.2.3.2.3).

4.2.3.4. *The effect of centring the picture*

If the electron beam does not enter the deflection field along the axis of symmetry, and it is required to prevent non-linearity, asymmetrical pincushion distortion and keystone distortion from occurring, the deflection field must be respectively uniform, barrel-shaped and cushion-shaped in planes which are perpendicular to the axis of symmetry. It is thus impossible to eliminate all the faults at the same time. The field is usually made slightly cushion-shaped so as to compensate, partially or wholly, for the much more serious pincushion distortion of the raster. If the beam is eccentric, a combination of the three faults occurs.

In the ideal case, the undeflected electron beam, the axis of symmetry of the deflection fields and the axis from the centre of the screen and perpendicular to the screen, all coincide. But even then it may be necessary to use the centring magnet, because the centre of the picture may be displaced relative to the centre of the screen, because of non-linearity in the time-base or eccentricity of the flyback period in the blanking period. In this case, the picture faults discussed in this section will still occur.

The faults are not generally noticeable in picture tubes whose maximum angles of deflection are not too large, but their effect is more serious in tubes with large angles of deflection and a narrow neck. In the latter case, the centring magnet must produce a greater deviation of the electron beam in order to give the same displacement on the screen, because the distance from the deflection point to the screen is smaller. In addition, the field has a smaller cross-section, so that the edge effects are stronger.

If it is required to apply picture-centring without introducing any distortion, the best method is to adjust the conventional centring magnet so that any distortion which is already present is reduced to a minimum.

Amongst other things, this compensates for the results of any eccentricities in the construction of the tube and of the deflection system, although, complete compensation with a single magnet is of course impossible. The final picture centring must then be done with a second centring system which is placed as near the screen as possible. The best way of doing it is to pass direct current through the deflection coils, but for economic reasons this has not yet been applied for black-and-white television.

4.2.4. Tilting of the picture

Tilting of the picture is usually caused by rotation of the deflection system relative to the neck of the tube. In magnetically-focused tubes, however, it may also be due to the deflection field penetrating the focusing field, which is axially directed. An electron entering the deflection field then receives e.g. a vertical velocity component from the field deflection field and this in its turn, in combination with the axial field, gives the electron a horizontal deviation.

With larger vertical angles of deflection, this horizontal deviation is also greater, because the horizontal force is proportional to the vertical velocity component. In addition, the horizontal deviation changes sign together with the vertical velocity component, so that the total effect is to tilt the picture. The picture can be returned to its correct position on the screen by rotating the deflection unit in the opposite direction.

4.2.5. Asymmetrical non-linear distortion

In addition to eccentricity of the electron beam, this type of distortion can also be caused by defects in the timebase circuits, although the possibility that the picture tube may have a part to play in distortion in the horizontal direction cannot be excluded.

As far as the line timebase circuit is concerned, the cause of distortion lies in the resistance of the booster diode and the coils in the deflection circuit. Because of this resistance, the voltage on the deflection coil during the scan is not constant, but decreases. As a result, the rate of variation of the current through the coils, and thus of the magnetic field, is greater at the beginning of the scan than it is at the end. This causes an asymmetrical distortion which is visible as a stretching of the picture at the left-hand side of the screen, which passes into compression at the right-hand side. To correct this distortion, a correction coil is usually connected in series with the line deflection coils. (see 6.3.7)

The picture tube itself can also have some effect. This becomes clear when we consider that on one hand the electron gun and on the other hand

the internal aluminium backing extend into the deflection field, so that eddy currents are induced in these metal components. Only those resulting from the very rapid line flyback can be of any importance. They develop heat, and the energy which is necessary for this is supplied by the timebase circuit, but is generally very small, being less than 0.5 watt.

As soon as the flyback is at an end, the eddy currents die out at a rate depending on the time constant which can be assigned to that part of the gun which projects into the deflection field. If the time constant is large, the effect of the disappearing eddy currents is visible in the picture, because they cause a magnetic field in opposition to the main field, so that the picture becomes somewhat compressed at the left-hand side of the screen. This distortion thus compensates that which is caused by the timebase itself.

Usually, however, the time constant is so slight that the effect has disappeared before the next line is visible on the screen. This is because there is a little time between the end of the flyback and that of the blanking period, and there is also some overscan in order to prevent the danger of black edges to the picture.

4.3. **Distortion of the light spot**

If the electron beam had an infinitely small cross-section, there would only be the question of geometrical picture distortion to be considered. It has, however, a finite cross-section which may differ in shape from the cross-section which we desire for the sake of good picture quality.

In order that a finely detailed picture may be produced on the screen, the cross-section of the beam where it reaches the screen must always be as small as possible, circular, and of the same dimensions over the whole screen. This is by no means always possible. We have already referred in previous chapters to distortion of the light spot owing to lack of symmetry in the gun, modulation defocusing, spherical aberration and the effect of the centring magnet. We must now pay some attention to the distortion which is due to the deflection.

The most important of these distortions are astigmatism, curvature of field and coma. It can be shown that astigmatism and curvature of field are in the first place proportional to the beam diameter at the point of deflection, and to the square of the angle of deflection, while coma is proportional to the angle of deflection and to the square of the beam diameter. Since the angle of deflection is large for black-and-white picture tubes while the diameter of the beam is not, coma can be left out of con-

sideration for this type of tube, as being insignificantly small. It should be noted that this does not apply to picture tubes for colour television.

4.3.1. Astigmatism

Astigmatism occurs because the deflection field exercises a focusing effect on the convergent electron beam, which is not the same in the direction of deflection as in a direction perpendicular to this. This focusing effect is determined both by the variation of the field in the direction of the axis of the tube and the variation of the field in the direction of deflection.

Astigmatism may be divided into isotropic astigmatism which occurs when only one deflection field is present, and anisotropic astigmatism which can only occur if both fields are deflecting the electron beam at the same time.

We assume that we have a uniform magnetic deflection field which begins and ends abruptly. In Fig. 4.3.1.1 this field is perpendicular to the

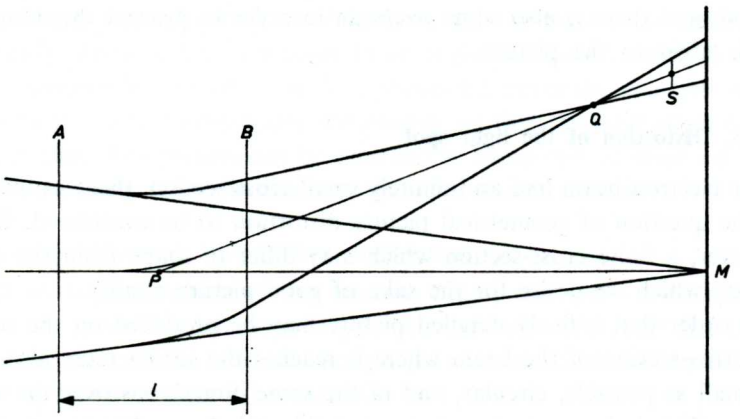

Fig. 4.3.1.1. Distortion of the spot due to deflection of the beam by a uniform magnetic field, perpendicular to the plane of the drawing and limited by the planes *A* and *B*.

plane of the drawing, and is directed towards the reader, being limited by the planes *A* and *B*, which are also perpendicular to the plane of the drawing.

The electron beam enters the field from the left-hand side, and is deflected upwards. If there was no field present, the beam would be focused at *M*, the centre of the screen. The figure only shows the rays at the edges of the beam, which lie in the *y*–*z* plane, i.e. the plane of deflection. If the beam is deflected, it does not remain focused on the screen, for, if we look at the

boundary rays shown in the drawing, we see that the lower ray enters the field at an obtuse angle while the upper ray enters it at an acute angle. Both rays are deflected with the same radius of curvature, so that the former remains longer in the field, and thus is deflected more than the latter. The result is that on leaving the field the two rays will intersect sooner than would be expected on the basis of their original convergence. Thus $PQ < PM$, where P is the deflection point. There has thus been an increase in the focusing power in the direction of deflection, while the focusing in the direction perpendicular to this remains constant, because the boundary rays which lie in the x–z plane enter the field under identical conditions.

As a result, when the beam is deflected vertically it first converges to a horizontal line (point Q), then diverges in the vertical direction while it continues to converge in the horizontal direction, until it forms a vertical line. This occurs at S, whose position is determined by $PS \approx PM$, so that the beam has not yet reached the screen, and so diverges in the horizontal direction. When the beam is deflected in the horizontal or vertical direction, we have the situation shown in Fig. 4.3.1.2. The spot on the screen has

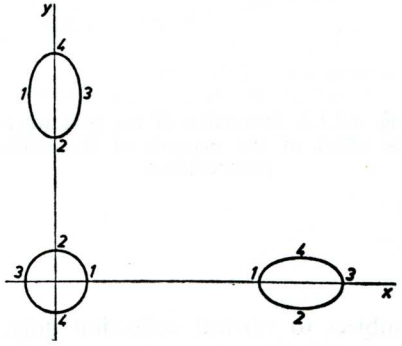

Fig. 4.3.1.2. Distortion of the spot on the screen for both horizontal and vertical displacement under the conditions shown in Fig. 4.3.1.1.

become elliptical. The major axis of the ellipse is in the direction of deflection, because the convergent effect is greatest in this direction and the beam starts to diverge sooner.

The above explanation, however, only applies to uniform fields, and in practice it is not possible to obtain such a field. It is possible to achieve uniformity in planes perpendicular to the axis of the tube, but the field will not begin and end abruptly. The increased convergence in the direction of deflection will continue to exist, and may even become greater, but in addition to this, increased convergence also occurs in the perpendicular direction. The explanation of this runs parallel to the explanation of the bending of straigth lines when the electron beam does not enter the field

along the axis. We now assume that the electron beam does enter the field along the axis. Because of the finite cross-section of the beam, half the electrons are above the x–z plane and half below it, so that the former experience a resultant force downwards and the latter a resultant force upwards.

Consequently, we finally have a convergent effect of the deflection field both in the direction of deflection and in the direction perpendicular to this. If the line and field deflection fields are completely identical, isotropic astigmatism disappears when the beam is deflected in a plane which passes through the axis and makes an angle of 45° with the horizontal plane.

The convergent effect is usually smaller in the direction of deflection than in the perpendicular direction. Fig. 4.3.1.3 represents the distortion of the spot in this case; the minor axis of the ellipse is now in the direction of deflection.

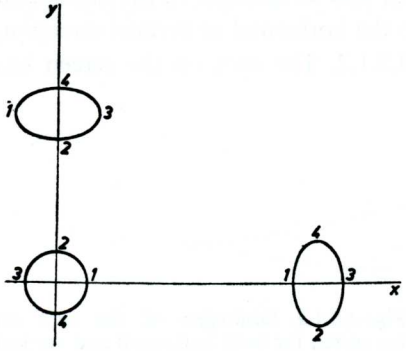

Fig. 4.3.1.3. Distortion of the spot when the effect of the margins of the fields predominates.

4.3.2. Curvature of field

Fig. 4.3.2.1 shows the electron beam subject to vertical deflection only, it being assumed that the convergent effect of the magnetic field is greatest in the horizontal direction. For this reason, the first focus line is vertical, and the second focus line is horizontal.

The loci of the centres of the focus lines in the direction of deflection form the sagittal image surface (A) and the loci of the centres of the focus lines perpendicular to the deflection form the tangential image surfaces (B). Somewhere between the two focus lines the beam has a circular cross-section and the loci of the centres of these circles is the surface of least confusion (C), in which the beam has its minimum cross-section. The three surfaces touch each other at the centre of the screen.

By making the field barrel-shaped it is possible to obtain a round spot on the screen, as shown in Fig. 4.3.2.2. The field becomes weaker towards

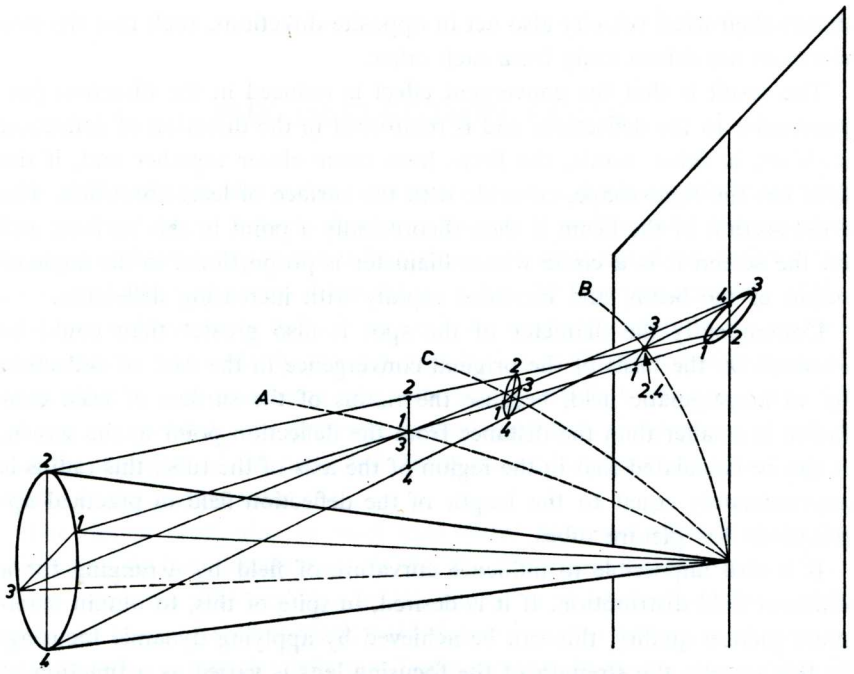

Fig. 4.3.2.1. Astigmatism and curvature of field.
A is the sagittal image surface, *B* is the tangential image surface, *C* is the surface of least confusion.

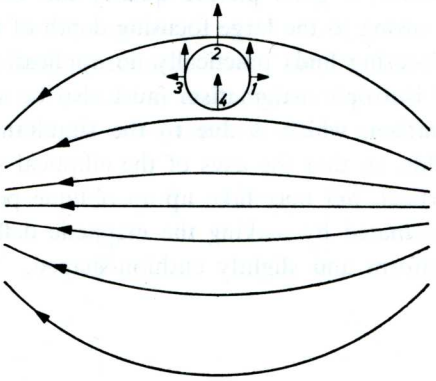

Fig. 4.3.2.2. The forces on the electron beam in a barrel-shaped field for vertical deflection

the top edge, so that electron 2 experiences a smaller force than electron 4. For electrons 1 and 3 the field also has a weak vertical component, but for electron 1 this component is in the opposite direction to the component for electron 3, so that the forces which the electrons experience

due to their axial velocity also act in opposite directions, such that the two electrons are driven away from each other.

The result is that the convergent effect is reduced in the direction perpendicular to the deflection, and is reinforced in the direction of deflection itself or, in other words, the focus lines come closer together and, if the field has the right shape, coincide with the surface of least confusion. The cross section of the beam is then theoretically a point in this surface, and on the screen it is a circle whose diameter is proportional to the angle of origin of the beam, and increases rapidly with increasing deflection.

Consequently the diameter of the spot is also greater than could be assumed on the basis of the original convergence in the case of deflection by an anastigmatic field, because the radius of the surface of least confusion is smaller than the distance from the deflection point to the screen. It can be calculated that in the region of the axis of the tube, this radius is approximately equal to the length of the deflection field in practical applications for picture tubes.

It is also impossible to influence curvature of field by arranging for a different field distribution. If it is desired, in spite of this, to obtain maximum picture quality, this can be achieved by applying dynamic focusing. In this system, the strength of the focusing lens is varied as a function of the deflection of the electron beam so that the instantaneous surface of least confusion cuts the screen at the point where the electron beam strikes it.

In practice, however, a good picture quality can be achieved without dynamic focusing, owing to the large focusing depth of the electron beam, so that dynamic focusing finds practically no application.

To the effect of isotropic astigmatism must also be added the effect of anisotropic astigmatism, which is due to the simultaneous operation of both deflection fields, so that the axes of the elliptical spot are no longer horizontal and vertical, but may take up an oblique position. This astigmatism can be eliminated by making the magnetic deflection field somewhere between uniform and slightly cushion-shaped.

CHAPTER 5

THE DEFLECTION COILS

One of the objects in view in the design of the deflection coils is to keep the energy requirements as low as possible. It is true that the electron beam is deflected under the influence of the magnetic field without the electrons taking up energy from the field, but the repeated recovery of the field energy in order to build it up again as magnetic energy in the volume of the coil is unavoidably accompanied by losses. These losses increase in proportion to the maximum magnetic energy which is required, and the energy requirements are determined, amongst other things, by the length and the diameter of the coil. Both these are limited, however, by the geometry of the picture tube.

The design must also be such that raster and spot distortions are a minimum. As has already been shown, the distortions depend on the form of the magnetic field and also on the geometry of the picture tube. In its turn, the form of the magnetic field depends on the geometry of the deflection coils, so that the deflection faults can thus be controlled by suitable shaping of the coils. However, they cannot all be removed simultaneously.

5.1. The deflection energy required

For calculating the deflection energy which is required, it is again assumed that the deflection field is uniform, that it begins and ends abruptly, and that it has a length l_0. The field strength is assumed to be H_0. In actual fact, the distribution of the field along the axis will be as indicated in Fig. 5.1.1.

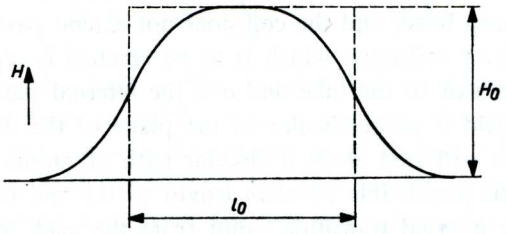

Fig. 5.1.1. The field strength as a function of position along the axis of the tube. l_0 is the effective length of the coil and H_0 is the maximum field strength.

If the peak value of the field strength is H_0, the effective length of the field,

and thus also of the coil, is defined as

$$l_0 = \frac{\int_{-\infty}^{+\infty} H \cdot dz}{H_0} .$$

This means that in Fig. 5.1.1, the area under the curve is equal to the area of the rectangle which is indicated by the broken lines.

For the deflection energy to be a minimum, the effective coil length must be made as great as possible, and the diameter of the coil as small as possible.

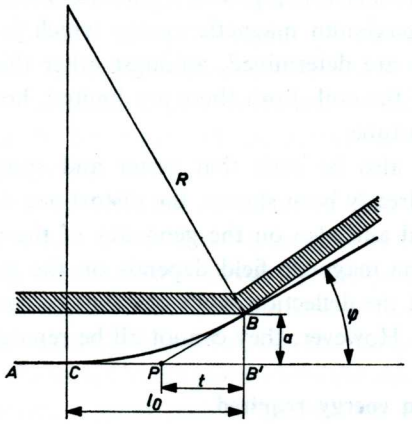

Fig. 5.1.2. The deflection of the electron beam in a magnetic field perpendicular to the plane of the drawing. l_0 is the effective length of the field. R is the radius of curvature of the path of the electrons in the field.

Fig. 5.1.2 shows part of the cross-section of the tube, i.e. at the transition from neck to cone. For the sake of simplicity, this transition has been drawn with a fairly sharp bend, and the coil does not extend past the bend. The maximum angle of deflection which is to be reached is represented by φ. A represents the axis of the tube and a is the internal radius of the neck. The magnetic field is perpendicular to the plane of the drawing and the electron beam is deflected along a circular path of radius R.

The maximum permissible effective length of the coil is now found as follows: At the internal transition point from the neck to the cone (B), draw a straight line at an angle φ to the axis of the tube A. The point of intersection with the axis is the deflection point P. Let the distance from P to B', the projection of B on the axis, be t. CP is equal to BP, sothat the radius of the electron path and the maximum permissible effective coil length $l_0 = CB'$ can be calculated in a simple manner. A longer coil would

result in the electron beam being intercepted by the neck of the tube when deflected at an angle φ. It follows from the figure that:

$$t = \frac{a}{\tan \varphi} \quad \text{and} \quad l_0 - t = \frac{a}{\sin \varphi},$$

so that

$$l_0 = \frac{a}{\tan \varphi} + \frac{a}{\sin \varphi} = \frac{a}{\tan \frac{1}{2}\varphi} \tag{5.1.1.}$$

In 4.2.1. we saw that $\sin \varphi = 0.3\, lH\, \sqrt{V_a}$, so that

$$H_0 = \frac{\sin \varphi}{0.3\, l_0} \sqrt{V_a} \text{ oersted,} \tag{5.1.2}$$

if V_a is expressed in volts and l_0 in cm.

The total energy in the magnetic field follows from equation (4.1.3.1.)

$$W = \frac{H_0^2}{8\pi} V.$$

In this expression, V is the volume of the field. The length l_0 is made as long as possible, giving a larger volume, but H_0 is inversely proportional to l_0, and the square of the field strength appears in the expression for the energy. For the volume still to be as small as possible, the cross-sectional area of the field must be a minimum.

If the field is limited to the inside of the neck of the tube, $V = \pi a^2 l_0$. Substitution of this value and of (5.1.1) and (5.1.2) gives

$$W = \frac{a \sin^2 \varphi \tan \frac{\varphi}{2} V_a}{7200} \text{ m joule} \tag{5.1.3.}$$

It follows from this equation that the required deflection energy is proportional to the diameter of the neck of the tube and not to the square of this value. This is due to the shortening of the coil, which a narrower neck requires, so that the electron beam is not intercepted by the glass wall at its maximum deflection. The fact that a larger maximum angle of deflection leads to a shortening of the coil is expressed by the factor $\tan \frac{1}{2}\varphi$.

The energy required in practice is greater than that indicated by the above expression for W. There are two reasons for this:

1. The cross-section of the electron beam. Up to the present we have tacitly assumed that the electron beam was infinitely thin, but in practice

the diameter of the beam must be taken as 2 to 3 mm where the deflection occurs. To allow for this, a in equation (5.1.1.) must be replaced by $(a - r)$ where r is half the diameter of the beam in the deflection field.

2. The energy of the field is not limited to a cylindrical space of length l_0 and diameter $2a$, but to a space with diameter $2\ (a + q)$. The latter quantity is the internal diameter of the core on which the coil is fitted. A ferroxcube core with a very high permeability and low losses is always used in order to increase the efficiency. In practice, or at least in the case of saddle – type coils, the magnetic field is now limited by this core.

The quantity q is equal to half the difference between the internal diameters of the core and the neck, and is determined by the thickness of the glass, the thickness of the coil, and the tolerances on the dimensions of the glass, the coil and the internal dimensions of the core.

The expression for the required magnetic energy is finally:

$$W = \frac{(a+q)^2 \ \sin^2\varphi \ \tan\frac{\varphi}{2} \ V_a}{7200\,(a-r)} \text{ m joule} \qquad (5.1.4.)$$

This equation shows clearly that decreasing the diameter of the neck further and further finally means that more deflection energy is required. The equation also shows the great influence of q. It is because of this quantity that the increase in field energy required for the change from 70° to 90° and later from 90° to 110° picture tubes was not as great as would be expected from the increase in the angle of deflection. The above-mentioned tolerances in particular have been reduced. However, the largest part of the saving in energy at the larger angles of deflection has been obtained by fitting the 90° coils, and more particularly the 110° coils, with flaps which lie against the conical part of the tube, instead of cutting them short at the transition from the neck to the cone. Because of this, the straight part of the coils can also be increased in length while keeping the center of deflection (point P) in the same place, so that the effective length of the coils has been appreciably increased.

5.2. The number of ampere-turns required

The number of ampere-turns required can now be determined from the calculated field-strength. We will do this on the basis of Fig. 5.2. which represents two air-cored coils lying alongside the neck of the tube. The drawing shows only one turn of each coil. Each of the turns consists of two straight sides parallel to the axis of the tube z, and two curved sides in planes which are perpendicular to the axis of the tube. If currents flow through the coils as indicated by the arrows, the associated field will lie

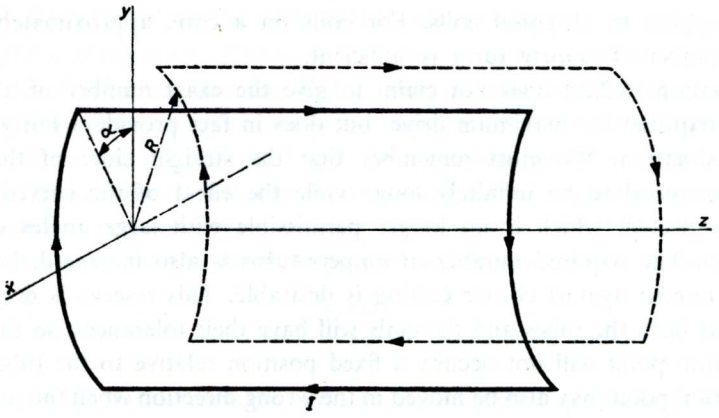

Fig. 5.2. Two air-cored coils, carrying a current I which produces a magnetic field in the negative x direction.

in the x direction, pointing away from us, and the electron beam will be deflected in the y direction. In order to calculate the number of ampere-turns required, we only need to determine the contribution which the straight sides of the coil make to the field strength. This is permissible for calculating the field strength at points on the axis or near it, because the contribution made by the curved sides of the coil is small in relation to that made by the straight sides. The length of the coils is l, and they lie on a cylindrical surface of radius R. If $R \ll l$, the error which results from assuming the straight sides of the coil to be infinitely long is also small. The contribution of each conductor to the field strength at the axis follows from $\int H \, \mathrm{d}l = 0.4 \, \pi I$. If we take the integration path as a circle whose centre is on the conductor, and which lies in a plane perpendicular to it, this circle must pass through the axis and $H = 0.2 \, I/R$ (5.2.1.).

If α is the angle between the vertical and an imaginary line connecting the conductor to the z axis, the required field strength on the axis is $H_x = \dfrac{0.2 \, I}{R} \cos \alpha$. However, there are 4 straight coil sides each consisting of n wires so that $H_x = \dfrac{0.8 \, nI \cos \alpha}{R}$. For a field which is more or less uniform in planes perpendicular to the axis, $\alpha \approx 30°$, as we shall see later. Substitution of this value and of H_x according to equation (5.1.2) finally leads to

$$n \, I = 4.8 \, \frac{R}{l_0} \sin \varphi \sqrt{V_a} \qquad (5.2.2.)$$

This applies to air-cored coils. For coils on a core, approximately half this number of ampere turns is sufficient.

Equation (5.2.2.) does not claim to give the exact number of ampere turns required for maximum drive, but does in fact provide a fairly good approximation. We must remember that the straight sides of the coil were assumed to be infinitely long, while the effect of the curved sides was neglected, which is no longer permissible with large angles of deflection. The required number of ampere-turns is also increased, because some reserve against corner cutting is desirable. This reserve is necessary because both the tubes and the coils will have their tolerances, so that the deflection point will not occupy a fixed position relative to the tube. The deflection point may also be moved in the wrong direction when the centring magnet is used, so that there is a danger that at maximum deflection the electron beam will be intercepted by the neck of the tube and the corners of the picture will remain dark. For this reason, it must be possible to slide the nominal coil a few mm back along the nominal tube before this corner-cutting takes place. This means that the effective length of the coil must be somewhat shorter, at the expense of extra ampere-turns, but against this l_0 increases again when the coils are extended over the conical portion of the tube. Equation (5.2.2.) therefore represents a good starting point from which the correct number of ampere turns can be determined experimentally.

5.3. Sensitivity

A deflection coil can be regarded as consisting of a selfinductance L and a resistance r in series. To scan the screen, a sawtooth current is passed through the coils. At the end and at the beginning of the scan respectively, the magnetic energy stored in the field is a maximum, and equals $\frac{1}{8} L\hat{\imath}^2$ where $\hat{\imath}$ is the peak-to-peak value of the sawtooth current.

If all the energy conveyed to the magnetic field was destroyed at the end of the scan, the power required would be $\frac{1}{8} L\hat{\imath}^2 f$, while in addition there is always a resistance loss of $\frac{1}{12} r\hat{\imath}^2$. The resistance loss is of the same order for vertical deflection as it is for horizontal deflection. For vertical deflection, the wattless power is negligible in relation to this loss, because of the low vertical scanning frequency, i.e. 50 or 60 c/s. The reverse is true, however, for horizontal deflection, where the scanning frequency is very high. As a first approximation, then, $\frac{1}{8} L\hat{\imath}^2$ is a measure of the sensitivity of the line deflection coils and $\frac{1}{12} r\hat{\imath}^2$ of the field deflection coils.

5.3.1. Sensitivity of the line deflection coils

As $\frac{1}{8} L\hat{\imath}^2 f$ is of the order of 15 to 40 VA, depending on the number of lines, the angle of deflection, and the E.H.T., the line deflection circuit is designed so that most of the energy stored in the magnetic field at the end of the scan can be recovered. In this case, too, the resistance losses remain uninteresting, but in spite of this, the resistance cannot be neglected, because it also causes a nonlinearity.

The coil must carry a sawtooth current which satisfies the equation

$$i_y = \frac{\hat{\imath}_y}{2}\left[\frac{2t}{t_s} - 1\right]$$

where t_s is the duration of the scan, and $\hat{\imath}_y/2$ is the direct current through the coil required in order to deflect the electron beam exactly to the edge of the raster. The required peak-to-peak value of the sawtooth current is thus $\hat{\imath}_y$.

If the coil has a purely inductive impedance, a constant voltage

$$V_L = \frac{L_y \hat{\imath}_y}{t_s}$$

is required during the scan. The product of voltage and current at the end of the scan can thus be taken as a measure of the sensitivity of the coil. This product is proportional to the above-mentioned deflection energy requirement. The smaller the product, the more efficiently can the deflection be carried out with the coil in question.

A sawtooth voltage is also developed across the resistance of the coil by the deflection current, and this voltage should be compensated. The voltage to be applied must thus satisfy the expression:

$$V_y = V_L + V_r = \frac{L_y \hat{\imath}_y}{t_s} + r_y \frac{\hat{\imath}_y}{2}\left[\frac{2t}{t_s} - 1\right].$$

Fig. 5.3.1. shows the voltages across the inductive and resistive components of the impedance, and also the total voltage. (V_L, V_r and V_y respectively).

At the end of the scan, the voltage must thus be an amount $\frac{r_y \hat{\imath}_y}{2}$ higher. As a result, the current – voltage product is now:

$$\frac{\hat{\imath}_y}{2}\left[\frac{L_y \hat{\imath}_y}{t_s} + \frac{r_y \hat{\imath}_y}{2}\right] = \alpha_h \frac{L_y \hat{\imath}_y^2}{2 t_s}.$$

where

$$\alpha_h = 1 + \frac{r_y t_s}{2 L_y}.$$

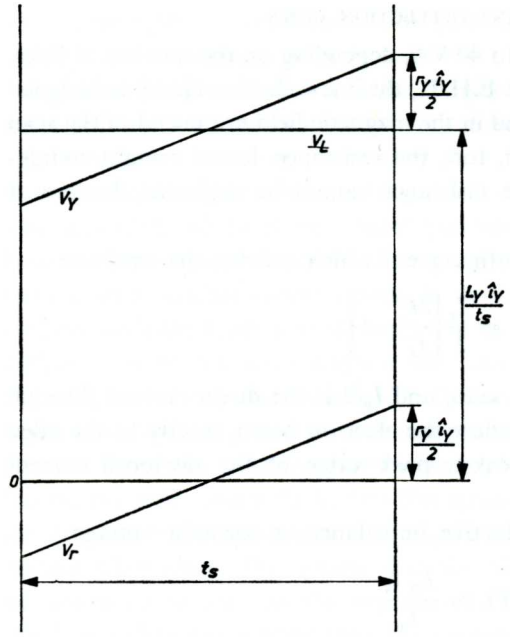

Fig. 5.3.1. The voltage required for a line deflection coil, in order to produce a pure sawtooth current. V_L is the voltage across the inductive component of the impedance of the coil, V_r is the voltage across the resistive component and V_y is the total voltage.

Consequently, if the merits of a particular type of coil are to be evaluated in connection with the design of a line output circuit, it is not sufficient merely to know $\hat{\imath}_y$, L_y and r_y. The value of α_h is also important.

The expression for α_h still contains t_s, or in other words, α_h depends on the particular television system which is employed.

If two different types of coil are being compared, it must be remembered that $\hat{\imath}_y$ also depends on the E.H.T. voltage on the picture tube, and sometimes also on the type of picture tube which is used to determine $\hat{\imath}_y$.

In practice, a pure sawtooth voltage such as indicated by V_y in Fig. 5.3.1. will never be applied, but instead a more-or-less constant voltage which is somewhat bigger than V_y at the end of the scan.

The difference between this voltage and V_y, which decreases according to a sawtooth curve during the scan, can be taken up by a so-called linearity coil in series with the line coil. This linearity coil has a Ferroxcube core which can be pre-magnetised by a small bar magnet parallel to the core. Its pre-magnetisation can be adjusted by varying the distance between the bar magnet and the core, in such a way that the coil shows a high impedance at the beginning and a low impedance at the end of the sweep.

Finally, $\hat{\imath}_y$ will also be made rather greater for the design of the line timebase, partly so that any tolerances can be taken up.

5.3.2. Sensitivity of the field deflection coils

For the vertical or field deflection, only the resistive losses are important. These are of the order of 0.5 watt, and thus are very low. In spite of this, however, they have to be taken into account, because the production of sawtooth currents in resistances takes place with very low efficiency. The energy taken up in the field timebase circuit is thus appreciable.

It has been pointed out already that the wattless power is negligible in relation to the resistance loss in the coils for field deflection. But neglecting the selfinductance of the coils gives rise to a nonlinearity. Compensation of this nonlinearity requires some extra energy, which has to be taken into account.

The field coil is connected to the secondary side of a transformer whose primary is included in the anode circuit of the field output pentode.

The current through the coil must satisfy the expression:

$$i_v = \frac{\hat{\imath}_v}{2}\left[\frac{2t}{t_v} - 1\right].$$

If we had only to deal with the resistance r, the voltage on the coil would also have to be a sawtooth voltage:

$$V_r = \frac{\hat{\imath}_v r_v}{2}\left[\frac{2t}{t_v} - 1\right].$$

Here too, we can take the current-voltage product at the end of the scan as a measure of the efficiency of the field coil:

$$\frac{\hat{\imath}_v^2 r_v}{4}.$$

The proportionality to the energy dissipation in the resistance is very obvious.

Because of the self inductance of the coil, a constant voltage

$$V_l = \frac{L_v \hat{\imath}_v}{t_v}$$

must be added to the sawtooth voltage.

The current-voltage product at the end of the scan thus becomes:

$$\frac{\hat{\imath}_v}{2}\left[\frac{\hat{\imath}_v r_v}{2} + \frac{L_v \hat{\imath}_v}{t_v}\right] = \frac{\alpha_v \hat{\imath}_v^2 r_v}{4},$$

$$\text{where } \alpha_v = 1 + \frac{2 L_v}{r_v t_v}$$

As we shall see later, the extra constant voltage is obtained by suitably driving the field output valve. This valve must supply an extra anode current of

$$\frac{\hat{\imath}_m L_s}{L_p}\left[\frac{2t}{t_v} - 1\right].$$

In this expression, L_p is the self inductance of the primary winding of the transformer and $\hat{\imath}_m$ and L_s are the values of $\hat{\imath}_v/2$ and L_v transformed to the primary.

5.4. The effect of the coil form on the distribution of the field

5.4.1. Concentrated turns

We will now investigate how the distribution of field in planes perpendicular to the axis can be affected by correct placing of the turns. For this purpose, we assume a field H_x in the direction of the x axis. This field can be represented as a function of y by means of the power series:

$$H_x = H_0 + H_2 y^2 + H_4 y^4 + \ldots .$$

In this series, H_0 is the field strength on the axis. The uneven terms in y do not appear because the field shows mirror-image symmetry relative to the $y - z$ plane, and H_x thus adopts the same value for equal but opposite values of y, always assuming that x and z have not changed.

If we limit ourselves to small deflections, the terms higher than the quadratic are negligible, so that all that remains is:

$$H_x = H_0 + H_2 y^2 .$$

We propose to calculate H_0 and H_2 for the case illustrated in Fig. 5.2., in which each coil consists of a single turn of wire.

In Fig. 5.4.1.1., one of the four sides of the coil is shown. According to equation (5.2.1.), the field strength at an arbitrary point P due to the current through this wire alone is given by:

$$H = \frac{0.2\, I}{r}$$

where r is the distance from P to the wire. H is perpendicular to the plane through the wire and through P. This plane makes an angle β with the $x - z$ plane, so that $H_x = H \sin \beta$. If P is determined by the running co-ordinates x and y, while the current-carrying wire is determined by the

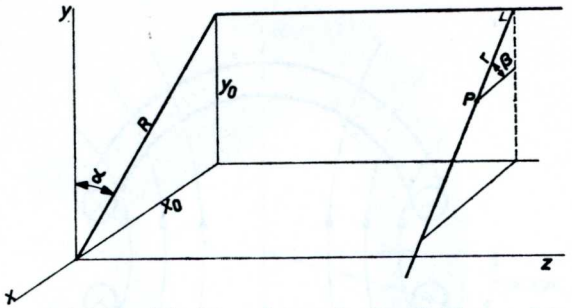

Fig. 5.4.1.1. One of the 4 straight sides of the pair of coils illustrated in Fig. 5.2. The wire is parallel to the z-axis and its position is determined by the coordinates x_o and y_o.

straight line x_0, y_0, we have $\sin\beta = \dfrac{y_0 - y}{r}$ and

$$r^2 = (x_0 - x)^2 + (y_0 - y)^2, \text{ so that}$$

$$H_x = \frac{0{,}2\, I (y_0 - y)}{(x_0 - x)^2 + (y_0 - y)^2}.$$

The contributions of the other three straight current-carrying conductors can be determined by an analagous method. The total result is:

$$H_x = 0{,}2\, I \left[\frac{y_0 - y}{(x_0 - x)^2 + (y_0 - y)^2} + \frac{y_0 + y}{(x_0 - x)^2 + (y_0 + y)^2} + \right.$$
$$\left. + \frac{y_0 - y}{(x_0 + x)^2 + (y_0 - y)^2} + \frac{y_0 + y}{(x_0 + x)^2 + (y_0 + y)^2}\right]$$

The quantities H_0 and H_2 are finally found by developing H_x in a series to y, after having first equated x to 0.

$$H_x = 0{,}4\, I \left[\frac{y_0 - y}{x_0^2 + (y_0 - y)^2} + \frac{y_0 + y}{x_0^2 + (y_0 + y)^2}\right] = 0{,}4\, I f(y)$$

$$H_x = 0{,}4\, I \left[f(0) + y f'(0) + \tfrac{y^2}{2} f''(0) + \ldots\ldots\right]$$

$$= 0{,}8\, I \left[\frac{y_0}{x_0^2 + y_0^2} + y^2 y_0 \left\{\frac{-3}{(x_0^2 + y_0^2)^2} + \frac{4\, y_0^2}{(x_0^2 + y_0^2)^3}\right\}\right]$$

$$= 0{,}8\, I \frac{y_0}{x_0^2 + y_0^2} \left[1 + \frac{y^2}{x_0^2 + y_0^2} \left\{-3 + \frac{4\, y_0^2}{x_0^2 + y_0^2}\right\}\right].$$

Substitution of $x_0^2 + y_0^2 = R^2$ and $\dfrac{y_0}{R} = \cos\alpha$ gives

$$H_x = \frac{0{,}8\, I}{R} \cos\alpha \left[1 + \frac{y^2}{R^2} \left\{-3 + 4\cos^2\alpha\right\}\right].$$

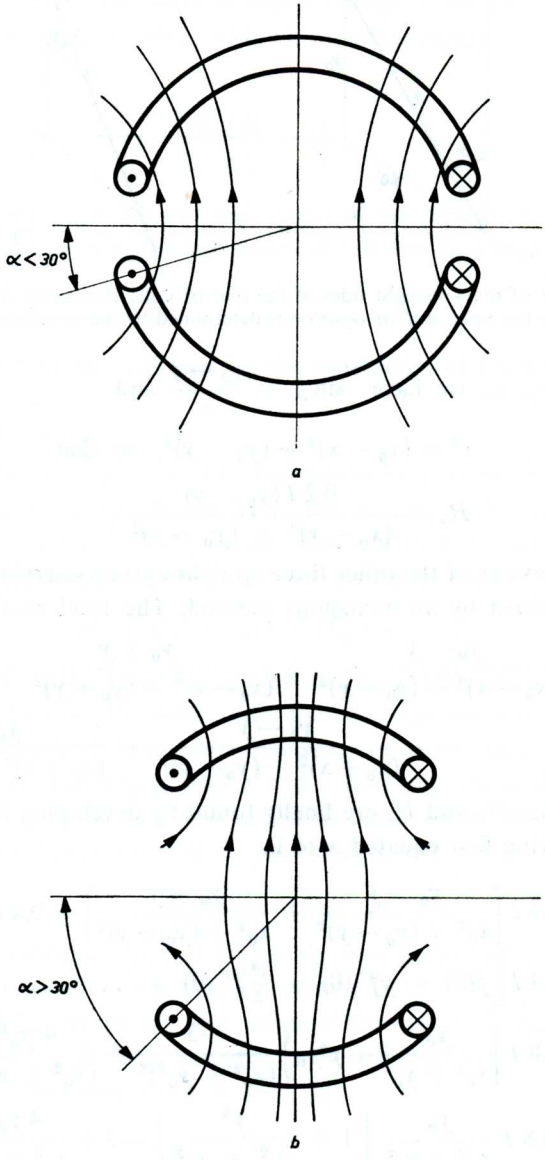

Fig. 5.4.1.2. A pair of coils for horizontal deflection of the electron beam.
a. $\alpha < 30°$. This leads to a pincushion field.
b. $\alpha > 30°$. This leads to a barrel-shaped field.

Fig. 5.5.1.1
Saddle coil, as used for line deflection for 110° picture tubes.

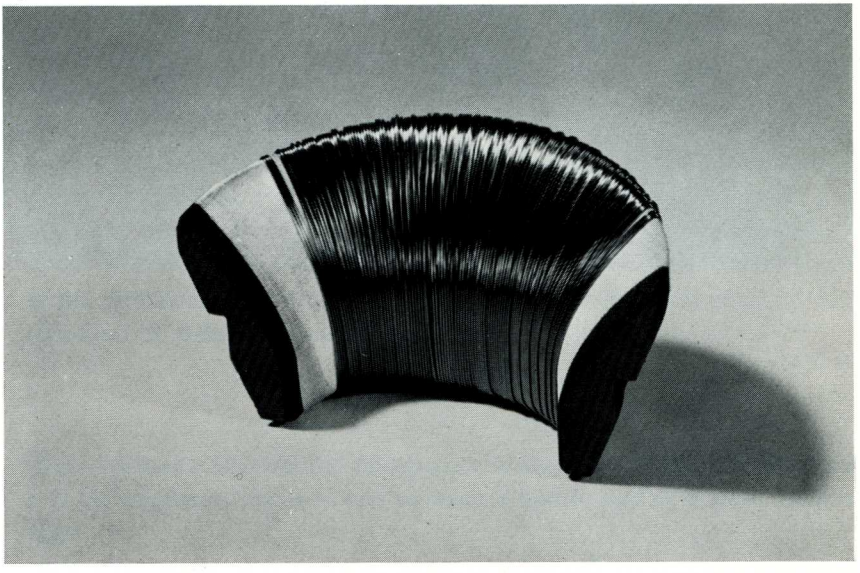

Fig. 5.5.2.1
Half a Ferroxcube core wound with a toroidal coil for field deflection for 110° picture tubes.

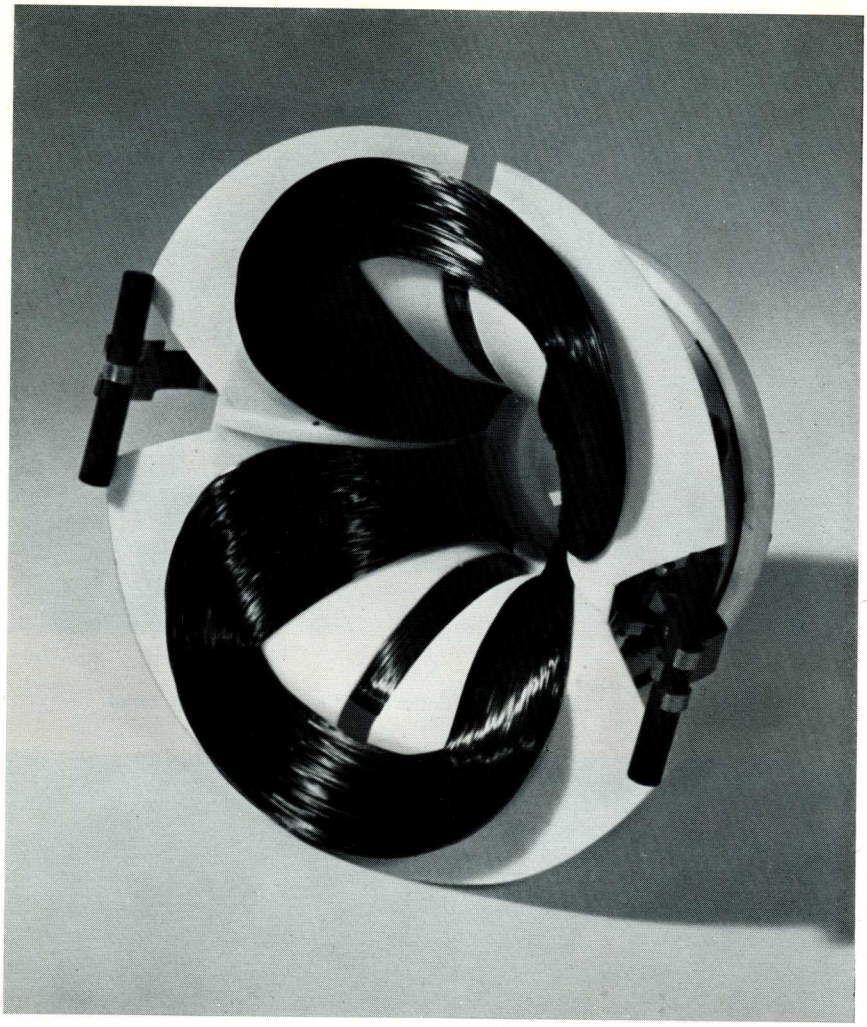

Fig. 5.5.7.1
Complete deflection unit for 110° deflection.

From which follow

$$H_0 = \frac{0.8\,I}{R}\cos\alpha \quad \text{and} \quad H_2 = \frac{8\,I}{R^3}\,(-3 + 4\cos^2\alpha)\,\cos\alpha.$$

The condition for a uniform field in planes perpendicular to the axis is thus:

$$\cos^2\alpha = 0.75 \text{ or } \alpha = 30°.$$

If $\alpha < 30°$, then H_2 is positive, and the field is pincushion shaped.
If $\alpha > 30°$, then H_2 is negative, and the field is barrel shaped.
The two situations are illustrated in Fig. 5.4.1.2.*a* and *b*. In practice, the coils do not consist of a single turn of wire, but of several turns. In this case, it is necessary to select the average angle α.

Although the above considerations form a good starting point for the coil design, it must be remembered that deviations can occur from the expected distortions of the raster and the spot of light. This is because, in the deduction of the field strength, the straight portions of wire were assumed to be infinitely long, the curved portions were neglected, and because the series development of H_x to y is only valid for the immediate neighbourhood of the axis while, with the present-day maximum angles of deflection, the electron beam passes close to the end of the coil. The form of the field deviates quite considerably here from that on the axis.

5.4.2. Distributed turns

A second possibility is to distribute the turns of the coil along the periphery of the core. Fig. 5.4.2. shows a cross-section through such a coil and core, for line deflection only, in a plane perpendicular to the axis. The cross sections through the wires constituting the coil are shown shaded. If the distribution of turns is such that the field strength is constant in the direction of deflection, we have:

$$H = \frac{0.4\,\pi\,nI}{l}.$$

This expression neglects the susceptance of the core. In the case illustrated, n is the number of turns of wire between A and B. As $l = R\sin\alpha$, it follows that:

$$H = \frac{0.4\,\pi\,nI}{R\sin\alpha}.$$

If H is to be constant, n must equal $\int N_0\cos\alpha\,d\alpha$ where N_0 is the maximum density of winding. A cosinusoidal distribution of the turns along

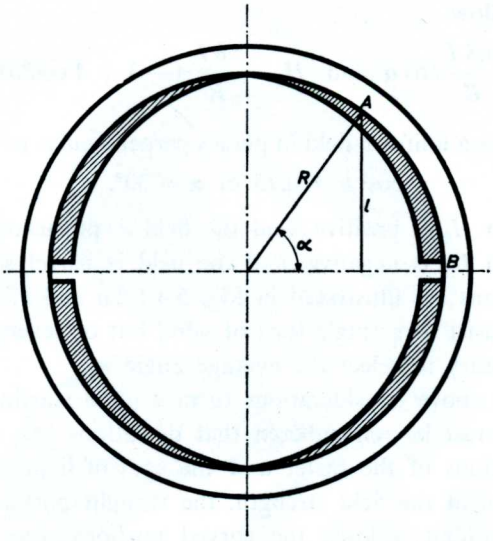

Fig. 5.4.2. Cross-section perpendicular to the axis of a coil with distributed turns.

the periphery of the core thus gives a uniform field. In more general terms the density of winding can be indicated by $N_0 \cos^p \alpha$. If $p > 1$, the density of winding decreases more sharply than with $\cos \alpha$, so that the resulting field is pincushion shaped. A barrel shaped field is obtained by choosing $p < 1$.

5.5. Construction

There are two types of coil, which are distinguished according to their shape, i.e. saddle coils and toroidal coils, each of which have their particular advantages and disadvantages and therefore their own ranges of application. The first type is used mainly for line or horizontal deflection, while the use of the second type is restricted to field or vertical deflection. In addition to the deflection coils, the complete deflection unit will often incorporate other components, such as raster-correction magnets.

5.5.1. The saddle coil

The coil illustrated in Fig. 5.2. is an example of a saddle coil. The reason for this name can be clearly seen from Fig. 5.5.1.1., in which the Ferroxcube core which meets round the outside of the coil is omitted. This coil is designed for use on picture tubes with 110° deflection. The photograph

shows clearly that one end of the coil is bent conically, so that the coil lies partly against the conical portion of the tube, as a result of which the deflection energy required is as low as possible.

Fig. 5.5.1.2. shows a cross-section perpendicular to the axis. The magnetic lines of force return through the core, which has a negligible susceptance, so that this too keeps the required number of ampere – turns down to a minimum. Finally, the diameter is always kept as small as possible; it is controlled by the external diameter of the neck of the tube, and the winding volume required for the coils. Because of the rather extended ends of the saddle coils, the average turn is fairly long. However, this coil remains very attractive for horizontal deflection, because the emphasis here falls on the magnetic energy, so that stray fields must be limited to a minimum.

5.5.2. The toroid coil

Fig. 5.5.2.1. is a photograph of half a Ferroxcube ring with a toroid coil, while Fig. 5.5.2.2 shows a cross-section perpendicular to the axis of two coils with distributed windings. These coils give a magnetic flux, part of which flows round outside the deflection unit. Thus they are less suitable for horizontal deflection.

The average turn-length is smaller than for saddle coils. These coils thus have a low R/L ratio, so that they are more suitable for vertical or field

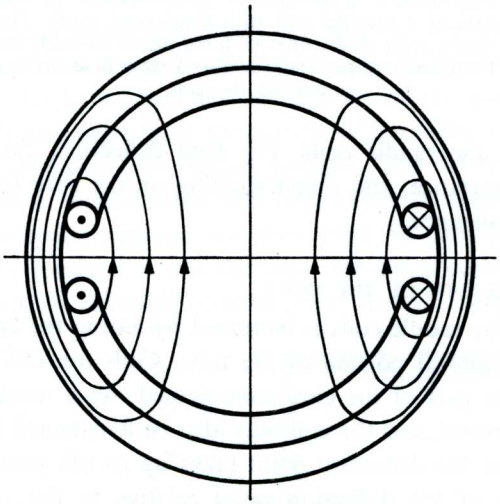

Fig. 5.5.1.2. Cross-section perpendicular to the axis of a saddle coil with concentrated turns. The return path of the lines of force is through the Ferroxcube core.

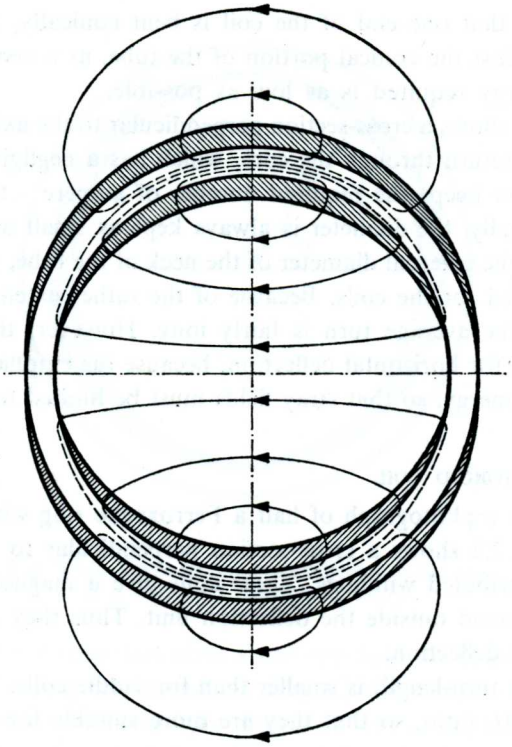

Fig. 5.5.2.2. Cross-section perpendicular to the axis of a toroidal coil with distributed turns. The return path of the lines of force passes through the Ferroxcube core. There is also a stray field present outside the coil.

deflection than the saddle coils. For field deflection, the resistive losses are of first importance, and direct winding on the core leads to a further reduction in resistance.

5.5.3. The length of the coils

The length of the saddle coils is increased by letting the heads of the coils lie against the conical portion of the tube. Coils for 110° deflection even have the greater part of the core cone-shaped. As a result, the deflection point moves forward, and the coil may also be lengthened in the backward direction so that the deflection point takes up its old position once more.

The position of the deflection point relative to the tube is very important. If it lies too far back, this results in corner-cutting. When selecting the position, we must take into account the tolerances in coil dimensions

and tube dimensions which are associated with the mass-production of these two components, as a result of which the deflection point may be shifted from the desired position. In addition, the chance of corner-cutting may be increased if the image on the screen has to be shifted by means of the centring magnet for electrical reasons, such as nonlinearity, and a lack of exact coincidence of the centre of the flyback period with the centre of the corresponding blanking period. In this connection, good engineering practice demands that, as far as its deflection point is concerned, it must be possible to move a nominal coil about 4 mm back on a nominal tube before corner-cutting takes place.

5.5.4. Correction magnets

It has been shown already that uniform deflection fields give rise to serious pincushion distortion of the raster, and that this can be prevented by making the fields themselves pincushion shaped. A field which is slightly pincushion shaped helps to prevent anisotropic astigmatism, but to prevent raster distortion at the same time, the pincushion character of the field must be more pronounced. In this case, the quality of the luminous spot deteriorates badly on account of isotropic astigmatism. The best compromise between raster distortion and distortion of the spot is obtained by not making the pincushion character of the field too strong, so that some raster distortion remains. This residue is suppressed by means of two or four permanent magnets attached to the deflection unit.

If only two magnets are used, they are fitted at the short sides of the cone of the tube. These magnets give the electron beam an extra horizontal deflection (Fig. 5.5.4.) so that the short sides of the picture are pulled straight. As they also drive back the corners of the raster at the same time, the horizontal sides are also pulled straight. The latter becomes more difficult to obtain in picture tubes with large angles of deflection (e.g. 110°), so that four correction magnets are often used. Of course, the amount of raster correction required is not the same for every combination of tube and coil, so that it is desirable to have some means of adjustment.

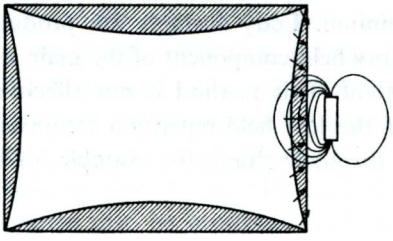

Fig. 5.5.4. The effect of a small correction magnet on the concave side of the picture.

It is obvious that the deflection sensitivity is also affected by the adjustment of the raster-correction magnets. The resulting spread in deflection sensitivity must be added to that which is due to spread in coils, picture tubes and deflection circuits, so that it is desirable to have some amplitude adjustment for the deflection.

5.5.5. Screening behind the deflection unit

The field distribution on the axis is more or less clock-shaped. Because of the attempt to make the coils as long as possible, fields penetrate quite a distance towards the gun, even reaching at the focusing lens. Because the electron gun penetrates partially into the deflection field, eddy-current losses arise in this gun during the line flyback pulses. The same is true for the aluminium coating which covers the inside of the tube. These eddy-current losses may amount to several percent of the total deflection energy which is required, and must also be covered by the timebase circuit.

Also the focusing lens affects the deflection sensitivity unfavourably. The chance of this occurring increases as continuing shortening of the tube is sought, not only in larger angles of deflection, but in shortening the neck of the tube, so that the focusing lens is pushed further and further into the deflection field. The result of this is that the first part of the field becomes more or less inoperative. This is because the focusing lens drives those electrons whose paths deviate from the axis of the tube, back to the axis, independent of the cause of the deviation.

The resulting loss of sensitivity applies to both horizontal and vertical deflection, and is worse for toroidal coils than for saddle coils, because the field of the former penetrates further back.

In addition to a loss in sensitivity, there is also a second effect, i.e. that of spherical aberration, because the deflection of the electron beam which is already present in the focusing lens means that more use is made of the edges of this lens than of the centre. In practice, the results are found to be much better than might be expected, but in spite of this, some coil manufacturers provide screening behind the coil. For the horizontal deflection, this can be done simply by means of a metal ring, e.g. of aluminium. Eddy currents are produced in this ring, which counteract the stray field component of the main field, and thus compensate it to a certain extent. This method is not effective for the field deflection field, because of the low field-repetition frequency. The only thing which helps here is a magnetic shunt, for example, of silicon iron.

5.5.6. Screening net

The line coils are the source of interfering radiations affecting radio receivers amongst other apparatus.

Direct electrical and magnetic radiation may occur, but voltages can also be induced in the domestic lighting mains, as we shall now explain with reference to Fig. 5.5.6. In this figure, V_1 represents the interfering

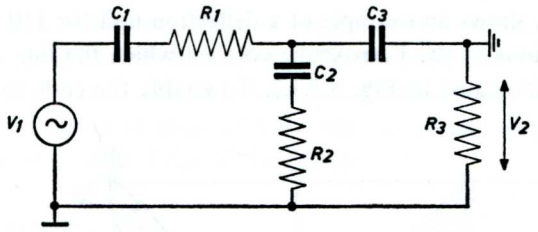

Fig. 5.5.6. Equivalent circuit diagram for the interfering voltage induced on the lighting mains via the picture tube, due to the flyback voltage peaks on the line coils.

voltage which results from the flyback voltage peaks on the line deflection coils. Higher harmonics of this voltage are coupled via C_1 to the internal conductive coating of the picture tube. C_1 is thus the capacitance between the coil and the internal conductor, while R_1 is the resistance of this conductor. C_2 is the capacitance between the internal conductor and the external aquadag coating of the tube. R_2 is the resistance of this coating, which in a television receiver is connected to the chassis. However, the internal conductor is also coupled to the surroundings (earth), principally at the screen end. This is represented by C_3. The return path to the source of interference is formed by the impedance of the lighting mains R_3 and the chassis. There is thus an interfering voltage V_2 present on the lighting mains connection.

If the coil is connected to the line output transformer in such a way that the connection is symmetrical relative to the chassis, this gives a considerable reduction of the interfering voltage.

By fitting a metal net between the coil and the neck of the tube, and connecting this net to the chassis, the remaining interfering voltage is practically short-circuited, and V_2 almost disappears. The net must not contain any short-circuiting contacts; if it does, this gives rise to damping of the line deflection field. For example, it may be comb-shaped. In addition, it must be insulated from the coil, so that it can withstand the peak voltages on the coil, and finally it must also be insulated from the

glass neck of the tube. This is because direct metallic contact of the chassis with the glass neck means that the E.H.T. voltage is applied across the glass wall of the neck. Electrolysis may take place at the higher temperature to which just this part of the tube is exposed, and after some time this will give rise to high-voltage breakdown.

5.5.7. Example of a deflection unit

Figure 5.5.7.1. shows an example of a deflection unit for 110° deflection *).

The dimensions of the Ferroxcube core on which the line and field coils are fitted are indicated in Fig. 5.5.7.2. To enable the coils to be fitted, the

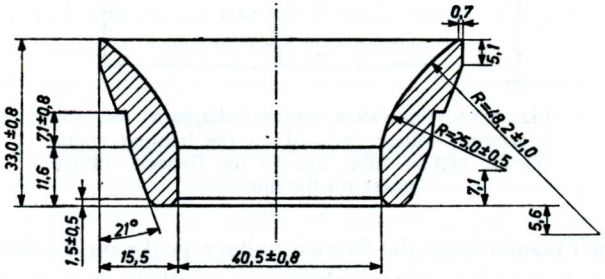

Fig. 5.5.7.2. Dimensions of the Ferroxcube core.

core is first divided into two equal halves. Fig. 5.5.7.3. shows one of these halves with a line coil and a field coil in position.

The field coils

These are toroidal and have distributed turns. They are wound directly onto the core after this has been wound round with linen tape, 9.5 mm wide and 0.076 mm thick. Inside the core the tape is half overlapping.

The coil is wound with 28 s.w.g. wire (= 0.376 mm) the total number of turns being 494. There are 8 layers containing respectively 96, 88, 78, 68, 58, 48, 38 and 20 turns.

The line coils

These are saddle shaped and also have distributed turns. They are insulated from the field coils by two suitably shaped P.V.C. sheaths, 0.635 mm thick. Each coil consists of 230 turns of 30 s.w.g. wire (= 0.315 mm).

The coils are wound with the aid of a special jig, and after winding, a

*) This deflection unit was developed in the Mullard Research Laboratories at Salfords, England.

current is passed through the coil, this current being high enough to slightly melt the insulation material on the wire. When it cools, the coil has assumed a permanent form, and can be placed over the field coil.

The correction magnets

The raster correction magnets are clearly visible in Fig. 5.5.7.1. They are made of Ferroxdur (Magnadur) and are 38.1 mm long and have a diameter of 5.1 mm. They are fixed to copper strips, so that they can be placed nearer to or further away from the tube. By this means it is possible to obtain a correctly-shaped raster. The magnets can also be moved slightly in the direction of their axes in order to correct any asymmetrical distortion of one or both sides of the picture.

The centring magnets

These are fitted behind the deflection unit (see Fig. 5.5.7.4) and consist of two rings, each of which is magnetised at two diametrically opposite places.

The magnetic material employed is Ferroxdur (Magnadur) which, because of its brittleness, is bonded with plastic. The advantage which Ferroxdur (Magnadur) magnets have over steel magnets is that they neither damp the line deflection field nor form a shunt for the field deflection field.

The maximum field strength on the axis is approximately 24 oersteds. This gives about 21 mm picture displacement on the screen of a 21 in. tube with 110° deflection and an E.H.T. of 16 kV.

The line coils are connected in parallel and the field coils in series.

	Line	*Field*
Coefficient of self inductance at 1 kc/s	4.55 mH	44.25 mH
Resistance at 24° C	6.4 Ω	12.8 Ω
Peak-to-peak current	1.882 A	0.645 A
α_h and α_v respectively	1.035	1.364

The calculation of α_h and α_v is based on the definitions given in sections 5.3.1. and 5.3.2.

The value chosen for t_s is 50 μsec, corresponding to a 625-line system with an increased flyback period (22%) and t_v is assumed to be 19 msec.

CHAPTER 6

DEFLECTION CIRCUITS

6.1. Measurement of the form and amplitude of the current required for horizontal and vertical deflection

As the previous chapters have shown, a purely linear relationship does not usually exist between the observed displacement of the spot on the screen and the variation of the currents through the deflection coils.

The required form and amplitude of these currents for a given combination of picture tube and deflection system can be determined in a simple manner, by determining the value of the direct current which has to be passed through the coils to give a certain displacement of the spot.

To do this, the picture tube can be marked with linear horizontal and vertical scales, both passing through the centre of the screen. As a focused stationary beam on one point of the screen would damage the phosphor coating, it is usual to pass an alternating current through the coil which is not taking part in the measurement, so that a long line will be produced on the screen instead of a spot. With the necessary operating voltages applied to the tube, the required data can be obtained by measuring the current for each position of the line.

If it is desired to displace the line linearly with time, the necessary variation of current per unit time is found to be a maximum when the line is passing the centre of the screen. To an increasing extent, this is found to be the case for picture tubes having large angles of deflection, with the result that the sawtooth current has to become more or less S-shaped. However, the deviation from linear variation is not so great that it has to be taken into account in the original layout of the deflection circuit. For calculating the matching transformer and the necessary currents and voltages, it is sufficient to assume a linear current form; the consequences of the S-shaped variation can be taken into account subsequently.

6.2. Differences between the voltages across the coils for horizontal and vertical deflection

The voltage which appears across the deflection coils during the deflection of the beam can be regarded as consisting of an inductive component $V_L = L\frac{\mathrm{d}i}{\mathrm{d}t}$ and a resistive component $V_r = ir$. Because the inductive component is much greater for horizontal deflection than it is for vertical

deflection, the voltage forms which occur are completely different. For a line frequency of 15625 c/s (625-line picture, $T = 64\,\mu s$) and a flyback period of 0.156 T ($t_f = 10\,\mu s$), the inductive voltage for a linear deflecting current is $L\hat{\imath}/54 \times 10^{-6}$ volts; the resistive voltage is $\hat{\imath}r$ volts (peak-to-peak). For the deflection coils in use at present, $r\,(\Omega) = 1{,}000$ to $1{,}500 \times L$ (henry) so that the inductive voltage is approximately 13 to 18 times the peak-to-peak value of the resistive voltage drop. The inductive voltage thus predominates; during the flyback it is many times greater. (Fig. 6.2.*a*). For a field frequency of 50 c/s, $T = 20$ ms and, assuming that the self inductance, the resistance and the necessary current are the same, and that the flyback period is 0.03 T, the inductive voltage is only

$$V_L = L\hat{\imath}/19.4 \times 10^{-3} \text{ volts}$$

while the resistive voltage is still $V_r = \hat{\imath}r$ volts. Thus the inductive voltage is now only $^1/_{20}$ to $^1/_{30}$ of the peak-to-peak value of the resistive voltage drop. Only during the flyback does the inductive voltage still have any significance. (Fig. 6.2.*b*).

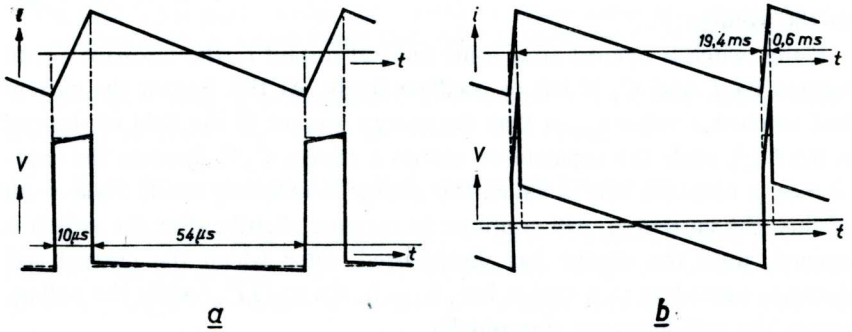

Fig. 6.2. *a*) Current and voltage of the deflection coil for horizontal deflection (idealised) *b*) The same for vertical deflection.

Because of the predominantly inductive character of the coil impedance for horizontal deflection, the circuit for this is very different from the circuit for vertical deflection. For the latter, the impedance of the coil is almost entirely resistive, so that it can be matched to the characteristics of the output valve in a manner corresponding to that employed for an output stage for audio reproduction.

6.3. Horizontal deflection

6.3.1. Representation of the deflection circuit by means of a switch

As can be seen from Fig. 6.2.*a*, the voltage across the line deflection coil during the scan is constant, apart from the resistive voltage drop.

A practically linear deflection current could thus be obtained by connecting the coil to a direct voltage source via a combination of valves having the characteristics of a switch. To describe the operation of the circuit, it is necessary to assume a capacitance parallel to the coil. This can normally consist of the parasitic capacitance of the coil, switch, wiring etc. For the sake of simplicity, we will start by assuming the coil to be loss-free.

If the switch in the circuit of Fig. 6.3.1.1. is closed, a linearly increasing

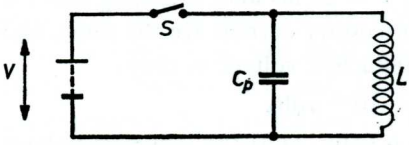

Fig. 6.3.1.1. Schematic representation of a deflection coil with a parallel capacitance, which can be connected to a direct voltage source by means of a switch.

current, $di/dt = V/L$ will be produced in the coil. The energy which is thereby generated in the magnetic field of the coil is $0.5\,Li^2$. At the instant when the switch is closed, the capacitance C_p suddenly becomes charged to the voltage V.

If the switch is opened after some time, at instant t_1, the resonant circuit formed by L and C_p is left to oscillate freely. At this instant the current had reached a value i_m, so that the energy present in the field of the coil is $0.5\,Li_m^2$, while the capacitance carries a charge C_pV. Because the capacitance is normally low in value, this charge is relatively small. As a result of this, the current i_m will continue to increase slightly after the switch is opened, until the charge has disappeared, after which the current will decrease according to a cosine law, $i_L = i_m \cos t/\sqrt{LC_p}$, while the voltage across the coil increases sinusoidally.

$$V_L = V_{\max} \sin t/\sqrt{LC_p} \qquad \text{(Fig. 6.3.1.2)}$$

At the instant $t = 0.5\,\pi\sqrt{LC_p}$, calculating from the instant when the voltage across the coil became zero (t_0), the current i_L will equal zero, and the voltage V_L will reach the maximum value $V_{\max}$. All the energy present in the circuit at the instant when the switch was opened is now collected in the capacitance, so that

$$0{,}5\,C_pV_{\max}^2 = 0{,}5\,Li_m^2 + 0{,}5\,C_pV^2$$

or

$$V_{\max} = \sqrt{\frac{L}{C_p}\,i_m^2 + V^2}.$$

At the instant $t = \pi\sqrt{LC_p}$, the current through the coil will again have reached a maximum value, and the capacitor will be discharged once more.

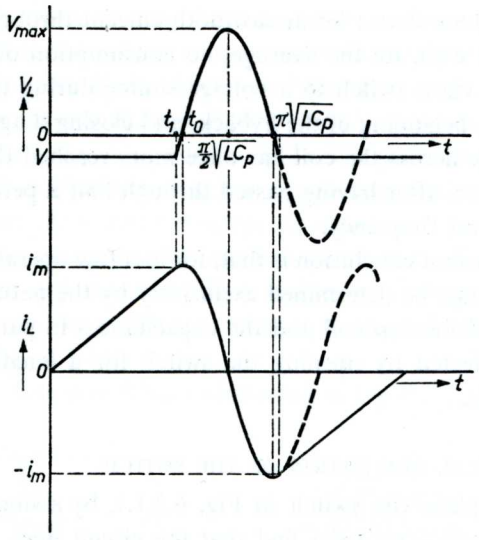

Fig. 6.3.1.2. Generation of sawtooth current with cosine-shaped flyback in the circuit of Fig. 6.3.1.1. For good linearity, and in order to prevent energy loss, the switch must remain open for slightly longer than half the natural period of oscillation.

A short time later, a situation will arise which is similar to the situation obtaining at the instant when the switch was opened, i.e.

$$V_L = Vc_p = V;\ \mathrm{d}i_L/\mathrm{d}t = V, \text{ but now we have } i_L = -i_m.$$

This is evidently a suitable moment to close the switch again, for it is only at this instant that $V_{C_p} = V$, so that no energy is transferred from or to C_p when the switch is closed. The energy present in the magnetic field of the coil is once more $0.5\,Li_m^2$, and this is returned to the power supply during the first half of the subsequent scan. The reason for this is that after some time the current through the coil will again become zero, while the voltage across the capacitance is kept constant. There is thus a quantity of energy returned to the voltage source, which is equal to the quantity drawn from it before the switch was opened, so that, on the average, no power has been consumed.

It is true that the same amount of energy could be returned to the voltage source by closing the switch later, but the first part of the next scan would not then be linear.

It is also incorrect to close the switch earlier. The voltage across the capacitance is then opposed to that of the voltage source, so that the charge which still remains will disappear abruptly and the current at the beginning of the scan may thus be considerably lower than it was before the flyback.

We thus conclude that a linear sawtooth current through a loss-free coil can be obtained with, on the average, no consumption of energy, by connecting the coil via a switch to a voltage source during the scan, opening the switch at the beginning of the flyback, and closing it again at the instant when the voltage across the coil has once more reached the same value as the voltage source, after having passed through half a period of oscillation at its own natural frequency.

Another important conclusion is that, for loss-free operation, the duration of the flyback must be determined exclusively by the natural period of oscillation of the deflection coil and the capacitances in parallel with it, and must not be affected by opening the switch for a length of time which differs from this.

6.3.2. Practical realisation of the switch

If we try to replace the switch in Fig. 6.3.1.1. by a single valve – triode, tetrode or pentode – we soon find that the circuit does not meet the requirements we have laid down. This is because the valve is only able to pass the current in one direction, so that there can be no question of recovering energy after the flyback. Such a circuit can only be suitable for small deflection powers where the recovery of energy is of no interest.

With the larger angles of deflection and the high accelerating anode voltages of present-day picture tubes, as little as possible of the circulating energy must be lost. It is thus necessary to use a second valve so that current can flow in the opposite direction.

It is quite sufficient to use a diode for this purpose, as control of the circuit is already guaranteed by the presence of a single multi-electrode valve. For example, let us take the circuit of Fig. 6.3.2.1.

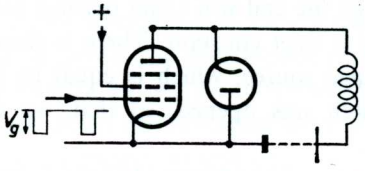

Fig. 6.3.2.1. Sawtooth current generator according to Fig. 6.3.1.1. in which the switch is formed by a pentode which is driven at the grid, and a diode connected in parallel, which allows current to flow in the reverse direction. The diode is switched into conducting or cut-off condition automatically by the anode voltages which occur.

The pentode is periodically cut off by a large negative pulse voltage on the control grid, initiating the flyback each time. This sharply increases the anode voltage of the pentode and the cathode voltage of the diode, so that the diode is also cut off. The anode voltage now completes half a period of oscillation as described above, until the voltage across the deflection coil is again equal to the supply voltage. The diode then becomes

conducting once more, so that from this instant the voltage across the coil is kept equal to the supply voltage; after this the pentode can also be made conducting again. It should be noted that the precise instant at which the switch closes again at the end of the flyback is automatically determined by the anode-to-cathode voltage of the diode. The pentode can be deblocked later, so that this half of the switch is conducting during the second half of the scan, when the current reverses its direction.

In this way, the switch is split into two parts, each of which allows the current to flow in one direction. This enables the energy which has been recovered to be used in a different manner to that which is possible with the circuit of Fig. 6.3.1.1.

We find the various possibilities illustrated in Fig. 6.3.2.1 to 6. Fig. 6.3.2.1

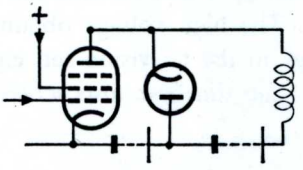

Fig. 6.3.2.2. As Fig. 6.3.2.1., but with a bias battery to give the pentode a small positive anode voltage during the forward sweep

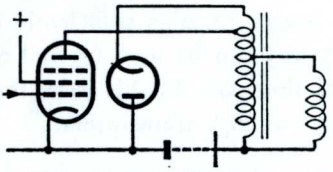

Fig. 6.3.2.3. As Fig. 6.3.2.2., but with a transformer to improve the matching. The anode voltage for the pentode during the scan is obtained from a tap on this transformer.

shows a ciruit corresponding to Fig. 6.3.1.1. The two switching valves are in parallel, so that the recovered energy flows back to the voltage source in the form of a return current. As the diode requires a slightly negative bias on the cathode in order to be able to conduct a current, while the pentode requires a slightly positive voltage on the anode, the circuit can be improved by giving the diode a small bias relative to the pentode. (Fig. 6.3.2.2). The same result is obtained with the circuit of Fig. 6.3.2.3., in which an autotransformer is used to generate this voltage automatically. In this connection, remember that the voltage across the deflection coil and thus also across that part of the transformer which is between diode and pentode is constant during the scan. The transformer also makes it possible to obtain good matching for the deflection coil, so that the required deflection can in fact be obtained with the available supply voltage. Although the diode is no longer connected exactly in parallel with the pentode in the circuits of Fig. 6.3.2.2 and 6.3.2.3, these are still classified as circuits having a *shunt efficiency diode*, because their operation corresponds to the principle of Fig. 6.3.2.1.

Fig. 6.3.2.4. shows a completely different form of the efficiency circuit.

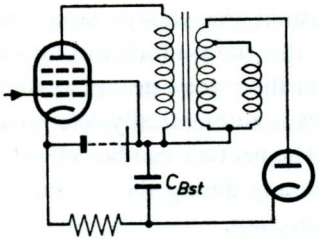

Fig. 6.3.2.4. Sawtooth current generator in which the energy remaining after the flyback is used to maintain a direct voltage across the capacitor $C_{B_{st}}$.

The current returned by the diode is no longer conveyed to the voltage source, but is used to charge the capacitor $C_{B_{st}}$. The resulting voltage on this capacitor can become considerably higher than the voltage of the voltage source. On the average, of course, the same charge must be drawn from this capacitor as is conveyed to it; otherwise, after a short time the diode no longer remains sufficiently conducting. The high voltage obtained in this way can be used to feed another stage in the television set, e.g. the field timebase. In this case, therefore, the line timebase also serves as a direct voltage transformer.

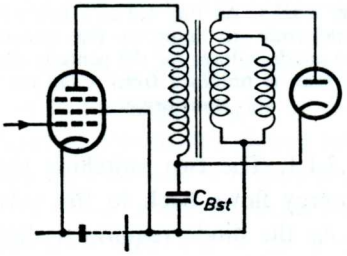

Fig. 6.3.2.5. Sawtooth current generator in which the voltage obtained across the capacitor $C_{B_{st}}$ is used to increase the supply voltage for the deflection circuit.

In the next circuit (Fig. 6.3.2.5), the increased voltage is used to supply the line timebase itself. This circuit with a *series efficiency diode* results in great advantages for the line timebase circuit. This is because the power output of the circuit is determined by the product of the current (peak value) and the voltage across the deflection coil. If a higher supply voltage is available, the currents which have to flow through the valves to give the same circulating power can be reduced. In addition, of course, it will be possible for the anode dissipations in these valves to be much lower, so that much less energy will be used. But even if special valves with extremely low internal resistance are made for use in the first circuit with a shunt efficiency diode, so that the anode dissipations no longer enter into the question, the circuit with the series efficiency diode still gives an indirect saving. This is because a valve with low internal resistance, which must be able to carry large currents, requires a large cathode surface and thus

Fig. 5.5.7.3
Half a Ferroxcube ring with a line coil and a field coil.

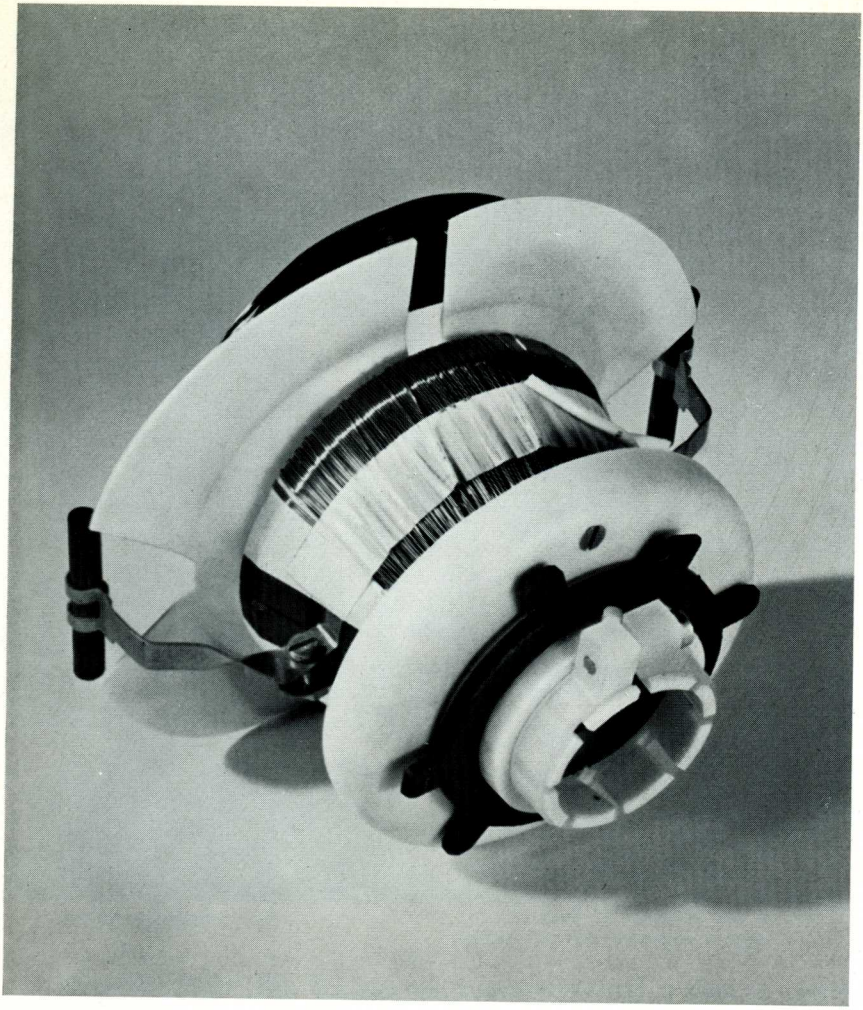

Fig. 5.5.7.4
The deflection unit seen from behind. The magnetic centring rings can be clearly seen.

more heater power. In addition, a large anode current in a pentode is unavoidably accompanied by a considerable screen-grid current which in itself is of no use to the circuit, while such valves would also have to be larger. Consequently, the circuit with a series efficiency diode has superseded all other possible arrangements.

We may now enquire if there is any point in making the supply voltage as high as possible. If we do this, we reach another limit, which is also set by the technological possibilities of the valves. We have already seen that during the flyback, i.e. with the switch open, a high inductive voltage arises across the latter. To prevent loss of energy, the valves will also have to be free of leaks, back emission and flashover. Since valves which can stand peak voltages above 6,000 to 7,000 volts, and which must also be able to carry quite large currents, are difficult to manufacture economically, there is no point in raising the supply voltage above 700 to 800 volts. The peak voltage during the flyback may reach seven to ten times the voltage during the scan, so that with a higher supply voltage the dangerous peak voltage limit would be exceeded. However, as the normal supply voltage in a television set is only 200–250 volts, a large increase in voltage is very welcome. The circuit with series efficiency diode, also termed a booster circuit, is thus eminently suitable for giving an economical horizontal deflection which is best adapted to the given supply voltage and the technological possibilities inherent in the valves.

This circuit is often combined with the circuit of Fig. 6.3.2.4. so that the increased voltage is also used to supply other stages in the television set. The resulting extra load is of course accompanied by a drop in the attainable voltage increase.

Finally, in Fig. 6.3.2.6., we recognize the same principle but the diode

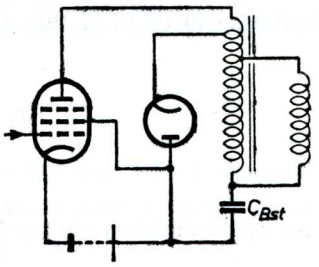

Fig. 6.3.2.6. The circuit of Fig. 6.3.2.5. with autotransformer.

has now been transferred to the primary side. This circuit was made possible by the production of a special type of diode, which can stand a high peak voltage between cathode and heater. With this arrangement, the losses in the transformer can be considerably lower than in the trans-

former with separate windings, principally because fewer losses occur due to leakage inductance.

As modern television sets make exclusive use of the circuit with series efficiency diode on the primary side, we will confine our attention to this type of circuit in our further consideration of horizontal deflection.

6.3.3. The flyback period

As can be seen from Fig. 6.3.1.2. the flyback period is somewhat longer than half an oscillation period. It is true that the current i_L continues to increase slightly in the interval between t_1 and t_0, but as this part of the curve is not linear, it is usually included in the flyback.

The flyback period is one of the starting points for calculating a deflection system, so it may be useful first of all to find an approximate expression for the relationship between the flyback period and the period of oscillation of the coil.

We have:

$$0{,}5\, C_p\, V_{\max}{}^2 = 0{,}5\, L\, i_m{}^2 + 0{,}5\, C_p\, V^2 \qquad (6.3.3.1.)$$

If the duration of the scan is t_s, the flyback is t_f and the angular frequency of the circuit formed by L and C_p is ω_f:

$$i_m = \frac{V t_s}{2\, L}.$$

Substituting in (6.3.3.1.) this gives:

$$V^2 = V_{\max}{}^2\, \frac{4\, LC_p}{t_s{}^2 + 4\, LC_p} \qquad (6.3.3.2.)$$

Now $LC_p = \dfrac{1}{\omega_f{}^2}$ and according to Fig. 6.3.1.2. :$V_{\max} \cos \omega_f \dfrac{t_f}{2} = V.$

Substituting in (6.3.3.2) this gives:

$$t_s = \frac{2}{\omega_f}\, \frac{\sin \omega_f \dfrac{t_f}{2}}{\cos \omega_f \dfrac{t_f}{2}}.$$

As an approximation $\sin \omega_f \dfrac{t_f}{2} \approx 1$ and

$$\cos \omega_f \frac{t_f}{2} = \sin \left(\omega_f \frac{t_f}{2} - \frac{\pi}{2} \right) \approx \omega_f \frac{t_f}{2} - \frac{\pi}{2}.$$

This gives:

$$t_s = \frac{4}{\omega^2{}_f t_f - \pi \omega_f}.$$

Which can be converted to:

$$\frac{\omega_f t_f}{\pi}\left(\frac{\omega_f t_f}{\pi} - 1\right) = \frac{4}{\pi^2}\frac{t_f}{t_s} = \frac{4}{\pi^2}\frac{p}{1-p} \qquad (6.3.3.3.)$$

where $p = \dfrac{t_f}{t_s + t_f}$, the fraction of a sawtooth period which is used for the flyback.

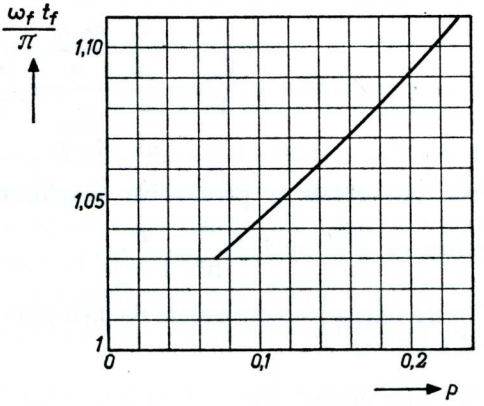

Fig. 6.3.3. Ratio of the flyback period to a half period of the natural oscillation period as a function of the flyback ratio p.

The value of $\dfrac{\omega_f t_f}{\pi}$, calculated according to equation (6.3.3.3.) is drawn in Fig. 6.3.3. as a function of p. This graph shows that for a normal value of p (0.15 — 0.16) the flyback period is about 7% longer than half an oscillation period.

This relationship between the oscillation period and the flyback period is not particularly interesting in itself, but it offers the possibility of finding an expression for the relationship between the voltage across the coil during the scan and the peak voltage which appears across it during the flyback.

6.3.4. Peak voltage

The maximum voltage V_m which occurs during the flyback can now be determined. It is of course proportional to the voltage V during the scan, and is also a function of p.

According to Fig. 6.3.1.2:

$$\frac{V_m}{V} = \frac{1}{\cos \omega_f \dfrac{t_f}{2}} .$$

By approximating to $\cos \omega_f \frac{t_f}{2}$ by $\omega_f \frac{t_f}{2} - \frac{\pi}{2}$ this becomes

$$\frac{V_m}{V} = \frac{\frac{2}{\pi}}{\frac{\omega_f t_f}{\pi} - 1} .$$

Substitution of equation (6.3.3.3) gives

$$\frac{V_m}{V} = \frac{\frac{2}{\pi} \quad \frac{\omega_f t_f}{\pi}}{\frac{4}{\pi^2} \quad \frac{p}{1-p}} = \frac{\pi}{2} \frac{1-p}{p} \frac{\omega_f t_f}{\pi} .$$

We can obtain a permissible simplification if we approximate to the value of $\frac{\omega_f t_f}{\pi}$ by $1 + \frac{4}{\pi^2} \frac{p}{1-p}$.

To do this, we simply equate the first term on the left-hand side of equation (6.3.3.3.) to 1.

We then have:

$$\frac{V_m}{V} = \frac{\pi}{2} \frac{1-p}{p} \left(1 + \frac{4}{\pi^2} \frac{p}{1-p}\right) = \frac{\pi}{2} \frac{1-p}{p} + \frac{2}{\pi} \qquad (6.3.4.)$$

This relationship, which is important for the determination of the peak voltage on the deflection coil and the switching valves will from now on be referred to as F_p. Fig. 6.3.4. shows the value of F_p as a function of the flyback ratio p.

It should be noted that this ratio is calculated for a sinusoidal flyback. However, the deflection transformer is usually designed so that an os-

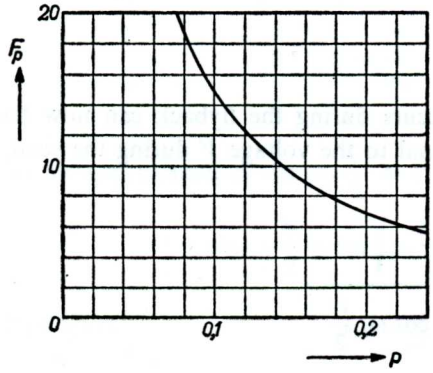

Fig. 6.3.4. Flyback to scan-voltage ratio, as a function of p.

cillation of still higher frequency is superimposed on the flyback voltage. Amongst other things, this results in a reduction of the maximum peak voltage which appears on the output valve and the diode. The value of F_p then determines the amplitude of the fundamental only; the actual value of the peak voltage can be found by applying a correction to the value of F_p, depending on the amplitude of the high frequency oscillation. Under favourable conditions, the value of F_p can in this way be reduced by approximately 20%.

6.3.5. The effect of losses during the flyback

Up to now, no account has been taken of the losses which will always occur in practice.

In this connection, the losses which occur during the flyback and which can be represented by a parallel resistance are particularly important. Such losses occur in the dielectric between the turns of the coil, plus the losses due to the changes in the direction of magnetisation of the Ferroxcube cores of the deflection coil and the transformer, and finally some of the energy is used for generating the final anode voltage (and current) for the picture tube.

The energy stored in the deflection coil (L_y) at the beginning of the flyback is: $W_1 = \frac{1}{2} L_y i_1^2$ and at the end of the flyback $W_2 = \frac{1}{2} L_y i_2^2$ where, in agreement with Fig. 6.3.5.1, i_2 is smaller than i_1 because of the losses which have occurred.

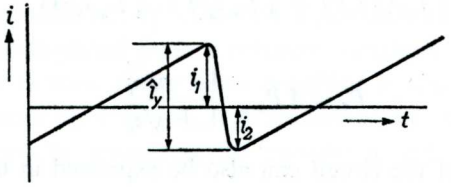

Fig. 6.3.5.1. Oscillogram of the sawtooth current through the deflection coil. Because of the losses during the flyback, i_2 has a smaller value than i_1.

The average power which is conveyed to the deflection coil during the scan is thus:

$$P_1 = W_1 f = \tfrac{1}{2} L_y i_1^2 f$$

and the power which is recovered after the flyback is

$$P_2 = P_1 - P_f = W_2 f = \tfrac{1}{2} L_y i_2^2 f,$$

where P_f is the loss during the flyback. This loss means that an extra

current $\frac{i_1 - i_2}{2}$ has to be supplied during the scan, resulting in a load of $P_f = V_y \frac{i_1 - i_2}{2}(1-p)$ on the supply, where V_y is the voltage across the deflection coil during the scan.

The efficiency of the circuit is:

$$\eta = \frac{P_1 - P_f}{P_1} = \frac{i_2^2}{i_1^2} \qquad (6.3.5.1.)$$

The peak current i_1, which is required in order to obtain the total deflection current $\hat{\imath}_y = i_1 + i_2$ then becomes:

$$i_1 = \frac{\hat{\imath}_y}{1+\sqrt{\eta}} \qquad (6.3.5.2.)$$

If P_{my} is the total magnetic power in the deflection coil, P_f can be expressed in terms of P_{my} and η.

$$P_{my} = \tfrac{1}{2} L_y (\tfrac{1}{2}\hat{\imath}_y)^2 f; \text{ and since } V_y = \frac{L_y \ \hat{\imath}_y \ f}{1-p} :$$

$$P_{my} = \tfrac{1}{8} V_y \ \hat{\imath}_y (1-p) \qquad (6.3.5.3.)$$

We have:

$$P_f = P_1 - P_2 = \tfrac{1}{2} L_y (i_1^2 - i_2^2) f = \tfrac{1}{2} L_y i_1^2 (1-\eta) f$$

and

$$P_{my} = \tfrac{1}{2} L_y (\tfrac{1}{2}\hat{\imath}_y)^2 f = \tfrac{1}{8} L_y \hat{\imath}_y^2 f = \tfrac{1}{8} L_y i_1^2 (1+\sqrt{\eta})^2 f \ .$$

From which:

$$P_f = 4 P_{my} \frac{1-\sqrt{\eta}}{1+\sqrt{\eta}} \qquad (6.3.5.4.)$$

The efficiency of the circuit can also be expressed in terms of the magnification Q_f of the resonant circuit formed by the self inductance of the deflection circuit with the stray capacitances.

During the flyback, the energy in this circuit decreases according to

$$W = W_1 \, e^{-\frac{\omega_f t}{Q_f}}$$

so that at the end of the flyback the remaining energy is:

$$W_2 = W_1 \ e^{-\frac{\omega_f t_f}{Q_f}} \ .$$

The efficiency now becomes $\eta = \frac{W_2}{W_1} = e^{-\frac{\omega_f t_f}{\pi} \ \frac{\pi}{Q_f}} \ .$

For a normal flyback ratio of 15%

$$\frac{\omega_f t_f}{\pi} \approx 1.07, \text{ so that } \eta = e^{-1.07 \frac{\pi}{Q_f}} .$$

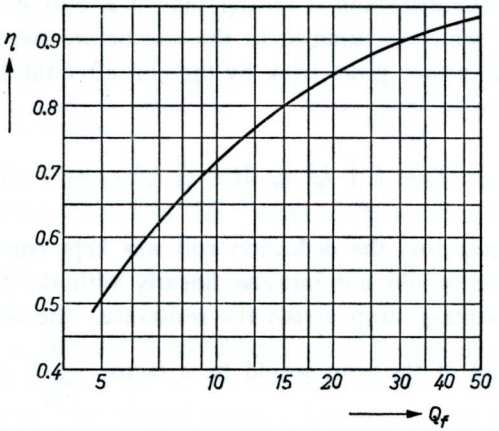

Fig. 6.3.5.2. Relationship between the Q factor at the flyback frequency and the current efficiency.

The relationship between Q and η is indicated in Fig. 6.3.5.2.

The practical usefulness of a Q measurement at the flyback frequency, however, is only relative, because the conditions – high voltages and currents – which apply in a working circuit remain unattainable during a Q measurement.

Nevertheless, a Q measurement could be used to compare the quality of different deflection coils, and it is also possible to obtain an indication of the efficiency to be expected from a complete timebase.

The final determination of the losses occurring in this circuit during the flyback, together with the value of η can be carried out in a simple manner in a working circuit by measuring the currents i_1 and i_2.

6.3.6. Losses during the scan

Since the deflection coils also have series resistance, the voltage across them during the scan for a linear variation of the deflection current will be made up of a constant inductive component and a sawtooth voltage of amplitude:

$$\triangle V_y = \hat{\imath}_y \, r_y \quad ,$$

and since

$$\hat{\imath}_y \approx \frac{V_y t_s}{L_y} \quad ,$$

we have:

$$\frac{\triangle V_y}{V_y} = \frac{r_y t_s}{L_y} \quad .$$

The voltage across the deflection coil is thus smaller at the beginning of the scan than at the end.

The average value of the product of current and voltage during the second part of the deflection is greater than it is during the first part, so that the power which is supplied to the coil before the flyback must be greater than the power given back by the coil after the flyback.

The losses are

$$P_s = f \int_0^{t_s} i_y^2 \, r_y \, dt = \tfrac{1}{12} \, \hat{\imath}_y^2 \, r_y \, (1 - p) \qquad (6.3.6.)$$

If the voltage across the deflection coil was kept constant during the scan, the current would not increase linearly with the time, because of the increasing voltage drop across the resistance. The deflection velocity $\left(\frac{di_y}{dt}\right)$ at the end of the scan would be a factor $\frac{\triangle V_y}{V_y}$ smaller than at the beginning.

For a practical coil, for which $r_y\,(\Omega) \approx 1000\, L_y\,(\mathrm{H})$ the non-linearity at a line frequency of 15,625 cycles per second becomes:

$$\frac{\triangle V_y}{V_y} = \frac{r_y \, t_s}{L_y} = 0{,}06.$$

Although a non-linearity of this order is not so serious – as a result of the very gradual decrease in the deflection velocity during the scan, the non-linearity cannot be observed so very clearly – a correction will as a rule be applied. The reason is that a constant voltage across the deflection coil cannot in fact be obtained without special precautions, because of the internal resistance of the valves, so that the non-linearity becomes appreciably greater. The linearity correction compensates for the deviations due to both the above causes.

6.3.7. Correction of the asymmetrical non-linearity

A much – used method of linearity correction consists of including a small coil, wound on a small Ferroxcube core which is pre-magnetised by means of a permanent magnet, in series with the deflection coil. (Fig. 6.3.7.)

At the beginning of the scan the direction of the current is such that the induced field cancels out or reduces the field of the permanent magnet. The self inductance of the small coil, and the voltage drop across it, are then a maximum.

During the second half of the scan, when the current changes in direction,

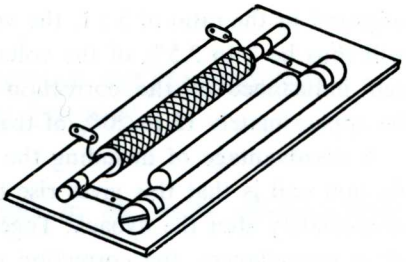

Fig. 6.3.7. A simple form of coil for correction of asymmetrical nonlinearity. The coil is wound on a small Ferroxcube rod, which is premagnetised by means of a permanent magnet. The eccentric mounting of the magnet on a rotatable support makes it possible to adjust the degree of premagnetisation.

the Ferroxcube is driven nearer and nearer to saturation, as a result of which the self inductance and the voltage drop are finally reduced to a minimum. With suitable dimensioning, the self inductance is then still approximately 20% of the self inductance at the beginning of the scan. The permanent magnet can be adjusted so that the increase in the voltage drop due to the resistances in the deflection coil and the circuit during the scan is exactly compensated by the decrease in the voltage drop across this correction coil. The desired result – linearization of the deflection – can thus be obtained, but of course at the cost of extra voltage loss in this correction coil.

Other methods of linearity correction also cause a similar loss. For the design of the transformer, however, it is important that this voltage drop only needs to be small at the end of the scan – of the order of a few per cent of the voltage across the deflection coil. This enables us to make a fairly accurate estimate of the total voltage required for the deflection coil and linearity correction at the end of the scan.

The voltage loss in the output valve and the diode can also best be estimated for the end of the scan, while as far as the peak current in the output valve is concerned, we are also only interested in the conditions which apply at this instant. Thus, the calculation of the deflection circuit can best be based on the situation at the *end of the scan*, neglecting for the time being the excess voltage which appears at the beginning of the scan, and which has to be compensated by the linearity correction.

This excess voltage depends in the first place on the internal resistance of the efficiency diode. If the current through this diode has an acceptable waveform, there is a much higher voltage drop across it at the beginning of the scan than at the end, so that the voltage across the deflection coil at the beginning of the scan can be approximately 4 to 10% higher than at the end. Without correction, the total nonlinearity will thus be 10 to 17%, remembering that the resistance of the transformer also has to be taken into account, in addition to that of the deflection coil.

Assuming that the voltage across the linearity correction coil can be

adjusted in the ratio of 5 : 1, the voltage loss in it at the end of the scan will thus be 2 to 3.5% of the voltage across the deflection coil, while the self inductance of the correction coil without pre-magnetisation must be approximately 12 to 20% of that of the deflection coil.

A disadvantage of including the correction coil in series with the deflection coil is that this gives rise to oscillations in the deflection current immediately after the flyback. Together with its self capacitance, and with stray capacitances, the correction coil forms a resonant circuit in which high-frequency oscillations are generated by the rapid variation in current during the flyback. These oscillations then die out slowly at the beginning of the scan, and also modulate the voltage appearing across the deflection coil, so that the current in it no longer varies continuously. Whether the image is modulated or not, this manifests itself in the appearance of light and dark vertical stripes at the left-hand side of the screen. The oscillations can usually be reduced sufficiently by connecting a damping resistor in parallel with the correction coil.

THE DEFLECTION CIRCUIT WITH SERIES EFFICIENCY DIODE

7.1. Relationships between the currents in the series efficiency-diode circuit

In order to arrive at a simple picture of the relationships between the currents which appear in the output circuit, it will again be assumed to begin with that the effect of the resistance of the deflection coil is negligible, that the booster capacitor C_{Bst} (Fig. 7.1.1.) has such a high value that the ripple voltage is very small in relation to the direct voltage, and that the booster diode has such a small internal resistance that the voltage drop across it is also negligible in relation to the direct voltage across the capacitor. The transformer will be regarded provisionally as an ideal transformer.

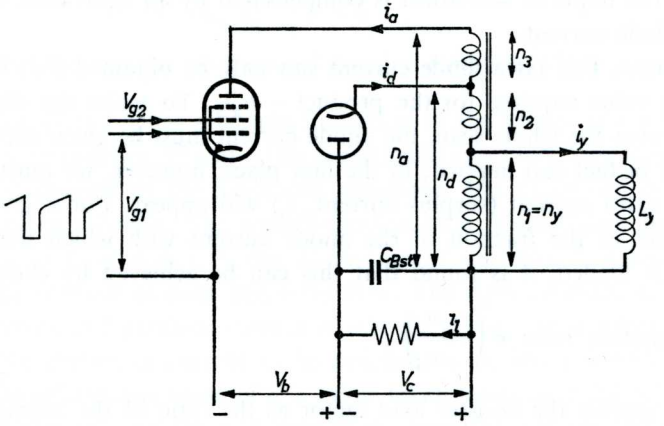

Fig. 7.1.1. The general form of the circuit with series efficiency diode.

As long as the diode in the circuit of Fig. 7.1.1. remains conductive, the voltage across L_y is constant, so that i_y has the required linear form. To generate this current, the combined currents of the pentode and the diode through n_a and n_d must give linear magnetisation, so that a constant magnetic flux is obtained in the (ideal) transformer:

$$\text{thus:} \quad n_a\ i_a + n_d\ i_d = -n_y\ i_y \ .$$

An example of how this can happen is shown in the "reduced current oscillogram" of Fig. 7.1.2., in which the individual current oscillograms are multiplied by the number of turns through which these currents pass.

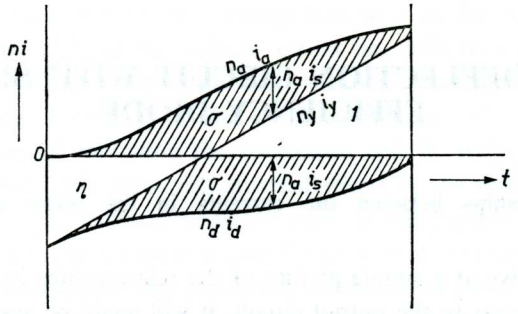

Fig. 7.1.2. Reduced current oscillogram for the circuit of Fig. 7.1.1., obtained by multiplying the currents by the number of turns through which they flow. The flyback is not drawn.

The contribution above the 0-axis to the product $-n_y i_y$ is supplied by $n_a i_a$, while the part below the axis is supplied by $n_d i_d$. The deviation of i_a from the required waveform is compensated by an equivalent deviation of the diode current.

Of course, this extra diode current can only be obtained if i_a is greater than the value required for the product $-n_y i_y$. To make the diode conducting over the whole scan, the anode current must be given such a form that this in fact can happen; in the first place, however, we must arrange that an extra current (surplus current, i_s) will appear. For a given value of η, and of the fraction of the anode current with which the booster voltage is loaded, it is found that this can be achieved by choosing the transformation ratio $n \left(= \frac{n_d}{n_a}\right)$.

If we express the booster load factor as the ratio of the average anode currents of diode and pentode

$$\Psi = \frac{\bar{i}_d}{\bar{i}_a} = \frac{\bar{i}_a + \bar{i}_l}{\bar{i}_a}$$

and the average current surplus in the surplus factor,

$$\bar{\sigma} = \frac{\bar{i}_s}{\bar{i}_a - \bar{i}_s},$$

it is possible to deduce that the surplus factor is equal to

$$\bar{\sigma} = \frac{n\Psi - \eta}{1 - n\Psi} \tag{7.1.}$$

This result follows from the consideration that the *transformed* average surplus currents of diode and pentode must be equal, while the *non-transformed* diode current is equal to the sum of the anode current of the pentode and the booster load current.

According to the reduced current oscillogram of Fig. 7.1.2. we have, above the 0-axis:

$$n_a\,\bar{i}_a = n_a\,\bar{i}_a\,\frac{1}{1+\bar{\sigma}}\ \text{(not shaded)} + n_a\,\bar{i}_a\,\frac{\bar{\sigma}}{1+\bar{\sigma}}\ \text{(shaded)}$$

Below the 0-axis

$$n_d\bar{i}_d = \eta\, n_a\,\bar{i}_a\,\frac{1}{1+\bar{\sigma}}\ \text{(not shaded)} + n_a\,\bar{i}_a\,\frac{\bar{\sigma}}{1+\bar{\sigma}}\ \text{(shaded)}$$

from which

$$\frac{n_d}{n_a}\,\frac{\bar{i}_d}{\bar{i}_a} = \frac{\eta+\bar{\sigma}}{1+\bar{\sigma}} = n\Psi$$

This expression can be re-arranged to give equation (7.1.)

Equation (7.1) implies a certain limitation of the values of n which can be chosen. In practice, Ψ and η (for a particular case) will have fixed values which are imposed by the conditions obtaining, and which can usually be determined in advance. The transformation ratio n must then be chosen so that $\bar{\sigma} > 0$. If it is not, the diode current will have dropped to zero before the pentode current begins to flow. The right connection between diode current and pentode current is missed, giving rise to a troublesome kink in the deflection current i_y. In practice, to ensure a good deflection current waveform, the value of $\bar{\sigma}$ is never taken lower than 0.2, which thus gives a minimum limit for n. A maximum value for n is reached because, as will be explained later, the flyback voltage on the valves will increase with increasing n. Under given conditions (supply voltage, anode voltage during the scan, flyback period) this results in a flyback voltage which reaches the limiting value for the diode or the pentode.

Between these minimum and maximum values of n, there is usually a certain freedom in the choice of the transformation ratio, so that various methods of driving are possible.

Besides the transformation ratio, the form of the anode current (grid voltage) also affects the drive; this cannot change the value of $\bar{\sigma}$, but it can affect the distribution of the surplus during the course of the scan. This is illustrated, for example, in the current diagrams in Fig. 7.1.3.

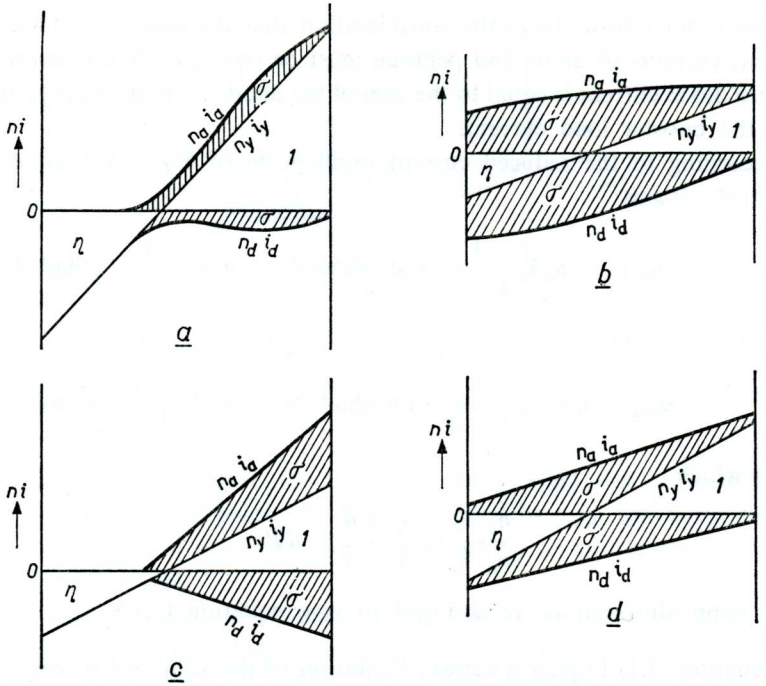

Fig. 7.1.3. Reduced current oscillograms under various conditions.
a) Transformation ratio calculated for small $\bar{\sigma}$, resulting in a high ratio between peak anode current and average anode current.
b) Transformation ratio calculated for large $\bar{\sigma}$, giving a more favourable ratio between peak current and average current. However, the peak voltage during the flyback is increased by just as much relative to a, as the peak current has decreased.
c) Transformer calculated for medium $\bar{\sigma}$, but with the peak current too high because of incorrect driving. The pentode is blocked for too long.
d) The same transformer as in *c*, but with optimum drive.

Figs. 7.1.3.*a* and *b* show the reduced current oscillograms for two different transformer designs. Fig. 7.1.3.*a* is the diagram for a small $\bar{\sigma}$ (in the region of 0.2) so that, according to equation (7.1) the product $n\Psi$ is only slightly higher than η. Such a small surplus means that the pentode must be carefully driven, so that the diode still remains conductive during the whole scan.

By contrast, we have the current diagram of Fig. 7.1.3.*b*., in which the transformation ratio is calculated for a large surplus ($\bar{\sigma}$ approx. 2.) The advantage of this method of driving, compared with the previous one, is to be found in the lower value of the peak current which is required for a given deflection. This is easy to understand if we remember that, with the same supply voltage in both cases, the average values of the currents for the same deflection will be approximately equal.

However, a low peak current is attractive because it is then possible to use a small valve, or a lower screen-grid voltage (and current), even though the average anode current remains practically the same. Consequently, designers will always try to obtain the highest possible surplus, but as the circulating magnetic energy is determined by the product of peak current and peak voltage, the drop in peak current will be accompanied by an increase in the peak voltage. The maximum permissible voltage on the output valves thus sets a limit to their attempts.

The current diagrams of Figs. 7.1.3.*c* and *d* are for one and the same transformer, so that the values of $\bar{\sigma}$ are the same. The difference lies entirely in a different method of driving the pentode. With the method of driving represented by Fig. 7.1.3.*c*, as in Fig. 7.1.3.*a*., a larger sawtooth voltage is applied to the grid of the output valve than the grid base of this valve can take. The pentode thus continues to be cut off for some time after the flyback (suppressed sawtooth drive).

As this transformer works with a greater surplus than that of Fig. 7.1.3.*a* there is now a large surplus current at the end of the scan, so that the peak current which the pentode has to supply is again much higher than it is for the driving method of Fig. 7.1.3.*d*.

There is practically no advantage to be set against this high peak current; it is not accompanied by a reduced peak voltage, because the surplus in the pentode current is simply compensated by an equivalent surplus in the diode current, and thus takes no part in building up the magnetic field.

The above considerations show that on one hand we must choose the transformation ratio to give the greatest permissible surplus, with an eye to the peak voltages, but on the other hand the pentode drive must be arranged so that the surplus at the end of the scan is as small as possible. The oscillogram of the diode current, taken across a small resistance in series with the diode, provides a simple check on the drive.

7.2. Voltage relationships

7.2.1. The effect of the drive on the voltage form, current form and distribution of the surplus

In considering the voltage relationships, the resistances and the leakage inductance of the transformer will again be neglected at first. In the voltage oscillogram of Fig. 7.2.1.1 it is also assumed that the diode current at the end of the scan has just reached zero. The diode peak current immediately

after the end of the flyback then has a value:

$$\hat{\imath}_d = \frac{\sqrt{\eta}\,\hat{\imath}_a + i_{ai}}{n}$$

where i_{ai} represents the anode current of the pentode at the beginning of the scan. In Fig. 7.2.1.1., however, this has been made equal to 0. The diode current causes a voltage drop $V_d = \hat{\imath}_d r_d$ across the diode, and this voltage gradually decreases to zero during the scan. The voltage on the cathode of the diode thus rises from $V_b - V_d$ to V_b.

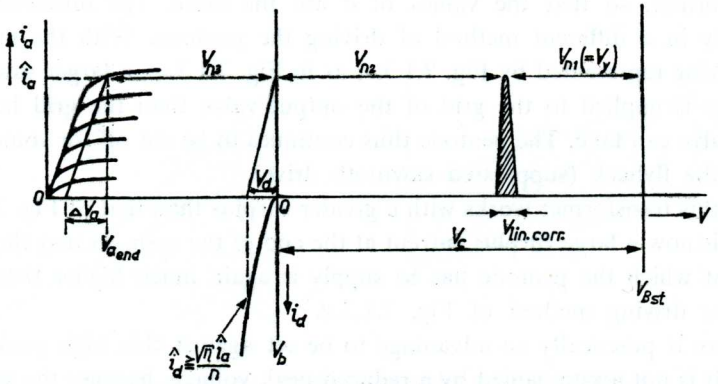

Fig. 7.2.1.1. Voltages occurring during the scan in the circuit of Fig. 7.1.1.

The booster capacitor C_{Bst}, which is periodically being charged by the diode current, is so large that after a number of periods the voltage across it reaches the constant value V_c. The total supply voltage thus reaches the value $V_{Bst} = V_b + V_c$.

As this voltage is constant, the load line of the pentode must also have a slope, i.e. $\triangle V_a = \frac{V_d}{n}$. Let us assume that this load line is situated to the right of the steep part of the i_a/V_a characteristic (above the knee).

Of course, this slope can only be obtained if the grid drive is such that the load line cuts the successive characteristics at the points shown in the diagram. If this was not the case, the diode current would not have been able to adopt the suitable form which has been assumed for it.

With the same output transformer, a strong suppression of the anode current at the beginning of the scan (suppressed sawtooth drive) will, for example, result in a shift of the load line as in Fig. 7.2.1.2. The diode current then shows a large surplus at the end of the scan. This method of driving favours linearity, as it results in a constant or even increasing

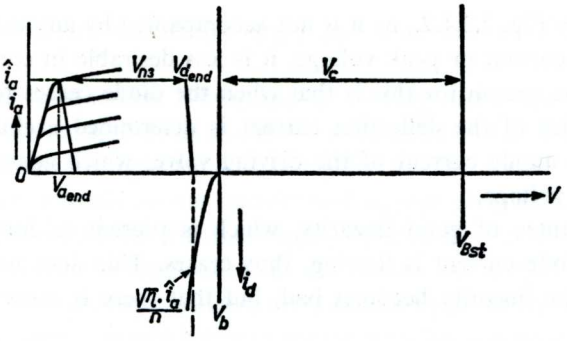

Fig. 7.2.1.2. Voltage occuring in the circuit of Fig. 7.1.1., when incorrectly driven. The sawtooth voltage on the grid of the pentode is too large, so that there is an excess surplus at the end of the scan.

voltage across the deflection coil during the scan. However, the large diode current at the end of the scan means that a much higher peak current is required from the pentode than would normally be the case (See Fig. 7.1.3.*c*.)

The method of driving indicated by Fig. 7.2.1.3 shows a deviation in the opposite sense, in that the pentode is opened too far shortly after the flyback. (pulse drive). Again with the same output transformer, this causes a large surplus in the diode current shortly after the flyback, so that the average surplus for which the transformer was calculated is used during the first half of the scan.

The diode thus becomes cut off during the second half of the scan. Although this condition is less harmful than the above-mentioned one

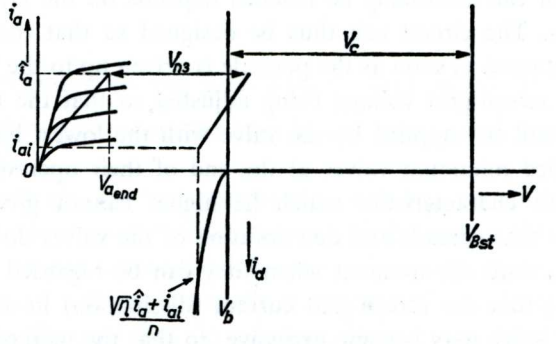

Fig. 7.2.1.3. The sawtooth voltage on the grid of the pentode is too small, so that there is an excess surplus at the beginning of the scan. The diode current is interrupted before the end of the scan.

illustrated by Fig. 7.2.1.2., as it is not accompanied by any useless increase in the peak current or peak voltage, it is less desirable in connection with linearity. The reason for this is that when the diode ceases to take a current, the form of the deflection current is determined exclusively by the form of the anode current of the driving valve, which again depends on the driving voltage.

The guarantee of good linearity, which is present as long as a compensating diode current is flowing, thus ceases. This does not necessarily mean that the linearity becomes bad, but that there is more chance of it doing so.

7.2.2. Driving below the knee of the i_a/V_a characteristic

In all the previous cases it was assumed that the load line of the pentode was situated to the right of the knee line, so that the predominant influence on the size of the anode current is exercised by the grid and screen-grid voltages. If these voltages are increased, the increasing current and the greater voltage drop across the transformer winding n_3 will cause the load line to move over to the left until it coincides with the steep part of the i_a/V_a characteristic below the knee.

Any further increase in the current is now impeded by the accompanying drop in anode voltage, even if the grid voltage or the screen-grid voltage were increased still further. Now the position of the i_a/V_a characteristic below the knee is much less subject to change due to variations in emission losses in the valve, and due to production spreads, than the position of the characteristic above the knee. Only the maximum value of the anode peak current which can eventually be reached depends on the grid and screen-grid voltages. The circuit can thus be designed so that the required deflection is obtained as soon as the pentode is driven up to the knee, the grid voltage and screen-grid voltage being adjusted so that the required peak current can still be supplied by the valve with the lowest lying characteristic. (So-called minimum valves at the end of their operating life).

Valves with characteristics which lie higher cannot give any greater deflection, so that spreads and deterioration of the valves do not have any visible effect, until the moment when they can be regarded as worn out. It is possible that the screen-grid current (dissipation) in a "normal" or "maximum" valve may become excessive, so that the method can only be advantageous if the required peak current is a certain fraction (e.g. 30%) lower than the current which can be supplied by a new valve having the nominal ratings, with the maximum permissible screen-grid dissipation. For

that matter, similar restrictions apply just as much to driving above the knee.

Against the considerable advantages of driving below the knee, a disadvantage is the reduced flexibility in the form of the drive. This is because the anode current is determined principally by the anode voltage, and this in its turn depends on the transformed voltage drop across the diode. The form of the currents will thus depend principally on the relationship between the internal resistances of the two valves. As neither of these can be zero, it is not possible to realise a drive according to the current diagrams of Fig. 7.1.3. *b* and *c*, in which one of the currents has a practically constant value during the scan, and thus causes a constant voltage drop across the valve, while the other current must be markedly sawtoothed. However, it will usually be possible to achieve one's object with a form of drive corresponding approximately to that of Fig. 7.1.3. *a* or *d*, in which both currents are more or less sawtoothed. In addition, the internal resistances of the two valves can be matched by connecting a small resistor in series with one of them, while it always remains possible to affect the current form by means of the grid voltage. In this case, of course, the load line cannot coincide with the steep part of the i_a/V_a characteristics over all its length, but must deviate partly to the right, which will cause a worsening of the stabilisation. Particularly for large deflection powers, driving below the knee is also accompanied by the objection of heavy loading of the screen grid, and an increasing chance of parasitic oscillations. As a result, driving above the knee, for which a new stabilisation technique has been developed, is once more being increasingly employed. The advantages and disadvantages of various circuits will be discussed further in sections 9.3.1 to 9.3.3.

7.2.3. Calculation of the scan and flyback voltages

The voltages during the scan can now be determined with the aid of Figs. 7.1.1 and 7.2.1.1.

As these voltages are not completely constant, we choose a certain instant during the scan, for which the end of the scan is found to be the most suitable. At that instant the deflection coil requires the highest voltage, while the primary voltage across the transformer is a minimum, because of the slope of the load line. In addition, there is practically no voltage drop across either the diode or the linearity correction coil.

In agreement with Fig. 7.2.1.1 we then have

$$V_{n_3} = V_b - V_{a_{\text{end}}},$$

where $V_{a\text{end}}$ represents the anode voltage at the end of the scan.

The voltage across the whole primary winding of the transformer is:

$$V_{n_a} = \frac{V_b - V_{a\text{end}}}{1-n} \qquad (7.2.3.1.)$$

The booster voltage V_{Bst} is:

$$V_{B_{st}} = V_{n_a} + V_{a\text{end}} = \frac{V_b - V_{a\text{end}}}{1-n} + V_{a\text{end}} \qquad (7.2.3.2.)$$

We can now calculate the value of the transformation ratio n_y/n_a to give the required deflection, starting from the voltage V_y required on the deflection coil at the end of the scan:

$$V_y = \frac{L_y \hat{\imath}_y f}{1-p} + \tfrac{1}{2}\hat{\imath}_y r_y \qquad (7.2.3.3.)$$

If a linearity correction coil (and perhaps an amplitude-control coil) is included in the current circuit of the deflection coil, the self inductance L_y of the deflection coil must be increased by that of the linearity coil at the end of the scan.

If this is not known, it can be represented provisionally by a small fraction (say 3%) of the self inductance of the deflection coil; r_y represents the combined resistance of the deflection coil and the correction coil.

A further voltage loss, which cannot be neglected, may be occasioned by the leakage inductance of the transformer between the windings n_y, and n_a and n_d. The size of this loss depends on a number of factors which will be discussed in section 7.3.3.

It can be compensated by making the *e.m.f.* V_y' induced in the transformer a fraction s higher than V_y; this fraction can be estimated on the basis of experience obtained with earlier designs, or with the aid of Figs. 7.3.3.6. *a* and *b* and 7.3.3.5.2, which give the size of the coupling factor k and the associated leakage losses for a number of commonly used transformer cores. (s is approximately 0.01 — 0.05)

We then have

$$V_y' = (1+s)\,V_y \qquad (7.2.3.4.)$$

and

$$\frac{n_y}{n_a} = \frac{V_y'}{V_{n_a}} = \frac{V_y'\,(1-n)}{V_b - V_{a\text{end}}} \qquad (7.2.3.5.)$$

The peak voltages which appear across the deflection coil and the output valves during the flyback can now be calculated if the flyback ratio p is known. If necessary this ratio can be changed or adapted by connecting

a coil or a capacitor in parallel across the deflection coil or any other winding on the transformer.

The ratio F_p of the flyback voltage to the inductive voltage during the scan can be found from equation (6.3.4.) or from Fig. 6.3.4; if oscillations of higher frequency still occur in the flyback, F_p will have to be corrected slightly.

The peak voltage on the deflection coil is then:

$$\hat{V}_y = F_p \frac{L_y i_y f}{1-p} \qquad (7.2.3.6.)$$

The peak voltage on the output pentode (between anode and cathode) is found from:

$$\hat{V}_a = F_p (V_{Bst} - V_{a_{end}}) + V_{Bst} \approx (1 + F_p)(V_{Bst} - V_{a_{end}}) = \\ = \frac{(1 + F_p)(V_b - V_{a_{end}})}{1-n} \qquad (7.2.3.7.)$$

The peak voltage on the diode (between anode and cathode) is:

$$\hat{V}_d = (1 + F_p)(V_{Bst} - V_b) = (1 + F_p)\left[\frac{V_b - V_{a_{end}}}{1-n} - (V_b - V_{a_{end}})\right] = \\ = \hat{V}_a - (1 + F_p)(V_b - V_{a_{end}}) \approx n\,\hat{V}_a \qquad (7.2.3.8.)$$

The peak voltage between cathode and heater of the diode is $\hat{V}_f = \hat{V}_d + V_b + V_{fe}$, where V_{fe} is the maximum potential between the heater and the negative pole of the voltage source V_b.

That the voltages during the scan and flyback will increase sharply with increasing values of the transformation ratio n, is clear from equations (7.2.3.1 -2, -7 and -8), if we assume that in every case we shall try to make the best possible use of the available supply voltage V_b, and that consequently $V_{a\text{end}}$ will always be made as low as possible. As a rule, V_b will have a given value, e.g. because it is obtained by direct rectification of the mains voltage without the use of a transformer; $V_{a\text{end}}$ will always be either on the knee or else slightly above it, e.g. 40 to 70 volts, so that the losses in the pentode can remain low. For a good design, therefore, care must be taken when choosing the transformation ratio to see that the maximum permissible peak voltage limits of the output valves are not exceeded.

7.3. The design of the output transformer

7.3.1. Determination of the transformation ratios

In the design of a line output transformer, the choice of the transformation ratio has a great effect on the result, as we have seen above.

Although the design may allow a certain latitude where only small deflection powers are involved, with the greater powers which are required for 110° deflection, for example, the peak currents and peak voltages must be carefully aligned with the possibilities and the limiting values of the output valves.

In such a case, it is preferable to take the maximum permissible peak voltage on the valves as the starting point, while in addition the available supply voltage and the desired flyback ratio be regarded as given.

The first step is to calculate the value of F_p from equation (6.3.4). (Fig. 6.3.4). The anode voltage of the output valve at the end of the scan can be put at a reasonable value, say 40 to 70 volts, depending on whether the design is intended for driving below or above the knee. As the peak voltage limits will not usually be reached simultaneously on both valves, we must find which valve reaches this limit first.

According to equation (7.2.3.8) the difference in the peak voltages is

$$\hat{V}_a - \hat{V}_d = (1 + F_p)(V_b - V_{a_{end}}) \quad .$$

If this difference is greater than the difference between the maximum permissible voltages, the pentode reaches the limit first, and vice versa. In the first case, the transformation ratio n can be calculated from equation (7.2.3.7), substituting the maximum design centre value for $\hat{V}_a$:

$$n = 1 - \frac{(1 + F_p)(V_b - V_{a_{end}})}{\hat{V}_a} \quad .$$

If the diode is the valve which limits the peak voltages, n can be found from equation (7.2.3.8.)

$$n = \frac{\hat{V}_d}{(1 + F_p)(V_b - V_{a_{end}}) + \hat{V}_d} \quad .$$

Whether or not a reasonable surplus current can be expected with the value of n found in this way, can be checked by means of equation (7.1)

$$\bar{\sigma} = \frac{n\Psi - \eta}{1 - n\Psi} \, .$$

The value of η can be estimated on the basis of previous experience, Q measurements, etc. It is usually between 0.6 and 0.65, and the product $n\Psi$ should then lie between 0.65 and 0.87.

After the transformation ratio n has been decided, the ratio n_y/n_a can also be calculated. To do this, the voltage required across the deflection coil must first be calculated from equation (7.2.3.3), after which n_y/n_a follows from equations (7.2.3.4) and (7.2.3.5).

7.3.2. Calculation of the required peak current

We can now calculate the peak current which the pentode has to supply.

The sawtooth current transformed to the "primary" winding (n_a) is:

$$\hat{\imath}_y^* = \frac{n_y}{n_a}\,\hat{\imath}_y \quad .$$

In addition to the transformed deflection current, the magnetising current of the transformer must also be supplied.

As the transformer, like the deflection coil itself, constitutes an inductive load, the magnetisation current is also a sawtooth current.

If m is the fraction of the transformed deflection current which is used for magnetising the transformer, the total "primary" current which is required is

$$\hat{\imath}_t = \frac{n_y}{n_a}\,\hat{\imath}_y\,(1+m) \quad .$$

In accordance with equation (6.3.5.2), the portion of this which will be delivered by the pentode is:

$$\hat{\imath}_a = \frac{\frac{n_y}{n_a}\,\hat{\imath}_y\,(1+m)}{1+\sqrt{\eta}} \qquad (7.3.2.)$$

In practice, a slightly higher value will be found for $\hat{\imath}_a$ if the diode is still taking a current at the end of the scan. We can attempt to limit this current as much as possible (e.g. to 20 to 30 mA) by a suitable choice of the waveform on the control grid of the pentode.

As the selected transformation ratios already lead to the maximum allowable peak voltage on the valves, the calculated peak current is the lowest with which the design can be realised. Of course, if it is found that the output valve has a large reserve of peak current, it is preferable to start with a somewhat lower peak voltage for the design, thus increasing the safety margin against flashover in the output valves.

7.3.3. Dimensioning of the transformer

The dimensioning of the transformer core is based largely on finding a suitable compromise between the dimensions and the efficiency of the transformer. Particular attention must be paid to obtaining low losses in the leakage inductance. These losses are accompanied by oscillations in the deflection current, and thus become visible in a troublesome manner.

It is not possible to give a simple method of calculation for determining

the most suitable dimensions. In particular, the simplest way to find the required number of turns and the coupling of the E.H.T. coil with the primary winding is by experiment.

It is possible, on the basis of the data for a particular core, to determine if it is possible to construct a transformer with a reasonable efficiency, using this core. These various points will now be briefly discussed.

7.3.3.1. *General shape of the core*

In comparison with its cross section, the core of the line output transformer has a very large window opening. This is necessary in order to obtain sufficient space between the windings and between the windings and the core, so as to prevent flashover and corona effect of the parts carrying an E.H.T. voltage.

An example of the construction of a line output transformer with E.H.T. output is shown in Fig. 7.3.3.1.1. The core is composed of two *U*-shaped Ferroxcube limbs, whose ends are ground flat and clamped against each other. The dimensions of some transformer cores now in general use are given in Fig. 7.3.3.1.2.

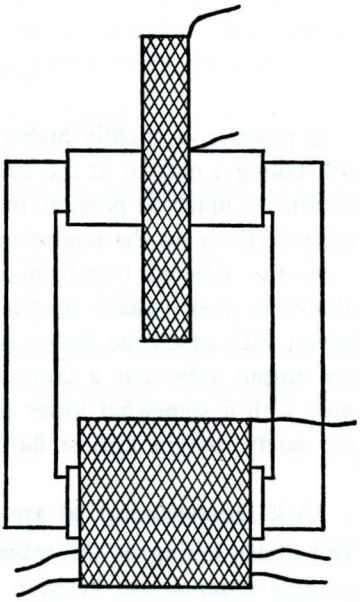

Fig. 7.3.3.1.1. Construction of a line output transformer with E.H.T. coil.

7.3.3.2. *The material of the core*

Ferroxcube is the only core material to be considered for the line output transformer. This uniform magnetic material is characterised by its high

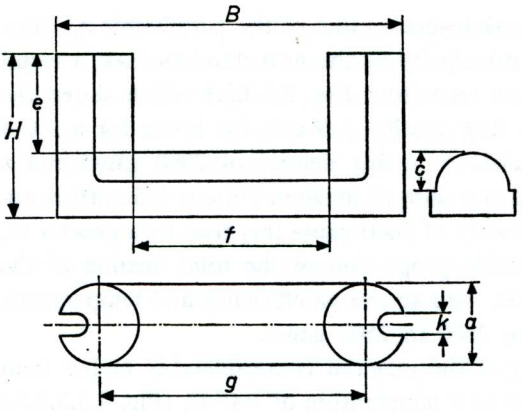

core	B mm	H mm	a mm	c mm	e mm	f mm	g mm	k mm
A	68.35	31.75	15.9	7.6	19.05	38.45	54	4.8
B	63.7	29.35	13.85	5.2	17.9	37.3	50.8	3.6
C	59	28.6	11.35	4.75	17.9	37.85	48.9	3.2

Fig. 7.3.3.1.2. Dimensions of a number of *U*-cores now in general use for line output transformers.

permeability and it also has such a high resistance that eddy current losses are kept very low.

This characteristic makes it the outstandingly suitable material for use at the relatively high line frequencies, at which normal iron cores would develop inacceptably high eddy current losses.

Because of its high resistance, Ferroxcube can be used in a compact mass, pressed to the required shape. Various types are manufactured, which can be used for widely differing purposes. Ferroxcube 3 C 4, which allows of fairly high flux densities, can be used for line output transformers.

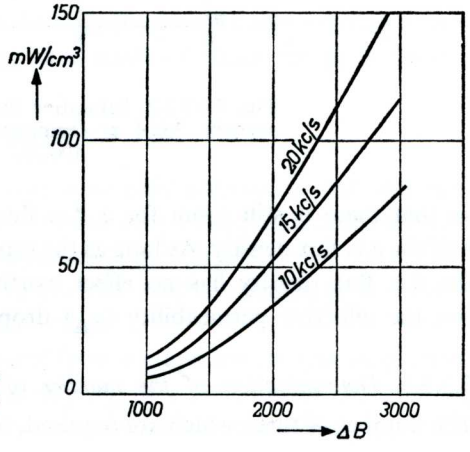

Fig. 7.3.3.2.1. Losses in Ferroxcube 3 C 4 as a function of the magnetisation at various line frequencies.

For this application, the peak-to-peak value of the permissible a.c. flux density ($\triangle B$) is determined principally by the heat developed as a result of the core losses. This can be seen from Fig. 7.3.3.2.1 which shows the relationship between the a.c. flux density $\triangle B$ and the losses for a 3 C 4 core at various line frequencies. At a flux density of 2000 gauss and a frequency of 15 kc/s, the loss in a core of medium volume (35 cm^3) is approximately 2 W; at a flux density of 3000 gauss this rises to a good 4 W.

This constitutes a considerable proportion of the total heating of the transformer, and it is advisable, with an eye on efficiency and temperature, not to make $\triangle B$ higher than 2000 to 2500 gauss.

The saturation flux density of the material is considerably higher than 0.5 $\triangle B$, viz. about 2,300 gauss at a temperature of 100° C. (Fig. 7.3.3.2.2.)

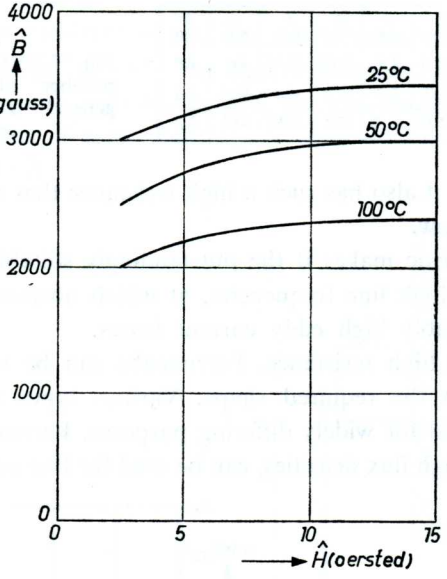

Fig. 7.3.3.2.2. Saturation flux density of Ferroxcube 3 C 4 at temperatures from 25° to 100° C.

so that there is still room for a d.c. flux density approximately equal to half the a.c. flux density. As long as the saturation flux density is not reached, the d.c. flux density has no effect worth mentioning on the core losses, but the effective permeability (μ_Δ) drops.

7.3.3.3. *Determination of the number of turns required*

The number of turns which are required, in order to give an a.c. flux density

$\triangle B$ (gauss) with a core of cross-section A (cm^2) can be calculated quite simply from the self inductance and the sawtooth current needed for the deflection coil. Neglecting the resistances and leakage inductances, we can see from the circuit of Fig. 7.1.1, that if a sawtooth current i_y flows through the deflection coil L_y, a sawtooth magnetising current will flow through winding n_1. The peak-to-peak value of this current is practically equal to $m\hat{\imath}_y = \hat{\imath}_y L_y/L_s$, where L_s is the effective self inductance of the transformer on the winding n_1. The peak-to-peak value of the resulting flux density in the transformer core is:

$$\triangle B \text{ (gauss)} = \frac{L_s m \hat{\imath}_y}{n_1 A} 10^8 \left[\frac{\text{henry. ampere}}{\text{cm}^2}\right]$$

where A is the cross-sectional area of the core.

The required number of turns n_1 thus follows from:

$$n_1 = \frac{L_y \hat{\imath}_y}{\triangle B A} 10^8 \qquad (7.3.3.3.)$$

n_a can now be found from the known transformation ratio according to equation 7.2.3.5, after which n_d follows from $n = n_d/n_a$. (n is determined in section 7.3.1)

The number of turns calculated in this way is the minimum number with which there will be no trouble with excessive losses and increase in temperature of the core. A larger number of turns is not generally to be recommended, because this will result in greater d.c. magnetisation and higher losses due to the leakage inductance.

7.3.3.4. *The effect of the d.c. magnetisation*

The average currents which flow through the transformer winding cause a pre-magnetisation B_0 of the core, as a result of which the peak value of the flux density is increased to:

$$\hat{B} = B_0 + 0{,}5 \triangle B.$$

As the a.c. flux density of the core may only amount to half the value of the saturation flux density, a d.c. flux density of approximately the same size can be permitted without objection (Fig. 7.3.3.4.1)

As a general rule, an air gap in the core will be necessary, in order to reduce the d.c. flux density to this value.

The size of the air gap can be found from a graph for the core in question, which shows the effective permeability μ_Δ as a function of the pre-magnetising flux and of the air gap, for the relevant a.c. flux density $\triangle B$. This

curve is formed by the upper tangents to a number of curves, each of which is for a particular air gap. The sizes of the (optimum) air gaps are indicated at the points of contact of the curve with the original graphs. Fig. 7.3.3.4.2. shows a curve of this type for 3 C 4 cores, the length of

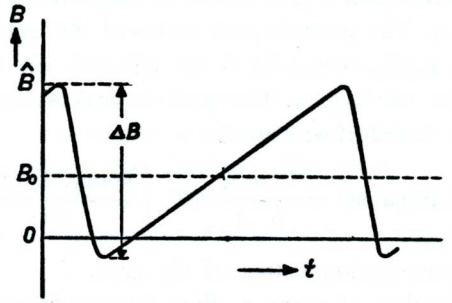

Fig. 7.3.3.4.1. Flux density in the core of a line output transformer with premagnetisation by direct current, during a line period.

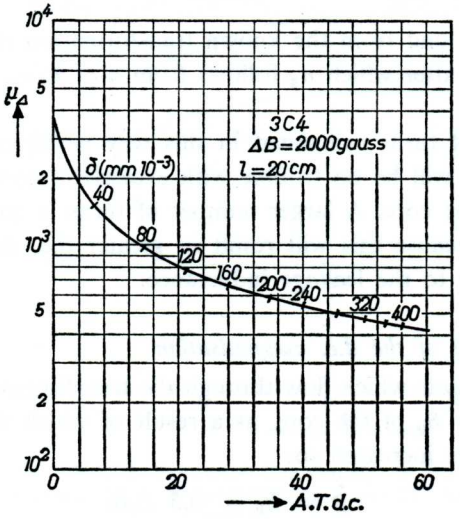

Fig. 7.3.3.4.2. Incremental permeability of Ferroxcube 3 C 4 cores, as a function of the premagnetisation in ampere-turns. The length of the magnetic circuit is 20 cm. The optimum air gap sizes are marked on the graph.

whose magnetic circuit is about 20 cm., for a flux density of 2,000 gauss.

To make use of this curve, we must first estimate the direct current through the winding n_3.

The direct current serves to cover the losses in the deflection circuit

during the scan and flyback. To the extent that they occur in the circuit and not in the valves, the losses during the scan can be neglected in this estimate, because they are usually very small in relation to the flyback losses. According to equation (6.3.5.4.) the latter can be calculated from

$$P_f = 4\,P_m \frac{1-\sqrt{\eta}}{1+\sqrt{\eta}} .$$

For a deflection circuit in which there is no E.H.T. load, and no current is drawn from the booster capacitor, and with which care has been taken to obtain a reasonable efficiency, partly by using Ferroxcube for the transformer and deflection coil, $\sqrt{\eta}$ can be taken as 0.8.

Then
$$P_f = 4\,P_m \frac{0.2}{1.8} = 0.444\,P_m \qquad (7.3.3.4.1.)$$

P_m can be found from the sum of $P_{my} = \frac{1}{8} L_y \hat{i}_y^2 f$ in the deflection coil and the power in the output transformer. The latter can be estimated as 0.1 to $0.15\,P_{my}$.

If we now estimate the load on the E.H.T. voltage (P_{EHT}) and the load on the booster voltage (P_c), the total losses in the deflection circuit outside the valves become:

$$P_{\text{tot}} = P_f + P_{EHT} + P_c .$$

The direct current through winding n_3, across which the voltage at the end of the scan is $V_b - V_{a\text{end}}$, now becomes:

$$\bar{i}_a = \frac{P_{\text{tot}}}{V_b - V_{a_{\text{end}}}} \qquad (7.3.3.4.2.)$$

This method of estimating the direct current is accurate enough for determining the air gap. To determine the anode dissipation of the output valve, greater accuracy may be required. This is referred to further in section 8.6.1.

It will be obvious that choosing a larger air gap will make μ_Δ less dependent on variations in the direct current, which may be a means of keeping the transformer characteristics more constant with large variations of load.

The effective self inductance of the transformer can now be calculated from:

$$L_s = \frac{0.4\pi\, n_1^2\, A\, \mu_\Delta}{l} \times 10^{-8} \text{ henry} \qquad (7.3.3.4.3.)$$

in which A is in cm^2 and l is the length of the iron path in cm.

We may now enquire what effect the diameter of the core will have on the self inductance. For constant $\triangle B$ it is found that the self inductance will increase slightly with decreasing diameter of the core, in spite of the larger air gap which will be required, provided that the d.c. magnetisation is not too high. The thinner core thus requires a smaller magnetisation current, and in this respect is not at a disadvantage. However, we must also take into account the leakage inductance, which will be much greater with the thin core, and which can completely nullify the above advantage under certain conditions. The effect of the leakage inductance will be discussed in the following section.

7.3.3.5. *The effect of the leakage inductance*

In addition to the E.H.T. winding, which will be treated separately, the line output transformer has three other windings, each of which will have a certain leakage inductance relative to the other two. An exact treatment of the resulting losses is very complicated, but the problem becomes much simpler if only the most important leakage inductance is taken into account, i.e. that of the winding to which the deflection coil is connected, relative to the whole primary winding.

The admissibility of this simplification rests on the consideration that the transformation ratio between diode and pentode windings is so close to 1, that with an autotransformer the coupling between these windings is very tight. In addition, the fraction of the leakage inductance which is thus neglected is completely or partially compensated by regarding the diode as being transformed to the pentode winding, instead of the other way round, since the coupling between n_y and n_a will not be so tight as that between n_y and n_d. Following this line of approach, the coupling of the deflection coil with the output valves can be discussed in accordance with the equivalent circuit diagram of Fig. 7.3.3.5.1, in which, to simplify matters still further, the resistances and stray capacitances are neglected.

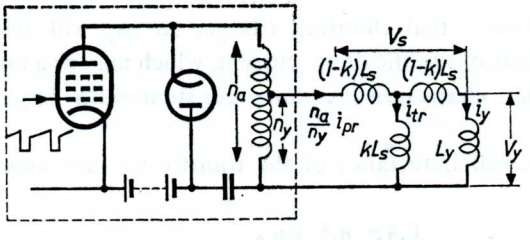

Fig. 7.3.3.5.1. Equivalent circuit diagram of the line output transformer (without E.H.T. winding) to determine the losses due to the leakage inductance. The sawtooth current is conveyed to the circuit under consideration via the valves and an ideal transformer with a transformation ratio n_y/n_a.

The sawtooth current which flows through the two valves, and which is fed, after transformation, to the circuit, is divided between the two branches kL_s and $(1-k)\,L_s + L_y$ in such a way that:

$$m = \frac{i_{tr}}{i_y} = \frac{L_y + (1-k)\,L_s}{kL_s} = \frac{L_y}{L_s}\frac{1}{k} + \frac{1-k}{k} \qquad (7.3.3.5.1.)$$

If $k > 0.99$, $m \approx L_y/L_s$.

The relative voltage loss which occurs as a result of the leakage inductance now follows from:

$$s = \frac{V_s}{V_y} = \frac{i_y\,(1-k)\,L_s + (i_y + i_{tr})\,(1-k)\,L_s}{i_y\,L_y} = \frac{L_s}{L_y}\,(2+m)\,(1-k) \qquad (7.3.3.5.2.)$$

The ratio of the magnetisation current of the transformer to the current in the deflection coil, and the ratio of the voltage loss due to the leakage inductance, to the voltage across this coil, – calculated from equations (7.3.3.5.1 and 2) – are expressed graphically in Fig. 7.3.3.5.2 as functions of L_s/L_y and of the coupling factor k.

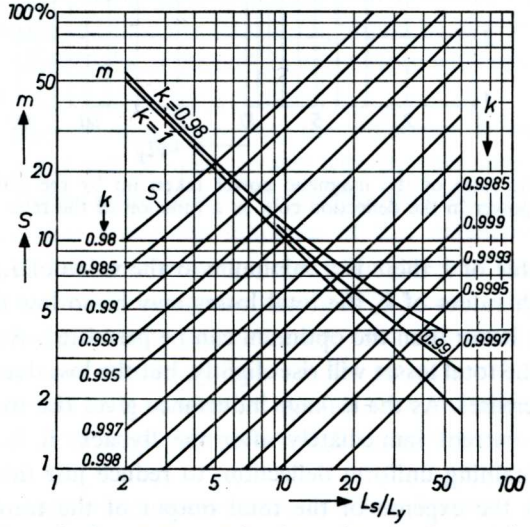

Fig. 7.3.3.5.2. Magnetisation current and voltage drop in the transformer, due to the leakage inductance, expressed as fractions of the current through and the voltage across the deflection coil respectively, as a function of the ratio of the self inductance of the transformer to that of the deflection coil. The coupling factor k is taken as the parameter.

The magnetic power $P_{m\,\mathrm{tot}}$ which the valves supply to the circuit can now be found from:

$$P_{m\,\mathrm{tot}} = P_{my}\,(1+m)\,(1+s)$$

The fraction lost in the transformer is thus:

$$\frac{P_{mtr}}{P_{my}} = (1 + m)(1 + s) - 1 \qquad (7.3.3.5.3.)$$

This ratio is expressed in Fig. 7.3.3.5.3 as a function of L_s/L_y and of k. This figure shows how much the output of the transformer is affected by the coupling factor; the losses increase sharply for lower values of k.

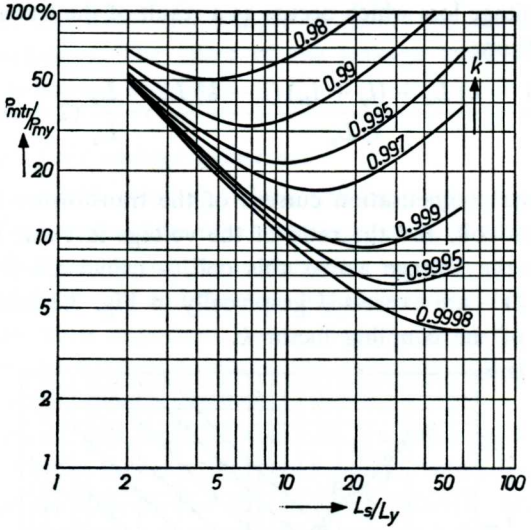

Fig. 7.3.3.5.3. The ratio of the magnetic power taken up by the output transformer to the magnetic power in the deflection coil, as a function of the ratio L_s/L_y and of k.

For each value of k there is a minimum at the value of L_s/L_y for which $m = s$. At high values of k, the total losses may be so low that a value of L_s/L_y which is lower than the optimum can be permitted. At a lower value it is true that the total losses will rise slightly, but the loss due to the leakage inductance decreases. As the leakage inductance gives rise to oscillations in the deflection current immediately after the flyback, it is desirable, for the sake of obtaining uniform deflection, to reduce just this leakage loss, if necessary at the expense of the total output of the transformer. That such oscillations can occur is easily deduced from the equivalent circuit diagram of Fig. 7.3.3.5.1. The leakage inductance brings about an inductive separation between the deflection coil and the booster diode. With the parasitic capacitances (not shown in the diagram) the leakage inductance forms a free resonant circuit which is not damped by the diode. This circuit is made to oscillate by the high voltage pulses during the flyback, and because of the low damping the oscillation will only die

away slowly. It will thus modulate the beginning of the scan voltage across the deflection coil.

This effect is so troublesome that in order to reduce it one always aims for the lowest permissible L_s/L_y ratio which can be reached with a given core. Consequently the number of turns, and thus the self inductance of the transformer, will depend in the first place on the maximum permissible flux density, as in equation (7.3.3.3.) After this, it is only necessary to check the size of the losses due to the magnetisation current and the leakage inductance of the transformer. It depends on the result, whether it is perhaps better to choose a thicker or a thinner core for the design.

7.3.3.6. *The effect of the diameter of the core on the ratio L_s/L_y and on the coupling factor k*

Starting in each case with the same $\triangle B$, we will now investigate how the ratio L_s/L_y and the coupling factor depend on the diameter of the core.

It has already been noted in section 7.3.3.4 that the self inductance of the transformer will increase with a smaller core diameter.

If there was no d.c. magnetisation, so that no air gap was necessary, the self inductance and thus the ratio L_s/L_y would be inversely proportional to the cross-sectional area of the coil, in accordance with equations (7.3.3.3.) and (7.3.3.4.3.)

With d.c. magnetisation, however, the difference is smaller, because the magnetising flux will be much greater with the thin core, which requires more turns, with the result that μ_Δ decreases. With the aid of Fig. 7.3.3.4.2. we can deduce that under the influence of d.c. magnetisation, the self-inductance of the transformer with a core which has half the cross-sectional area of another core will be approximately 30% greater than with the latter core. In considering the influence of the diameter of the core on the coupling factor, we may note that in addition to the air gap and the diameter of the core, k depends on a number of other factors including the method of winding, the thickness of the wire and the transformation ratio of the autotransformer.

To draw a comparison between the coupling factors for different core diameters, therefore, is pointless unless it is done under identical conditions. Figs. 7.3.3.6. *a* and *b*, in which the measured coupling factor for two cores having different diameters is given as a function of the transformation ratio, can serve as an example. With these two cores, which have equal window openings, the winding takes up the same fraction of the total winding space, and in both cases a layer winding is employed, while only one thickness of wire is used for the whole winding.

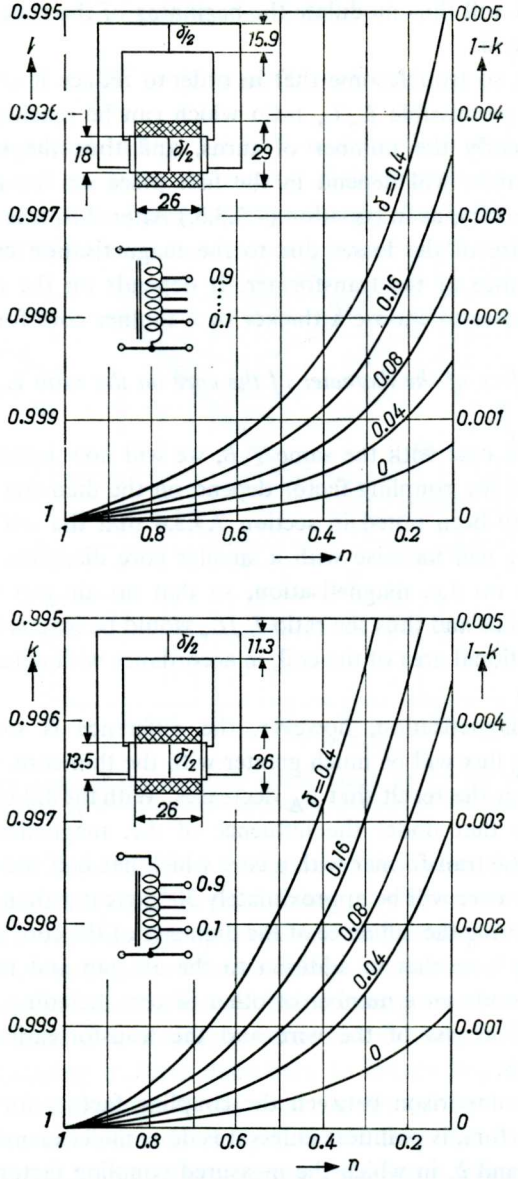

Fig. 7.3.3.6. *a* and *b*. Characteristic variation of the coupling factor of an autotransformer, as a function of the transformation ratio and of the size of the air gap for Ferroxcube 3 C 4 cores with the same window opening, but of different diameter.

The values of k which are given here can serve as an indication of what can be attained under comparable conditions. Because of the many factors

involved, however, too much significance should not be attached to the absolute values which are quoted.

It now appears that k is considerably smaller for the thin core, particularly because of the air gap, which must be larger for this core. In combination with the slightly higher ratio L_s/L_y, this means that the leakage loss is the greatest for the thin core, in accordance with Fig. 7.3.3.5.2. In addition, Fig. 7.3.3.6. shows that the transformation ratio has a very great effect on k. Therefore, a thin core can be used with success, provided that n_y/n_a is high enough. As a general rule it may be assumed that no troublesome oscillations in the picture will be caused by the leakage inductance if the leakage loss $s = V_s/V_y < 0.03$. If the required transformation ratio gives too high a leakage loss, a thicker core is recommended.

In the following paragraphs we shall reconsider what we have said above, with the aid of an example.

7.4. Example of calculation of an output transformer

As an example we now give a calculation for an output transformer for the horizontal (line) deflection in a picture tube with a diagonal deflection angle of 110°, and an E.H.T. voltage of 16 kV. The deflection coil has a self inductance L_y of 2.9 mH, and a resistance r_y of 5 Ω, while the peak-to-peak value of the current required to displace the electron beam from edge to edge of the picture is 2.2 amperes.

In addition:

The line frequency = 15,625 c/s
The flyback ratio $p = 0.16$.

The maximum permissible peak voltages on the output valves are: 7,000 volts for the pentode, 5,000 volts for the diode. The h.t. rail voltage $V_b = 220$ volts, nominal, but it must be possible to maintain the deflection with 10% undervoltage.

First of all, the sawtooth current $\hat{\imath}_y$ through the deflection coil must be determined. With a flyback ratio of 16%, the remainder of the blanking period is about 2%. Because of the aspect ratio of the tube (width to height, approximately 5 : 4), there must be about 6% over-deflection in the horizontal direction, relative to the vertical deflection, since the aspect ratio of a transmitted picture is 4 : 3. Further, in order to have a margin for eccentricity of the picture (the edges of the picture must not be visible), both the horizontal and vertical deflection are increased by another 2% so that the total over-deflection in the horizontal direction must be approximately 10%. With the 110° picture tube, the amplitude of the saw-

tooth current needed to give this value is only 5% more than the current required for displacement of the spot from edge to edge of the picture because, as a result of the shape of the picture tube, the displacement at the edges of the screen increases much more rapidly than the angle of deflection. The required deflection current thus becomes:

$\hat{\imath}_y = 1.05 \times 2.2$ amperes $= 2.3$ amperes.

It is now necessary to find the transformation ratios. To do this, we find out which valve reaches the limit of maximum peak voltage first.

From equation (6.3.4.) we have

$$F_p = \frac{\pi}{2}\frac{1-p}{p} + \frac{2}{\pi} = 9$$

and from equation (7.2.3.8)

$$\hat{V}_a - \hat{V}_d = (1 + F_p)(V_b - V_{a_{end}})$$

In order to be able to obtain sufficient deflection with low mains voltage, $V_{a_{end}}$ must still remain slightly above the knee. Now the knee depends on the peak current, which is not known at this stage. For a peak current (estimated) of 300 mA, $V_{a_{end}}$ for an output valve like the *PL* 36 would have to be at least 40 V, so that there is sufficient margin available if $V_{a_{end}}$ is put at 70 V for the rated supply voltage.

Then: $$\hat{V}_a - \hat{V}_d = 10\,(220 - 70) = 1500 \text{ V}.$$

In this case, then, the diode reaches the maximum peak voltage first and the maximum peak voltage on the pentode is 5000 + 1500 volts = 6500 volts.

With these peak voltages as the starting point, the transformation ratio $n = n_d/n_a$ can be calculated from equation (7.2.3.8)

$$n = \frac{\hat{V}_d}{\hat{V}_a} = \frac{5000}{6500} = 0.77\,.$$

We can now check to see if a reasonable surplus is obtained with this transformation ratio.

According to equation (7.1)

$$\bar{\sigma} = \frac{n\Psi - \eta}{1 - n\Psi}\,.$$

As there is no booster load, and no E.H.T. load is required, $\Psi = 1$, and η can be put at 0.64, so that

$$\bar{\sigma} = \frac{0.77 - 0.64}{0.23} = 0.56.$$

The usable values of $\bar{\sigma}$ are 0.2 to 2, so that the calculated transformation ratio can be employed.

The voltage across the whole transformer winding n_a now becomes: (equation 7.2.3.7).

$$V_{Bst} - V_{a_{end}} = \frac{\hat{V}_a}{1 + F_p} = 650 \text{ V}.$$

To find the transformation ratio n_y/n_a, we must calculate the voltage which has to be present across the deflection coil at the end of the scan. According to equation (7.2.3.3):

$$V_y = \frac{L_y \hat{\imath}_y f}{1 - p} + 0.5 \hat{\imath}_y r_y = 130 \text{ V}.$$

In determining the voltage which has to be generated in the transformer, account must also be taken of the voltage which is lost across the linearity correction coil, and of the voltage drop caused by the leakage inductance of the transformer. With respect to the latter, we can assume that the voltage may be increased by not more than 3%, as otherwise the oscillations after the flyback can become troublesome.

In order to take both factors into account, the e.m.f. induced in the transformer at the end of the scan can be taken as:

$$V_y' = 1.05 \, V_y = 136 \text{ V}.$$

The transformation ratio n_y/n_a must thus be:

$$\frac{n_y}{n_a} = \frac{V_y'}{V_{Bst} - V_{a_{end}}} = 0.21.$$

To calculate the number of turns we now select the core diameter and the value of $\triangle B$ which can be permitted for the chosen core. The calculation can be made, for example, for a core with a diameter of 11.35 mm, core C of Fig. 7.3.3.1.2. ($A = 1$ cm^2). Because of the small volume of this core, an a.c. flux density of 2,400 gauss is permissible at the required line frequency of 15,625 c/s.

According to equation (7.3.3.3):

$$n_y = \frac{L_y \hat{\imath}_y 10^8}{\triangle B \, A} = \frac{2.9 \times 2.3 \times 10^5}{2{,}400} = 278$$

$$n_a = \frac{278}{0.21} = 1325$$

$$n_d = 0.77 \times 1325 = 1020.$$

The required peak anode current can be calculated according to equation (7.3.2):

$$\hat{\imath}_a = \frac{\frac{n_y}{n_a}\hat{\imath}_y(1+m)}{1+\sqrt{\eta}}.$$

If the required magnetisation current through n_y is estimated as $0.1\,\hat{\imath}_y$ (thus $m = 0.1$), we have:

$$\hat{\imath}_a = \frac{0.21 \times 2.3 \times 10^3 \times 1.1}{1.8} = 295 \text{ mA}.$$

To determine the air gap and the self inductance of the transformer, we next estimate the direct current. With $m = 0.1$, the total magnetic power, taking into account the loss through the leakage inductance and the linearity coil, (equation 6.3.5.3) is:

$$P_{m\,\text{tot}} = 1.15\,P_{my} = \frac{1.15}{8}\,V_y\,\hat{\imath}_y\,(1-p) = 36 \text{ VA}$$

The flyback losses in the output circuit are then approximately (equation 7.3.3.4.1) $P_f = 0.444\,P_m = 16$ W.

The direct current through the winding n_3 ($n_a - n_d$ turns) is now (equation 7.3.3.4.2):

$$\bar{\imath}_a = \frac{P_f}{V_b - V_{a_{\text{end}}}} = 107 \text{ mA}.$$

The pre-magnetisation is thus given by

$$(1325 - 1020) \times 0.107 = 31 \text{ ampere-turns}.$$

Fig. 7.3.3.4.2 shows that for this core and this pre-magnetisation an air gap of 0.18 mm is required, and that μ_Δ is approximately 600.

According to equation (7.3.3.4.3), the self inductance of the transformer is:

$$L_s = \frac{0.4\pi\,n_y^2\,A\,\mu_\Delta\,10^{-8}}{l} = 30 \text{ mH}.$$

The ratio L_s/L_y is thus $\frac{30}{2.9} \approx 10.3$. From Fig. 7.3.3.6.*b* we can deduce that the coupling factor to be expected with this core, with a transformation ratio of 0.21 and an air gap of 0.18 mm, will be 0.995.

Fig. 7.3.3.5.2 shows that the magnetisation current will be 10% of i_y, but that the leakage inductance also causes a voltage loss of over 10% of V_y. This is considerably more than was assumed, and will almost certainly give rise to unacceptable oscillations. We can now repeat the cal-

culation for a thicker core, e.g. core A of Fig. 7.3.3.1.2 with $A = 1.9$ cm². As this core has twice the volume of the first one, a lower value of $\triangle B$ will be chosen, for example 2,000 gauss, so as to limit the losses. We then have $n_y = 168$ turns, $n_a = 800$ turns and $n_d = 615$ turns. The pre-magnetisation becomes 19 ampere-turns, so that $\delta = 0.12$ mm and $\mu_\Delta = 800$. Then $L_s = 28$ mH, $L_s/L_y \approx 9.7$ and $k = 0.9982$.

In this case, $m = 11\%$ and $s = 3.5\%$, which is a considerable improvement on the thin core.

We may now enquire under what conditions a thin core can be used. To this end, we will re-calculate the above example for the thin core, but this time for a deflection coil having a self inductance of 26 mH and a resistance of 45 Ω, which requires a deflection current $\hat{\imath}_y$ of 0.77 ampere. This coil is just as sensitive as the previous one, so that P_m, i_a, $\hat{V}_a$, $\hat{V}_d$ and n remain unchanged. Now $V_y' = 410$ volts and $n_y/n_a = 0.63$. n_y becomes 835 turns, while n_a and n_d remain unchanged. Consequently the air gap and μ_Δ remain the same size, so that the ratio L_s/L_y also remains unchanged. According to Fig. 7.3.3.6.*b*, however, k now rises to 0.999 for this transformation ratio.

With $L_s/L_y = 10.3$ and $k = 0.999$, Fig. 7.3.3.5.2. gives $m = 9\%$ and $s = 2.2\%$.

With this high-impedance deflection coil, therefore, the thin core is completely acceptable.

The question now arises, whether an improvement can be brought about in those cases where the leakage inductance is too high, by preventing pre-magnetisation of the core. A well-known method of doing this is to compensate for the pre-magnetisation by arranging for a direct current to flow in the opposite direction in another winding. The air gap can then be left out, so that k will rise in accordance with Fig. 7.3.3.6. The cause of this, however, is the increase in μ_Δ and not the decrease in the leakage inductance. The increased μ_Δ cannot be used to reduce the number of turns on the transformer because then $\triangle B$ will increase, and with it the losses. Consequently the leakage inductance cannot be reduced by this measure, although the higher self inductance means a smaller magnetisation current, so that the efficiency of the circuit improves slightly. However, this does not prevent the appearance of oscillations, and so does not serve the object stated above.

7.5. **Correction of the symmetrical non-linearity**

For picture tubes with a relatively flat screen, which means that the deflection coil is placed a long way in front of the centre of curvature of the screen,

the displacement on the screen is not proportional to the angle of deflection. To ensure that the spot moves across the screen at a constant speed, the voltage across the deflection coil must be made to vary parabolically, so that the voltage is at a maximum when the spot passes the centre of the screen. A simple method of doing this is to connect a capacitor in series with the deflection coil. The value of the capacitor is such that the resonant frequency of this series circuit is far below the line frequency. The sawtooth current which flows through the capacitor produces an approximately parabolic voltage across it. During the first half of the period the capacitor is charged by a decreasing current, which charge flows back during the second half of the period by an increasing current.

The voltage which is present across the deflection coil during the scan is now formed by the sum of the constant voltage across the transformer and the parabolic voltage across the capacitor; because of this, the current becomes more or less S-shaped.

As the capacitor is reduced in value and the resonant frequency approaches the line frequency, the parabolic form of the voltage becomes more sinusoidal, while the impedance of the series circuit decreases. For this reason, the series circuit of capacitor and deflection coil must be connected to a lower tapping of the transformer than would be necessary for the deflection coil alone.

If only a little linearity correction is required, it is sufficient to reduce the value of the booster capacitor. The primary sawtooth current which flows through this capacitor causes a parabolic voltage component across the primary winding of the transformer. As the sawtooth current through this capacitor is not linear, this method is not suitable for large corrections. In addition, the load line of the output pentode would become more unfavourable, because of too large a primary parabolic component, resulting in increased anode dissipation of the output valve.

CHAPTER 8

GENERATION OF THE HIGH ACCELERATING VOLTAGE (E.H.T.) FOR THE PICTURE TUBE

8.1. Circuit for obtaining the E.H.T. supply from the output transformer

The high peak voltages which occur during the flyback of the line timebase are frequently used to supply the high accelerating voltage for the picture tube. The required voltage is 14 to 18 kilovolts, while the highest permissible voltage on the line output pentode is 6 to 7 kilovolts; this voltage must thus be transformed up before it is rectified. It would also be possible to use a cascade rectification circuit, but as this is more complicated, it is preferable to use an extra winding on the transformer.

Fig. 8.1. shows a circuit for obtaining the E.H.T. supply from the flyback.

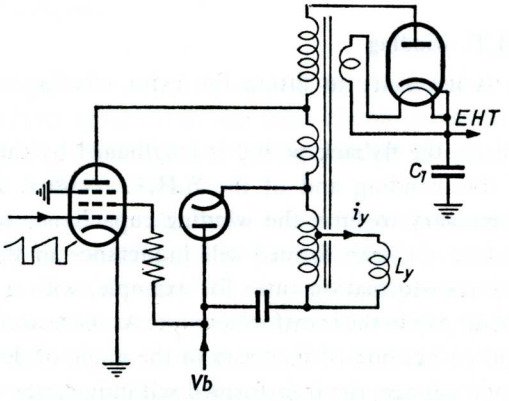

Fig. 8.1. Circuit of a line output transformer with E.H.T. generation.

The transformed peak voltage is rectified by means of a diode whose heater voltage comes from a single well-insulated turn on the same transformer, so that when there is no load, the capacitor C_1 becomes charged to the maximum value of this peak voltage. One advantage of the method of generating the E.H.T. supply from the line timebase is that, because of the high frequency, only a small buffer capacitor needs to be used. With a capacitance of 1,000 pF and a current output of 1 mA, for example, which represents approximately the maximum anode current of the picture

tube, the voltage drop per period (one line time $\times$ $(1-p) \approx 50\,\mu s$) is:

$$\triangle V = \frac{i\ t}{C} = \frac{10^{-3} \times 50 \times 10^{-6}}{10^{-9}} = 50\ \text{V},$$

which is certainly permissible at a level of 14 to 18 kilovolts.

When there are several white lines in succession, a greater voltage drop will be experienced, due to the internal impedance of the E.H.T. source. To prevent excessive discharge during white portions of the picture, the value of C_1 is usually taken around 2,000 pF (for 21″ tubes).

The pulse-shaped voltage also means that the maximum reverse voltage which the E.H.T. rectifier has to stand is only a little higher than the direct output voltage.

The buffer capacitance C_1 is mainly obtained by providing the outside of the bulb of the picture tube with an aquadag coating, which must be earthed by means of a contact spring or similar arrangement. Together with the internal coating of the glass bulb, which is connected to the E.H.T. voltage, this coating forms the required high tension capacitor.

8.2. **The E.H.T. winding**

Particular care is necessary in fitting the extra winding onto the output transformer.

In the first place, the flyback period is lengthened by the extra parasitic capacitance of this winding and of the E.H.T. rectifier. For this reason it used to be necessary to limit the winding capacitance to the minimum and even to reduce the transformed self inductance in the output stage, by means of the transformation ratio for example, with a parallel coil or with an enlarged air gap in the transformer core. As more and more deflection energy was required because of increases in the angle of deflection and the accelerating anode voltage, the transformed self inductance of the deflection coils decreased, so that more parasitic capacitance can be permitted for 90° or 110° deflection. This change is reflected in the form of the E.H.T. winding. Fig. 8.2.1. shows a transformer design for 70° deflection, using a tall narrow coil; Fig. 8.2.2. shows a transformer for 110° deflection, on which the E.H.T. coil is much lower and wider.

We may wonder why the larger capacitance should be concentrated in the E.H.T. coil. The reason is that this increases the load capacity of the E.H.T. supply. The E.H.T. rectifier draws the current largely from the reservoir formed by the parasitic capacitance on the anode of the rectifier; for the pulse-shaped loading currents, the unavoidable leakage inductance forms an impedance which partially insulates the E.H.T. rectifier from the

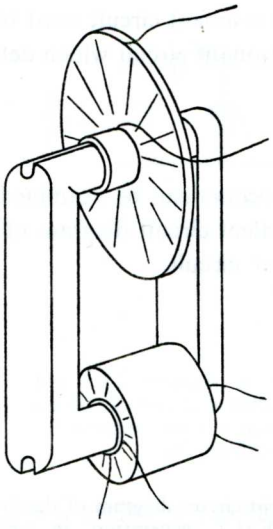

Fig. 8.2.1. Typical design of a line output transformer with tall narrow E.H.T. coil for 70° deflection.

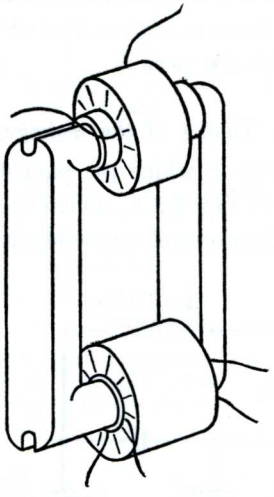

Fig. 8.2.2. Typical design of a transformer for 110° deflection.

much greater capacitance which is present on the primary winding. Consequently it is advantageous that the total circuit capacitance required in view of the flyback period should be concentrated as much as possible at the anode of the E.H.T. rectifier.

That the leakage inductance forms a factor which cannot be neglected, is not due to any impossibility of keeping it small enough, with reference to the load capacity of the E.H.T. supply. On the contrary, the leakage inductance is deliberately made greater than it need be, so that no trouble is experienced from parasitic oscillations after the flyback. These oscillations are of the same type as, although lower in frequency than, those which are due to the primary leakage inductance discussed in section 7.3.3.5. The latter can be countered by ensuring a sufficiently low leakage inductance, while this is not possible for the leakage inductance of the E.H.T. winding, partly because of insulation problems.

It is found that these oscillations can only be adequately prevented if the resonant circuit formed by the leakage inductance and the stray capacitance is tuned to the flyback period in such a way that the parasitic oscillation which is generated in this circuit at the beginning of the flyback is cancelled out again during the second half of the flyback.

In principle, a number of tuning frequencies are possible, but only the lowest is accompanied by advantages which lead to its being used in practice;

it is found that the tuning frequency of this resonant circuit must be nearly three times as high as that of the primary resonant circuit which determines the flyback period.

8.3. Tuning of the leakage inductance

The way in which the parasitic oscillation occurs can be examined on the basis of Fig. 8.3.1., which shows the equivalent circuit diagram of the self inductances and capacitances of the output circuit.

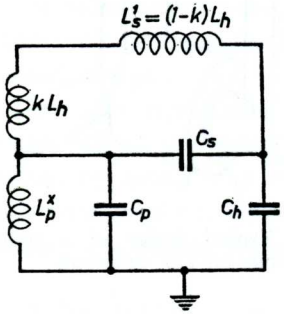

Fig. 8.3.1. Equivalent circuit diagram of the line output transformer with E.H.T. generation, in which there is an appreciable leakage inductance between the "primary" and the E.H.T. coil.

In this figure, $L_p{}^x$ is the self inductance of the deflection circuit consisting of the primary of the transformer and the transformed self inductance of the deflection coil; kL_h is that portion of the E.H.T. winding which can be regarded as coupled with $L_p{}^x$; $L_s{}^1$ is the leakage inductance of the E.H.T. winding relative to the primary; C_p is the total capacitance present and transformed to the primary; C_h is the capacitance of the E.H.T. rectifier with wiring, and C_s is the capacitance of the E.H.T. winding. We thus have two coupled resonant circuits, principally determined by $L_p{}^x$ and C_p and by $L_s{}^1$, C_s and C_h, but affecting each other to a great extent because of the high degree of coupling, both capacitive via C_h and inductive.

The behaviour of the secondary resonant circuit during the flyback in the primary circuit will now be examined separately for each method of coupling.

The situation in regard to the capacitive coupling can be represented as in Fig. 8.3.2. Neglecting the self inductance and capacitance transformed from the primary circuit to the secondary circuit via the inductive coupling (which does not, in fact, make any difference to our considerations), we can say that the resonant circuit is formed by $L_s{}^1$ and C_s, and that a periodic negative pulse derived from $L_p{}^x$ is fed in via C_h.

To start with, we will regard this as an ideal rectangular pulse. At the beginning of the pulse, at the instant t_1, a very large current surge abruptly

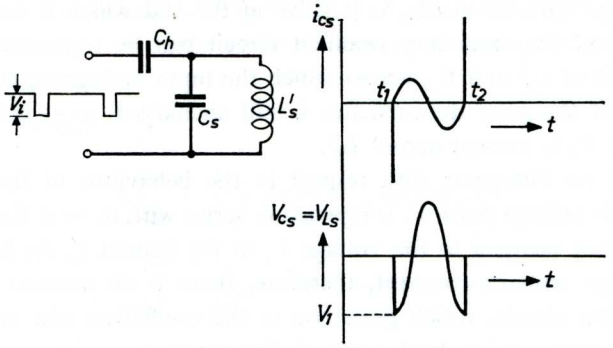

Fig. 8.3.2. Current in and voltage across a parallel resonance circuit, to which a rectangular pulse voltage is applied via a capacitance, with a pulse time which is equal to the period of oscillation of the tuned circuit.

charges the capacitor C_s to the voltage

$$V_1 = \frac{V_i\, C_h}{C_s + C_h}\,.$$

As long as the input voltage V_i remains constant, the energy ($\frac{1}{2}\, C_s V_1^2$) imparted to the circuit will give rise to a sinusoidal oscillation. If L_s^1 and C_s are tuned so that exactly one period has been completed at instant t_2 when the pulse ends, the capacitor, which had just reached the full voltage V_1 again, is discharged by an equally large current surge in the opposite direction. As the current through the coil at that instant had just become zero, the circuit is now without energy, so that the oscillation breaks off as abruptly as it started.

If we consider the course of events for the inductive coupling (Fig. 8.3.3.) the result is found to be completely analogous to the above. The

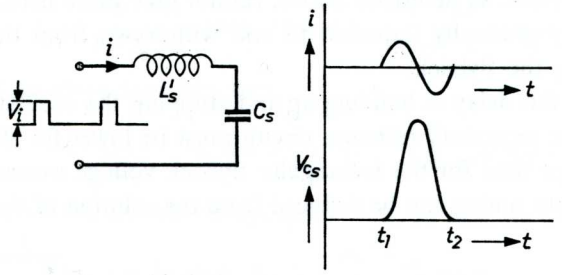

Fig. 8.3.3. Current in and voltage across a series resonant circuit to which a pulse voltage is applied with a pulse time equal to the period of ocillation of the tuned circuit.

pulse voltage induced in kL_h is positive at the end which is turned away from L_p, and the secondary resonant circuit can be represented by the series circuit of L_s^1 and C_s, across which the input voltage V_i acts. At the beginning of the pulse the capacitor is still uncharged, so at instant t_1 the full voltage V_i is present across L_s^1.

It makes no difference with respect to the behaviour of the resonant circuit if this voltage pulse V_i is injected in series with it, or if the capacitor C_s is suddenly charged to the voltage V_i at the instant t_1. As long as the input voltage remains constant, therefore, there is an amount of energy $\frac{1}{2} C_s V_i^2$ in the circuit, which gives rise to the oscillation and maintains it until the energy is taken back again at the instant t_2.

Figs. 8.3.2. and 8.3.3. show that both methods of coupling produce oscillations of the same polarity, so that they reinforce each other.

Whether the oscillations will stop completely after instant t_2 is determined by two factors, i.e. by correct tuning, so that $i_L = 0$ at instant t_2, and by the size of the discharge current, so that C_s is completely discharged. Since there are losses in both circuits, the voltage V_{C_s} at instant t_2 will be slightly lower than at instant t_1, so that complete cessation of the oscillations would require a corresponding reduction of the discharge current relative to the charging current at instant t_1. If the above mentioned prerequisites are not fullfilled, some oscillation will remain active after the instant t_2 during the succeeding scan. Although this oscillation will also modulate the voltage across the deflection coils, the damping effect of the booster diode during the scan means that this need not have any noticeable effect on the linearity of the deflection.

In practice, we cannot assume a rectangular input pulse voltage, but must start in the first instance from a periodic half sine-wave pulse.

The abrupt starting and ending of the oscillation at the beginning and end of the flyback, as described above, cannot take place here, because the energy is only gradually imparted to and withdrawn from the secondary circuit during the flyback.

Because of this delay in building up and stopping the oscillation, the LC product of the secondary resonant circuit must be lower for the sinusoidal flyback voltage than for the rectangular flyback voltage assumed above.

The optimum tuning can be deduced from the solution of the differential

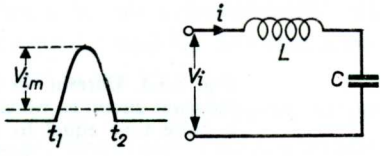

Fig. 8.3.4. Series resonant circuit to which the voltage $V_i = V_{i\,max} \sin(\omega t - \varphi)$ is applied.

equation for the circuit of Fig. 8.3.4, but now with an input voltage $V_i = V_{im} \sin(\omega t - \varphi)$ in the interval between t_1 and t_2. (The flyback of the line timebase).

At every instant:

$$L\frac{di}{dt} + \frac{1}{C}\int i\,dt = V_{im}\sin(\omega t - \varphi)$$

or

$$\frac{d^2i}{dt^2} + \frac{i}{LC} = \frac{\omega V_{im}}{L}\cos(\omega t - \varphi) \ .$$

The general solution of the reduced equation:

$$\frac{d^2i}{dt^2} + \frac{i}{LC} = 0 \text{ has the form } i = A\,e^{-j\frac{t}{\sqrt{LC}}}$$

or

$$i = A_1\cos\frac{t}{\sqrt{LC}} + A_2\sin\frac{t}{\sqrt{LC}} \ .$$

To find a particular solution we put:

$$i = p\sin\omega t + q\cos\omega t \ .$$

Then:

$$\frac{di}{dt} = \omega p\cos\omega t - \omega q\sin\omega t$$

and

$$\frac{d^2i}{dt^2} = -\omega^2 p\sin\omega t - \omega^2 q\cos\omega t \ .$$

Substitution in the differential equation gives:

$$-\omega^2 p\sin\omega t - \omega^2 q\cos\omega t + \frac{p}{LC}\sin\omega t + \frac{q}{LC}\cos\omega t = \frac{\omega V_{im}}{L}\cos(\omega t - \varphi)$$

This can only be satisfied if:

$$p = \frac{\omega C V_{im}}{1-\omega^2 LC}\sin\varphi \text{ and } q = \frac{\omega C V_{im}}{1-\omega^2 LC}\cos\varphi \ .$$

The complete solution now becomes:

$$i = A_1\cos\frac{t}{\sqrt{LC}} + A_2\sin\frac{t}{\sqrt{LC}} + \frac{\omega C V_{im}}{1-\omega^2 LC}\cos(\omega t - \varphi) \ .$$

At the instant t_1, t in the above equations $= 0$, so that we have:

1.) $i = 0$, thus $A_1 = \dfrac{-\omega C V_{im}}{1-\omega^2 LC}\cos\varphi$

2.) $\dfrac{di}{dt} = 0$, thus $A_2 = \dfrac{-\omega^2 C V_{im}\sqrt{LC}}{1-\omega^2 LC}\sin\varphi$.

Then:

$$i = \frac{\omega C V_{im}}{1-\omega^2 LC}\left[\cos(\omega t-\varphi) - \cos\varphi\cos\frac{t}{\sqrt{LC}} - \omega\sqrt{LC}\sin\varphi\sin\frac{t}{\sqrt{LC}}\right] \tag{8.3.1.}$$

In addition:

$$V_L = L\frac{\mathrm{d}i}{\mathrm{d}t} = \frac{\omega\sqrt{LC}\,V_{im}}{1-\omega^2 LC}\left[-\omega\sqrt{LC}\sin(\omega t-\varphi) + \right.$$

$$\left. + \cos\varphi\sin\frac{t}{\sqrt{LC}} - \omega\sqrt{LC}\sin\varphi\cos\frac{t}{\sqrt{LC}}\right] \tag{8.3.2.}$$

If no further oscillations are to occur after instant t_2, both i and V_L must equal 0 at this instant. ($\omega t = \pi + 2\varphi$).

From $i = 0$ follows:

$$\cos(\pi+\varphi) - \cos\varphi\cos\frac{\pi+2\varphi}{\omega\sqrt{LC}} - \omega\sqrt{LC}\sin\varphi\sin\frac{\pi+2\varphi}{\omega\sqrt{LC}} = 0.$$

This is satisfied for $\dfrac{\pi+2\varphi}{\omega\sqrt{LC}} = (2n+1)\pi$ (n a whole number)

For the lowest attainable tuning, $n = 1$ so that $\dfrac{1}{\sqrt{LC}} = \dfrac{\pi}{\pi+2\varphi}3\omega$.

In order to distinguish it from the other possible tuning frequencies this tuning, for which one and a half periods of the oscillation occur during the flyback, is known as "third harmonic", although this expression is not completely applicable on the basis of the tuning and of the waveform.

If we substitute this value of $1/\sqrt{LC}$ in equation (8.3.2.), we find that V_L is not exactly zero for $\omega t = \pi + 2\varphi$, so that a small oscillation will remain after instant t_2. This is due to the term $\sin\varphi\cos t/\sqrt{LC}$ in this equation, which is of opposite sign after one and a half periods. As the angle φ is very small (for a normal flyback period $\varphi \approx 0.035\,\pi$) this term is small in comparison with the two others. In fact, the presence of this in the expression for i and V_L is due to the second boundary condition not being stated absolutely accurately. In practice, a small direct voltage caused by the preceding pulses will be found across the coil during the scan, so that $\mathrm{d}i/\mathrm{d}t$ cannot be zero at instant t_1.

Because this deviation is so slight, it can be neglected. As a matter of fact, the minimum is influenced to a considerable extent by the damping which is not included in the calculation, from both the primary and the secondary resonant circuits. In addition, the damping on the secondary

resonant circuit is variable, because of the variable load constituted by the E.H.T. rectifier with changes of brightness of the spot. In spite of these shortcomings, tuning of the leakage inductance is generally employed, partly because of the other advantages associated with it.

8.4. Additional advantages of the tuned leakage inductance

Besides the main object of tuning – the prevention of interfering oscillations during the scan – other important subsidiary advantages can be achieved, which can contribute to raising the efficiency of the circuit as a whole.

The peak voltage across the leakage inductance is added to the input voltage V_i, giving an appreciable gain in voltage for the E.H.T. supply; in addition, due to the reaction of the oscillating current on the primary of the transformer, the primary flyback voltage is distorted in such a way that a lower primary peak voltage is reached. This is shown graphically in Fig. 8.4. The form of the current i, which is made up of the three components given by equation (8.3.1) is shown in Fig. 8.4.1, while Fig. 8.4.2. shows the voltage V_L according to equation (8.3.2.).

The resulting peak voltage across the whole E.H.T. winding is represented in Fig. 8.4.3, while the resulting primary peak voltage – in a particular case – is shown in Fig. 8.4.4.

According to equation (8.3.2), the maximum voltage $V_{L\,\max}$ which can be obtained with correct tuning for a normal flyback period ($p = 0.15$, $\omega\sqrt{LC} = 0.36$, $\cos\varphi = 0.99$) is:

$$V_{L\,\max} = 0.55\, V_{im}$$

In practice a lower value will always be found, because of the damping. The oscillation appears in phase opposition at the two ends of the leakage inductance because a capacitive tapping of this circuit, consisting of C_h and C_p, is earthed as in Fig. 8.3.1. As a result, only part of the oscillating voltage contributes to the increase in peak voltage at the end which is connected to C_h, and the remainder reduces the voltage across C_p.

The inductive coupling also contributes to reducing the primary peak voltage. The oscillating current i_L passes through that part of the E.H.T. winding, kL_h, which is tightly coupled with the primary, and thus induces the oscillation back into the primary circuit. The maximum reduction of the primary peak voltage is attained with a certain amplitude of this oscillation and amounts to about 20%.

This amplitude can be affected by means of C_h and C_p, and by increasing or reducing the self-capacitance C_s of the E.H.T. winding, but the effect on the flyback period must always be taken into account.

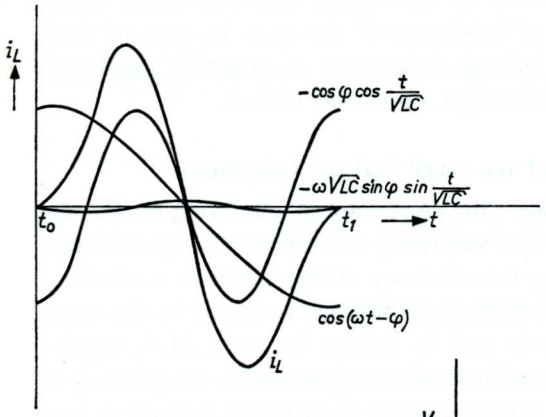

Fig. 8.4.1. Waveform of the current in the resonant circuit of Fig. 8.3.4.

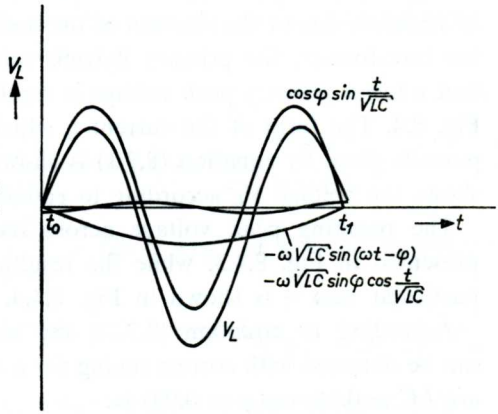

Fig. 8.4.2. Waveform of the voltage across the self inductance in the circuit of Fig. 8.3.4.

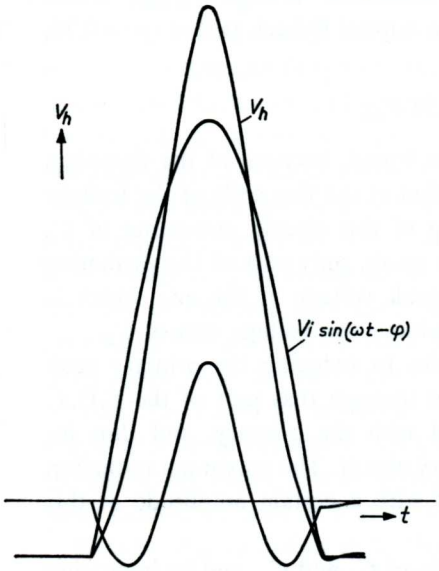

Fig. 8.4.3. Increase of the peak voltage in the E.H.T. coil as a result of the tuned leakage inductance.

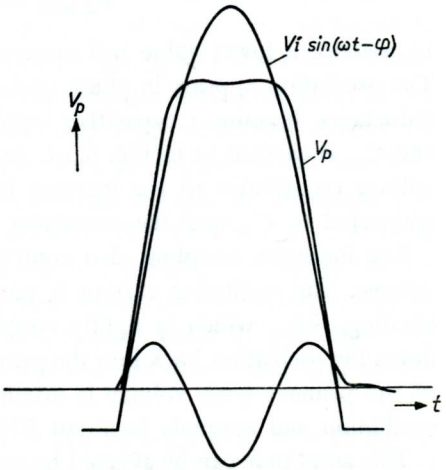

Fig. 8.4.4. Reduction of the primary peak voltage as a result of the tuned leakage inductance in an optimum case.

The correct tuning can best be obtained by bringing the leakage inductance to the required value, e.g. by placing the E.H.T. winding on a different part of the core from the primary, by applying coupling turns with the primary or short-circuiting turns round the stray field, by fitting a spacing ring between the primary and the E.H.T. winding, or some similar measure. This only has a slight effect on the flyback period.

A simple method of determining whether the correct tuning has been obtained in practice is to look at the oscillogram of the oscillations, which is obtained by connecting the ends of a single loop to the vertical amplifier of an oscilloscope, and placing the loop near the core of the transformer, i.e. in the stray field. The correct tuning has been obtained if the amplitude of the oscillations during the flyback is considerably greater than during the scan. (Fig. 8.4.5.)

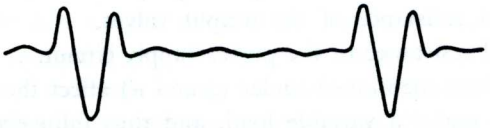

Fig. 8.4.5. Oscillogram of the decay of the leakage field of the transformer during and after the flyback in an optimum case.

Of course, it will not always prove possible to obtain the theoretical maximum reduction of the primary peak voltages, because of the limited possibilities of variation of the above-mentioned capacitances. However, a reduction of 10 to 15% in the F_p factor can usually be realised.

This reduction in F_p makes it possible to increase the magnetic power handled by a given valve, by a similar percentage, without exceeding the peak voltage limit. This is an important advantage, which is one of the factors making it possible to obtain larger angles of deflection (110°), at which this reduction can be better utilised with output valves the same as, or only slightly larger than, the ones which were used for 70° and 90° deflection.

8.5. Internal impedance of the E.H.T. source

Because of the internal impedances in the E.H.T. source, the output voltage will depend on the current which is taken.

The load will also reduce the current output of the transformer, so that the deflection current will depend on the E.H.T. load. With suitable dimensioning, however, the deflection which is observed on the screen can remain practically constant under the influence of these two factors.

To this end, the increase in deflection sensitivity which is caused by the decreasing E.H.T. voltage must just be compensated by the decrease in the deflection current.

As the angle of deflection is more or less proportional to the deflection current, and is inversely proportional to the root of the E.H.T. voltage, a constant ratio must therefore be maintained between these two quantities, even with large fluctuations of brightness.

$$\frac{\hat{\imath}_y}{\sqrt{EHT}} = C \quad .$$

To the internal impedance contribute,

a) the internal resistance of the E.H.T. rectifier,

b) the leakage inductance between the E.H.T. winding and the primary,

c) the internal resistance of the "primary" part of the circuit, including the internal resistance of the output valves,

d) the internal resistance of the power supply circuit.

The contributions mentioned under *c*) and *d*) affect the stability of the primary voltage under a variable load, and thus influence the deflection current as well as the E.H.T. voltage. It is easy to appreciate that the condition of a constant relationship between $\hat{\imath}_y$ and $\sqrt{EHT}$ can be met if the contributions mentioned under *a*) and *b*), which only affect the E.H.T. voltage, are nearly as large as the contributions mentioned under *c*) and *d*), which affect both E.H.T. voltage and deflection current at the same time. With increasing load, the relative drop in the E.H.T. voltage will be twice as great as the relative drop in the deflection current, so that the above condition is satisfied.

Consequently a low internal impedance is not essential for good regulation, as the width of the picture can be kept constant at every level of internal impedance. However, it has the advantage that the E.H.T. voltage can be maintained better with large load currents, and, as a result, greater brightness and better focusing are obtained with a large beam current.

We may wonder what happens to the field deflection when the E.H.T. voltage drops.

Naturally, the field deflection sensitivity also increases, so that the field deflection current has to be adapted to the E.H.T. voltage to the same degree as the line deflection current.

As the direct voltage across the booster capacitor is proportional to the line deflection current, the required correction can be obtained in a simple manner by using this voltage as the supply voltage for the sawtooth os-

cillator for field deflection. This oscillator then has to be set up so that the sawtooth voltage obtained is proportional to the supply voltage.

In the field timebase, the deflection current depends on the size of the driving sawtooth on the grid of the output valve, in contrast with the line timebase, in which the output valve only has a switching function. To correct the field amplitude, therefore, it is sufficient to feed the oscillator from the booster voltage, and this need only constitute a very small extra load on the line output circuit.

Included among the possible methods of obtaining a low internal impedance are:

a) Ensuring a sufficiently high heater voltage for the E.H.T. rectifier, particularly for high load current.

b) Reducing the leakage inductance as far as possible, with reference to the flyback period and "third harmonic" tuning.

c) Driving the line output valve in an anode voltage range with low internal resistance (below the knee) or using a feedback circuit.

Provided that a reference element is used, a feedback circuit can also neutralise the effect of the internal impedance of the power supply circuit.

8.6. The influence exercised on the circuit by the E.H.T. load

8.6.1. Increase of the average anode current

The load which is applied to the circuit via the E.H.T. generator will generally have to be accompanied by an increase in the average current in the output valve. The size of this increase will depend on the internal impedance of the E.H.T. generator, amongst other things, as can be shown in a simple manner by means of an example. It must be noted that we are thinking only of the behaviour of a circuit for which the deflection remains constant with variations in the beam current, as discussed in the previous section.

Suppose that the unloaded E.H.T. voltage is 16 kV, and that the total internal impedance is 5 MΩ. With a beam current of 200 μA the E.H.T. voltage drops to 15 kV, so that the load on the circuit is 3 watts. If no extra current was supplied to the circuit, this load would be entirely at the expense of the deflection power. The deflection power must in fact decrease, because of the drop in the E.H.T. voltage, but not more than proportionally with the E.H.T. voltage, thus by $^1/_{16}$ in this case. In a practical case, P_m may be 36 VA for example. Then P_f would equal 16 W, if $\sqrt{\eta}$ is 0.8. As a result of the decrease in the E.H.T. voltage, P_m must also decrease bij $^1/_{16}$, which means that P_f drops to $^{15}/_{16} \times 16 = 15$ W. Consequently only 1 watt

may be taken from the deflection power as a result of the E.H.T. load, so that the remaining 2 watts must be drawn from the power supply.

With no load, therefore, the power requirement is 16 watts, and in the loaded condition 18 watts. We will now investigate what this means for the average current.

If it is assumed that $V_b - V_{a\text{end}} = 160$ V with no load on the transformer, the average anode current would be

$$\bar{i}_{a0} = \frac{16}{160}\,\text{A} = 100\,\text{mA}.$$

With the E.H.T. supply loaded, $V_b - V_{a\text{end}}$

$$\text{must drop to } \sqrt{\frac{15}{16}} \times 160\,\text{V} = 155\,\text{V}$$

in order to adapt the deflection current to the reduced E.H.T. voltage.

The average anode current now becomes

$$\bar{i}_a{}^1 = \frac{18}{155}\,\text{A} = 116\,\text{mA}.$$

In the following discussion, quantities corresponding to the unloaded E.H.T. will be given a suffix "0" and those corresponding to the loaded E.H.T. will be indicated by the index "1". We then have:

$$\bar{i}_{a0} = \frac{P_{f0}}{V_b - V_{a_{\text{end}}0}}$$

$$\bar{i}_a{}^1 = \frac{P_f{}^1}{V_b - V_{a\text{end}}{}^1}$$

and

$$\frac{V_b - V_{a_{\text{end}}0}}{V_b - V_{a_{\text{end}}}{}^1} = \sqrt{\frac{EHT_0}{EHT^1}}\,.$$

With the given internal impedance of the E.H.T. generator (R_i), the required increase in the average anode current as a result of the increased beam current (i_{EHT}) is given by:

$$1 + \gamma = \frac{\bar{i}_a{}^1}{\bar{i}_{a0}} = \frac{P_f{}^1}{P_{f0}} \sqrt{\frac{EHT_0}{EHT^1}} \qquad (8.6.1.1.)$$

The total power $P_f{}^1$ in the loaded condition is the sum of the power required for the deflection and the power which is taken from the E.H.T. voltage source, thus:

$$P_f{}^1 = P_{f0}\,\frac{EHT^1}{EHT_0} + EHT^1\, i_{EHT}\,.$$

It follows that:

$$1 + \gamma = \sqrt{\frac{EHT^1}{EHT_0}} + \frac{i_{EHT}\sqrt{EHT_0\, EHT^1}}{P_{f0}} \qquad (8.6.1.2.)$$

In addition:

$$EHT^1 = EHT_0 - i_{EHT}\, R_i$$

The increase in the average anode current due to the load on the E.H.T. voltage supply thus depends on P_{f0} and consequently on P_{m0}, as well as on EHT_0 and R_i.

Fig. 8.6.1 shows the value of γ for different values of EHT_0, R_i and P_{f0}.

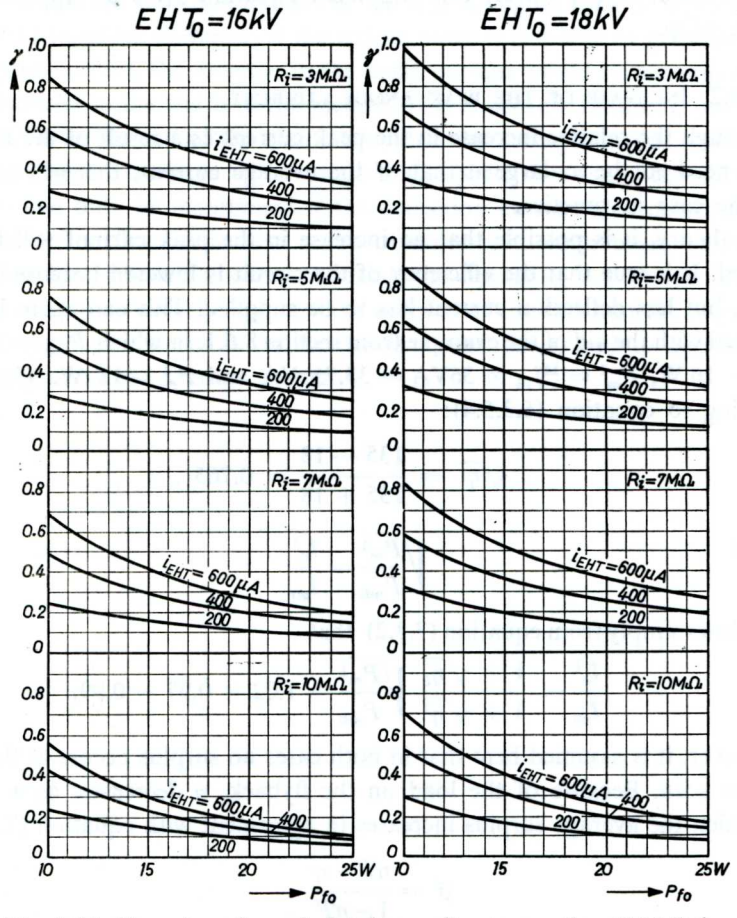

Fig. 8.6.1. The value of γ, calculated according to equation (8.6.1.2) for unloaded E.H.T. voltages of 16 and 18 kV and different values of the internal impedance, as a function of the flyback losses in the unloaded condition.

In the above, it is assumed that there is no load worth mentioning on the booster voltage. If there is, the direct current will already be higher for no load on the E.H.T. voltage, so that the fractional increase resulting from loading the E.H.T. supply will be smaller. This condition, which very seldom occurs now, can be represented in the above equations by replacing P_{f0} by the sum of the flyback losses and the booster load (i.e. $0.444\,P_{m0}+V_c i_l$).

For $R_i = 0$, it follows from equation (8.6.1.2) that

$$\gamma = \frac{EHT_0\ i_{EHT}}{P_{f0}} \qquad (8.6.1.3.)$$

For a small R_i ($< 3\ \mathrm{M}\Omega$) this simplified equation gives an approximate value of γ.

8.6.2. Increase of the peak anode current

Although the relative increase in the peak current as a result of the E.H.T. load need not be as large as that of the average current, this will usually be the case in practice.

In theory, it is possible that no increase in the peak current will be required. It is true that the efficiency of the circuit is lowered because of the load, but less deflection current has to be supplied. This can again be explained with the aid of the example from section 8.6.1. in which $P_{m0} = 36\mathrm{VA}$, $P_{f0} = 16\ \mathrm{W}$, $P_m{}^1 = {}^{15}/_{16} \times 36\mathrm{VA} = 33.75\ \mathrm{VA}$ and $P_f{}^1 = 18\ \mathrm{W}$. Then according to equation (6.3.5.4):

$$\sqrt{\eta^1} = \frac{135 - 18}{135 + 18} = 0.765\ .$$

Since

$$\sqrt{\frac{P_m{}^1}{P_{m0}}} = \frac{i_y{}^1}{i_{y0}}$$

it follows simply from equation (7.3.2) that

$$\frac{i_a{}^1}{i_{a0}} = \frac{1 + \sqrt{\eta_0}}{1 + \sqrt{\eta^1}} \sqrt{\frac{P_m{}^1}{P_{m0}}} = 1.02 \times 0.97 = 0.99.$$

However, it is assumed here that in both cases no surplus occurs at the end of the scan. Because of the load on the flyback, η decreases, as a result of which the average surplus increases in agreement with equation (7.1.):

$$\bar{\sigma} = \frac{n\Psi - \eta}{1 - n\Psi}\ .$$

The increase in the average surplus will also find expression in an increase in the surplus at the end of the scan, which will result in a higher peak

anode current unless a deliberate change in the waveform of the driving voltage is made simultaneously with the application of the load. If this is not done, the increase in the average anode current – whether obtained by lowering the grid bias, raising the screen grid voltage or the anode voltage, or by a combination of these – will have little effect on the waveform of the current, so that the peak current will increase in proportion with the average current, i.e.

$$i_a^1 = (1 + \gamma)\, i_{a0} \qquad (8.6.2.)$$

The appearance of a surplus at the end of the scan means that in the loaded condition the peak anode current will be higher than is required by the power supplied. However, if the output valve is not able to produce this high peak current, the increase in the beam current would be accompanied by a decrease in the width of the picture. This is because failure to produce the surplus at the end of the scan means that the average surplus would be too low, which conflicts with equation (7.1.). In that case, the average surplus can only be maintained if the deflection current also decreases.

If the full deflection is also to be obtained with high beam currents, it is therefore advisable, when choosing the operating conditions of the output valve (particularly V_{g2}), to take account of the fact that the required peak current also depends on the beam current load, and to about the same degree as the average current.

CHAPTER 9

THE OUTPUT VALVES

After paying particular attention to the design of the output transformer in the previous chapter, we will now discuss the output valves, the choice of operating conditions for them and their behaviour in various circuits.

9.1. The booster diode

Although the booster diode has a more passive role in the deflection circuit than the output pentode, the valve which is used here must satisfy high requirements if the circuit is to function correctly.

The diode must be able to pass large peak currents and average currents with a slight voltage drop, and at the same time it must be able to stand much higher peak voltages than is usual for normal rectifier valves in television or radio receivers.

These higher voltages do not only occur between anode and cathode, but also between cathode and heater. Consequently some distance must be allowed between the cathode sleeve and the heater, while care must also be taken to see that no electrons are drawn from the heater to the cathode during the flyback, when the cathode is at a high positive voltage. For this reason the heater is surrounded with an insulating material.

Because of these measures, more time elapses between switching on and obtaining emission from the cathode of this diode than is necessary for other valves. One result is that the screen grid of the output pentode starts to take current some time before the anode voltage begins to increase.

It is fortunate in this connection that the same series resistor, which prevents excessive screen-grid dissipation during normal operation of the set, also prevents excessive screen-grid current during the warming-up time of the diode.

As a higher screen-grid dissipation is permitted for the output valves during the warming-up time than for normal operation, no extra safety precautions have to be taken during warming-up.

The PY 81 and PY 88 are two of the special types of valve designed for use as booster diodes. The maximum peak voltages V_{a-k} of these valves are 5,000 V and 6,000 V respectively; the maximum average anode currents are 150 mA and 220 mA respectively.

These values are the so-called design centre maxima, which must not be

exceeded when nominal valves, components and operating voltages are employed. Absolute maximum values (5,600 V and 7,500 V respectively) are however indicated for the peak voltages for these valves, and these values must not be exceeded even under extreme operating conditions such as increased supply voltage, unfavourably placed tolerances, lack of synchronisation of the timebase etc.

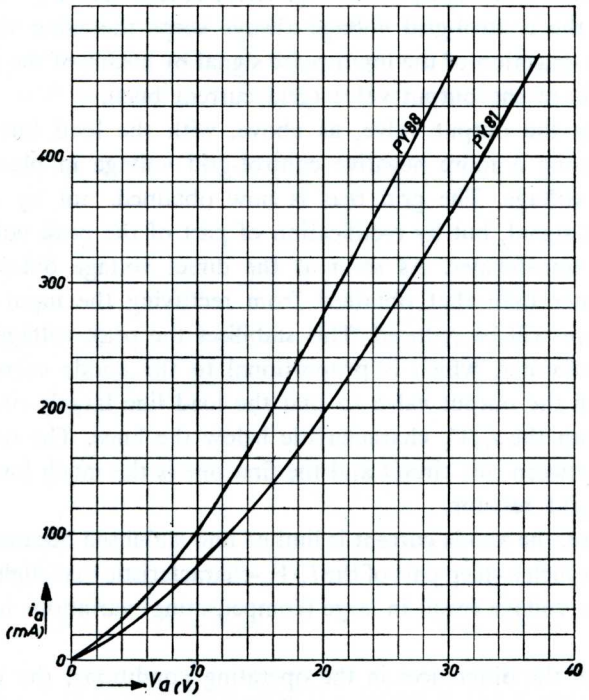

Fig. 9.1. i_a/V_a characteristic of the booster diodes PY 81 and PY 88.

The internal resistance of these valves is low, as can be seen from their characteristics (Fig. 9.1.). This means, amongst other things, that in most cases the slope of the load line in the i_a/V_a diagram for the pentode will not be less than that of the i_a/V_a characteristic below the knee of output valves such as the PL 81 and PL 36. (Also see section 7.2.1. and 7.2.2.)

9.2. **Operating conditions of the output pentode**

The choice of operating conditions for the output pentode has a great influence on the behaviour of the circuit.

In principle, the anode current, supplied to the deflection circuit, can

be mainly determined either by the screen-grid voltage, by the control-grid voltage, or by the anode voltage. This gives the following possibilities.

1) Driving the output valve in such a way that the load line always remains above the knee of the i_a/V_a characteristic. To achieve this, a relatively high resistance is connected in series in the screen-grid circuit, so as to limit the anode current to such a value that the voltage drop across the transformer winding n_3 (from Fig. 7.1.1) is less than $V_b - V_{a\ \text{knee}}$. In this circuit the control-grid voltage always keeps the same value, and is obtained by detection of the input pulse signal by means of the grid current characteristic of the output valve (grid current bias).

2) Driving the output valve, as above, with the load line above the knee, but using a more negative control-grid voltage in place of a low screen-grid voltage. The grid bias is now obtained, not by rectification of the input signal, but by rectification of part of the peak voltage across the output transformer. As soon as the direct voltage obtained in this way is greater than that obtained from rectifying the input signal, the anode current will be reduced. This stabilises the peak voltage across the output transformer, which is proportional to the anode current.

3) Driving the output valve so that the load line largely or completely coincides with the i_a/V_a characteristic below the knee. The only external difference between this circuit and the first one is the much lower value of the screen-grid resistor.

In this case, the anode current is limited and stabilised because the anode voltage is on such a steep part of the i_a/V_a-characteristic that slight variations in the anode voltage result in large (compensating) variations in the anode current.

Because of the differences in the operating conditions, the circuits will behave very differently with variations in the supply voltage, with changes in screen brightness (variations of the current which is drawn from the E.H.T. rectifier), and on deterioration of the characteristic of the output valve as a result of loss of emission. These points will now be examined in the following paragraphs.

9.3. Behaviour of the output circuits

9.3.1. The non-stabilised circuit above the knee

In this circuit, the transformer is dimensioned so that the nominal deflection and E.H.T. voltage are obtained if the voltage across the transformer winding n_3 at the end of the scan is less than the nominal supply voltage minus the minimum anode voltage $V_{a\ \text{knee}}$ at which the output valve is

able to produce the required peak current. In order to prevent the deflection becoming too great, the peak current is limited by means of a series resistor in the screen-grid circuit. The negative grid voltage is obtained by means of grid current which is drawn at the end of each scan. At that moment the grid voltage is slightly positive (approx. +1 V).

It is now easy to investigate the behaviour of the circuit with the aid of the i_a/V_a diagram of the output valve for $V_{g1} = +1$ V with V_{g2} as parameter. We draw the line which connects the point $V_a = V_b$ nom (for $i_a = 0$) with the working point at the end of the scan ($V_{a\text{end}}$, $\hat{\imath}_a$). A line of this type, such as line PQ in Fig. 9.3.1. does not represent the working

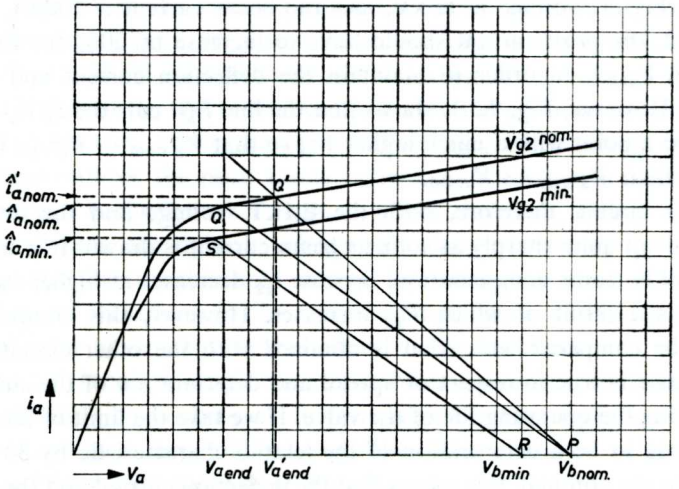

Fig. 9.3.1. Variations of $\hat{\imath}_a$ and $V_{a\,\text{end}}$, due to variations in the supply voltage and the load on the E.H.T. voltage in the non-stabilised circuit.

line itself, but the line on which the working point at the end of the scan would always be if $\hat{\imath}_a$ were changed, while keeping the same waveform. The reason for this is that as long as the impedance in the anode circuit, the waveform and the frequency remain constant, the voltage drop across the transformer is proportional to the peak current. However, if the anode impedance is changed, for example by placing a heavier load on the E.H.T. voltage, this condition is represented by a new line PQ^1 through V_b, which comes out at a higher peak current value for the same value of $V_{a\text{end}}$. Finally, if we alter the supply voltage without changing the load on the transformer, this line moves along the V_a axis parallel to the first line, e.g. *RS*.

Variations in the supply voltage will also be accompanied by variations of V_{g2}. It may be assumed that V_{g2} will be proportional to V_b.

It may be deduced from Fig. 9.3.1. that, partly due to the change in anode voltage, the peak current and $V_b - V_{a\text{end}}$ will also vary almost in proportion with V_b. Consequently, both the deflection current and the E.H.T. voltage vary about proportionally to the supply voltage, which means that variations of the deflection on the picture tube screen are only half the value of the percentage variations in the supply voltage.

The behaviour of the circuit for variations of the load on the E.H.T. voltage can also be deduced from Fig. 9.3.1. Let us assume that the line PQ refers to an unloaded circuit, for which $P_f = 15$ W.

If the E.H.T. voltage is 15 kV, and the beam current is 200μA, that is 3 W load, the peak current should have to increase by 20% for the same value of $V_{a\text{end}}$, in order to maintain the deflection current and E.H.T. voltage. However, Fig. 9.3.1. shows that the line PQ^1 cuts the i_a/V_a characteristic at a point with a much higher V_a, so that $V_{b\ \text{nom}} - V_a{}^1{}_{\text{end}}$ is much smaller than $V_{b\ \text{nom}} - V_{a\text{end}}$.

In this circuit, therefore, both the E.H.T. voltage and the deflection current drop quite sharply as soon as beam current is drawn. It is true that there will be some compensation, because i_{g2} decreases at higher values of $V_{a\text{end}}$, as a result of which V_{g2} increases. However, this compensation cannot be compared with what is obtained with the other circuits.

The same is true in respect of spread and deterioration of the characteristic during the operating life of the valve. If we take the limit of the spread and ageing to be a deteroration of the (static) characteristic by 30% with respect to the nominal, this means that the deflection current and the E.H.T. voltage are subject to large variations when valves are replaced, and during the life of the valves. To compensate this, the screen-grid voltage should really be adapted to the emissive condition of the valve by changing the series resistance. This method of amplitude regulation is not usually employed, as it is accompanied by the risk that the user may adjust the set to an E.H.T. voltage which is too high.

Another method of regulating the amplitude which can be used in this circuit is an adjustable coil, which is connected in parallel with the deflection coil or one of the windings of the transformer. This coil consumes part of the deflection current supplied by the transformer. During the operating life of the valve the deflection can be returned to its original level by increasing the self inductance of this coil. To prevent changes in the flyback period and the E.H.T. voltage, a small coil is sometimes included in series with the deflection coil, in addition to the parallel regulating coil, the

amplitude control being done by shifting a Ferroxcube core from the series coil into the parallel coil and vice versa. By this means the inductive load on the transformer can be kept constant during the amplitude adjustments.

In this circuit which is driven above the knee, there is no point in including only a series coil, because then the peak current will hardly vary, due to the high internal resistance of the pentode.

9.3.2. The stabilised circuit

In contrast with the previous circuit, the peak anode current in the stabilised circuit is adjusted as required by means of the grid bias. For this purpose, a part of the flyback voltage, which lies above a certain threshold value, is rectified, after which the resulting voltage is fed to the control grid of the output valve as an extra negative voltage. As long as the flyback has not reached this threshold voltage, there will be no regulating voltage, and grid current will flow at the end of the scan just as in the previous circuit. If the flyback voltage rises above the threshold voltage, the resulting negative grid voltage reduces the peak anode current, and this works against any further increase in the flyback voltage. It will be clear that, with an effective stabilising system, the flyback voltage will always be equal to, or only slightly greater than the threshold voltage. By making this threshold voltage independent of variations in the mains voltage, these variations can be prevented from having any further effect on the deflection.

Fig. 9.3.2.1. shows a simple form of stabilisation circuit, with which an effective stabilisation is obtained. In this circuit a voltage dependent resistor (VDR) is used as a threshold pulse rectifier. The operation of the VDR can be explained with the aid of Fig. 9.3.2.2.

The VDR has a symmetrical non-linear characteristic; the resistance decreases with increasing voltage. The VDR can thus operate as a rectifier for an asymmetrical voltage form. As the curvature of the VDR characteristic is continuous, small pulse voltages will also be rectified by an unloaded VDR circuit. By connecting another resistor in parallel with the VDR resistor, the rectifying effect is made dependent on the input voltage. This is because the parallel circuit has a characteristic which is almost linear for small voltages, so that rectification will only occur if the pulse voltage is large enough for its positive peaks to reach the curved part of the characteristic. In addition, a given rectified voltage can only be produced by maintaining a given current through the parallel resistor. This current is much greater than the current required by the VDR itself for the same voltage, so that the input signal must have a much greater amplitude. It is therefore possible to adjust the threshold value, and with it the line amplitude,

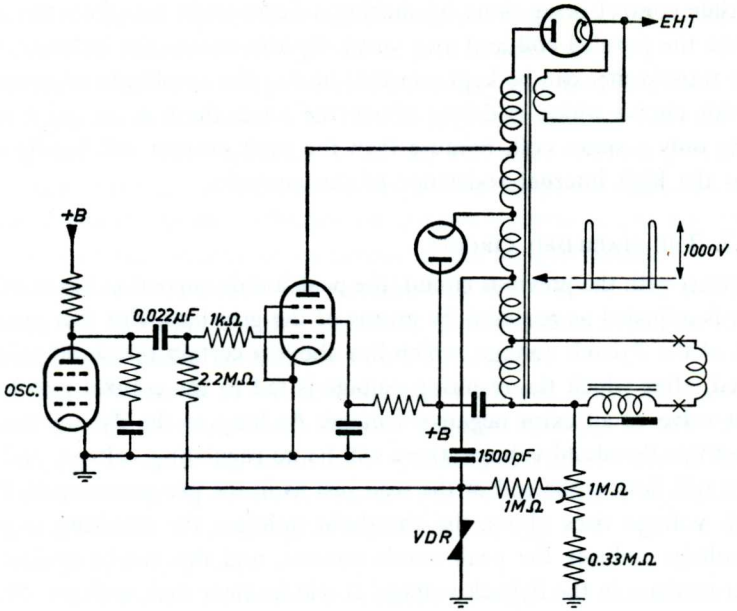

Fig. 9.3.2.1. Stabilised line output circuit.

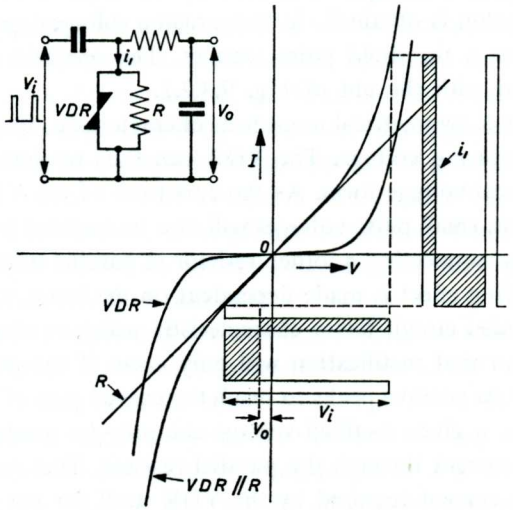

Fig. 9.3.2.2. Illustration of the operation of the VDR circuit.

by varying the value of the resistor *R*. A further possible means of adjustment is obtained by connecting a high adjustable positive voltage to the lower end of this resistor, e.g. part of the booster voltage, as shown in Fig. 9.3.2.1. There is now a bias voltage across the VDR, which must first be cancelled out by the rectification, before a negative control voltage can appear. The bias which is obtained is stabilised by the VDR itself. As a matter of fact, this characteristic makes it difficult to adjust the bias voltage, because a slight variation of voltage requires a large variation of current through the VDR.

Fig. 9.3.2.3. shows a better method of adjustment, in which the input pulse voltage is itself adjustable, by means of a capacitive voltage divider. However, the trimmer must be able to withstand high pulse voltages, because effective stabilisation is only obtained if the flyback voltage used for this purpose has reached a value of approximately 1,000 V.

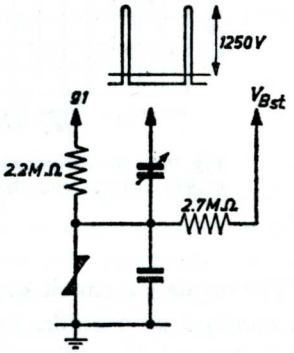

Fig. 9.3.2.3. VDR circuit with capacitive adjustment of the flyback pulse.

As the VDR is not subject to wear, and few components are used with it, the chance of failure of the regulating circuit is very small. One suitable VDR is the Philips type E 298 ZZ/01, which draws about 2 mA peak current at 1,000 V peak voltage.

The average negative voltage which appears at the top of the VDR is filtered by the grid leak resistance of the output valve, in combination with the coupling capacitor and the anode circuit of the oscillator which generates the drive voltage. In order to prevent hunting, the coupling capacitor must have a greater value than is usual in non-regulated circuits.

It is not recommended that extra *R–C* filters should be included in the lead from the regulator circuit to the control grid of the output valve, as the extra phase shift for low frequencies encourages the appearance of hunting.

The behaviour of the stabilised circuit can now be examined with the

aid of Fig. 9.3.2.4. The lines on which the working point must be situated at the end of the scan are now drawn in the i_a/V_a graph with V_{g1} as parameter. V_{g2} is taken as having a fixed value.

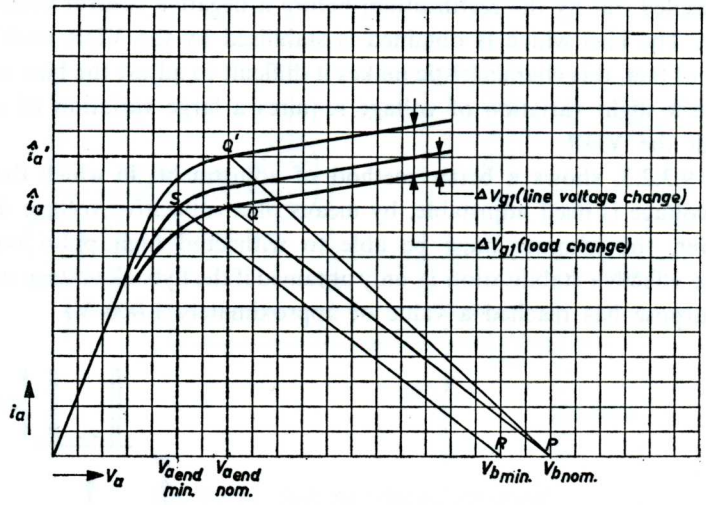

Fig. 9.3.2.4. Variations of $\hat{i}_a$, $V_{a\,end}$ and V_{g1} due to variations in the supply voltage and the load on the E.H.T. voltage in the stabilised line output circuit.

The regulation circuit keeps the flyback voltage, and with it $V_b - V_{a\text{end}}$, as constant as possible, by means of adjustment of the grid voltage. If V_b is changed, $V_{a\text{end}}$ therefore moves along by practically the same amount, which happens, as can be seen from Fig. 9.3.2.4. because the regulating circuit caused V_{g1} to vary by an amount $\triangle V_{g1}$. In practice, the movement of V_{g2} with V_b will mean that there must be a still greater change of the grid voltage. In order to keep the deflection as constant as possible, steps are taken to see that this $\triangle V_{g1}$ is obtained from a small alteration of the flyback voltage. For this reason, a large flyback pulse is used for the regulating circuit (approx. 1,000—1,200 V peak-to-peak). When such a voltage is used, the stabilisation circuit reduces the amplitude variations which occur with mains voltage variations of 10%, to about 0.5%. However, the stabilising effect stops as soon as $V_{a\text{end}}$ comes into the steep part of the i_a/V_a characteristic, since $V_b - V_{a\text{end}}$ can no longer remain constant. Consequently, the transformer for this circuit is calculated in such a way that the voltage drop across the winding n_3 at the end of the scan is not more than the minimum supply voltage minus the minimum anode voltage which

the output valve in question requires, in order to be able to produce the required peak current, i.e.

$$Vn_3 < (V_{b\,\min} - V_{a\,\text{knee}}).$$

With increasing E.H.T. load, the slope of the line on which the working point is situated at the end of the scan also increases. As $V_b - V_{a\text{end}}$ will remain practically constant, this means a considerable increase in the peak current, in contrast to the previous circuit.

The additional power which is drawn from the E.H.T. supply is much less of a drain on the deflection power than it was in the previous case, and is largely drawn from the supply circuit.

This results in constant raster widths and E.H.T. voltage, i.e. low internal resistance. Of course, the peak current can only increase as long as V_{g1} is still negative. The same is true of loss of emission in the valve; the screen-grid voltage is preferably made so high that sufficient beam current can be drawn from a valve at the end of its operating life and at undervoltage, before the grid voltage at the end of the scan has become 0 V.

9.3.3. The circuit with drive below the knee

For this circuit, the output transformer is calculated so that the voltage drop across the transformer winding n_3 is equal to $V_{b\,\text{nom}} - V_{a\,\text{knee}}$ when the required deflection is obtained with all reserves and the correct E.H.T. voltage. The grid voltage is again obtained by grid rectification of the input signal and is thus approx. +1 V at the end of the scan.

Fig. 9.3.3. shows that a certain amount of stabilisation of the scan voltage $V_b - V_{a\text{end}}$ is obtained by driving below the knee both for variations of the E.H.T. load and for ageing of the valve. In this respect it can be remarked that the steep part of the i_a/V_a characteristic hardly changes with valve ageing. Variations in the supply voltage however have a proportional effect on $V_b - V_{a\text{end}}$, so that in this respect this circuit is no better than the first. The range of the amplitude regulating circuit must therefore be large enough to deal with variations due to changes in the supply voltage, as well as tolerances of the components which are used.

In this circuit, at least one adjustable coil must be included in series with the deflection coil, as an adjustable shunt coil by itself is ineffective in this circuit with low internal resistance of the output valve. Here too, a combined series-shunt adjustment is preferably used to keep the flyback period constant, while another possible means of adjustment is switching over the deflection coil to suitable taps on the output transformer.

One result of driving below the knee, is the high ratio of screen-grid

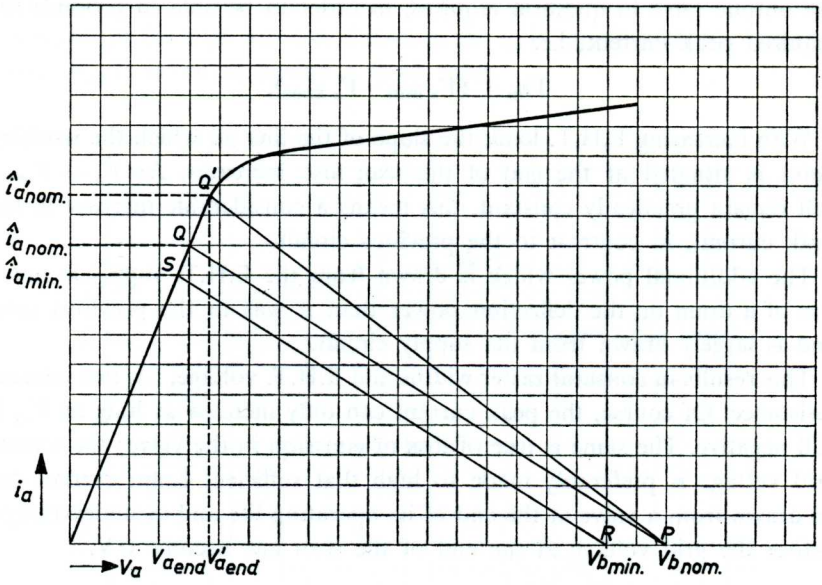

Fig. 9.3.3. Variations of $\hat{i}_a$, and $V_{a\,\mathrm{end}}$ in a line output circuit with partial stabilisation obtained by driving below the knee of the i_a/V_a characteristic.

current to anode current. This ratio depends to a large extent on the degree to which the anode voltage is driven below the knee. If a fixed screen-grid voltage was employed, very large variations would occur in the screen-grid current, because practically the whole difference in the cathode current of different valves has to be taken up by the screen grid. However, a sliding screen-grid voltage is obtained by using a series resistor, so that the differences in the cathode currents are automatically reduced. If this series resistor is not decoupled, the screen-grid voltage does not only adapt itself to the average, but also does so instantaneously, so that the occurrence of high instantaneous values of the screen-grid current is also prevented.

Although the situation is greatly improved by the screen-grid resistor, the dissipation which occurs in the screen grid is difficult to calculate. For this reason, it is customary in such circuits to give the series resistor a value such that the screen grid can never be overloaded. The minimum value for the resistance can be roughly calculated from:

$$R_{g2\,\mathrm{min}} = \frac{0.75\ (0.5\ V_{b\,\mathrm{nom}})^2}{P_{g2\,\mathrm{max}}} \qquad (9.3.3)$$

The factor 0.75 in this expression is only applied if the resistor is not

decoupled. This takes into account the fact that the screen-grid current is suppressed at least during the flyback period, while it is also unlikely that the screen-grid voltage would be exactly equal to 0.5 V_b during the whole scan. Because of this, the theoretical maximum screen-grid dissipation is never reached during the scan, so that the series resistor may be reduced correspondingly.

In practice, the circuit with drive below the knee is found to give sufficient stabilisation against changes in the valve characteristics and variations of the load.

In addition to the objection, mentioned above, of dependence on the mains voltage, however, there is also the possibility of Barkhausen oscillations occurring. The occurrence of these oscillations will be explained briefly in the following section.

9.3.4. Barkhausen oscillations

Barkhausen oscillations owe their origin to the electrons which turn back from the anode, pass between the wires of the screen grid, and are finally braked and sent back again as a result of the negative potential of the control grid. If large groups of electrons start doing this at the same time, a high frequency oscillation of quite large intensity will be produced. The oscillations can only be observed when the valve is driven below the knee.

The frequency which is generated depends only on the construction of the output valve, and on the voltages on the electrodes. The impedances connected to the electrodes have no effect on the frequency, because the whole oscillation takes place within the valve. As the valve passes through a large number of different operating settings during each period, the frequency spectrum which is generated is very extensive. Measurements show that oscillations of fairly high intensity may occur in the range between 300 and 500 Mc/s, while the half frequencies also occur at lower intensities.

These oscillations have no effect on the operation of the timebase circuit and the course of the sawtooth current. However, if the radiated energy reaches the aerial, there is the chance that one or more vertical stripes will appear on the screen. The stripes are black in a receiver for negative modulation and white in a receiver for positive modulation; the position of the stripes on the screen is determined by the instant at which the operating conditions of the valve are suitable for generating frequencies within the channel being received by the set.

The interfering effect can be reduced by good screening of the line time-

base. In addition, precautions are taken in modern line timebase valves, in order to counter the appearance of interference due to Barkhausen oscillations. In the PL 36 for example, a plate is connected to the anode and is placed in the path of the electrons, thus hindering the simultaneous return of large groups of electrons. These precautions make it possible to obtain interference-free operation, even for driving below the knee, provided that the screen-grid resistance is not too low.

9.3.5. Dynatron oscillations

In addition to Barkhausen oscillations, dynatron oscillations can also appear in the line timebase, but only when the valve is driven just above the knee. These oscillations or instabilities can occur when there is a region of negative slope in the i_a/V_a characteristic. As is well known, this is often the case for beam tetrode and pentode valves at fairly low currents.

If instability is to occur, the impedance in the anode circuit must be higher than the reciprocal value of the negative slope of the i_a/V_a characteristic. Because of the damping which the booster exercises on the circuit during the scan, the load impedance of the anode of the output valve is only a few hundred ohms for high frequencies.

However, if a non-decoupled resistor is included in the screen-grid circuit of the valve, positive feedback occurs in passing through those parts of the characteristic which have a negative slope, as a result of which instability can still occur.

This form of instability can be observed in the oscillograms of the anode current of diode and pentode as bumps or sudden changes in the current, but they are scarcely noticeable in the deflection current. However, these oscillations may cause the working line to jump to the knee, as a result of which Barkhausen oscillations will also be produced. In that case, the visible effect is identical to that of the interference described in the previous section.

However, it is easy to prevent dynatron oscillations, because it is sufficient to connect a decoupling capacitor across the screen-grid resistor of the output valve. When an autotransformer is being used, there is unlikely to be a high leakage inductance, which could favour the appearance of oscillations, in the transformer between the diode and pentode windings.

9.3.6. The choice of the screen-grid resistance

After it has been determined what value the minimum anode peak current must have in order to obtain sufficient deflection, we must decide what

value the screen-grid resistor must have, for the output valve to be able to produce the required current during a reasonable operating life.

For a line output valve, it is customary to allow a margin of about 30% reduction on the nominal value of the anode current, for spreads in the characteristic and reduction of the current due to emission loss.

The "end of operating life" is reached when the anode current has dropped to 70% of the published nominal value for nominal heater voltage at anode voltages above the knee, and for fixed values of applied voltages; a further reduction in the anode current, of 10% of the nominal value, must be expected if the heater voltage is also 10% below the nominal value, as a result of low mains voltage. The static characteristics of an output valve at the end of its operating life, and for underheating, can

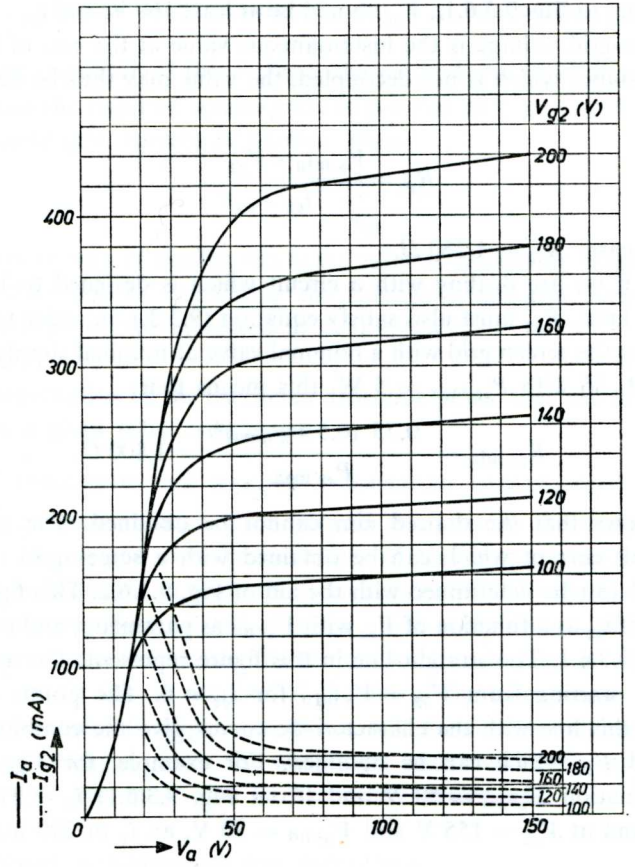

Fig. 9.3.6.1. i_a/V_a characteristics of a PL 36 at the end of its operating life, with 10% underheating, with V_{g2} as parameter for $V_{g1} = +1$ V.

thus be deduced from the nominal characteristics by reducing the values of the current scales by 40%. This only refers to anode voltages above the knee, because the characteristic below the knee hardly alters at all during the operating life of the valve.

As an example, Fig. 9.3.6.1. shows these characteristics for a PL 36, at $V_{g1} = +1$ V. This is about the maximum grid voltage which can be reached in a circuit under the minimum conditions described above. From this characteristic, we can determine the screen-grid voltage required by an underheated "end of life" PL 36, in order to produce the required $\hat{\imath}_a$ at a given $V_{a\text{end}}$.

As an example, we can choose a circuit for which $V_b = 220$ V nominal, 200 V minimum, $\hat{\imath}_a = 300$ mA minimum and for which $V_{a\text{end}}$ could be approximately 50 V under the minimum conditions.

According to Fig. 9.3.6.1., V_{g2} should be at least 160 V, and $i_{g2} = 32$ mA. This screen-grid voltage is the instantaneous value at the end of the scan. For a resistance which is not decoupled, the value may thus be determined from:

$$R_{g2} = \frac{V_{b\,\text{min}} - V_{g2}}{i_{g2}} .$$

In this case, $R_{g2} = 1{,}250\ \Omega$.

However, if we are dealing with a circuit which is designed to be driven below the knee, R_{g2} must also satisfy equation (9.3.3.), in order to prevent overloading the screen grid with a nominal valve at nominal supply voltage. For the PL 36 with $P_{g2\,\text{max}} = 5$ W, this means that:

$$R_{g2\,\text{min}} = \frac{0.75\ (0.5\ V_{b\,\text{nom}})^2}{P_{g2\,\text{max}}} = 1{,}800\ \Omega.$$

This shows that the desired aim cannot be obtained. The maximum anode peak current which can be obtained with a screen-grid resistance of 1,800 Ω can be determined with the aid of Fig. 9.3.6.2. This figure gives the value of i_{g2} as a function of V_{g2} with $V_{a\text{end}}$ as parameter, and is deduced from Fig. 9.3.6.1. The straight line in this figure represents the screen-grid resistance, starting from $V_{g2} = V_{b\,\text{min}}$ for $i_{g2} = 0$. The points of intersection of this line with the characteristic curves give the combinations of $V_{a\text{end}}$ and V_{g2} which can be obtained. For example, for $V_{g2} = 150$ V, the combination $V_{a\text{end}} = 50$ V and (from Fig. 9.3.6.1) $\hat{\imath}_a = 270$ mA is possible, and at $V_{g2} = 155$ V and $V_{a\text{end}} = 70$ V, an $\hat{\imath}_a$ of 290 mA can be obtained.

In stabilised circuits it is customary to decouple the screen-grid resistor

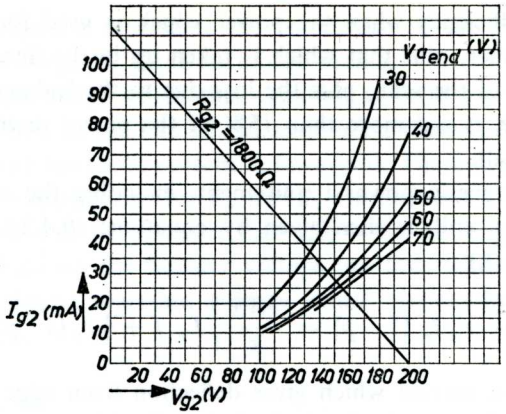

Fig. 9.3.6.2. I_{g2} as a function of V_{g2} with $V_{a\,end}$ as parameter for a PL 36 at the end of its operating life, with 10% underheating.

with a large capacitor. If this is done, the method described above cannot be used, and the required screen-grid resistor can only be calculated if the average screen-grid current is known. Then

$$R_{g2} = \frac{V_{b\ min} - V_{g2}}{\bar{i}_{g2}} .$$

The simplest way of finding the exact value is usually by measurement. However a method of calculating the average screen-grid current for a stabilised circuit will be discussed in section 9.4.9.

9.4. Determination of the maximum deflection power that can be obtained with a given valve complement

9.4.1. Prerequisites for making a simplified calculation

The previous chapters have given general guidance in the design of the deflection circuits and the dimensioning of the output transformer. It may often be desirable to find out if, and under what conditions, a given deflection can be obtained with a given valve complement, without carrying out a detailed calculation for the output transformer. It will be obvious that, to do this, a number of factors in the calculation, which in practice are subject to slight variations, will have to be allocated fixed values or percentages, while the conditions under which the expressions used are applicable must also be accurately determined.

9.4.2. Power requirements for deflection

With reference to the power requirements for deflection, the circuit has

a reasonable efficiency when the power which is used for magnetisation of the transformer, plus that which is taken up in the linearity correction coil at the end of the scan, plus the loss due to the leakage inductance of the transformer, is not more than 15% of the power required by the deflection coil itself.

The total magnetic power requirement, including the resistance losses of the deflection coil, is then given by equation: (9.4.2.), derived from equation (6.3.5.3.)

$$P_m = \frac{1.15}{8} V_y \hat{\imath}_y (1-p) = \frac{1.15}{8} \left\{ L_y f + \tfrac{1}{2} r_y (1-p) \right\} \hat{\imath}_y^2 . \quad (9.4.2.)$$

The deflection current which gives deflection from edge to edge of the raster is often taken as a basis of calculation. To this current must be added a margin for adapting the aspect ratio of the picture to the transmission standard, while the difference between the flyback period and the blanking must be added on or subtracted, according to whether the difference is positive or negative. In addition, allowance must be made for tolerances in the sensitivity of the deflection coil, and for a slight over-deflection in the vertical direction, to which the horizontal deflection must be adapted. When determining the deflection current which is required, it must also be remembered that the deflection usually increases more rapidly than the current; for example in a picture tube with a deflection angle of 110°, only about 5% more current is required for an over deflection of 10% than for deflection from edge to edge.

When an (inductive) amplitude regulator is used, the power taken up by this must also be taken into account.

As loading the E.H.T. voltage results in an increase γ of both the average current and the peak current, the total power taken by the loaded deflection circuit can be put at:

$$P_m{}^1 = (1+\gamma) P_m.$$

9.4.3. Peak anode current requirements

The peak current which the output valve has to supply can be expressed in terms of the value of the power requirements for deflection. To this end, the product $1.15\, V_y \hat{\imath}_y$ in equation (9.4.2.) is replaced by the product of the total primary voltage and current:

$$(1+\gamma) P_m = \tfrac{1}{8} (V_{Bst} - V_{a_{\text{end}}}) \hat{\imath}_a (1 + \sqrt{\eta}) (1-p),$$

from which:

$$\hat{\imath}_a = \frac{8 (1-a) (1+F_p) (1+\gamma) P_m}{\hat{V}_a (1+\sqrt{\eta}) (1-p)} \quad (9.4.3.)$$

In this expression a represents the percentage of the reduction of the primary peak voltage by third harmonic tuning.

The conditions under which this equation is valid are firstly, that no diode current flows at the end of the scan when there is no E.H.T. load, secondly, that the sawtooth current is linearised. These are the conditions under which the expressions for P_m and $\hat{\imath}_a$ are deduced.

In addition, it will be assumed that $\sqrt{\eta} = 0.8$ as long as the E.H.T. load and the load on the booster voltage are low, while $(1 - a)$ is put at 0.85. These figures represent average values measured in a number of practical circuits.

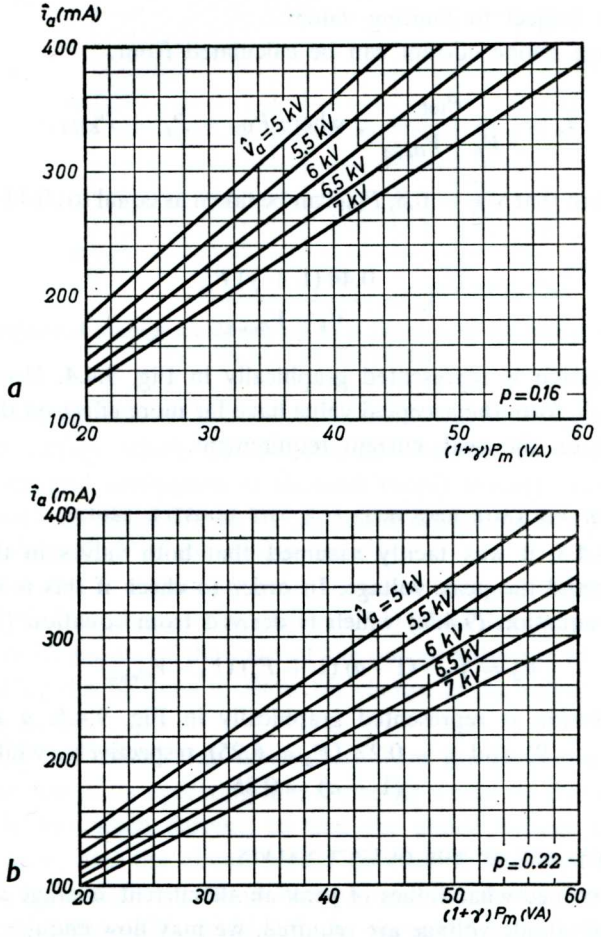

Fig. 9.4.3. Required peak anode current as a function of the deflection power with $\hat{V}_a$ as parameter, (*a*) for a flyback ratio of $p = 0.16$ and (*b*) for $p = 0.22$.

The peak anode current requirement given by this expression, and under the stated conditions, is shown graphically in Fig. 9.4.3.*a* and *b*, as a function of $(1 + \gamma) P_m$ with the anode peak voltage $\hat{V}_a$ as parameter, for $p = 0.16$ $(F_p = 9)$ and $p = 0.22$ $(F_p = 6.25)$ respectively. Any deviation of $\sqrt{\eta}$ from the accepted value has little effect on the required peak current.

9.4.4. Average anode current

In addition to the peak current, the average anode current which the output valve has to supply is also important. The average anode current is one of the factors determining the losses in the valve and the cathode load, and is subject to limiting values.

The average anode current can be calculated from:

$$\bar{i}_a = \frac{P_{\text{tot}}}{V_b - V_{a_{\text{end}}}} \text{ , where } P_{\text{tot}} = P_f^1 + P_{EHT}.$$

On condition that $\sqrt{\eta} = 0.8$, P_{tot} can be taken as equal to: $0.44\,(1+\gamma)\,P_m$ so that

$$\bar{i}_a = \frac{0.44\,(1 + \gamma)\,P_m}{V_b - V_{a_{\text{end}}}} \qquad (9.4.4.)$$

This expression is represented graphically in Fig. 9.4.4. However, deviations of $\sqrt{\eta}$ from the accepted value have far more effect on the average current than on the peak current requirement.

9.4.5. Peak voltage required for the booster diode

In section 9.4.3, it was tacitly assumed that both valves in the output circuit can stand the peak voltage. In order to check if this is in fact so, we can use equation (9.4.5.) which is derived from equation (7.2.3.8):

$$\hat{V}_d = \hat{V}_a - (1 - a)\,(1 + F_p)\,(V_b - V_{a_{\text{end}}}) \qquad (9.4.5.)$$

This expression is represented graphically in Fig. 9.4.5. *a* and *b* for $p = 0.16$ $(F_p = 9)$ and $p = 0.22$ $(F_p = 6.25)$ respectively, while

$$(1 - a) = 0.85.$$

9.4.6. Limits set by the output valves

Having determined what values of peak anode current, average anode current and peak anode voltage are required, we may now enquire what currents can and must be supplied by the valves at a given supply voltage.

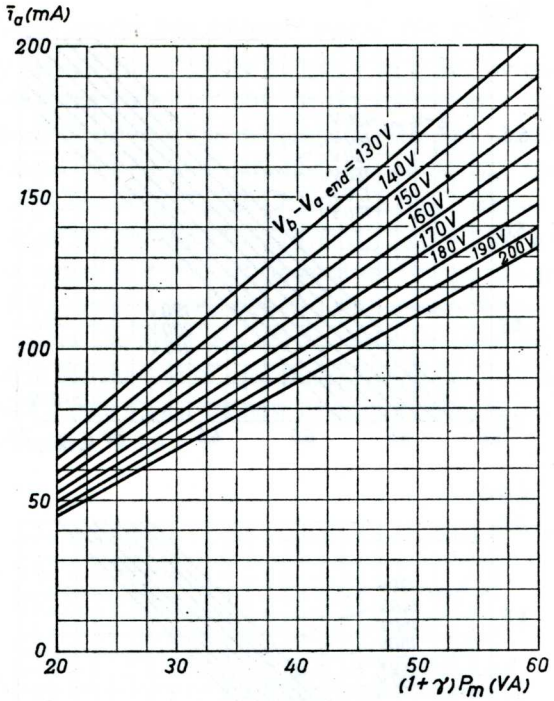

Fig. 9.4.4. Required average anode current as a function of the deflection power with $V_b - V_{a\,end}$ as parameter.

As far as the currents are concerned, the limits will be set by the maximum screen-grid voltage which can be obtained without exceeding the permitted screen-grid dissipation at nominal supply voltage. There are also cases in which the limits are set by the anode dissipation or by the average cathode current limit of the output valves.

It is clear that a distinction must be made between different types of circuits. In the case (discussed in section 9.3.1) when there is no stabilisation at all, either by means of the knee of the output valve, or by a regulating circuit nothing can be done to allow for change in the valves, as has been mentioned earlier.

If R_{g2} for this circuit was determined from the characteristic for the valve at the end of its operating life, the result would be that a new valve would draw too much current, so that the anode voltage would again reach the knee, and the circuit would go over to the type discussed in section 9.3.3. In addition, the deflection and the E.H.T. voltage would increase too much, which could only be prevented by adjustment of the set (e.g. increase of the screen-grid resistance).

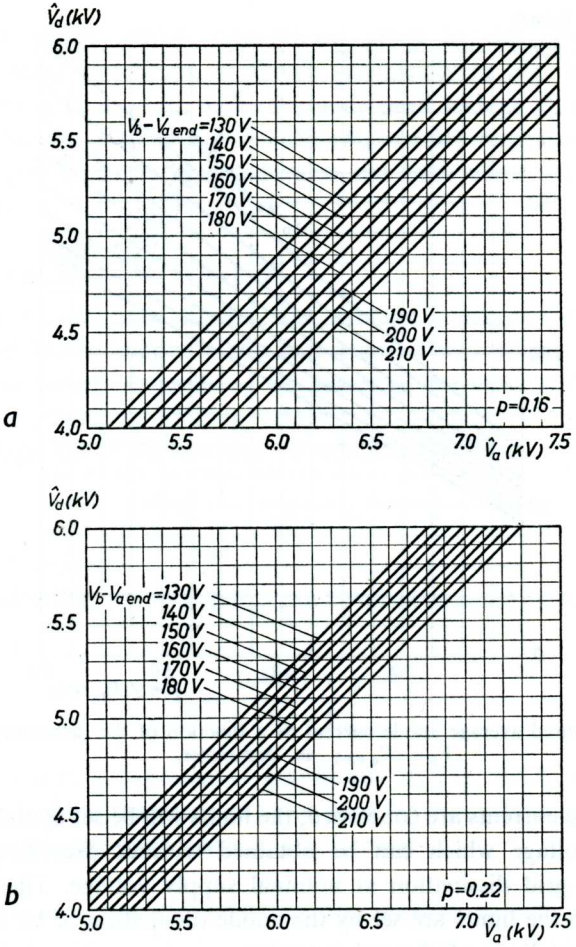

Fig. 9.4.5. V_d as a function of V_a with $V_b - V_{a\,end}$ as parameter for (*a*) $p = 0.16$ and (*b*) $p = 0.22$.

In the other types of circuit however, there is a reserve, which is called upon automatically as soon as this becomes necessary. For these types of circuit, the following section indicates a method of determining the maximum deflection power which can be obtained at nominal voltage. This calculation is based on the assumption that the output valve must still be able to give sufficient deflection and good linearity until it reaches the end of its operating life, even with 10% undervoltage of the power supply.

9.4.7. Maximum power for driving below the knee

The maximum power which can be supplied by a line output valve when it is driven below the knee, can now be determined in a simple manner. With this method of driving, the minimum screen-grid resistance is determined by equation (9.3.3.) and depends only on $V_{b\,\mathrm{nom}}$ and $P_{g2\,\mathrm{max}}$.

This value is indicated in Fig. 9.4.7.1. If we now transfer the resulting minimum values of R_{g2} for the PL 36, with $P_{g2\,\mathrm{max}} = 5$ W, to Fig. 9.3.6.2, but place these values at 0.9 $V_{b\,\mathrm{nom}}$ instead of $V_{b\,\mathrm{nom}}$, this gives the maximum value of V_{g2} which can be expected with undervoltage. $V_{a\mathrm{end}}$ can be taken slightly above the knee, e.g. 70 V, which is quite acceptable as a limiting condition for the end of operating life and for undervoltage. With these values of V_{g2} and $V_{a\mathrm{end}}$, we now determine the minimum obtainable value of $\hat{\imath}_a$ from Fig. 9.3.6.1.

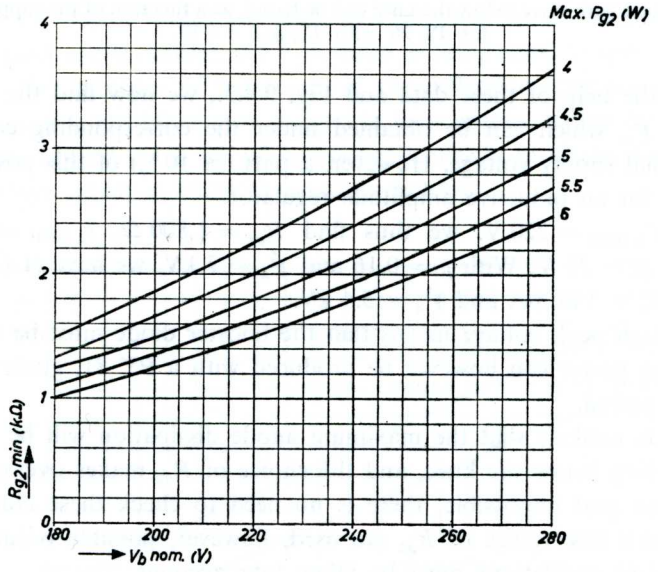

Fig. 9.4.7.1. Minimum value of the screen-grid resistance as a function of the nominal supply voltage with $P_{g2\,\mathrm{max}}$ as parameter, for driving below the knee of the i_a/V_a characteristic.

At nominal supply voltage the peak anode current will then be at least 10% higher, in agreement with what was discussed in section 9.3.3., while $V_{a\mathrm{end}}$ will drop until it reaches the steep part of the family of i_a/V_a characteristics. We can now determine the value of $(1 + \gamma)\ P_m$ from Fig. 9.4.3., while the corresponding average anode current and the required

peak voltage on the booster diode can be found with the aid of Figs. 9.4.4. and 9.4.5. These last figures also indicate which booster diode is required in order to give this maximum deflection power.

As an example, the procedure outlined above will now be followed for a PL 36, for which $\hat{V}_a = 7{,}000$ V and $P_{g2} = 5$ W.

Table 9.4.7.2 gives the values of R_{g2}, V_{g2}, and $\hat{\imath}_a$ for undervoltage, and, in the last two columns, $\hat{\imath}_a$ nominal and $V_{a\text{end}}$ nominal.

V_b nom	V_b min	R_{g2} min	V_{g2} min	$\hat{\imath}_a$ min	$\hat{\imath}_a$ nom	$V_{a\text{ end}}$ nom
(V)	(V)	(Ω)	(V)	(mA)	(mA)	(V)
180	162	1250	138	245	270	30 V
200	180	1500	146	270	295	33 V
220	198	1800	155	295	325	35 V
240	216	2150	160	310	340	37 V
260	234	2550	163	315	345	40 V

Fig. 9.4.7.2. Maximum value of the peak anode current, on which the design of an output circuit with drive below the knee can be based, as a function of the supply voltage, for PL 36 with $P_{g2\,\max} = 5$ W.

With the help of these data and Fig. 9.4.3., we now find the value of $(1 + \gamma)\ P_m$ which can be obtained under the corresponding conditions of nominal supply voltage. However, a part ($\approx 10\%$) of this power must be used for an inductive amplitude regulator.

For $V_{b\text{ nom}} = 220$ V, we thus find $R_{g2} = 1{,}800\ \Omega$, $\hat{\imath}_{a\text{ nom}} = 325$ mA and $V_{a\text{end}} = 35$ V. With $p = 0.16$ and $\hat{V}_a = 7$ kV, we have $(1+\gamma)\,P_m = 50$ VA, $\bar{\imath}_a = 140$ mA and $\hat{V}_d = 5.4$ kV.

This high peak voltage means that the booster diode must be a PY 88. The same power can however be produced with a PY 81, given a longer flyback period.

As it is unlikely that the maximum anode dissipation will be exceeded with driving below the knee, and the choice of R_{g2} makes overloading of the screen grid impossible, there is no need to check these conclusions. When such low values of R_{g2} are used, however, possible occurrence of Barkhausen oscillations must be taken into account.

9.4.8. Maximum power for the stabilised circuit

The maximum power which can be obtained in the stabilised circuit with a given valve complement also depends on the peak current, and thus on the screen-grid voltage. In this case the screen-grid resistor will be decoupled, so that the screen-grid voltage is now determined by the average screen-grid current.

Because of the position of the working line at nominal supply voltage,

the ratio of average anode current to average screen-grid current is much more favourable than for a circuit driven below the knee.

The maximum screen-grid dissipation is only reached at a considerably higher voltage; therefore, the series resistor can usually have a lower value. This also means that a higher screen-grid voltage can be present at low mains voltage, when the working line comes closer to the knee of the valve.

As was explained in section 9.3.2., when the supply voltage changes, the working line moves along by practically the same amount, while the peak current remains almost unchanged. For this reason, the anode current for a valve at the end of its operating life, and with undervoltage, must be at least equal to the peak anode current for which the circuit was designed, while the anode voltage must be at least equal to the knee voltage. For the PL 36, the nominal value of $V_{a\text{end}}$ can thus be found by adding 0.1 V_b to the value given in Fig. 9.3.6.1. The nominal screen-grid voltage can be found by multiplying the indicated required minimum value by 1.1. These values are given in Fig. 9.4.8. as a function of the required peak anode current; 0.1 V_b is taken as being equal to approximately 20 Volt. The influence of tolerances of the deflection components on the anode voltage is not taken into account in these graphs, so that these figures should be applied to a set of components which produces the lowest anodevoltage which is likely to occur in practice.

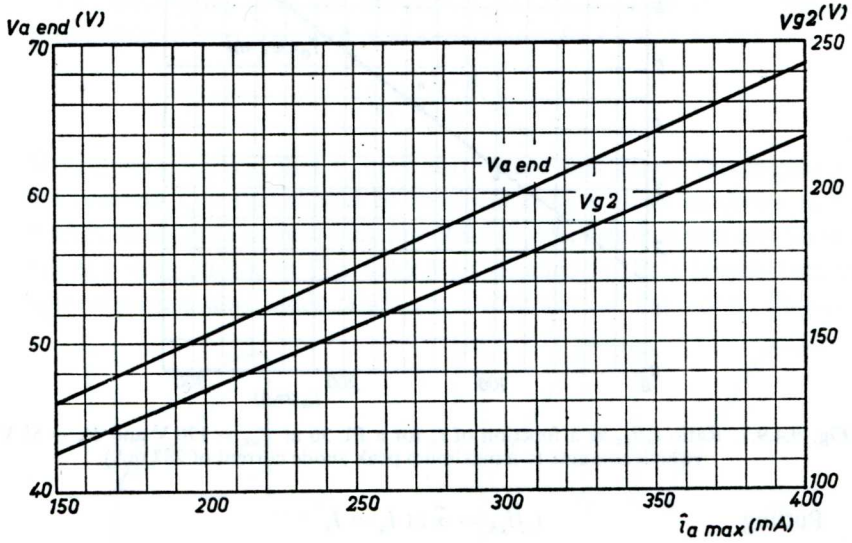

Fig. 9.4.8. Required nominal anode voltage at the end of the scan, $V_{a\text{ end}}$, and required nominal screen-grid voltage, V_{g2}, of an end-of-life PL 36 with underheating, as functions of the peak anode current $\hat{\imath}_{a\text{ max}}$ for which the stabilised time base circuit is designed.

Just as for driving below the knee, the relationship between the anode current and the screen-grid current of the valve is one of the important criteria which determine the behaviour and the possibilities of the valve.

In the stabilised circuit with decoupled screen-grid resistor, it is the average value which is important, instead of the instantaneous value at the end of the scan. A method of finding the ratio $\bar{\alpha} = \bar{i}_a/\bar{i}_{g2}$ for the values of anode and screen-grid voltages given in Fig. 9.4.8. will now be worked out in section 9.4.9.

9.4.9. Ratio of average anode current to average screen-grid current

To ascertain the value of $\bar{\alpha} = \bar{i}_a/\bar{i}_{g2}$, it is necessary to know the functions $i_a = f(t)$ and $i_{g2} = f(t)$.

As a first approximation, the function $i_a = f(t)$ will be assumed to be linear. Measurements reveal that the function $i_{g2} = f(t)$ can also be approximated by a straight line (see Fig. 9.4.9.1.)

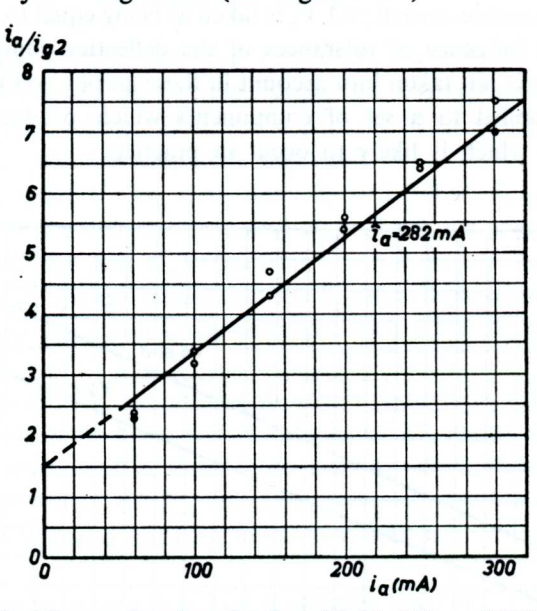

Fig. 9.4.9.1. Ratio i_a/i_{g2} as a function of i_a for a PL 36 at $V_{g2} = 170$ V and $V_a = 58$ V (which amounts to a maximum peak anode current of 282 mA).

Putting $\quad i_a/i_{g2} = \hat{\alpha}$ at $i_a = \hat{i}_a$

and $\quad i_a/i_{g2} = \alpha_0$ at $i_a = 0$

in which the value of α_0 is derived by extrapolating the measured function

$i_a/i_{g2} = \mathrm{f}(i_a)$, we may write:

$$i_a/i_{g2} = \alpha_0 + (\hat{\alpha} - \alpha_0)\, i_a/\hat{\imath}_a \qquad (9.4.9.1.)$$

where

$$i_a = \hat{\imath}_a\ t/\tau_1 \qquad (9.4.9.2.)$$

τ_1 denoting the duration of the scan.

From equations (9.4.9.1) and (2)

$$i_{g2} = \frac{\hat{\imath}_a}{\hat{\alpha}-\alpha_0}\ \frac{t}{t + \tau_1\alpha_0/(\hat{\alpha}-\alpha_0)}$$

whence

$$\bar{\imath}_{g2} = \frac{1}{\tau_1}\ \frac{\hat{\imath}_a}{\hat{\alpha}-\alpha_0} \int_0^{\tau_1} \frac{t}{t + \tau_1\alpha_0/(\hat{\alpha}-\alpha_0)}\,\mathrm{d}t$$

$$= \frac{1}{\tau_1}\ \frac{\hat{\imath}_a}{\hat{\alpha}-\alpha_0} \left| t + \frac{\tau_1\alpha_0}{\hat{\alpha}-\alpha_0} \left\{ 1 - \log_e \left(t + \frac{\tau_1\alpha_0}{\hat{\alpha}-\alpha_0} \right) \right\} \right|_0^{\tau_1}$$

$$= \frac{\hat{\imath}_a}{\hat{\alpha}-\alpha_0} \left(1 - \frac{\alpha_0}{\hat{\alpha}-\alpha_0} \log_e \frac{\hat{\alpha}}{\alpha_0} \right) \qquad (9.4.9.3.)$$

It should be recognised that this expression gives the average value of the screen-grid current *during the scan.*

The assumption that the function $i_a = \mathrm{f}(t)$ is linear is not generally permissible, for in that case the average anode current would be

$$\bar{\imath}_a = \frac{1-p}{2}\ \hat{\imath}_a\ .$$

Measurements reveal that $\bar{\imath}_a$ may also exceed this value. This implies that the function $i_a = \mathrm{f}(t)$ should be represented by a curve as shown in Fig. 9.4.9.2. In order to correct equation (9.4.9.3), it is assumed that this function has the form shown in Fig. 9.4.9.3 (A detailed analysis reveals that this approximation also holds when the waveform of the curve shown in

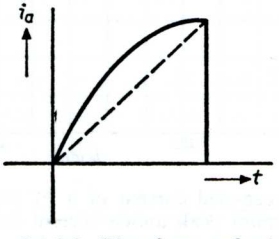

Fig. 9.4.9.2. Waveform of the anode current as a function of time.

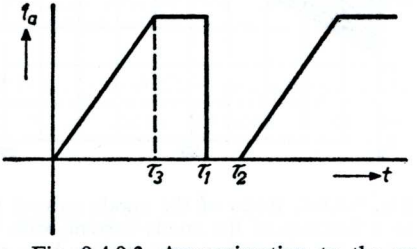

Fig. 9.4.9.3. Approximation to the waveform shown in Fig. 9.4.9.2.

Fig. 9.4.9.2 is not convex but concave. In that case the second term of equation (9.4.9.6) becomes negative instead of positive.)

The average value of the screen-grid current is then given by the expression:

$$\bar{\imath}_{g2} = \frac{1}{\tau_2}\left\{\frac{\tau_3 \hat{\imath}_a}{\hat{\alpha}-\alpha_0}\left(1 - \frac{\alpha_0}{\hat{\alpha}-\alpha_0}\log_e \frac{\hat{\alpha}}{\alpha_0}\right) + (\tau_1 - \tau_3)\frac{\hat{\imath}_a}{\hat{\alpha}}\right\} \qquad (9.4.9.4.)$$

and the average value of the anode current by:

$$\bar{\imath}_a = \frac{1}{\tau_2}\left\{\tau_3 \frac{\hat{\imath}_a}{2} + (\tau_1 - \tau_3)\hat{\imath}_a\right\} \qquad (9.4.9.5.)$$

By substituting $(\tau_2 - \tau_1)\tau_2 = p$, and combining equations (4) and (5):

$$\frac{1}{\bar{\alpha}} = \frac{2\{\hat{\alpha}-\alpha_0+\alpha_0 \log_e(\alpha_0/\hat{\alpha})\}\{(1-p)\hat{\imath}_a/\bar{\imath}_a - 1\}}{(\hat{\alpha}-\alpha_0)^2} + \frac{2-(1-p)\hat{\imath}_a/\bar{\imath}_a}{\hat{\alpha}} \qquad (9.4.9.6.)$$

A family of curves representing the obtainable ratio i_a/i_{g2} as a function of i_a for a nominal PL 36 line output valve is plotted in Fig. 9.4.9.4. This

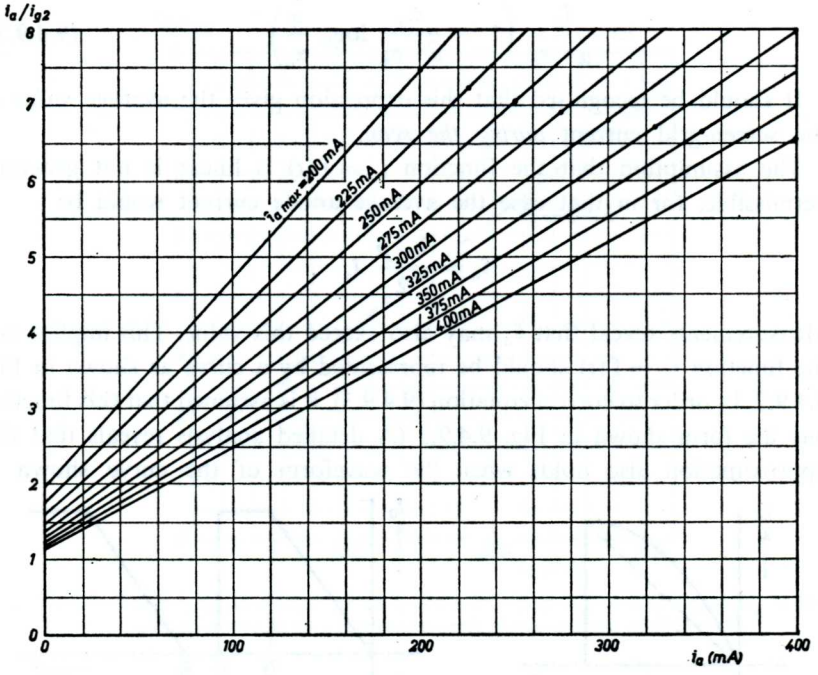

Fig. 9.4.9.4. Ratio of the anode current to the screen-grid current of a PL 36, as a function of the anode current, with the maximum peak anode current for which the circuit has been designed, as parameter. From this graph, the value α_0 at $i_a = 0$ and that of $\hat{\alpha}$ at $i_a = \hat{\imath}_a$ can be derived for different values of the maximum anode current $\hat{\imath}_{a\,max}$.

ratio depends both on the anode voltage and on the screen-grid voltage, but since the required values of these voltages depend exclusively on the maximum peak anode current $\hat{\imath}_{a\,\max}$ for which the circuit has been designed, curves are plotted with $\hat{\imath}_{a\,\max}$ as parameter. From Fig. 9.4.9.4. it is possible to derive the value of $\hat{\alpha}$ at $i_a = \hat{\imath}_a$ and that of α_0 at $i_a = 0$ for a nominal PL 36 for any value of $\hat{\imath}_{a\,\max}$.

These values of $\hat{\alpha}$ and α_0 have been substituted in equation (9.4.9.6) so as to obtain a graph for the PL 36 representing $\bar{\alpha}$ as a function of $\hat{\imath}_{a\,\max}$ for different values of the ratio $\hat{\imath}_{a\,\max}/\bar{\imath}_a$. This ratio is constant for a given design once the values of $\hat{V}_d$ and $\hat{V}_a$ have been chosen. Fig. 9.4.9.5 is ap-

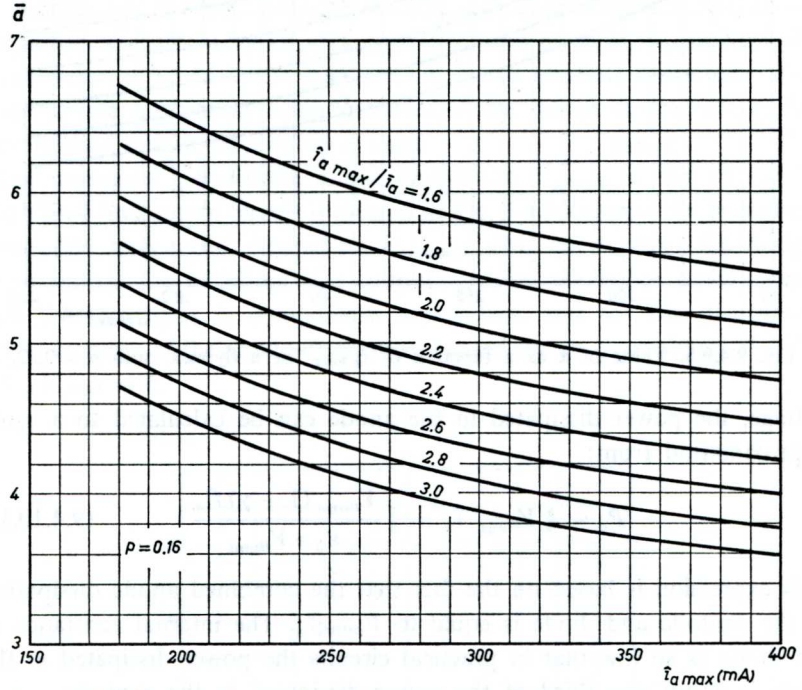

Fig. 9.4.9.5. Value of $\bar{\alpha}$ as a function of $\hat{\imath}_{a\,\max}$, with the ratio $\hat{\imath}_{a\,\max}/\bar{\imath}_a$ as parameter, for a flyback ratio $p = 0.16$.

plicable to $p = 0.16$ and Fig. 9.4.9.6 to $p = 0.22$. Comparison of these graphs clearly shows the important improvement obtained at the higher flyback ratio.

9.4.10. Anode and screen-grid dissipation

In practical circuits, in which line voltage fluctuations do not exceed 10% and the minimum value of $V_{a\,\mathrm{end}}$ is only slightly higher than the knee

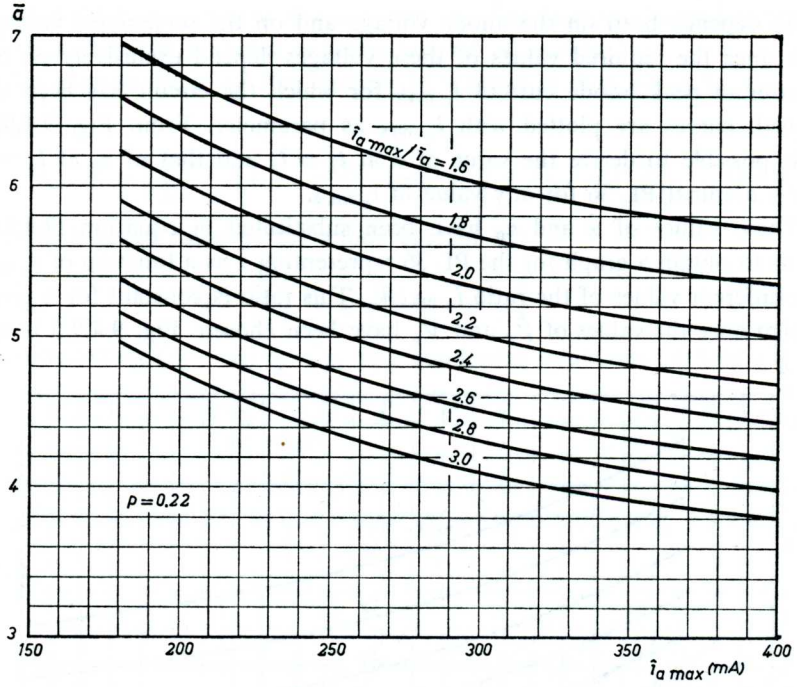

Fig. 9.4.9.6. Value of α as a function of $\hat{\imath}_{a\,max}$ for a flyback ratio $p = 0.22$.

voltage, the power dissipated in the anode can be calculated to a good approximation from:

$$P_a \approx \tfrac{3}{4} V_{a_{end}} \bar{\imath}_a = \tfrac{1}{3} \frac{V_{a_{end}} (1+\gamma) P_m}{V_b - V_{a_{end}}} \qquad (9.4.10.1.)$$

This expression is based on the fact that the combined anode dissipation of the pentode and diode is equal to $V_{a\,end}\bar{\imath}_a$. The internal resistance of the diode is so low that in practical circuits the power dissipated in the diode is about one third of the power dissipated in the pentode.

It should be recognised however, that the actual dissipation depends on the driving waveform; therefore somewhat lower values may be found when the ratio of peak to average anode current is low, as occurs in pulse-driven circuits.

It may therefore be advisable to check the anode dissipation by measurement in those cases where equation (9.4.10.1) indicates that the value is rather too high.

As far as the anode dissipation is concerned, it is not sufficient, in stabilised line output stages, to satisfy the conditions imposed by the design

centre ratings for conventional circuits. In fact, these design centre ratings do take into account the increase in the anode dissipation caused by an overvoltage of 10% in conventional circuits, which results in an increase of the anode dissipation by approximately 20%, but in stabilised line output circuits such an overvoltage may result in a considerably higher increase of the anode dissipation.

This can be explained by examining equation (9.4.10.1) more closely. Since $V_b - V_{a\,\mathrm{end}}$ is kept substantially constant, an increase in the nominal line voltage will result in $V_{a\,\mathrm{end}}$ increasing by the same *absolute* amount, that is *relatively* by $V_b/V_{a\,\mathrm{end}}$ times the relative increase in V_b. An increase of the line voltage by 10% will therefore cause the anode dissipation to increase by $(V_b/V_{a\,\mathrm{end}}) \times 10\%$, and since $V_b/V_{a\,\mathrm{end}}$ is usually of the order of 3.5 to 4, this might result in the absolute maximum value of the anode dissipation being exceeded if the design centre ratings for conventional output circuits were used.

The maximum permissible anode dissipation $P_{a\,\max}$ of the PL 36 in a stabilised line output circuit is plotted in Fig. 9.4.10 against the maximum permissible screen-grid dissipation $P_{g2\,\max}$. This curve gives the design centre ratings for stabilised line output circuits, allowance having been made for tolerances in components and valves, and for the disproportionate increase of the anode dissipation caused by an overvoltage of 10% at $V_b/V_{a\,\mathrm{end}} = 4$.

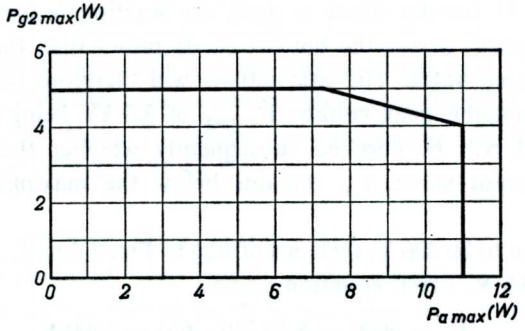

Fig. 9.4.10. Design centre ratings of $P_{a\,\max}$ and $P_{g2\,\max}$ of the PL 36 in a stabilised line output circuit with $V_b/V_{a\,\mathrm{end}} = 4$.

The screen-grid dissipation is:

$$P_{g2} = V_{g2}\,\bar{\imath}_{g2} = V_{g2}\,\bar{\imath}_a/\bar{\alpha} \qquad (9.4.10.2.)$$

in which V_{g2} is the nominal screen-grid voltage derived from the graph of Fig. 9.4.8. In this graph the function $V_{g2} = \mathrm{f}(\hat{\imath}_{a\,\max})$ is approximated by

a straight line which is given by the expression:

$$V_{g2} \approx 53 + b\,\hat{\imath}_{a\,\max} \qquad (9.4.10.3.)$$

where $b \approx 415$ V/A denotes the slope of the V_{g2} curve.

Substitution of equation (9.4.10.3) in equation (9.4.10.2) and combination with equations (9.4.3.) and (9.4.4.) gives:

$$P_{g2} = \left\{ 53 + \frac{1570\ (1+F_p)}{(1-p)\,\hat{V}_a} P_m (1+\gamma) \right\} \frac{4}{9} \frac{P_m (1+\gamma)}{(V_b - V_{a\,\mathrm{end}})\,\bar{\alpha}} \qquad (9.4.10.4.)$$

For practical calculations it is more convenient to use equation (9.4.10.2) combined with equation (9.4.10.3); equation (9.4.10.4) has been derived only to show the dependence of P_{g2} on P_m (if the ratio $\bar{\alpha}$ were constant, P_{g2} would even be a square function of P_m).

9.4.11. Example for $p = 0.16$

The method of investigating the performance of a given combination of line output valve and booster diode will now be illustrated by ascertaining, by way of example, the maximum obtainable value of $(1+\gamma)\,P_m$ when a PL 36 is used in combination with a PY 81 at a nominal line voltage of 220 V.

It is further assumed that the flyback ratio $p = 0.16$ and that the third harmonic content during the flyback is 15%, giving $0.85\ (1+F_p) = 8.5$.

Since a PY 81 booster diode is used, the limiting factor will probably be the peak voltage across the booster diode rather than the peak voltage of the line output valve. The calculations will therefore be based on the maximum permissible peak voltage $\hat{V}_{d\,\max}$ of 5.0 kV being applied to the PY 81, and it will be checked subsequently whether the peak voltage of the line output valve, $\hat{V}_a$, remains below the maximum permissible value.

If V_{g2} is taken to be 200 V, then, according to Fig. 9.4.8., $\hat{\imath}_{a\,\max} = 355$ mA and $V_{a\mathrm{end}} = 65$ V. From equation (9.4.5.)

$$\hat{V}_a = 5000 + 8.5\,(220 - 65) = 6300 \text{ V}.$$

Hence, from equation (9.4.3.)

$$(1+\gamma)\,P_m = \frac{1.8 \times 0.84 \times 6300}{8 \times 8.5} \times 355 \times 10^{-3} = 50 \text{ VA},$$

and from equation (9.4.4.)

$$\bar{\imath}_a = \frac{4}{9} \times \frac{50}{220 - 65} = 143 \text{ mA}.$$

The anode dissipation is calculated from equation (9.4.10.1)

$$P_a = \tfrac{3}{4} \times 65 \times 143 \times 10^{-3} = 7.0 \text{ W}.$$

The ratio $\hat{\imath}_{a\,\max}/\bar{\imath}_a = 355/143 = 2.5$, so that at $\hat{\imath}_{a\,\max} = 355$ mA, according to Fig. 9.4.9.5., $\bar{\alpha} = 4.2$, which gives $\bar{\imath}_{g2} = 143/4.2 = 34.0$ mA. According to equation (9.4.10.2) the screen-grid dissipation would then be:

$$P_{g2} = 200 \times 34.0 \times 10^{-3} = 6.8 \text{ W}.$$

Fig. 9.4.10. shows that this value is in excess of the maximum permissible screen-grid dissipation, which implies that the chosen value of $V_{g2} = 200$ V is too high.

The calculation is now repeated on the same lines for lower values of V_{g2}; the results thus obtained are tabulated below:

V_{g2}	200	190	180	170	160	V
Va_{end}	65	63	60	58	56	V
$\hat{\imath}_{a\,\max}$	355	331	306	282	257	mA
$\hat{V}_a$	6.3	6.3	6.4	6.4	6.4	kV
$P_m(1+\gamma)$	50	46	43	40	37	VA
$\bar{\imath}_a$	143	130	120	110	100	mA
P_a	7.0	6.1	5.4	4.8	4.2	W
$\hat{\imath}_{a\,\max}/\bar{\imath}_a$	2.5	2.6	2.6	2.6	2.6	
$\bar{\alpha}$	4.2	4.2	4.3	4.4	4.5	
$\bar{\imath}_{g2}$	34.0	31.0	27.9	25.0	22.0	mA
P_{g2}	6.8	5.9	5.0	4.2	3.5	W

The table reveals that 180 V is the highest screen-grid voltage that may be used without the maximum permissible screen-grid dissipation of 5 W (at $P_a \leq 7.3$ W) being exceeded. The maximum obtainable value of $(1+\gamma)P_m$ thus amounts to 43 VA.

9.4.12. Influence of the flyback ratio

The above calculations were based on the assumption that the flyback ratio $p = 0.16$, and it should be recognised that even a slight increase of this ratio gives a considerable improvement. This can best be illustrated by reconsidering the example given above, in this case, however, taking $p = 0.18$. The flyback factor F_p is then reduced from 9 to 7.8, which gives $0.85\ (1 + F_p) = 7.5$ instead of 8.5.

The results of the calculations, made on the same lines as those for $p = 0.16$, are summarised in the following table:

V_{g2}	200	195	190	185	180	V
Va_{end}	65	64	63	62	60	V
$\hat{\imath}_{a\,max}$	355	342	331	318	306	mA
$\hat{V}_a$	6.2	6.2	6.2	6.2	6.2	kV
$P_m(1+\gamma)$	54	52	51	49	47	VA
$\bar{\imath}_a$	155	148	145	138	131	mA
P_a	7.6	7.1	6.9	6.4	5.9	W
$\hat{\imath}_{a\,max}/\bar{\imath}_a$	2.3	2.3	2.3	2.3	2.3	
$\bar{\alpha}$	4.6	4.6	4.6	4.7	4.7	
$\bar{\imath}_{g2}$	33.7	33.2	31.6	29.3	27.9	mA
P_{g2}	6.7	6.3	6.0	5.4	5.0	W

The table reveals that in this case, too, a screen-grid voltage of 180 V should be chosen. The magnetic power that can be obtained is approximately 10% higher than for $p = 0.16$.

The results that are obtained by raising the flyback ratio to 0.22, which gives $F_p = 6.3$ and $0.85\,(1 + F_p) = 6.2$, are entered in the following table for three different values of V_{g2}.

It can be seen from this table that at $p = 0.22$ the screen-grid voltage should also be 180 V. The magnetic power that is attained at this setting is 51 VA.

V_{g2}	185	180	175	V
Va_{end}	62	60	59	V
$\hat{\imath}_{a\,max}$	318	306	294	mA
$\hat{V}_a$	5.9	5.9	5.9	kV
$P_m(1+\gamma)$	53	51	49	VA
$\bar{\imath}_a$	149	142	135	mA
P_a	6.9	6.4	6.0	W
$\hat{\imath}_{a\,max}/\bar{\imath}_a$	2.1	2.2	2.2	
$\bar{\alpha}$	5.2	5.3	5.3	
$\bar{\imath}_{g2}$	28.6	26.8	25.2	mA
P_{g2}	5.3	4.9	4.4	W

9.4.13. Use of a combined design chart

The various graphs governing the design of a stabilised line output circuit, and given in the preceding section, can advantageously be combined in a single comprehensive design chart. Fig. 9.4.13.1 shows such a design chart plotted for the PL 36 and based on the following data:

Flyback ratio	p	$= 0.16$
Flyback factor	F_p	$= 9$
Peak voltage reduction $(1 - a)$		$= 0.85$
Energy recovery factor	$\sqrt{\eta}$	$= 0.8$
Max. screen-grid dissipation	P_{g2}	$= 5$ W

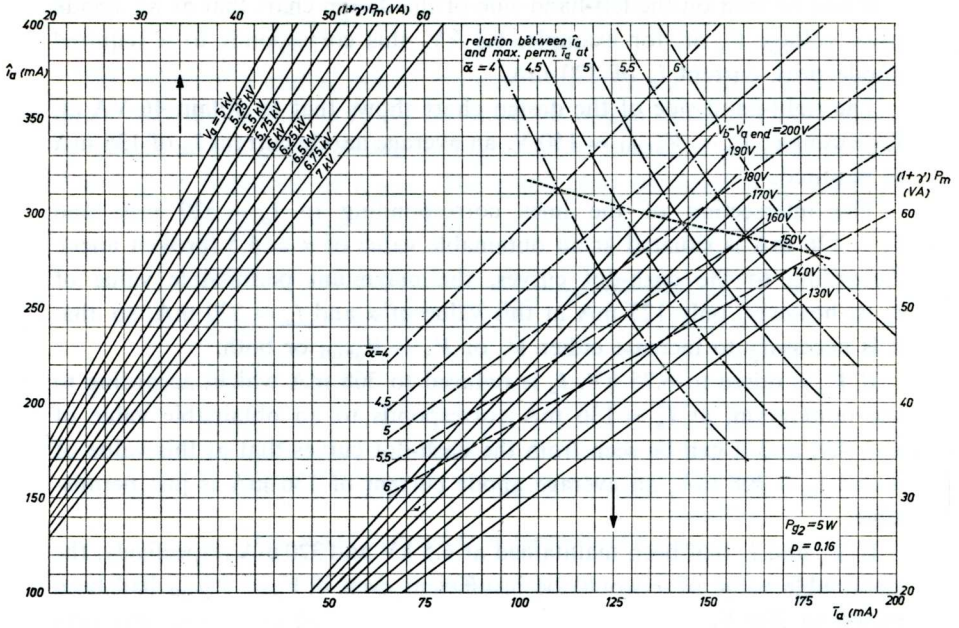

Fig. 9.4.13.1. Comprehensive design chart by means of which a line output circuit can be investigated. For the conditions under which this design chart is valid, see text.

At the left-hand side of this design chart is plotted, according to equation (9.4.3.), the required peak anode current $\hat{i}_a$ as a function of the desired deflection power $(1 + \gamma) P_m$ with the peak anode voltage $\hat{V}_a$ as parameter.

Similarly, at the right-hand side of the design chart is plotted, according to equation (9.4.4.), the required average anode current $\bar{i}_a$ as a function of the desired deflection power $(1 + \gamma) P_m$ with $V_b - V_{a\text{end}}$ as parameter.

According to the graph of Fig. 9.4.8., a minimum value of V_{g2} (and also of $V_{a\text{end}}$) is required for any value of $\hat{i}_{a\,\max}$, and since $V_{g2} = P_{g2}/\bar{i}_{g2}$ and, moreover, $\bar{i}_{g2} = \bar{i}_a/\bar{\alpha}$, it is possible to plot curves which represent the relation between $\hat{i}_{a\,\max}$ on the left-hand scale and the *maximum permissible* value of $\bar{i}_a$ (at which $P_{g2} = 5$ W is reached) on the scale at the bottom of the design chart for different values of $\bar{\alpha}$. These curves are traced in dash-dot lines.

Finally, the value of $\bar{\alpha}$ obtainable from equation (9.4.9.6.) is plotted against $\hat{i}_a$ and $\bar{i}_a$ (broken lines).

The application of this design chart is explained by the following example. Assume that a coil with a deflection power requirement of $P_m = 37$ VA at 625 lines is to be used and that $\gamma = 0.24$, giving $(1 + \gamma) P_m = 46$ VA.

It can be seen on the left-hand side of the design chart that at an anode peak voltage $\hat{V}_a$ of, for example, 6.5 kV, this corresponds to a required anode peak current $\hat{\imath}_a$ of 320 mA.

The right-hand side of the design chart shows that to obtain 46 VA at, for example, $V_b - V_{a\text{end}} = 150$ V, an average anode current $\bar{\imath}_a$ of 136 mA is required.

The intersection of the lines corresponding to $\hat{\imath}_a = 320$ mA and $\bar{\imath}_a = 136$ mA is situated at an obtainable value of $\bar{\alpha} = 4.5$ (broken lines). According to the dash-dot curves, the maximum permissible value of $\bar{\imath}_a$ is, however, only 125 mA at this value of $\bar{\alpha}$ and $\hat{\imath}_a = 320$ mA, so that it is necessary to increase either $\hat{V}_a$ or $V_b - V_{a\text{end}}$ or both.

If $\hat{V}_a$ is raised to 6.75 kV, $\hat{\imath}_a$ is reduced to 308 mA which, according to the nomogram, at $\bar{\imath}_a = 136$ mA corresponds to an obtainable value of $\bar{\alpha} = 4.7$, and it can be seen from the dash-dot curves that at this value of $\bar{\alpha}$ and $\hat{\imath}_a = 308$ mA, an average anode current of 136 mA is just permissible.

If $\hat{V}_a$ and $\hat{\imath}_a$ had been maintained at 6.5 kV and 320 mA respectively, the obtainable value of $\bar{\alpha}$ would be insufficient even if $V_b - V_{a\text{end}}$ had been raised to 200 V.

Such a design chart thus enables the designer to ascertain immediately whether and under what conditions a given project can be realised. It is in fact sufficient to determine the point corresponding to the required values of $\hat{\imath}_a$ and $\bar{\imath}_a$, and to check whether the *obtainable* value of $\bar{\alpha}$ (broken lines) is at least equal to the *required* value of $\bar{\alpha}$ (dash-dot lines). *This will be the case for all combinations of $\hat{\imath}_a$ and $\bar{\imath}_a$ situated below the dashed line* which interconnects the intersection points of the corresponding curves for the permissible and obtainable values of $\bar{\alpha}$.

By means of the expressions and graphs given in the preceding sections, similar design charts can be readily prepared for different values of the flyback ratio or of the screen-grid dissipation.

To facilitate the construction of the design chart, a method is outlined by which the dashed line mentioned above can be plotted directly for a given valve, without the necessity of plotting curves of the permissible and obtainable values of $\bar{\alpha}$.

For this purpose, equation (9.4.9.6) may be rewritten:

$$\frac{1}{\bar{\alpha}} = P\,(1-p)\,\hat{\imath}_a/\bar{\imath}_a + Q \cdot$$

where

$$P = \frac{\hat{\alpha}^2 - \alpha_0{}^2 + 2\,\hat{\alpha}\,\alpha_0 \log_e(\alpha_0/\hat{\alpha})}{\hat{\alpha}\,(\hat{\alpha} - \alpha_0)^2}$$

and

$$Q = \frac{-2\,\hat{\alpha}\,\alpha_0 + 2\,\alpha_0^2 - 2\,\hat{\alpha}\,\alpha_0 \log_e(\alpha_0/\alpha)}{\hat{\alpha}\,(\hat{\alpha} - \alpha_0)^2} .$$

The values of $\hat{\alpha}$ and α_0 can be evaluated for different values of the maximum peak anode current $\hat{\imath}_{a\,\max}$ on which the design of the circuit is based, by means of the graph shown in Fig. 9.4.9.4. It is thus possible to plot P and Q as functions of $\hat{\imath}_{a\,\max}$. The graph thus obtained (Fig. 9.4.13.2)

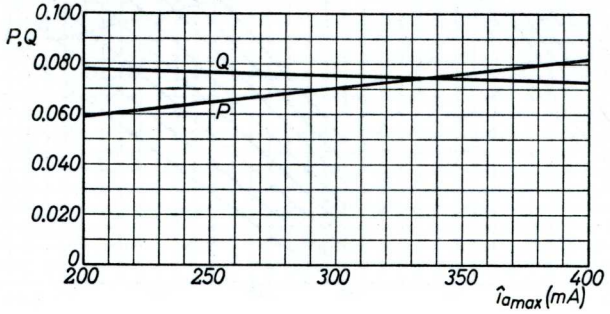

Fig. 9.4.13.2. P and Q as functions of $\hat{\imath}_{a\,\max}$.

reveals that for the PL 36 both P and Q are very nearly straight lines, approximately given by:

$$P = 0.036 + 0.115\,\hat{\imath}_{a\,\max}$$

and

$$Q = 0.083 - 0.025\,\hat{\imath}_{a\,\max} .$$

Hence

$$1/\bar{\alpha} = (0.036 + 0.115\,\hat{\imath}_{a\,\max})\,(1-p)\,\hat{\imath}_{a\,\max}/\bar{\imath}_a + 0.083 - 0.025\,\hat{\imath}_{a\,\max} .$$

Now $P_{g2} = V_{g2}\bar{\imath}_a/\bar{\alpha}$, whilst, for a minimum end-of-life PL 36,

$$V_{g2} = 53 + 415\,\hat{\imath}_{a\,\max} \quad \text{(see Fig. 9.4.8.)}$$

Hence:

$$P_{g2} = (53 + 415\,\hat{\imath}_{a\,\max})\,\bar{\imath}_a\,\{(0.036 + 0.115\,\hat{\imath}_{a\,\max})\,(1-p)\,\hat{\imath}_{a\,\max}/\bar{\imath}_a + (0.083 - 0.025\,\hat{\imath}_{a\,\max})\} =$$

$$= (53 + 415\,\hat{\imath}_{a\,\max})\,(0.036 + 0.115\,\hat{\imath}_{a\,\max})\,\hat{\imath}_{a\,\max}\,(1-p) + (0.083 - 0.025\,\hat{\imath}_{a\,\max})\,\bar{\imath}_a\,(53 + 415\,\hat{\imath}_{a\,\max}),$$

which gives:

$$\bar{\imath}_a = \frac{P_{g2} - (53 + 415\,\hat{\imath}_{a\,\max})\,(0.036 + 0.115\,\hat{\imath}_{a\,\max})\,\hat{\imath}_{a\,\max}\,(1-p)}{(0.083 - 0.025\,\hat{\imath}_{a\,\max})\,(53 + 415\,\hat{\imath}_{a\,\max})}$$

$$= \frac{P_{g2} - (1-p)\,\hat{\imath}_{a\,\max}\,(47.6\,\hat{\imath}_{a\,\max}^2 + 21.0\,\hat{\imath}_{a\,\max} + 1.91)}{-10.4\,\hat{\imath}_{a\,\max}^2 + 33.1\,\hat{\imath}_{a\,\max} + 4.4} \qquad (9.4.13)$$

By means of this expression, it is therefore possible to plot in the combined design chart the limit at which the permissible and obtainable values of $\bar{\alpha}$ are equal, and below which the working point must be chosen. This has been done in Figs. 9.4.13.3–10 for different values of P_{g2} and p.

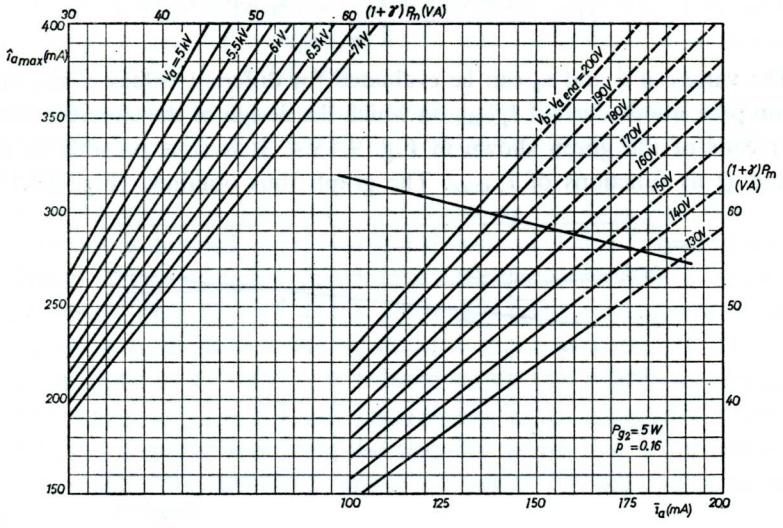

Fig. 9.4.13.3. Combined design chart for $P_{g2} = 5$ W ($P_a = 7.3$ W) and $p = 0.16$.

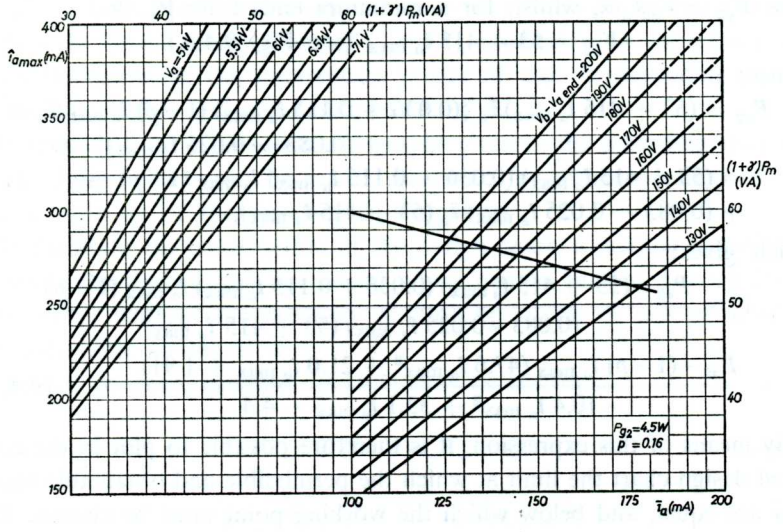

Fig. 9.4.13.4. Combined design chart for $P_{g2} = 4.5$ W ($P_a = 9$ W) and $p = 0.16$.

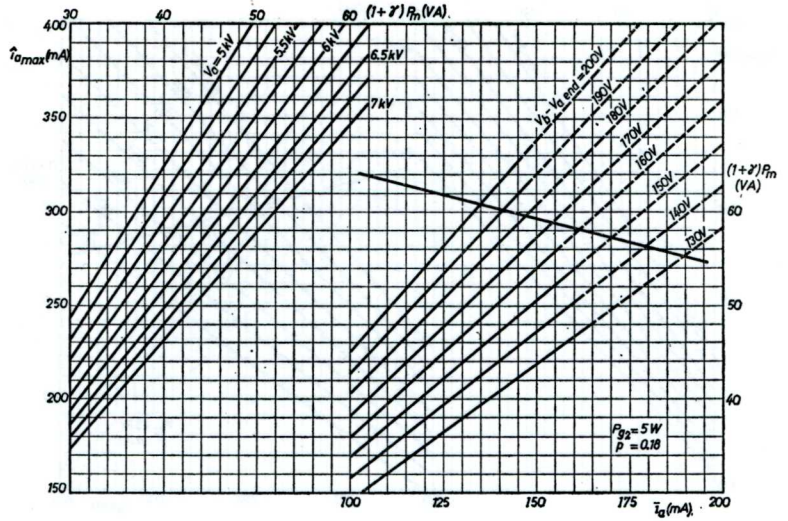

Fig. 9.4.13.5. Combined design chart for $P_{g2} = 5$ W ($P_a = 7.3$ W) and $p = 0.18$.

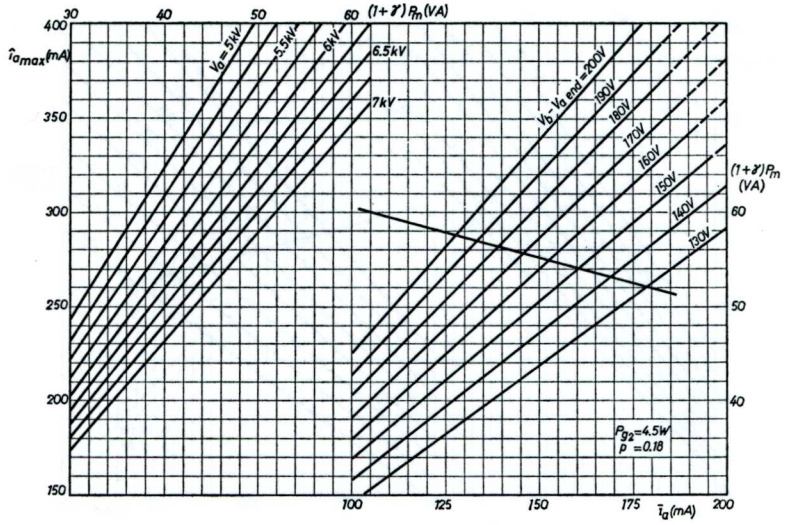

Fig. 9.4.13.6. Combined design chart for $P_g = 4.5$ W ($P_a = 9$ W) and $p = 0.18$.

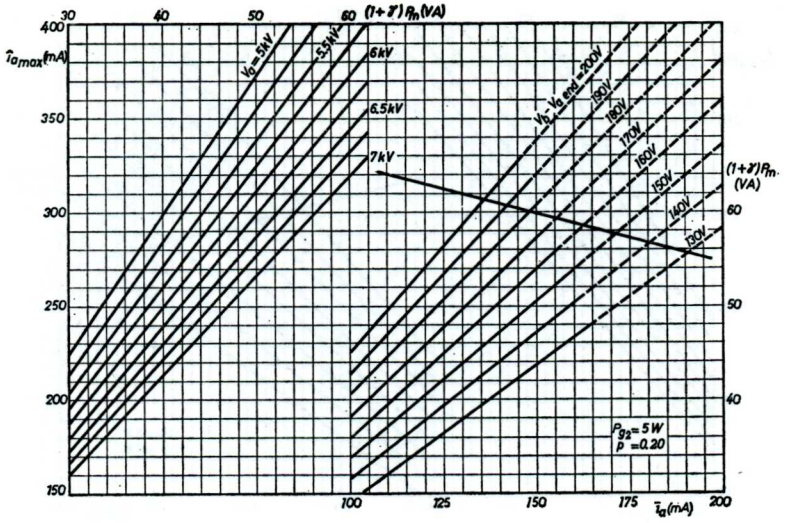

Fig. 9.4.13.7. Combined design chart for $P_{g2} = 5$ W ($P_a = 7.3$ W) and $p = 0.20$.

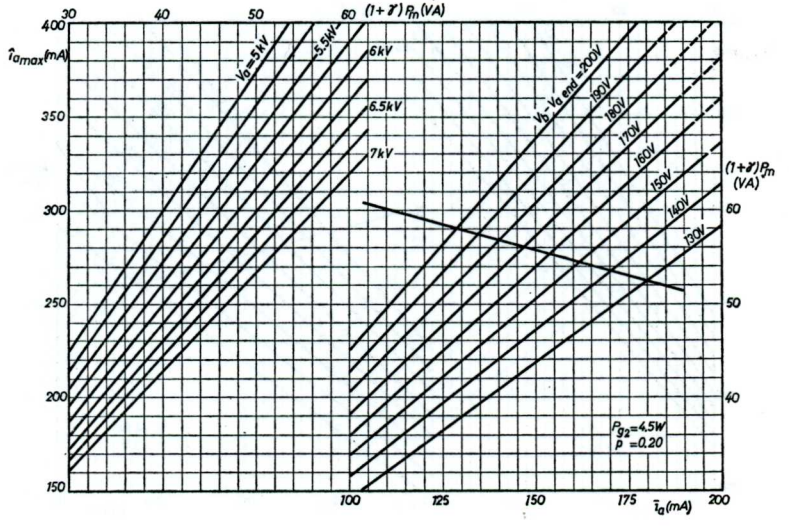

Fig. 9.4.13.8. Combined design chart for $P_{g2} = 4.5$ W ($P_a = 9$ W) and $p = 0.20$.

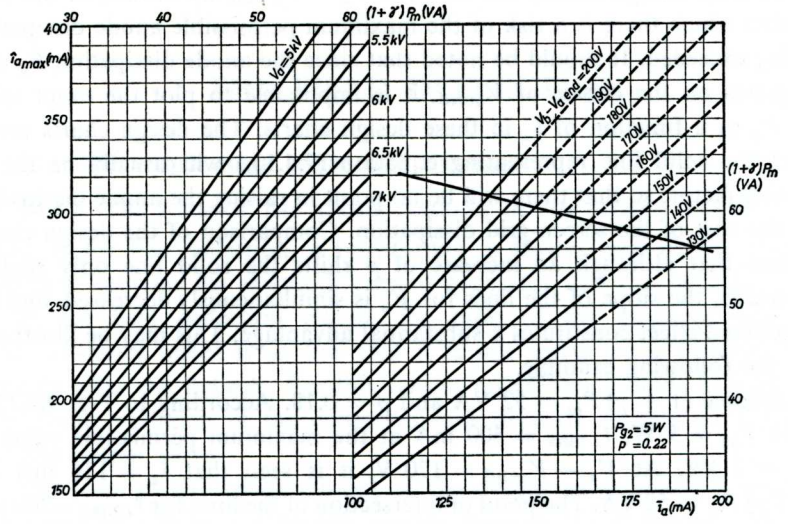

Fig. 9.4.13.9. Combined design chart for $P_{g2} = 5$ W ($P_a = 7.3$ W) and $p = 0.22$.

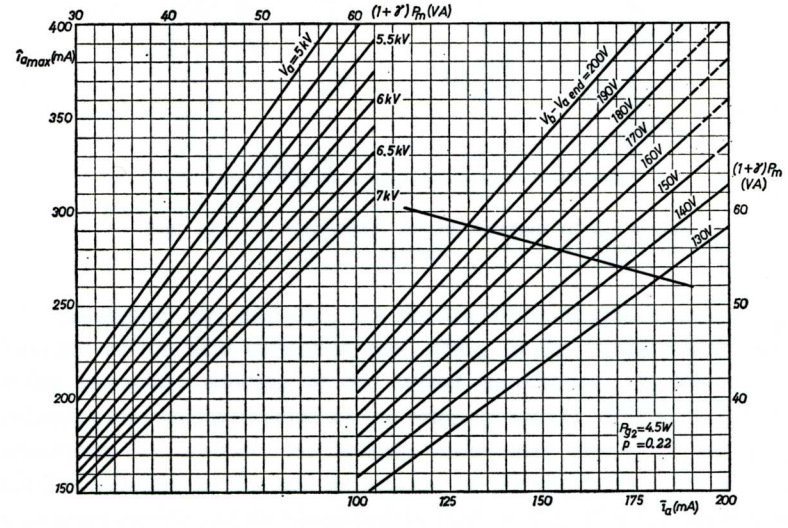

Fig. 9.4.13.10. Combined design chart for $P_{g2} = 4.5$ W ($P_a = 9$ W) and $p = 0.22$.

In these design charts, the lines for $V_b - V_{a\,\mathrm{end}}$ are broken in the area within which there is a risk of the maximum permissible anode dissipation being exceeded. It should be noted that since the anode dissipation P_a also depends on the choice of $V_{a\mathrm{end}}$, it is impossible to plot the exact value of P_a as a function of $\bar{\imath}_a$ in these design charts. The design charts reveal that the solid line representing equation (9.4.13.) will usually be the limiting factor, so that there will be no point in raising the anode dissipation at the cost of the screen-grid dissipation. Comparison of the design charts shows that although an increase of p shifts the solid line only slightly upwards, the slope of the lines for $\hat{V}_a$ is simultaneously decreased, and the combined effect constitutes a substantial advantage. This may be illustrated by the following example.

Assume $(1 + \gamma) P_m = 52$ VA and $p = 0.18$. According to Fig. 9.4.13.5, with $P_{g2} = 5$ W, $\hat{\imath}_{a\,\max} = 300$ mA at the maximum permissible value of $\hat{V}_a = 7$ kV. At $V_b - V_{a\mathrm{end}} = 170$ V, it is seen that $\bar{\imath}_a = 136$ mA for $(1+\gamma) P_m = 52$ VA. The point of intersection of the lines for $\hat{\imath}_{a\,\max} = 300$ mA and $\bar{\imath}_a = 136$ mA, lies just below the limit given by equation (9.4.13.)

If p had been 0.16 (Fig. 9.4.13.3.), $\hat{\imath}_{a\,\max}$ would have become 330 mA at $\hat{V}_a = 7$ kV, and it is seen that its point of intersection with this line for $\bar{\imath}_a = 136$ mA lies far above the limit.

If p is raised to 0.22 (Fig. 9.4.13.9), a peak anode voltage of $\hat{V}_a = 6$ kV is sufficient, resulting in $\hat{\imath}_{a\,\max} = 302$ mA, a value readily obtainable at $\bar{\imath}_a = 136$ mA.

CHAPTER 10

THE FIELD DEFLECTION

10.1. The output stage of the field timebase

10.1.1. The form of the anode current in the output valve

Just as for line deflection, a transformer is always used as the coupling element between the sawtooth current generator and the deflection coil.

In the field deflection circuit, the ratio of the magnetic power to the resistance losses is so low that it is not worth while recovering the energy after the flyback. For this reason no efficiency diode is used, and the linear variation of the deflection now depends entirely on the drive to the output valve.

The form of the anode current of the output valve which is required, in order to obtain a sawtooth current through the deflection coil, will now be subjected to a closer examination. As for the line timebase, we shall start from a linear sawtooth current through the deflection coil. The equivalent circuit diagram of the anode circuit of the output stage is given in Fig. 10.1.1.1.

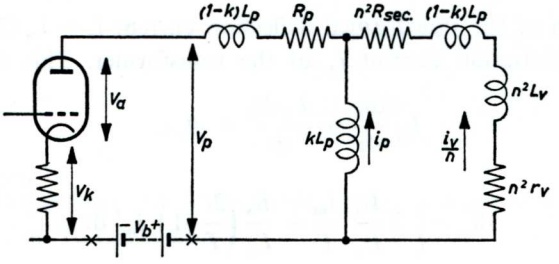

Fig. 10.1.1.1. Equivalent circuit diagram of the anode circuit.

In this figure, n^2r_v and n^2L_v are the transformed resistance and self inductance of the field deflection coil, n^2R_{sec} is the transformed resistance of the secondary winding of the output transformer, R_p and L_p are the resistance and self inductance of the primary, and $(1 - k)\,L_p$ is the leakage inductance. In practice, the leakage inductance proves to be negligibly small in relation to the self inductance of the deflection coil, so that the equivalent circuit can be simplified to that of Fig. 10.1.1.2. In this figure, R_s is the total resistance of the secondary circuit, transformed to the pri-

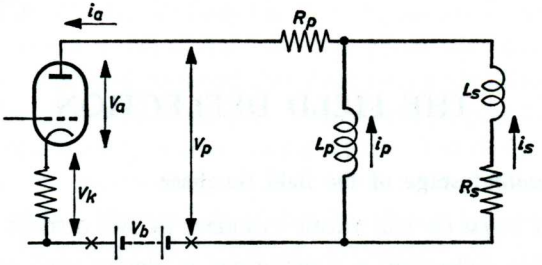

Fig. 10.1.1.2. Simplified equivalent circuit diagram.

mary, L_s is the transformed self-inductance of the coil, and i_s is the transformed deflection current, as shown in Fig. 10.1.1.3. The anode current

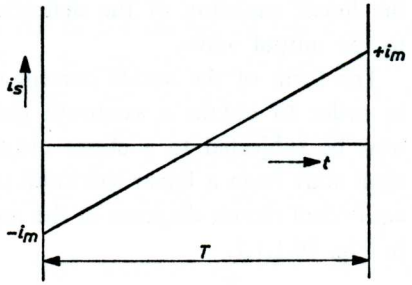

Fig. 10.1.1.3. Transformed deflection current as a function of time.

i_a is the sum of the transformed deflection current $i_s = i_m\,(2t/T - 1)$ and of the magnetisation current i_p of the transformer. This follows from:

$$L_p \frac{\mathrm{d}i_p}{\mathrm{d}t} = \frac{L_s\,\mathrm{d}i_s}{\mathrm{d}t} + R_s\,i_s$$

or

$$\mathrm{d}i_p = \left\{ 2\frac{L_s}{L_p}\frac{i_m}{T} + \frac{R_s}{L_p}\left(\frac{2t}{T} - 1\right) i_m \right\} \mathrm{d}t \ .$$

Consequently

$$i_p = 2\frac{L_s}{L_p}\, i_m \frac{t}{T} + \frac{R_s}{L_p}\left(\frac{t^2}{T} - t\right) i_m + C \ .$$

As the integrated value of i_p has to produce the average anode current i_{ag}, the integration constant can be found from:

$$i_{ag} = \frac{1}{T}\int_0^T i_p\,\mathrm{d}t$$

or

$$i_{ag} = \frac{1}{T}\left[\frac{L_s}{L_p}\, i_m \frac{t^2}{T} + \frac{R_s}{6L_p}\left(\frac{2t^3}{T} - 3t^2\right) i_m + Ct \right]_0^T$$

$$i_{ag} = \frac{L_s}{L_p} i_m - \frac{i_m R_s T}{6 L_p} + C$$

so that

$$i_p = i_{ag} + \frac{i_m R_s T}{6 L_p}\left(\frac{6t^2}{T^2} - \frac{6t}{T} + 1\right) + \frac{i_m L_s}{L_p}\left(\frac{2t}{T} - 1\right)$$

Consequently

$$i_a = i_p + i_s = \underbrace{i_{ag}}_{a} + \underbrace{\frac{i_m R_s T}{6 L_p}\left(\frac{6\,t^2}{T^2} - \frac{6t}{T} + 1\right)}_{b} +$$

$$+ \underbrace{\frac{i_m L_s}{L_p}\left(\frac{2t}{T} - 1\right)}_{c} + \underbrace{i_m\left(\frac{2t}{T} - 1\right)}_{d} . \qquad (10.1.1.)$$

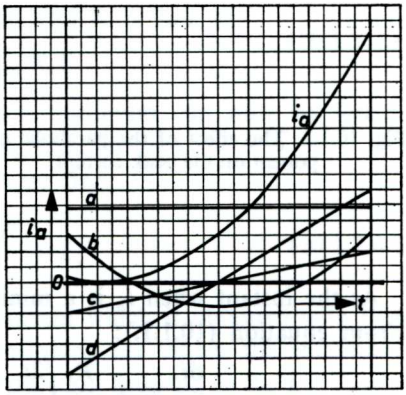

Fig. 10.1.1.4. Anode current as a function of time, composed of 4 components according to equation (10.1.1.) when $L_p < 0.5\, R_s T - L_s$.

According to equation (10.1.1) the anode current consists of 4 components, as shown in Fig. 10.1.1.4., i.e.:

a) The average anode current.

b) The parabolic magnetisation current of the transformer, the relative size of which (in relation to the deflection current) is determined by the ratio R_s/L_p.

c) An extra sawtooth current through the primary, the relative size of which is determined by the ratio L_s/L_p, and

d) The transformed deflection current.

10.1.2. Choice of L_p

The choice of L_p affects the size of the parabolic component and of the sawtooth component in i_p. As the value of L_p increases, the sawtooth

current component decreases more and more, so that the minimum required peak current would be reached for very high values of the ratio L_p/L_s. In practice however, this is accompanied by large dimensions of the transformer, or by a higher resistance of the windings, so that the resistance loss then becomes too great.

The parabolic component of i_p does not contribute to the peak anode current as long as the value of the latter is so small that the minimum in the anode current comes at the beginning of the scan. This will be clear from Fig. 10.1.2. As soon as the parabolic component becomes so large, that the minimum anode current does not appear at the instant $t = 0$, the peak-to-peak value of the anode current will be greater than the sawtooth current component.

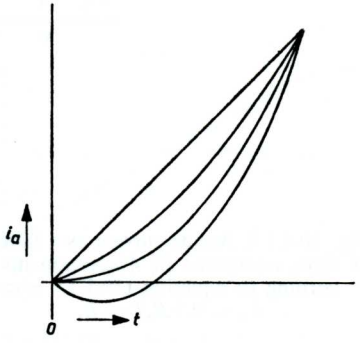

Fig. 10.1.2. The effect of the parabolic component on the peak current.

At the instant when i_a is a minimum: $\mathrm{d}i_a/\mathrm{d}t = 0$.
From equation (10.1.1.):

$$\frac{\mathrm{d}i_a}{\mathrm{d}t} = i_m \frac{R_s}{L_p}\left(\frac{2t}{T} - 1\right) + 2\frac{i_m}{T}\left(1 + \frac{L_s}{L_p}\right) .$$

The time t_m, at which the anode current is a minimum, can thus be found from:

$$\frac{R_s T}{L_p}\left(\frac{2t_m}{T} - 1\right) = -2\frac{L_p + L_s}{L_p}$$

from which

$$\frac{t_m}{T} = \tfrac{1}{2} - \frac{L_p + L_s}{R_s T} \qquad (10.1.2.1.)$$

If this minimum is to occur at the beginning of the scan ($t_m = 0$), L_p must thus have a value which is given by:

$$L_p = \tfrac{1}{2} R_s T - L_s \qquad (10.1.2.2.)$$

The advantage of this dimensioning (zero initial slope: z.i.s.) is that it is easy to cut off the output valve during the flyback by means of a small

negative pulse, and that a simple method of linearisation can be used, e.g. an adjustable cathode resistance by means of which the linearity at the beginning of the scan can be adjusted. We shall return to this in section 10.2.

At a lower value of L_p, the anode current (for ratios of L_s and R_s which occur in practice) will reach the minimum at a later instant. Both the parabolic component and the sawtooth current component in i_p then cause an increase in the peak anode current, so that the required peak anode current (at least if the transformation ratio is to remain the same) increases sharply with decreasing L_p. On the other hand, it is possible that the direct anode current will decrease. This can be determined by putting $i_a = 0$ for $t = t_m$ in equation (10.1.1.)

By substituting from equation (10.1.2.1.) in equation (10.1.1) and evaluating, we find:

$$\frac{i_{ag}}{i_m} = \frac{(R_sT)^2 + 12\,L_p^2 + 12\,L_s^2 + 24\,L_sL_p}{12\,L_p\,R_sT} \qquad (10.1.2.3.)$$

The value of L_p at which i_{ag} becomes a minimum can now be found by equating the differential quotient $\mathrm{d}i_{ag}/\mathrm{d}L_p$ to zero.

After solving the differential equation we find:

$$L_p = \sqrt{\frac{(R_sT)^2}{12} + L_s^2} \qquad (10.1.2.4.)$$

The reduction in the average anode current which is obtained with this dimensioning, in relation to the dimensioning for which the minimum anode current occurs at the beginning of the scan, depends on the L_v/r_v ratio of the deflection coil. For a certain ratio, the two dimensionings coincide. This ratio is found by substituting equation (10.1.2.4.) in equation (10.1.2.2.); It is found that the two dimensionings coincide for $L_s = \frac{1}{6}\,R_sT$. For the sake of comparison, it may be noted that for the Philips toroidal field deflection coil for 110° deflection, $L_s \approx \frac{1}{10}\,R_sT$, while for other coils of the saddle type $L_s \approx \frac{1}{20}\,R_sT$.

Although the decrease in the direct current for the circuit dimensioned to minimum direct current, is slight in comparison with "zero initial slope", while the necessary peak current is higher, this dimensioning may still be attractive, because, with a lower value of L_p a smaller transformer can be constructed.

Or, if the dimensions of the transformer are not reduced, the lower self inductance leads to lower resistance losses, as a result of which the available supply voltage can be used to better effect. In this case, the trans-

formation ratio can be increased so that i_s, the deflection current transformed to the primary side, will decrease. Consequently, this still leads to reduction of the peak anode current $\hat{\imath}_a$ and i_{ag}.

If the anode current does not reach the minimum value at the beginning of the scan, there is a large chance of non-linearity, due to the curvature of the characteristic near the cut-off point. To prevent this, it is recommended that the drive should not be allowed to come too close to the cut-off point of the output valve during the scan, so that a small residual current will always continue to flow. This also gives a margin for variations in the direct anode current due to fluctuations in the supply voltage, and other causes. The non-linearity which results from the curvature of the characteristic can also be countered by applying a high degree of negative feedback in the output stage. The choice of L_p will thus be partly determined by the possibilities of negative feedback. It may be concluded from the above, that for simple circuits, dimensioning according to equation (10.1.2.2.) is to be prefered to dimensioning to equation (10.1.2.4), while the latter offers the possibility of using a smaller output transformer, particularly if any distortion can be taken up by negative feedback.

Finally it may be noted, that the magnetic deflection energy in the field must be destroyed after every scan, in order to prevent oscillations after the flyback. These are partly prevented by the hysteresis losses of the transformer, while the remaining part must be taken up by the output valve or by another damping element, connected in parallel with the transformer. Up to the present, the hysteresis losses during the scan have not been taken into consideration. In practice they cause a 5 to 10% increase in the required anode current, depending on the quality of the material of the core, amongst other things.

10.1.3. Anode voltage during the scan

The anode voltage during the scan is found from $V_a = V_b - V_p$, in which V_p is the voltage on the primary of the output transformer. (Fig. 10.1.1.2.). This voltage is the sum of the voltage $L_p\,\mathrm{d}i_p/\mathrm{d}t$ and the voltage drop across the primary resistance of the transformer $i_a R_p$:

$$V_p = \underbrace{i_{ag}R_p}_{(a)} + \underbrace{\frac{i_m R_s T R_p}{6\,L_p}\left(6\frac{t^2}{T^2} - 6\frac{t}{T} + 1\right)}_{(b)} + \underbrace{+\frac{i_m}{L_p}\left(2\frac{t}{T} - 1\right)(R_p L_p + R_p L_s + R_s L_p)}_{(c)} + \underbrace{\frac{2L_s i_m}{T}}_{(d)} \qquad (10.1.3.)$$

The primary voltage V_p consists of 4 components as shown in Fig. 10.1.3:

a) A direct voltage component.

b) A parabolic component.

c) The sawtooth voltage component.

d) The inductive direct voltage.

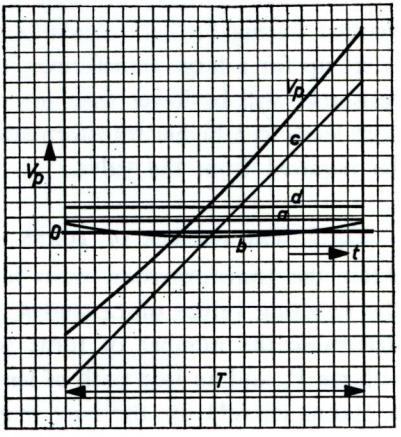

Fig. 10.1.3. Voltage across the primary winding of the transformer as a function of time, consisting of 4 components according to equation (10.1.3.)

The anode voltage of the valve is the difference between $V_b - V_p$ and the cathode voltage of the valve, and reaches a minimum value at the end of the scan. In order to prevent distortion, the anode voltage must always remain above the knee of the valve characteristic.

10.1.4. Transformation ratio

The choice of the transformation ratio is important for obtaining the optimum output of the circuit. Just as for line deflection, we have to take into account the unfavourable conditions under which we wish to make sure of complete deflection, that is of the lowest mains voltage, and of minimum valves at the end of their operating life. However, the deflection required under these circumstances also depends on the E.H.T. voltage on the picture tube, so that, when i_m is being determined, the question of whether or not the line timebase is stabilised must be taken into account.

As far as utilisation of the supply voltage is concerned, the deflection coil is optimally matched if the anode voltage under the above-mentioned minimum conditions still remains slightly above the knee of the i_a/V_a characteristic. The transformation ratio can thus be found from the relationship between the maximum permissible fluctuation in the primary voltage and the required voltage across the deflection coil, both at the

end of the scan:

$$n = \frac{V_{b\,\min} - V_{a\,\min} - V_{cat} - \hat{\imath}_a R_p}{0.5\,\hat{\imath}_v\,(r_v + R_{sec}) + \dfrac{L_v\,\hat{\imath}_v}{T}} \qquad (10.1.4.)$$

To start with, the values of $\hat{\imath}_a$, R_p and R_{sec} are still unknown, so that a provisional estimate of these quantities must be made, which can be verified during further calculations. It is obvious that if the calculation is set up for a large transformer, the losses in the primary and secondary resistance will be lower than for a small one, so that the use of a large core leads to a higher transformation ratio, and thus less peak current will be required from the valve.

10.1.5. The number of turns required

After the transformation ratio has been provisionally determined, and the resulting values of L_p and i_{ag} have been calculated, it is possible to determine the number of turns required on a transformer core with a volume V_k and an iron path of length l_k. The best way to do this is to use a Hanna curve*) for the core material in question. This curve gives the value of

$$\frac{L_p i_{ag}^2}{V_k} \text{ as a function of } \frac{n_p i_{ag}}{l_k}.$$

The curve forms the top limit of a number of curves, each of which refers to a given air gap; at the points of contact of a Hanna curve with the individual curves, the corresponding value of the air gap is indicated. For example, Fig. 10.1.5. shows a Hanna curve for iron cores consisting of annealed dynamo sheet with a silicon content of 1.5%, for an a.c. flux density $\triangle B = 5000$ gauss (peak-to-peak).

Ferroxcube is not used for field output transformers, because the low loss characteristics of this material are not fully utilised at low frequencies, and in addition the saturation flux density is much lower than that of the normal types of iron.

At present, wound strip cores made of grain orientated steel, are frequently used for field output transformers. The Hanna curve of this material is situated appreciably higher than that of silicon iron, as a result of which better or smaller transformers are possible with this material.

When determining the size of the air gap, attention must of course be paid to the average anode current which will be drawn by a new output

*) Journal of the Am. Inst. of El. Eng. **46**, 1927, p. 128.

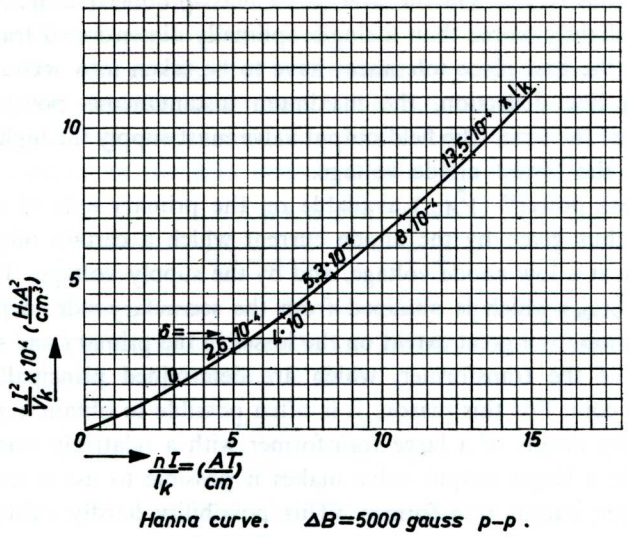

Fig. 10.1.5. Hanna curve of transformer lamination with a silicon content of 1.5% at a high value of the a.c. flux density.

valve, at a high supply voltage. This current can be considerably higher than the calculated minimum direct anode current requirement, and depends on the way in which the working point of the valve is adjusted. If a fixed cathode resistor is used, the value of which is chosen so that a valve which is on undervoltage and is at the end of its operating life can just draw sufficient direct current, it may be assumed that with a maximum new valve on overvoltage the direct anode current will be approximately 80% higher than the required minimum value. Under these conditions too, saturation of the core of the output transformer must be prevented.

10.1.6. Efficiency of the output transformer

After we have calculated the number of turns required on a transformer of given dimensions, in order to provide the required self inductance, we can determine the thickness of the wire to be used for the primary and secondary windings. In order to obtain a high efficiency, the available winding space should be used as efficiently as possible. This problem appears in the same form for practically every a.f. transformer and can be solved with the aid of tables of wire thickness, resistivity, tolerances etc. In this way, the primary and secondary resistances which can be realised with a given winding space can be roughly calculated before the trans-

former is constructed. On the average, a mass-produced transformer will come out slightly worse than a single optimally dimensioned transformer, because in the first place tolerances have to be taken into account.

As with line deflection, the maximum instantaneous power appears at the end of the scan. The field output valve must supply the highest anode current at the lowest anode voltage.

The "peak power" ($\hat{V}A_{pr}$) available on the primary side of the transformer is thus given by the anode current which a certain output valve can deliver at a low anode voltage, and by the supply voltage. The "peak power" ($\hat{V}A_{sec}$) which is obtained from the secondary side, depends, for field deflection, to a great extent on the losses in the primary and secondary resistance of the transformer, which are determined principally by the size of the core. For this reason, it is often possible to obtain a given field deflection by means of a large transformer with a relatively small output valve, while a larger output valve makes it possible to use a smaller and thus cheaper output transformer. (This possibility hardly exists for line deflection, because if the core is too small it always causes unacceptable decaying oscillations in the picture, as a result of the leakage inductance).

The efficiency of the transformer can now be defined as the ratio of the peak power utilised in the deflection coil to the peak power supplied to the primary. This ratio can be found from the product of the separate ratios of the primary and secondary peak-to-peak currents and of the voltages at the end of the scan.

By substitution from equation (10.1.2.3.) in equation (10.1.1.) for $t = T$, we find the relationship Φ between the primary peak current $\hat{\imath}_a$ and the (transformed) deflection current $2i_m$;

$$\Phi = \frac{\hat{\imath}_a}{2i_m} = \frac{(0.5\, R_s T + L_p + L_s)^2}{2\, L_p\, R_s\, T} \qquad (10.1.6.1.)$$

Φ can be regarded as a "design factor" and is principally determined by the choice of L_p, e.g. dimensioning according to equation (10.1.2.2.) or equation (10.1.2.4.) The value of Φ is fairly constant for each of these dimensionings, although the (transformed) resistance of the secondary winding of the transformer is included in R_s.

When the transformer is dimensioned according to equation (10.1.2.2.) ($L_p + L_s = 0.5\ R_s T$), equation (10.1.6.1.) can be reduced to:

$$\Phi = \frac{0.5\, R_s T}{L_p}\ .$$

The value of $1/\Phi$ can be regarded as a peak current efficiency of the transformer.

The voltage efficiency (η) can now be calculated from the ratio of the (transformed) voltage across the deflection coil to the primary voltage for $t = T$. The voltage efficiency is determined by the voltage drop across the primary and secondary resistances of the transformer windings, whereby Φ affects the voltage drop across the primary resistance. If R_c is the transformed resistance of the field deflection coil ($R_c = n^2 r_v$) then:

$$\eta = \frac{0.5\, R_c T + L_s}{0.5\, R_s T + L_s + \Phi\, R_p T} \qquad (10.1.6.2.)$$

The ratio of the primary to the secondary "peak powers", that is between what is given up at the deflection coil to what is supplied to the transformer by the output valve, is now:

$$\frac{V\hat{A}_{sec}}{V\hat{A}_{pr}} = \frac{\eta}{\Phi} \qquad (10.1.6.3.)$$

It must be remembered that the above-mentioned "peak power" does not represent any actual power, but only the product of the current and the voltage which are important for the output valve, while on the secondary side of the transformer this product represents a quantity which is proportional to the measure of sensitivity for the deflection coil, as given in section 5.3.2.

The quotient η/Φ thus forms a quantity which can be used to indicate the total "efficiency" of the output transformer. However, this efficiency cannot be used as a quantity which can be applied to a given transformer without further consideration, because the ratio L_v/r_v of the deflection coil which is connected to it affects the efficiency. It should also be noted that this "efficiency" is not an actual energy efficiency, but only the ratio of the secondary and primary products of current and voltage at the end of the scan. The efficiency defined in this way forms a logical link between the data for the deflection coil and those for the output valve which is to be used, and can be utilised to compare the merits of different transformer designs.

To illustrate the above, we shall now use a number of examples to examine the effect of the transformer dimensions, and the choice of L_p, on the efficiency. Here we run into the difficulty that calculation of the primary and secondary resistances of the transformer by means of a fixed formula does not quite represent practical conditions, as the choice of wire thickness is limited to certain standardised dimensions.

If it is found that there is just not enough winding space for a given wire thickness, it is possible that the next smaller cross-section cannot

make full use of the available winding space. In addition the copper filling factor depends on the thickness of the insulation, stiffness of the windings, tolerances etc. It is obvious that it will be difficult to include all these factors in comparative table for transformers, before the transformers themselves have been constructed.

In the following examples of calculation, therefore, careful use will be made of practical formulae to determine the resistance of the primary and secondary windings, the secondary winding being wound above the primary and the primary and secondary winding spaces being kept equal.

Under these conditions the resistances can be roughly calculated from:

$$R_p \approx 74 \times 10^{-6} \frac{n_p^2}{q\,a} \text{ and } R_{sec} \approx 104 \times 10^{-6} \frac{n_s^2}{q\,a} .$$

In these expressions, n is the number of turns, q is the fraction of the winding space which is available for the winding, and a is the unit dimension of the core lamination. (Fig. 10.1.6.)

For $a = 13$, we can calculate with $q \approx 0.25$, while $q \approx 0.2$ for a small transformer with $a = 10$.

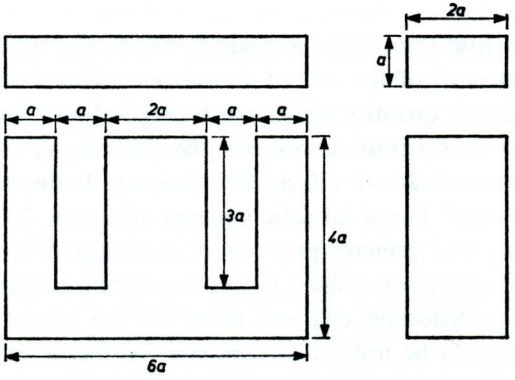

Fig. 10.1.6. A transformer core.

The number of turns will now be determined with the aid of the Hanna curve (Fig. 10.1.5.) for an a.c. flux density $\triangle B = 5000$ gauss.

The calculations will be set up for transformers with $a = 13$ and $a = 10$, each with L_p values according to equation (10.1.2.2.) (zero initial slope) and equation (10.1.2.4.) (minimum i_{ag}).

With these dimensions it is a simple matter to find i_{ag}. By substitution

from equation (10.1.2.2.) in (10.1.2.3.) we find:

$$i_{ag} = i_m \frac{R_s T}{3 L_p}$$

for dimensioning to "zero initial slope", and by combination with equation (10.1.6.1.) we find:

$$i_{ag} = \tfrac{1}{3}\, \hat{\imath}_a \quad . \qquad (10.1.6.4.)$$

By substitution from equation (10.1.2.4.) in equation (10.1.2.3.) we find:

$$i_{ag} = i_m \frac{L_p + L_s}{0.5\ R_s T} \quad . \qquad (10.1.6.5.)$$

for dimensioning to minimum i_{ag}.

The calculations included in the following table were carried out for

L_p calcutated for: Unit dimension of the transformer core		min i_{ag} $a = 10$	z.i.s. $a = 10$	min i_{ag} $a = 13$	z.i.s. $a = 13$
Estimated values	$R_p \Omega$	250	350	100	150
	$R_{sec}\ \Omega$	10	15	3	5
	$\hat{\imath}_a$ mA	100	90	80	70
Calculated transformation ratio (equation (10.1.4))	η	6.8	6	8.8	8.3
$i_m = \frac{0.5\, \hat{\imath}_v}{n}$ mA		34	38.5	26	28
$R_c = n^2 r_v \Omega$		2300	1800	3880	3440
$R_s = n^2 (r_v + R_{sec})\ \Omega$		2760	2340	4100	3780
$L_s = n^2 L_v$ H		4.6	3.6	7.7	6.9
Primary self inductance:					
equations (10.1.2.2) and (10.1.2.4) L_p H		16.6	19.4	24.8	30.1
	Φ	1.3	1.2	1.33	1.25
Calculated minimum value of $\hat{\imath}_a$ ($\hat{\imath}_a = 2\, \Phi\, i_m$)	mA	89	92	70	70
Minimum value of i_{ag} (equations 10.1.6.4) and (10.1.6.5)	mA	26	31	21	23.5
$i_{ag\ nom} = i_{ag\ min} + 10$ mA		36	41	31	33.5
$\frac{L_p\, i_{ag}^2}{V_k} \cdot \frac{\mathrm{H \cdot A^2}}{\mathrm{cm^3}}$		4.8	7.3	2.4	3.4
From the Hanna curve, $\frac{n_p\, i_{ag}}{l_k} \cdot \frac{\mathrm{A}}{\mathrm{cm}}$		8	11	4.7	6
n_p		2670	3200	2360	2800
$R_p\ \Omega$		264	380	127	178
n_s		392	533	268	337
$R_{sec}\ \Omega$		8	14.8	2.3	3.7
Voltage efficiency with calculated R_p and R_{sec}	η	0.72	0.6	0.9	0.85
Total efficiency	η/Φ	0.55	0.5	0.68	0.68
Voltage across primary winding at end of scan					
$V_p = i_m \left(R_s + \frac{2 L_s}{T} + 2\, \Phi\, R_p\right)$ V		130	139	135	135

a deflection coil with $L_v = 100$ mH, $r_v = 40\ \Omega + 10\ \Omega$ feedback resistance, $\hat{i}_v = 460$ mA, while the circuit must be able to operate with a minimum supply voltage $V_b = 200$ V. The minimum anode voltage is approximately 50 V, while V_{cat} can be put at 15 V and $T = 20$ msec. (These figures refer to vertical deflection at 50 c/s in the AW 43–88 picture tube with a diagonal angle of deflection of 110° and the Philips AT 1009 deflection unit).

The results in the above table show that a change in the transformer dimensions is accompanied by an appreciable difference in efficiency. We can also conclude that there is no difference in efficiency for the large transformer, whether it is dimensioned to minimum i_{ag} or to zero initial slope. In this case, there is little point in dimensioning to minimum i_{ag}, because the difference in i_{ag} is only small, and the linearity is easier to maintain at zero initial slope. In contrast, there is an improvement in the efficiency of the small transformer for minimum i_{ag}, so that in this case, this dimensioning is the most suitable.

Finally, it should be noted that the iron losses have not yet been taken into account, and that when a small core is used, the a.c. flux density $\triangle B$ and thus the losses will increase with decreasing values of L_p.

10.1.7. Anode dissipation

An important quantity which, together with the required peak current, can be decisive for the possibility of using a given output valve, is the anode dissipation which will occur in the circuit for a given supply voltage.

The simplest way to determine the anode dissipation is to find the total power taken from the supply circuit, and to subtract from this the power that is dissipated in the deflection coil, the transformer and the cathode resistance.

The power P_c which is conveyed to the circuit during the scan is

$$P_c = \frac{1}{T} \int_0^T i_a\ V_p\ \mathrm{d}t \quad .$$

Substitution from equations (10.1.1.) and (10.1.3.) and evaluation of this function gives:

$$P_c = i_{ag}^2\ R_p + 2\ i_{ag}\ i_m \frac{L_s}{T} + 0.2 \left(\frac{i_m\ R_s\ T}{6\ L_p}\right)^2 R_p + \frac{i_m^2}{3} \left\{ R_s \left(1 + \frac{L_s}{L_p}\right) + \right.$$

$$\left. + R_p \left(1 + \frac{L_s}{L_p}\right)^2 \right\} \qquad (10.1.7.1.)$$

In addition to the terms with R_p and R_s which represent the direct

resistance losses, there is a term $2\, i_{ag} i_m\, L_s/T$ which represents the (necessary) destruction of magnetic energy in the deflection coil during the flyback.

The magnetic energy which is stored up in the field of the transformer by the parabolic component of the magnetisation current is largely retained, and supplies the beginning of the following scan.

Up till now we have not yet taken into account the iron losses which are caused by the magnetisation.

The iron losses (P_y) can be calculated if the specific losses of the material are known, e.g. the losses in watts per kg at a peak-to-peak a.c. flux density of 10,000 gauss (P_{10}).

Then $$P_y = P_{10}\, G\, \triangle B^2\, 10^{-8} \text{ watts} \qquad (10.1.7.2.)$$

In this expression, G is the weight of iron in kg and $\triangle B$ is the a.c. flux density occurring in the circuit, in gauss. The a.c. flux density can be calculated from:

$$\triangle B = \frac{L_p \dfrac{i_m R_s T}{4 L_p}}{n_p A}\, 10^8 = \frac{i_m R_s T}{4 n_p A}\, 10^8 \text{ gauss} \qquad (10.1.7.3.)$$

(A = the cross section of the core in cm^2, and $\dfrac{i_m R_s T}{4 L_p}$ = the peak-to-peak value of the parabolic component of i_p, which is found from the sum of the positive and negative peak values of this component in equation (10.1.1.) for $t = 0$ and $t = \frac{1}{2} T$ respectively).

The following table gives an impression of practical values of transformer losses and anode dissipations, based on the four transformer calculations given as examples in section 10.1.6. The dissipations are calculated for the nominal supply voltages of 220 V, while the core material has a density of 7.2 kg/dm^3 and a specific loss of 2.6 W/kg for a flux density variation of 10,000 gauss.

The results given in this table confirm the expectation that dimensioning to minimum i_{ag} will give the lowest power requirement and the lowest anode dissipation. In addition, of course, a large transformer is always better than a small one.

One advantage of dimensioning to "zero initial slope", however, is the better wave form of the anode current, which means that it is easier to achieve good linearity of the deflection current.

The table also shows that the contribution of the third term in equation (10.1.7.1.) to the total losses is negligibly small, and can be omitted when drawing up the table. This term only covers the losses in the primary

L_p calculated for: unit dimension of the transformer core		I min i_{ag} $a = 10$	II z.i.s. $a = 10$	III min i_{ag} $a = 13$	IV z.i.s. $a = 13$
For values, see table in section 10.1.6.	L_p H	16.6	19.4	24.8	30.1
	L_s H	4.6	3.6	7.7	6.9
	$R_s\ \Omega$	2760	2340	4100	3780
	$R_p\ \Omega$	264	380	127	178
	n_p	2670	3200	2360	2800
	i_m mA	34	38.5	26	28
	i_{ag} mA	36	41	31	33.5
Dissipated power, according to equation (10.1.7.1)	$i_{ag}^2 R_p$ W	0.34	0.64	0.12	0.2
	$2\, i_{ag}\, i_m \frac{L_s}{T}$ W	0.56	0.57	0.62	0.65
	$0.2\left(\frac{i_m R_s T}{6 L_p}\right)^2 R_p$ W	0.02	0.02	0.018	0.004
	$\frac{i_m^2}{3}\left\{R_s\left(1+\frac{L_s}{L_p}\right)+R_p\left(1+\frac{L_s}{L_p}\right)^2\right\}$ W	1.5	1.65	1.26	1.28
	P_c W	2.42	2.88	2.02	2.14
Equation (10.1.7.3.)	ΔB gauss	4400	3500	3400	2800
Weight of core ($48a^3 \times 7 \times 2 \times 10^{-3}$)	kg	0.35	0.35	0.76	0.76
Iron loss (equation (10.1.7.2)) P_y	W	0.18	0.12	0.23	0.16
Total power dissipated in transformer and coil $= P_t = P_c + P_y$	W	2.6	3	2.25	2.3
Cathode resistance $P_{Rcat} = i_{ag}^2 R_{cat}$	W	0.54	0.62	0.47	0.5
Power taken from power supply $P_b = V_{b\,\mathrm{nom}}\, i_{ag}$	W	8	9	6.8	7.4
Anode dissipation of the output valve $P_a = P_b - P_{Rcat} - P_t$	W	5	5.4	4.1	4.6

resistance of the transformer due to the parabolic component of the magnetisation current.

10.1.8. The choice of the output valve

In each case, the anode dissipations which were calculated in the above table were low enough to remain within the published maximum values of the ECL 82 or PCL 82 output valves. This is not true, however, of the peak current values ($\hat{\imath}_a$) calculated in the table in section 10.1.6. In addition, the discrepancy increases when the iron losses are also taken into account, which means that the peak current must be increased by a fraction P_y/P_c.

To obtain a fair comparison of the four examples given in the table, the primary voltage V_p, at the bottom of the table, must be made the same

for each example. The differences are due to the estimated values R_p and R_s not being absolutely accurate, which can be corrected by continued repetition.

For a comparison of efficiency, as in this table, this is not necessary, because we are concerned with the product of $\hat{\imath}_a$ and V_p, but the available supply voltage must always be used to the full to determine the minimum peak current requirement. For case I, this means a small increase and for case II a small decrease of the transformation ratio. The recalculated values of $\hat{\imath}_a$, including iron losses, are then 93, 99, 78 and 76 mA respectively.

If we compare these currents with the current which can be supplied by a PCL 82, we find that this valve will definitely be inadequate for the first two cases, while the other two fall just inside the possible performance of this valve. This is also determined by the available screen-grid voltage, and the permissible screen-grid dissipation. In the chosen examples, no more than 185 V are present between screen-grid and cathode at the minimum supply voltage of 200 V. According to the published data, the maximum peak anode current of this valve at the end of its operating life, and with 10% underheating of the cathode, is approximately 77 mA at 50 V anode voltage and $V_{g2} = 185$ V.

The maximum screen-grid dissipation is 1.8 W, so that the maximum i_{g2} which can occur at the nominal V_{g2} of approximately 200 V, is 9 mA. It is unlikely that the screen-grid current would be so high for an average anode current of approximately 35 mA, but it is a point that must be checked by measurement in doubtful cases.

In the first two cases, a larger output pentode is required, e.g. a PCL 85 or a PL 84. The PL 84 also allows of a much higher anode dissipation.

10.1.9. Operating conditions of the output valve

In the above it has been assumed that a cathode resistor is used in order to obtain the required operating conditions for the output valve.

For field deflection, there is a close relationship between the peak anode current and the required minimum direct current. With a circuit dimensioned to "zero initial slope", $i_{ag} \geqslant 0.33\,\hat{\imath}_a$, while with dimensioning to minimum direct current, $i_{ag} \geqslant 0.3\,\hat{\imath}_a$.

Now the peak current requirement remains practically constant, particularly with a stabilised deflection circuit, so that the direct current should also preferably remain constant.

However, in the field deflection circuit, stabilisation occurs in quite a different way to the line deflection, i.e. by keeping the a.c. amplitude of

the output valve constant. The direct anode current does not play any part in this, and must be separately stabilised.

The simplest way of doing this is to employ a cathode resistor, which provides a high degree of direct current stabilisation. Although still greater stabilisation is attractive, in connection with preventing variations of the self inductance of the output transformer, and with keeping the anode dissipation at a low level, this has not yet been applied.

The value of the cathode resistor should preferably be chosen so that an end-of-life valve on undervoltage still draws sufficient current.

The correct value can be found as follows. In Fig. 10.1.9, curve I is the static i_a/V_g characteristic of a nominal PCL 82 at nominal heater voltage and at $V_a = V_{g2} = 200$ V. This agrees with the previous calculated examples, in which $V_{b\ \mathrm{nom}}$ was 220 V and $V_{cat\ \mathrm{nom}} \approx 20$ V. Curve II, for a valve at the end of operating life at the same V_a and V_{g2} but with 10% underheating of the cathode, is deduced from the first curve by reducing

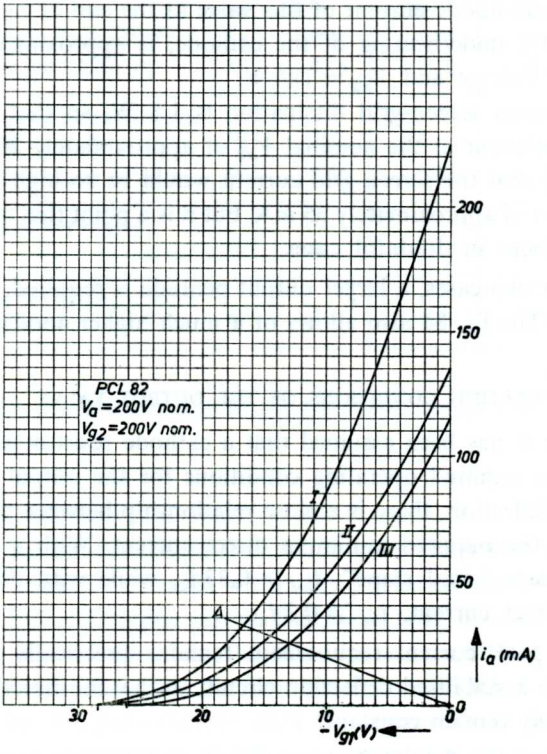

Fig. 10.1.9. Adjustment of the working point of the output valve.

the anode current by 40%. As undervoltage also means that the screen-grid voltage will drop, the current decreases still further. This is represented, for a 10% voltage drop, by curve III, which is obtained by moving curve II along the $-V_g$ axis by an amount $\frac{0.1\ V_{g2\ \text{nom}}}{\mu_{g1g2}}$.

In this figure, we can now draw a line A from the origin, through the required minimum anode current on curve III, e.g. 25 mA. Then

$$-V_{g1} = 13 \text{ V}$$

and the value of the cathode resistance R_{cat} follows from:

$$R_{cat} = \frac{-V_{g1}}{I_a + I_{g2}} .$$

With an average i_a/i_{g2} ratio of approximately 4, which is found in practice for the PCL 82, we then have $R_{cat} \approx 420\ \Omega$.

Fig. 10.1.9. also shows that the line A cuts the nominal curve I at $i_a = 32$ mA. This shows that the assumption made in the table in section 10.1.6., that $i_{ag\ \text{nom}}$ will be approximately 10 mA higher than the minimum i_{ag} requirement, proves to be quite ample in this case.

10.2. **A simple field deflection circuit**

In the following paragraphs, we will discuss a number of complete field deflection circuits.

Fig. 10.2.1. shows a simple form of field deflection circuit.

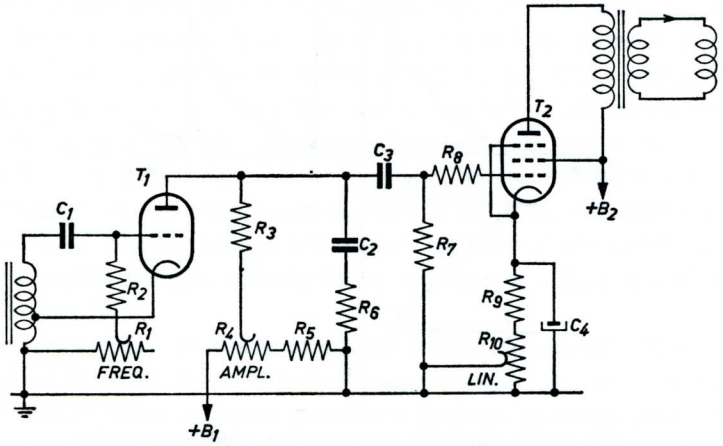

Fig. 10.2.1. A simple form of field deflection circuit.

The circuit consists of a sawtooth voltage generator, which is immediately

followed by the output amplifier which converts the sawtooth voltage into a sawtooth current.

The sawtooth voltage generator consists of the blocking oscillator circuit round the triode T_1. The sawtooth voltage is produced by periodic discharging of capacitor C_2 by means of the anode current of T_1, while in the intervals between discharging, the triode is blocked and the capacitor is charged via resistors R_3 and R_4. As is well known, the sawtooth voltage obtained in this way forms the beginning of an exponential charging curve; the non-linearity can be limited by maintaining a very high voltage across resistor R_3, this voltage being many times greater than the sawtooth voltage across C_2. For this reason the booster voltage from the line time base is often utilised as the supply voltage for the oscillator. The sawtooth voltage is conveyed to the grid of the pentode output valve T_2 via C_3.

The required parabolic component in the anode current is obtained by making use of the curvature of the i_a/V_g characteristic of the output valve (Fig. 10.2.2.). The sawtooth voltage at the control grid can be brought to a region of the characteristic which has a more or less pronounced curvature, by shifting the working point of the output valve. Consequently, this offers a possibility of adjusting the linearity of the raster, particularly in the range of low current values (beginning of the scan), where the curvature changes most rapidly.

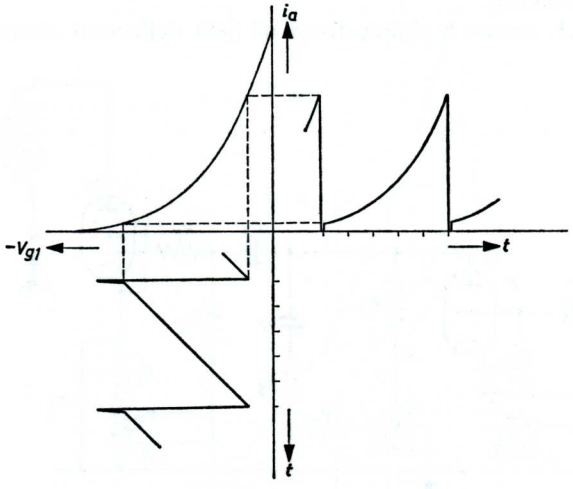

Fig. 10.2.2. Parabolic component in anode current due to curvature of the i_a/V_g characteristic.

The parabolic component obtained in this way is not large in relation

to the sawtooth current, so that this circuit requires a transformer with relatively high self-inductance, which only needs a low magnetisation current.

During the flyback a large positive peak voltage must of necessity appear at the anode of the output valve, because of the self inductance of the deflection coil. In order to prevent this flyback voltage being damped too heavily, which would make the flyback too slow, the anode current of the output valve is completely or almost completely suppressed during the flyback. For this purpose, a resistor R_6 is included in series with capacitor C_2 in the anode circuit of the blocking oscillator. The peak anode current of the oscillator triode T_1, which discharges capacitor C_2, causes a negative voltage pulse across this resistor, which is also conveyed to the control grid of the output valve. The amplitude of the sawtooth voltage on the grid of the output valve can be regulated by adjusting the charging current through R_3 to C_2 by means of potentiometer R_4.

10.3. **Circuit with triode output valve**

The pentode output valve which was used in the previous circuit has such a high internal resistance that the form of the anode current is largely determined by the form of the control voltage on the grid, and hardly at all by the anode voltage. If a triode with a low internal resistance was used in the same circuit, it would not be the form of the anode current, but the form of the anode voltage, which would adapt itself to the form of the grid voltage. Now the anode voltage approaches the sawtooth form far more closely than does the anode current, as was found in section 10.1.3. For this reason, a triode of this type can still be driven in the same sawtooth manner as the pentode in the circuit of Fig. 10.2.1., even although a relatively large parabolic component is required in the anode current. The only thing is that the amplitude of the control voltage must be far greater for the triode than for the pentode, because of the effect of the anode voltage on the anode current. This is no great objection in itself, seeing that the booster voltage will always be many times higher than the required control voltage, and the latter can thus be obtained with a reasonable linearity.

However, a great drawback of triodes is that the anode voltage which is required in order to provide the required peak current with a given cathode surface is much higher than for a pentode. Consequently, a triode can only be used when the supply voltage B_2 is high, e.g. when the output valve as well as the oscillator are supplied by the booster voltage from the line timebase.

10.4. **Circuit with pentode output valve and negative voltage feedback**

The normal supply voltages of 180 to 240 volts necessitate the use of a pentode output valve, which can still supply a large anode current at a very low anode voltage. By means of negative voltage feedback in the output stage, it is possible to reduce the internal resistance of the pentode to such an extent that the dynamic i_a/V_g characteristic is equivalent to that of a triode, while maintaining all the advantages of the pentode. V_g is, of course, not the control voltage on the grid of the output valve, but the control voltage at the input circuit, which includes the negative feedback voltage to the grid as well as the control voltage.

This solution offers further possible means of linearising the anode voltage by the application of frequency-dependent feedback. Fig. 10.4. shows an example of such a circuit, which is applied in countless variations.

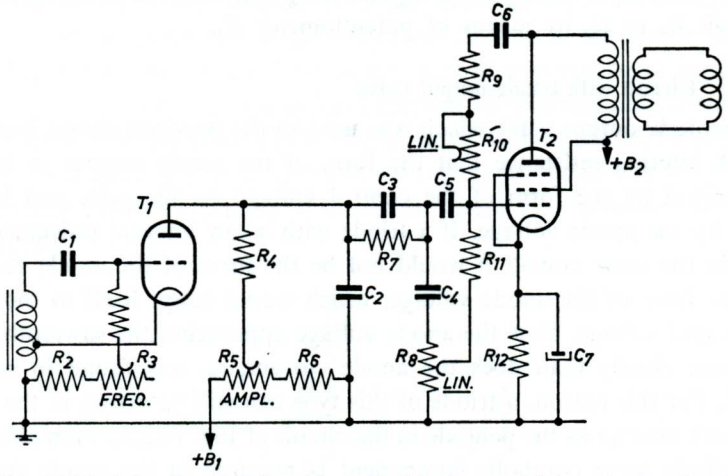

Fig. 10.4. Field deflection circuit with pentode output valve and negative voltage feedback.

The circuit offers two possible means of adjusting the linearity. The potentiometer R_8 enables one to introduce distortion of the sawtooth voltage on the grid of the output valve, in such a way as to obtain a certain curvature in the sawtooth current through the deflection coil, both in the positive and the negative sense. This affects the linearity over the whole picture screen.

In addition, potentiometer R_{10} makes it possible to correct the form of the control voltage shortly after the flyback; consequently this affects the linearity at the top of the screen.

These separate adjustments can hardly be avoided in a circuit with

negative voltage feedback, because the spread in components and valves, and variations of the operating point, can have a great influence on the linearity.

The simple circuits which we have discussed have the disadvantage that a really linear deflection can seldom be realised, because the causes of non-linearity cannot be completely compensated by the means which have been indicated. The causes of non-linearity can be listed as:

a) The output voltage of the simple capacitive sawtooth oscillator, which forms part of an exponential function.

b) Deviations of the parabolic form of the magnetisation current of the output transformer, due to variations in the permeability of the core material during the scan.

c) The curvature of the characteristic of the output valve, which is subject to spread, and can vary with the supply voltages.

d) Possible asymmetry of the deflection coil and of the picture tube, and deviations from linearity due to the relative flatness of the screen.

It goes without saying, that distortions of such differing types cannot all be compensated by the curvature of the valve characteristic, or by means of simple integrating networks. Nevertheless, many irregularities can be removed by a high degree of negative feedback. In particular negative feedback assists in keeping the form of the current constant.

With negative voltage feedback (as in Fig. 10.4.) there is the difficulty that the height of the picture will decrease gradually due to heating up of the deflection coil after switching on. This is because the negative feedback will always try to keep the voltage across the deflection coil constant, while the resistance of the coil increases due to the higher temperature. The current thus decreases. To counter this effect, a thermistor (resistor with negative temperature coefficient) is sometimes included in series with the deflection coil.

A second difficulty is presented by the high positive voltage peak which appears in the anode circuit, and which is conveyed to the feedback network. This peak voltage must not reach the grid of the output valve. This can be prevented in two ways, i.e. by compensation by means of a negative pulse which is fed to the network and which is generated by the sawtooth generator, or by removing the voltage peak from the feedback signal by means of an integrating filter. In the latter case, the feedback becomes ineffective for high frequencies. As far as suppression of any microphony in the output valve is concerned, this is a disadvantage. The first method is not accompanied by this disadvantage, and can thus profit from the not unimportant adventitious advantage of negative feedback, that all internal

interfering signals are also suppressed. In both cases, the network which determines the size of the pulse on the grid of the output valve must be accurately adjusted. (potentiometer R_{10}).

10.5. **Circuit with pentode output valve and negative current feedback**

One method of completely avoiding the above-mentioned disadvantages, is to apply negative current feedback.

To this end, a resistor is included in series with the deflection coil, and the sawtooth voltage which appears across this resistor is conveyed in phase opposition to the input of the amplifier. The voltage obtained in this way is too small to produce an effective feedback by applying it directly to the grid of the output valve, so that a pre-amplifier or transformer are required. Figs. 10.5.1 and 10.5.2 show possible circuits.

The circuit of Fig. 10.5.1. is suitable for a deflection coil with very low impedance ($r_v = 4\ \Omega$, $L_v = 9$ mH). In order to prevent too much loss of energy, the series resistor cannot be more than about 1 Ω, with which a sawtooth voltage of approximately 1 V peak-to-peak is obtained.

A high feedback factor is obtained by choosing a pre-amplifier with high amplification factor, for which a (low microphony) a.f. pentode is the most suitable.

The sawtooth voltage which is conveyed to the amplifier is generated by periodic rapid discharge of capacitor C_6 by the triode T_1, while in the intervals between discharges the capacitor is slowly charged by a current which is drawn, via R_6 and R_7, from a stabilised voltage supply.

The triode T_2 is connected as a cathode follower and is responsible, amongst other things, for maintaining a constant voltage across resistor R_6. As a result of this, the charging current remains practically constant during the scan, so that a very linear sawtooth voltage is obtained. This sawtooth voltage is positive-going. Since the control voltage of the output valve must always be positive-going, the oscillator voltage in this case must be fed to the cathode of the pre-amplifier T_3. In spite of the low input impedance, there is no objection to this, because the output impedance of the cathode follower is also low. Because of the very linear control voltage and the high degree of negative feedback (15—20 times) the circuit will be satisfactorily reproducible, and the current through the deflection coil will be able to remain very constant and linear under widely differing conditions. In the amplifier stage, precautions are also taken to ensure that the form of the current can be modified slightly, so that it is possible to compensate non-linearity due to asymmetry of coil and picture tubes.

It may be noted as a peculiarity of this circuit that the oscillation is

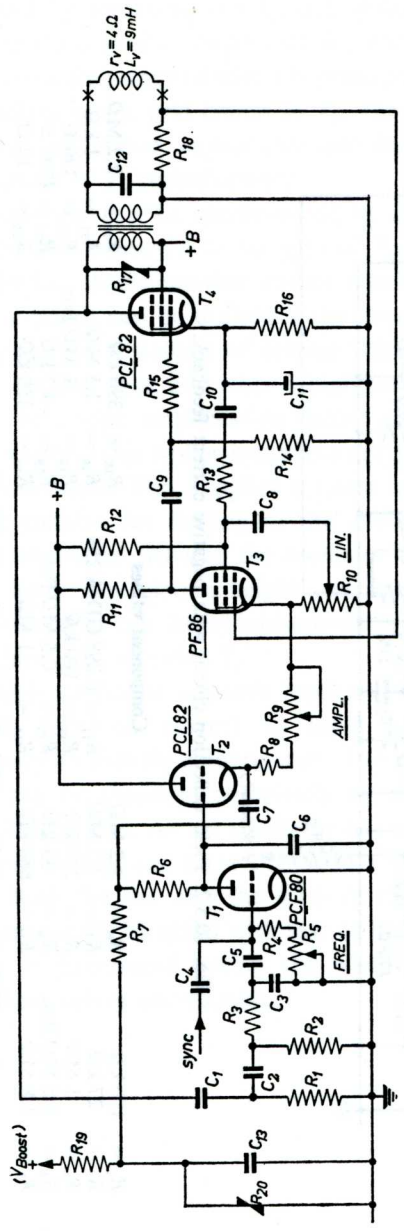

Fig. 10.5.1. Field deflection circuit with negative feedback by the current through the deflection coil.

Component values

R_1	= 120 kΩ	R_5	= 500 kΩ	R_9	= 20 kΩ	R_{14}	= 2.2 MΩ	R_{18}	= 1.2 Ω
R_2	= 120 kΩ	R_6	= 820 kΩ	R_{10}	= 1 kΩ linear	R_{15}	= 1 kΩ	R_{19}	= 680 kΩ
R_3	= 56 kΩ	R_7	= 220 kΩ	R_{11}	= 390 kΩ	R_{16}	= 470 kΩ	R_{20}	= VDR E 298/ GD/A 258
R_4	= 220 kΩ	R_8	= 15 kΩ	R_{12}	= 1.8 MΩ	R_{17}	= VD 9011		
				R_{13}	= 39 kΩ				
C_1	= 0.015 μF	C_4	= 5600 pF			C_9	= 0.047 μF	C_{12}	= 0.1 bis
C_2	= 0.015 μF	C_5	= 0.015 μF	C_7	= 0.1 μF	C_{10}	= 0.47 μF		= 0.5 μF
C_3	= 0.022 μF	C_6	= 0.033 μF	C_8	= 0.47 μF	C_{11}	= 25 μF	C_{13}	= 0.1 μF

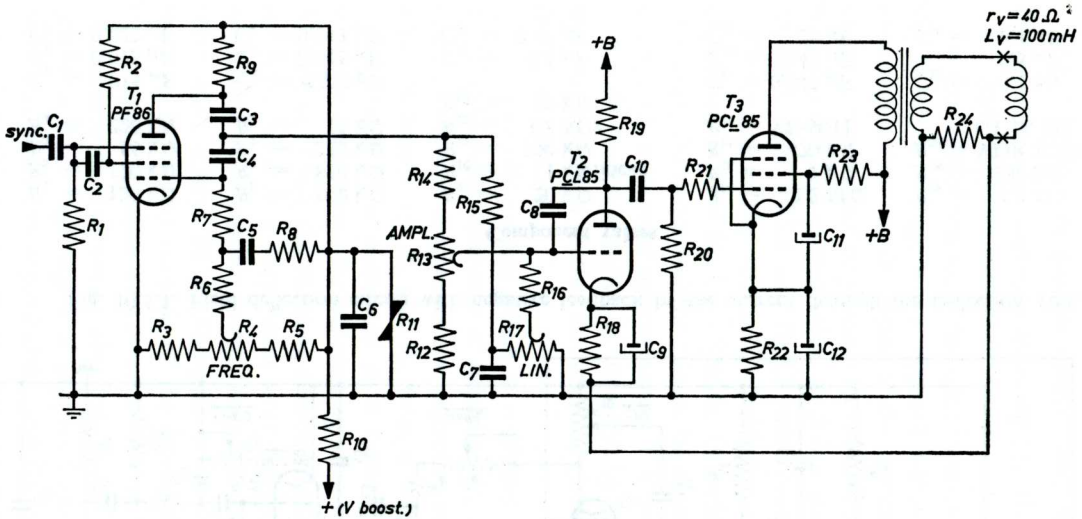

Fig. 10.5.2. Field deflection circuit with negative current feedback.

Component values

R_1 =	100 kΩ	R_6 =	1.2 MΩ	R_{11} =	E 298 GD/A 258	R_{15} =	390 kΩ
R_2 =	27 kΩ	R_7 =	1.2 MΩ	R_{12} =	100 kΩ	R_{16} =	1.5 MΩ
R_3 =	1 MΩ	R_8 =	270 kΩ	R_{13} =	0.5 MΩ Pot.	R_{17} =	1 MΩ Pot.
R_4 =	0.5 MΩ Pot.	R_9 =	33 kΩ	R_{14} =	1 MΩ	R_{18} =	4.7 kΩ
R_5 =	1.8 MΩ	R_{10} =	680 kΩ			R_{19} =	330 kΩ

R_{20} =	2.2 MΩ	C_1 =	1500 pF	C_4 =	6800 pF	C_7 =	0.039 μF
R_{21} =	1 kΩ	C_2 =	0.015	C_5 =	8200 pF	C_8 =	47 pF
R_{22} =	390 Ω	C_3 =	0.033 μF	C_6 =	0.47 μF	C_9 =	100 μF
R_{23} =	4700 Ω					C_{10} =	0.1 μF
R_{24} =	10 Ω					C_{11} =	10 μF
						C_{12} =	100 μF

maintained by returning the flyback pulse at the anode of the output valve T_4 to the grid of T_1; as a result, the whole circuit forms a multivibrator, the repetition frequency of which is principally determined by the discharge time-constant in the grid circuit of T_1. The flyback period depends mainly on the self inductance, capacitance and damping which are present in the anode circuit of T_4 (transformed).

The timebase can be synchronised by means of positive raster pulses, which are also conveyed to the grid of T_1.

Fig. 10.5.2. shows another circuit which is simpler than the previous one. This circuit can be utilised if the impedance of the deflection coils is high enough for a voltage of several volts to be obtained across a series resistor. In that case, and when a high slope pentode output valve is used, a triode with high amplification factor can be used as pre-amplifier.

A transitron with Miller-integration (T_1) is employed here as sawtooth voltage oscillator. This supplies a linear negative-going sawtooth voltage which is suitable for feeding to the grid of the amplifier valve T_2. The network connected between the oscillator and the amplifier makes it possible to adjust the picture height and linearity.

The oscillator can be synchronised by feeding negative raster pulses to the third grid of valve T_1.

The high degree of negative feedback means that in both circuits the ratio of deflection current to input voltage is very constant. It is unnecessary to include a thermistor. The effect of variations in the mains voltage can be absorbed completely by stabilising the supply voltage to the oscillator valve. As the oscillator has a very low current-consumption, the supply voltage can be stabilised in a simple manner with the aid of a V.D.R. Both the size and the form of the deflection current will always remain practically identical with that of the input voltage, so that optimum linearity is guaranteed within the whole range of driving voltages for which these valves are suitable.

LITERATURE REFERENCES

Books:

1. F. KERKHOF and W. WERNER, *Television*, Eindhoven Centrex 1954.
2. O. KLEMPERER, *Electron Optics*, Cambridge: University Press 1953 (2nd. edition).
3. A. A. RUSTERHOLZ, *Electronenoptik*, Basel: Birkhäuser 1950.
4. F. SCHRÖTER, R. THEILE and G. WENDT, *Fernsehtechnik*, erster Teil, Berlin: Springer 1956.
5. V. K. ZWORYKIN and G. A. MORTON, *Television*, New-York: Wiley 1940–1954.

Articles:

1. R. ANDRIEU, *Die Zeilenablenkung mit Spartransformator*, Telefunkenzeitung 95, 1952.
2. H. BÄHRING, *Magnetische Strahlablenksysteme*, Funk und Ton, Januar 1952.
3. K. G. BEAUCHAMP, *Overcoming line scan ringing*, Wireless World, September 1957.
4. C. H. BOERS and A. G. W. UITJENS, *Practical considerations on line timebase output stages with booster circuit*, Philips Electronic Application Bulletin, August 1951.
5. B. B. BYEER, *Design considerations for scanning yokes*, Tele-Tech, August 1950.
6. W. T. COCKING, *Deflector coil characteristics*, Wireless World, March, April, May, 1950.
7. E. T. EMMS, *The theory and design of television frame output stages*, Electronic Engineering, March 1952.
8. FÄLKER and HÜCKUNG, *Magnetische Messung an Ferrit U-Kernen für Horizontalausgangsübertrager*, Elektronische Rundschau, August 1958.
9. FÄLKER and HÜCKUNG, *Eigenschaften von Ferrit U-Kernen für horizontale Ausgangsübertrager*, Elektronische Rundschau, Januar 1959.
10. J. C. FRANCKEN, J. DE GIER and W. F. NIENHUIS, *A pentode gun for television picture tubes*, Philips Techn. Review, September 1956.
11. A. W. FRIEND, *Television deflection circuits*, RCA Review, March 1947.
12. Dr GOSWIN SCHAFFSTEIN, *Die Verlustleistung bei der Zeilenablenkung im Fernseher*, Radio Mentor, März 1960.
13. J. HAANTJES and G. J. LUBBEN, *Errors of magnetic deflection I*, Philips Res. Rep., February 1957, Idem II, February 1959.
14. G. W. O. HOWE, *Negative ions in cathode ray beams*, Wireless Engineer, August 1954.
15. R. G. E. HUTTER, *Electron beam deflection*, Journal of Applied Physics, August and September 1947.
16. J. L. H. JONKER, *A short length direct-view picture-tube*, Philips Techn. Review, July 1953.
17. W. F. NIKLAS, *An improved ion-trap magnet*, Philips Tech. Review, February-March 1954.
18. W. F. NIKLAS, *Negative Ionenkomponente des Elektronenstrahles in Kathodenstrahlröhren*, Philips Res. Rep., April 1954.
19. M. J. OBERT and W. A. NEEDS, *Ferrite-core yoke for wide deflection angle kinescopes*, Tele-Tech, October 1950.

20. S. L. Reiches and D. P. Ingle, *Magnetic centering of electrostatic C.R. tubes*, Electronics, January 1952.
21. H. Reker, *Der Zeilenablenkungstranformator mit abgestimmter Hochspannungswicklung*, N.T.Z. XI, März 1958.
22. O. H. Schade, *Characteristics of high-efficiency deflection and high voltage supply systems for kinescopes*, R.C.A. Review, March 1950.
23. K. Schlesinger, *Anastigmatic yoke for picture tubes*, Electronics, October 1949.
23*a*. K. Schlesinger, *Magnetic deflection of kinescopes*, Proceedings of the I.R.E., August 1947.
24. R. Suhrmann, *Kontrastfilter für Fernsehgeräte*, Elektronische Rundschau, Juli 1958.
25. J. A. Verhoef, *The focusing of television picture-tubes with ferroxdure magnets*, Philips Techn. Review, January 1954.
26. B. V. Vonderschmitt and W. H. Barkow, *Application of ferrites to deflection components*, Tube division R.C.A., Publication Nr. ST-993.
27. G. Wendt, *Bildfehler bei Ablenkung eines Kathodenstrahls in zwei gekreuzten Ablenkfeldern*, Zeitschrift für Physik, 1942, pag. 593–617.
28. G. Wendt, *Méthode pour la détermination d'un ensemble de deviation magnétique*, Ann. de Radioeléctricité, 1954, page 286–307.

LIST OF SYMBOLS

a = Internal radius of the picture tube neck; percentage of reduction of flyback peak voltage due to tuned leakage induction; unit dimension of transformer core
A = Cross-sectional area of transformer core
B = Brightness; magnetic flux density
B_0 = Premagnetisation by d.c.
ΔB = Variation of brightness; a.c. flux density
$\hat{B}$ = Peak value of the flux density
c = Velocity of light; crossover
C = Capacitance
d = Spotdiameter; distance between deflection plates
e = Charge of an electron
E = Electric fieldstrength
E.H.T. = Anode voltage of the picture tube (extra high tension)
f = Frequency
F = Force experienced by electrons
F_p = Ratio of flyback peak voltage to scan voltage with line deflection
g = Grid
H = Magnetic fieldstrength
i_a = Anode current
i_{ag}, $\bar{i}_a$ = Direct anode current
$\hat{i}_a$ = Peak anode current
i_{ai} = Anode current at the start of the scan
$\bar{i}_d$ = Average current of the booster diode
$\hat{i}_d$ = Peak current of the booster diode
i_{g2} = Screen-grid current
i_l = Extra load current, taken from the booster voltage
i_m = The value of $\hat{i}_v/2$, transformed to the primary of the field output transformer; value of the line scan current at the start of the flyback
i_p = Magnetising current of the field output transformer
i_s = Surplus current; field deflection current transformed to the primary of the output transformer
i_{tr} = Magnetising sawtooth current of the line output transformer
i_v = Current through the field deflection coil
$\hat{i}_v$ = Peak to peak value of i_v
i_y = Current through the line deflection coil
$\hat{i}_y$ = Peak to peak value of i_y
$\hat{i}_y{}^*$ = Value of $\hat{i}_y$ transformed to the primary
I_a = Beamcurrent in the picture tube
k = Cathode; coupling factor of transformer windings
l = Distance from the cathode to the screen; length of the deflection field
l, l_k = Length of the iron path of a transformer core
l_0 = Effective length of the deflection field

L = Distance from the centre of deflection to the screen; self inductance of coils
L_h = Self inductance of the E.H.T. winding
L_p = Self inductance of the primary winding of the field output transformer
L_p^* = Self inductance of the line deflection circuit transformed to the primary of the output transformer
L_s = Self inductance of the field deflection coil transformed to the primary of the output transformer; self inductance of the winding n_y of the line output transformer
L_s' = Leakage inductance of the E.H.T. winding, relative to the primary
L_v = Self inductance of the field deflection coil
L_y = Self inductance of the line deflection coil
m = Mass of an electron; ratio of the power required for magnetising the line output transformer, relative to the power in the deflection coil
n = Number of turns; transformation ratio
n_a = Number of turns of the line output transformer between the connections to the anode of the pentode and the booster capacitor
n_d = Number of turns of the line output transformer between the connections to the booster diode and the booster capacitor
n_p = Number of turns of the primary of the field output transformer
n_s = Number of turns of the secondary of the field output transformer
n_y = Number of turns of the line output transformer between the connections to the deflection coil
N_0 = Maximum density of winding
p = Fraction of sawtooth period in which the flyback takes place
P = Power
P_a = Anode dissipation
P_b = Power, delivered by the power supply
P_c = Power dissipated in the resistances of the primary and secondary of the field output transformer and of the field deflection coil
P_f = Power lost during the flyback of the line timebase
P_{g2} = Screen-grid dissipation
P_m = Magnetic power in the line deflection circuit
P_{my} = Magnetic power in the line deflection coil
P_{Rcat} = Dissipation in the cathode resistor caused by the anode current
P_s = Power lost during the scan in the line deflection coil
P_y = Iron loss of the field output transformer
q = Difference between the internal radii of the deflection yoke and the picture tube neck; fraction of winding space, available for a winding
Q_f = Magnification of resonant circuit at flyback frequency
r = Half the diameter of the electron beam in the deflection field
r_v = Resistance of the field deflection coil
r_y = Resistance of the line deflection coil

R = Radius of curvature of the electron path; radius of curvature of the screen; radius of coils with cylindrical shape
R_c = Resistance of the field deflection coil transformed to the primary
R_{cat} = Cathode resistor
R_i = Internal resistance
R_p = Resistance of the primary of the field output transformer
R_s = Resistance of the secondary circuit of the field output stage, transformed to the primary
R_{sec} = Resistance of the secondary of the field output transformer
s = Ratio of power lost due to leakage inductance of the transformer relative to the power in the deflection coil
S = Cross-section of a coil; surface area of deflection plates
t_f = Duration of the line flyback
t_s = Duration of the line scan
t_v = Duration of the field scan
T = Duration of a period
v = Velocity of electrons
V = Volume of the deflection field; potential
V_a = Anode voltage
$\hat{V}_a$ = Peak anode voltage
$V_{a\text{end}}$ = Anode voltage at the end of the scan
V_b = Supply voltage
V_c = Voltage across the booster capacitor
V_d = Voltage difference for electrostatic deflection; Voltage drop across booster diode during the scan
$\hat{V}_d$ = Peak voltage at the booster diode during the flyback
V_{g1} = Control grid voltage
V_{g2} = First anode voltage; screen-grid voltage
V_k = Cathode voltage; Volume of the iron core of a transformer
V_L = Voltage across the inductive component of the deflection coil impedance
V_p = Voltage across the primary of the field output transformer
V_r = Voltage across the resistive component of the deflection coil impedance
V_y = Voltage across the line deflection coil at the end of the scan
W = Screenwidth; energy stored in the deflection field
y = Displacement of the spot on the screen
$\bar{\alpha}$ = Ratio of average anode current to average screen-grid current
$\hat{\alpha}$ = Ratio of anode current to screen-grid current at the end of the scan
α_o = Extrapolated value of the ratio of anode to screen-grid current at zero anode current
α_h = Correction factor for the sensitivity of the line deflection coil
α_v = Correction factor for the sensitivity of the field deflection coil
γ = Increase of the current and power consumption of the linetime-base due to the load on the E.H.T., relative to the current and power consumption in the unloaded condition
ε = Relative permittivity

η = Ratio of the line deflection power at the end of the flyback to the power at the start of the flyback; Voltage efficiency factor of the field output transformer

μ = Permeability

μ_Δ = Incremental permeability

μ_{g1g2} = Amplification factor of the screen-grid to the control grid

$\bar{\sigma}$ = Average value of the surplus current factor

φ = Angle of deflection of the electron beam; phase angle

Φ = Ratio of peak anode current to the peak-to-peak value of the field deflection current, transformed to the primary

Ψ = Ratio of average diode current to average anode current of the pentode of the line output stage

INDEX